

UNIVERSITÄT
BAYREUTH

**Functional analysis of the metal
hyperaccumulation and hypertolerance
candidate genes *NAS4*, *ZIP6*, *CAX1* and *NRAMP3*
in *Arabidopsis halleri***

DISSERTATION

Zur Erlangung des akademischen Grades
Doktor der Naturwissenschaften (Dr. rer. nat.)
der Fakultät Biologie / Chemie / Geowissenschaften
der Universität Bayreuth

vorgelegt von
Hassan Ahmadi

geboren am 03.03.1981 in Noodsheh, Iran
Bayreuth, June 2017

This doctoral thesis was prepared at the department of Plant Physiology at the University of Bayreuth from February 2012 until June 2017 and was supervised by Prof. Dr. Stephan Clemens.

This is a full reprint of dissertation to obtain the academic degree of Doctor of Natural Science (Dr. rer. Nat.) and approved by the Faculty of Biology, Chemistry and Geoscience of the University of Bayreuth.

Date of submission: 28. 06. 2017

Date of defense: 05. 10. 2017

Acting dean: Prof. Dr. Stefan Peiffer

Doctoral committee:

Prof. Dr. Stephan Clemens (1st reviewer)

PD. Dr. Alfons Weig (2nd reviewer)

Prof. Dr. Angelika Mustroph (chairman)

Prof. Dr Egbert Matzner

Summary

Arabidopsis halleri is a model species for the study of mechanisms underlying metal hyperaccumulation and, more generally, for plant adaptation to extreme environments. Comparative transcriptome analysis between *A. halleri* and *A. thaliana* as well as QTL studies suggested *NAS4*, *ZIP6*, *NRAMP3* and *CAX1* as candidate genes for metal hyperaccumulation and hypertolerance in *A. halleri*.

The ability to successfully perform genetic manipulations is essential to enable reverse genetic studies in *A. halleri* aiming at dissecting molecular aspects of heavy metal hyperaccumulation and hypertolerance. Therefore, a seed independent and highly efficient method for *Agrobacterium*-mediated stable transformation of *A. halleri* was developed. RNAi knock-down lines of *A. halleri* in which transcript levels of *NAS4*, *ZIP6*, *CAX1* and *NRAMP3* were significantly reduced, were generated and used to analyze the direct role of each gene in metal hyperaccumulation and hypertolerance. Suppression of *AhNAS4* resulted in reduced root NA content with no effect on *A. halleri* Zn and Cd hyperaccumulation or hypertolerance. We suggest that *AhNAS4* is not a metal hyperaccumulation gene in *A. halleri*. Instead, suppression of *AhNAS4* resulted in more efficient root-to-shoot translocation specifically of Fe and higher tolerance towards Fe deficiency in *A. halleri*. It also changed the Fe distribution pattern in roots and while Fe mainly was accumulated in the epidermis layer of wild-type and control plants, it was distributed evenly among different cell types in roots of *AhNAS4* suppressed lines. Silencing of *AhNAS4* resulted in Ni hypersensitivity and a severe reduction in root elongation and root biomass in *A. halleri*. We assume that *AhNAS4* down regulation might increase synthesis and efflux of organic acids like citrate and malate into the xylem in *A. halleri*, which consequently would increase Fe translocation from roots to the shoot.

Furthermore, it was found that while *AhZIP6* had no measurable contribution to metal hyperaccumulation, it played a role in root Cd uptake in *A. halleri*, and while suppression of *ZIP6* had no effect on tolerance towards Ni, Zn and Pb, it specifically enhanced tolerance towards Cd in *A. halleri*. Suppression of *AhZIP6* decreased root short-term uptake of Cd in *A. halleri*. This study provides the first experimental evidence for the role of *AhZIP6* in root Cd uptake in *A. halleri*.

Suppression of *AhCAX1* increased H₂O₂ and superoxide accumulation following Cd treatment in *A. halleri* roots. These increases were Ca²⁺- dependent and completely absent when plants were cultivated in medium with the higher Ca²⁺ concentration. Our study strongly supports the hypothesis that *AhCAX1* is indeed explaining the QTL Cdtol2 and thus represents the second Cd hypertolerance factor identified in plants besides *HMA4*.

Finally, it was shown that suppression of *NRAMP3* has no detectable physiological effect in metal accumulation or metal tolerance in *A. halleri*.

Zusammenfassung

Arabidopsis halleri ist ein Modellsystem für die mechanistische Aufklärung von Metall-Hyperakkumulation und –Hypertoleranz sowie generell die Analyse der Anpassung von Pflanzen an Extremstandorte. Vergleichende Transkriptom-Studien und QTL-Analysen hatten *NAS4*, *ZIP6*, *NRAMP3* und *CAX1* als Kandidatengene für Metall-Hyperakkumulation bzw. –Hypertoleranz in *A. halleri* identifiziert.

Die molekulare Aufklärung der Mechanismen von Metall-Hyperakkumulation und –Hypertoleranz durch *reverse genetics*-Ansätze ist abhängig von der Fähigkeit *A. halleri* zu transformieren. Deshalb wurde in dieser Arbeit ein Protokoll für die effiziente, stabile und von der Anzucht aus Samen unabhängige Transformation von *A. halleri* entwickelt. Dies ermöglichte die Generierung von *Knockdown*-Linien mittels RNAi. Mehrere unabhängige Linien mit jeweils stark reduzierter Transkript-Abundanz der Kandidatengene *NAS4*, *ZIP6*, *CAX1* und *NRAMP3* wurden erzeugt und für die molekulare und physiologische Analyse der Rolle der jeweiligen Gene genutzt.

Suppression von *AhNAS4* resultierte in reduzierten Nicotianamin-Gehalten der Wurzel. Dies war jedoch ohne Effekt auf die Zn- bzw. Cd-Hyperakkumulation oder –Hypertoleranz. Stattdessen zeigte sich eine effizientere Translokation von Fe aus den Wurzeln in den Spross und eine höhere Toleranz gegenüber Fe-Mangel. Der Verlust von *AhNAS4*-Funktion führte außerdem dazu, dass die Verteilung von Fe in Wurzelgewebe verändert war. Eine Akkumulation in epidermalen Zellen wie im Wild-Typ war nicht mehr zu beobachten. Zudem verursachte *AhNAS4-Knockdown* Ni²⁺-Hypersensitivität. Die Arbeitshypothese zur Erklärung dieser Phänotypen ist, dass Reduzierung der *AhNAS4*-Transkriptmenge kompensatorische Reaktionen auslöst und über die Erhöhung z.B. der Sekretion von organischen Säuren in das Xylem zu verbesserter Fe-Translokation in den Spross führt.

Für das Kandidatengen *AhZIP6* wurde gefunden, dass es keinen messbaren Beitrag zur Metall-Hyperakkumulation oder –Hypertoleranz leistet, der *Knockdown* jedoch spezifisch die Cd²⁺-Toleranz erhöht. Es konnte gezeigt werden, dass *AhZIP6* signifikant zur Cd-Aufnahme in *A. halleri* beiträgt und damit einer der ersten pflanzlichen Cd-Transporter identifiziert ist.

Suppression von *AhCAX1* verursachte erhöhte Akkumulation von H₂O₂ und Superoxid-Radikalen in mit Cd²⁺ behandelten Pflanzen. Diese Effekte waren abhängig von externen Ca²⁺-Konzentrationen. Sie stützen damit die Hypothese, dass *AhCAX1* einen der Cd-Toleranz-QTLs (*Cdtol2*) erklärt und somit den zweiten Cd-Hypertoleranzfaktor neben *HMA4* darstellt.

Für *Nramp3* schließlich konnten in entsprechenden RNAi-Linien keine detektierbaren Beiträge zur Metall-Hyperakkumulation oder –Hypertoleranz gefunden werden.

Acknowledgements

I would like to extend my deepest gratitude to my supervisor Prof. Dr. Stephan Clemens, for giving me this opportunity to be part of his research team, for his remarkable ideas, guidance and encouragement during my research period and above all for his kindness and understanding that made my stay in the department enjoyable.

I extend my sincere thanks to Dr. Michael Weber, for his support during lab work and giving important suggestions during the course of the research.

I thank Dr. Ulrich Deinlein for answering my questions about his previous data and transformation protocol. I am very thankful to my lab bench mate Stephan Höreth, for the warm discussions and encouragements as well as for the good working environment.

I would like to express my gratitude to Dr. Shimpei Uraguchi, Dr. Jean-Yves Cornu and Dr. Blen Beyene for their assistance in the lab whenever I needed.

I am deeply grateful to Dr. Katarina Vogel-Mikus and Dr. Paula Pongrac for their help with μ PIXE experiments and data analysis.

My sincere appreciation goes to Prof. Dr. Angelika Mustroph, for her esteemed guidance and valuable suggestions during my research.

My heartfelt gratitude goes to Ursula Ferrera for her assistance in dealing with university formalities and heartily concern about my progress in general and to Christiane Meinen, Carmen Guenther and Silke Matros for their technical support of the research.

I am grateful to “Bundesministeriums für Bildung und Forschung” for financing this research.

I am very grateful to all members of the Department of Plant Physiology who were directly or indirectly involved in my journey throughout the PhD work.

Last, but not least, all this would not be possible without support from my family in Iran, who even that far away made me feel strong enough across this life-changing odyssey.

Table of Contents

Summary	I
Zusammenfassung	II
Acknowledgements	III
Table of Contents	IV
List of figures and tables	VIII
List of abbreviations	XI
1. Introduction	1
1.1 Plant mineral nutrition	1
1.1.1 Mineral nutrients roles in plant growth and development.....	1
1.1.2 Zn and Fe deficiency and toxicity in plants	2
1.2 Molecular mechanism of Zn and Fe uptake and distribution in plants	3
1.2.1 Zn uptake and sequestration.....	3
1.2.2 Xylem Zn loading and unloading.....	4
1.2.3 Phloem Zn loading and unloading.....	5
1.2.4 Fe uptake.....	5
1.2.5 Fe Translocation.....	6
1.2.6 Subcellular transport of Fe.....	7
1.2.7 Zn and Fe deficiency in Human.....	8
1.3 Nonessential toxic heavy metals uptake in plants	8
1.3.1 Cadmium toxicity in human and plants	9
1.3.2 Cadmium toxicity at the cellular level	10
1.4 Molecular mechanism of Cd uptake, chelation, sequestration, and translocation in plants	11
1.4.1 Cd uptake	11
1.4.2 Cd chelation and sequestration.....	11
1.4.3 Cd translocation	12
1.5 Metal hyperaccumulation and hypertolerance in plants	13
1.5.1 Metal hypertolerant and hyperaccumulator species	14
1.5.2 Molecular mechanisms of metal hyperaccumulation and hypertolerance	15
1.6 The aim of this study	19
2. Materials and methods	21
2.1. Generation of <i>A. halleri</i> RNAi lines	21
2.1.1 Generation of <i>AhNAS4</i> , <i>AhZIP6</i> , <i>AhNRAMP3</i> and <i>AhCAX1</i> RNAi constructs.....	21
2.1.2 <i>A. halleri</i> transformation.....	21
2.1.2.1 Optimal density of <i>Agrobacterium tumefaciens</i>	22
2.1.2.2 Acetosyringone effect on <i>A. halleri</i> transformation.....	22
2.1.2.3 Effect of genotype on <i>A. halleri</i> transformation	22

2.2. GFP analysis by florescent and confocal microscopy	23
2.3 Transcript analysis	23
2.4 Plant material and growth conditions.....	24
2.4.1 Hydroponic cultures	24
2.4.2 Short-term uptake experiment.....	24
2.4.3 Plant culture on soil.....	25
2.5 Elemental Analysis	25
2.5.1 ICP-OES Analysis.....	25
2.5.2 Perls staining of Fe coupled to DAB intensification	26
2.5.3 Quantitative mapping of elements by Particle-Induced X-ray Emission (μ PIXE).....	26
2.6 Determination of leaves chlorophyll content.....	26
2.7 Determination of catalase activity.....	27
2.8 ROS detection and quantification	27
2.9 Determination of NA content.....	27
2.10 Determination of soil pH.....	28
2.11 Statistical Analysis	28
3. Results.....	29
3.1 Optimization the <i>Agrobacterium</i>-mediated transformation of <i>A. halleri</i>.....	29
3.1.1 Media for callus induction and shoot regeneration.....	29
3.1.2 <i>A. halleri</i> regeneration steps	29
3.1.3 Analysis of plants stably transformed with GFP	30
3.1.4 Effect of <i>A. tumefaciens</i> density on <i>A. halleri</i> transformation efficiency.....	31
3.1.5 Effect of acetosyringone on <i>A. halleri</i> transformation efficiency.....	32
3.1.6 Effect of source of explants on <i>A. halleri</i> transformation efficiency.....	33
3.1.7 Effect of <i>A. halleri</i> genotype on transformation efficiency.....	34
3.2 The physiological role of <i>NAS4</i> in <i>A. halleri</i>	37
3.2.1 Confirmation of <i>AhNAS4</i> -RNAi lines with real-time PCR.....	37
3.2.1.1 Suppression of <i>AhNAS4</i> results in reduced root NA content in <i>A. halleri</i> grown in standard medium for 10 days.....	38
3.2.2 Elemental profiling of <i>AhNAS4</i> -RNAi lines hydroponically grown in standard <i>A. halleri</i> 1/10 Hoagland medium for 10 days.....	39
3.2.2.1 Suppression of <i>AhNAS4</i> slightly disturb Zn translocation in <i>A. halleri</i> grown in standard medium for 10 days.....	39
3.2.2.2 Silencing of <i>AhNAS4</i> results in more efficient root-to-shoot translocation specifically of Fe in <i>A. halleri</i> grown in standard medium for 10 days.....	40
3.2.2.3 <i>AhNAS4</i> suppression results in no change in root and shoot contents and root-to-shoot translocation of Mn, Ca and Mg.....	41
3.2.2.4 <i>AhNAS4</i> suppression results in change in Fe localization pattern in roots.....	42
3.2.3. Silencing of <i>AhNAS4</i> increases tolerance towards Fe deficiency in <i>A. halleri</i> grown in alkaline medium.....	43

3.2.3.1 Silencing of <i>AhNAS4</i> results in more efficient root-to-shoot translocation specifically of Fe in <i>A. halleri</i>	44
3.2.3.2 Silencing of <i>AhNAS4</i> does not change root-to-shoot translocation of Zn in <i>A. halleri</i> plants grown in alkaline medium	45
3.2.4. <i>AhNAS4</i> suppression causes Ni hypersensitivity in <i>A. halleri</i>	48
3.2.4.1. <i>AhNAS4</i> suppression has no effect on root and shoot Ni content in <i>A. halleri</i>	50
3.2.4.2. <i>AhNAS4</i> suppression specifically enhances Fe root-to-shoot translocation under control and Ni stress conditions	51
3.2.4.3. <i>AhNAS4</i> suppression has no effect on root and shoot Zn content in <i>A. halleri</i> hydroponically grown for 3 weeks under control and Ni stress conditions.....	52
3.2.5. <i>AhNAS4</i> suppression has no effect on excess Zn and Cd tolerance in <i>A. halleri</i>	53
3.2.6 Silencing of <i>AhNAS4</i> increases tolerance towards Fe deficiency in <i>A. halleri</i> grown in alkaline soil	55
3.2.6.1 Silencing of <i>AhNAS4</i> results in higher chlorophyll content in leaves of <i>A. halleri</i> in alkaline soil.....	56
3.2.6.2 Silencing of <i>AhNAS4</i> results in higher catalase activity in leaves of <i>A. halleri</i> grown in alkaline soil	57
3.2.6.4 <i>AhNAS4</i> suppression decreases shoot Mg content of alkaline soil grown plants	59
3.2.6.5 PIXE imaging of the whole leaves of <i>A. halleri</i> wild-type and <i>AhNAS4</i> -RNAi plants grown in normal and alkaline soils	60
3.2.7. Characterization of <i>AhNAS4</i> -RNAi lines on phenotyping and Bestwig soils	61
3.3 The physiological role of ZIP6 in <i>A. halleri</i>	65
3.3.1 Confirmation of <i>AhZIP6</i> -RNAi lines with real-time PCR.....	65
3.3.2 Elemental profiling of <i>AhZIP6</i>-RNAi lines	66
3.3.2.1 Elemental profiling of <i>AhZIP6</i> -RNAi lines hydroponically grown in standard <i>A. halleri</i> 1/10 Hoagland medium	66
3.3.2.2 <i>AhZIP6</i> suppression results in no phenotypic change in <i>A. halleri</i> plants grown under Zn and Fe depletion or in medium with sufficient or Zn excess content	67
3.3.2.3 <i>AhZIP6</i> suppression does not change root and shoot metal content of <i>A. halleri</i> plants grown in Zn and Fe depletion or in medium with sufficient or Zn excess content	69
3.3.3 Tolerance assay of <i>AhZIP6</i>-RNAi lines	70
3.3.3.1 Suppression of <i>AhZIP6</i> has no effect on Ni and Zn tolerance in <i>A. halleri</i>	70
3.3.3.2 Suppression of <i>AhZIP6</i> has no effect on root and shoot metal content in <i>A. halleri</i> plants under Ni and Zn stress conditions.....	72
3.3.3.3 Suppression of <i>AhZIP6</i> specifically enhances tolerance towards Cd in <i>A. halleri</i>	74
3.3.3.4 Suppression of <i>AhZIP6</i> has no effect on metal content in <i>A. halleri</i> grown under Cd stress conditions for 3 weeks	75
3.3.3.5 Suppression of <i>AhZIP6</i> decreases roots short-term uptake of Cd in <i>A. halleri</i>	77
3.3.3.6. Characterization of <i>AhZIP6</i> -RNAi lines on phenotyping and Bestwig soils	78
3.3.3.6 Suppression of <i>AhZIP6</i> has no effect on shoot metal content of soil-grown <i>A. halleri</i>	79
3.3.3.7 Suppression of <i>AhZIP6</i> has no effect on lead (Pb) tolerance in <i>A. halleri</i>	80
3.4 The physiological role of <i>CAX1</i> in <i>A. halleri</i>	81

3.4.1 Comparison of <i>CAX1</i> expression in <i>A. halleri</i> C-line and <i>Auby</i> individuals.....	81
3.4.2 Confirmation of <i>AhCAX1</i> -RNAi lines with real-time PCR	82
3.4.2 Tolerance assay of <i>AhCAX1</i>-RNAi lines.....	83
3.4.2.1 Suppression of <i>AhCAX1</i> has no effect on <i>A. halleri</i> biomass under Cd stress condition .	83
3.4.3 ROS detection and quantification in <i>AhCAX1</i> -RNAi lines.....	84
3.4.3.1 Suppression of <i>AhCAX1</i> increase H ₂ O ₂ accumulation following Cd treatment in <i>A. halleri</i>	84
3.4.3.2 Suppression of <i>AhCAX1</i> increases superoxide accumulation following Cd treatment in <i>A. halleri</i>	85
3.5 The physiological role of <i>NRAMP3</i> in <i>A. halleri</i>.....	86
3.5.1 Confirmation of <i>AhNRAMP3</i> -RNAi lines with real-time PCR.....	86
3.5.2 Elemental profiling of <i>AhNRAMP3</i>-RNAi lines.....	87
3.5.2.1 <i>AhNRAMP3</i> suppression has no effect on in <i>A. halleri</i> tolerance towards Cd	87
3.5.2.3 <i>AhNRAMP3</i> suppression has no effect on Ni tolerance in <i>A. halleri</i>	90
3.5.2.4 <i>AhNRAMP3</i> suppression has no effect on tolerance towards Fe deficiency in <i>A. halleri</i> .	91
3.5.2.5. Silencing of <i>AhNRAMP3</i> has no effect on roots and shoots metal content of <i>A. halleri</i> plants hydrponically grown in control or Fe depleted medium	92
4. Discussion.....	95
4.1 Optimized protocol for <i>Agrobacterium</i>-mediated transformation of <i>A. halleri</i>.....	95
4.2 <i>NAS4</i> plays an important role in Fe homeostasis in <i>A. halleri</i>	96
4.2.1 <i>AhNAS4</i> is not a Zn and Cd hyperaccumulation and hypertolerance gene in <i>A. halleri</i>	96
4.2.2 Suppression of <i>AhNAS4</i> enhances root-to-shoot translocation of Fe and consequently tolerance towards Fe deficiency	97
4.3 <i>ZIP6</i> plays a role in root Cd uptake in in <i>A. halleri</i>.....	99
4.3.1 <i>AhZIP6</i> is not a metal hyperaccumulation gene in <i>A. halleri</i>	99
4.3.2 Suppression of <i>AhZIP6</i> specifically enhances tolerance towards Cd in <i>A. halleri</i>	100
4.3.4 Suppression of <i>AhZIP6</i> decreases short-term uptake of Cd in <i>A. halleri</i> roots	100
4.4 <i>AhCAX1</i> is essential for suppressing Cd-induced generation of reactive oxygen species in roots of <i>A. halleri</i>	101
4.4.1 Suppression of <i>AhCAX1</i> has no visible phenotypical effects on <i>A. halleri</i> grown under sequential Cd tolerance assay.....	101
4.4.2 Suppression of <i>AhCAX1</i> leads to an increase in H ₂ O ₂ and superoxide accumulation following Cd treatment in <i>A. halleri</i>	102
4.5 <i>AhNRAMP3</i> has no major contribution to metal hyperaccumulation and hypertolerance in <i>A. halleri</i>.....	103
4.5.1 Suppression of <i>AhNRAMP3</i> did not reveal any physiological role in <i>A. halleri</i>	103
References	105

List of figures and tables

Fig. 1.1 Intercellular Zn and Fe transport in <i>A. thaliana</i>	8
Fig. 1.2 Mechanisms underlying Cd uptake and translocation in rice	13
Fig. 1.3 Plants differently response to Zn and Cd exposure	14
Table 1.1 Hyperaccumulation of trace elements in land plants	15
Table 1.2 Metal homeostasis genes that are highly expressed in <i>A. halleri</i> and <i>N. caerulescens</i> ..	17
Fig. 1.4 The common core set of metal transporter genes highly expressed in <i>A. halleri</i> and <i>N. caerulescens</i> and their role in hyperaccumulation and hypertolerance	19
Table 2.1 Primers were used for RNAi constructs of <i>AhNAS4</i> , <i>AhZIP6</i> , <i>AhNRAMP3</i> and <i>AhCAX1</i> ..	21
Fig. 2.1 Origin of the individuals selected for the assessment of variation in transformation competence	23
Fig. 3.1 <i>A. halleri</i> regeneration steps	30
Fig. 3.2 GFP expression in root tips of <i>A. halleri</i>	31
Fig. 3.3 Effect of <i>A. tumefaciens</i> density on <i>A. halleri</i> transformation efficiency 32Error! Bookmark not defined.	
Fig. 3.4 Effect of acetosyringone on <i>A. halleri</i> transformation efficiency	33
Tab. 3.1 and Fig. 3.5 Effect of source of explants on <i>A. halleri</i> transformation efficiency	34
Fig. 3.6 Effect of <i>A. halleri</i> genotype on callus induction	35
Fig. 3.7 Effect of <i>A. halleri</i> genotype on shoot regeneration	35
Tab. 3.2 and Fig. 3.8 Effect of <i>A. halleri</i> genotype on transformation efficiency	36
Fig. 3.9 Reduction of <i>AhNAS4</i> transcript level in independent RNAi lines	37
Fig. 3.10 Effect of <i>AhNAS4</i> suppression on <i>NAS1</i> , <i>NAS2</i> , <i>NAS3</i> and <i>NAS4</i> transcript abundance in roots and shoots of <i>A. halleri</i>	38
Fig 3.11 NA content in roots and shoots of hydroponically grown <i>A. halleri</i> wild-type and <i>AhNAS4</i> -RNAi plants	39
Fig. 3.12 Zn accumulation in <i>A. halleri</i> wild-type and <i>AhNAS4</i> -RNAi plants hydroponically grown in standard medium for 10 days	40
Fig. 3.13 Fe content in roots and shoots of <i>A. halleri</i> wild-type and <i>AhNAS4</i> -RNAi plants hydroponically grown in standard medium for 10 days	41
Fig. 3.14 Mn, Mg and Ca contents in roots and shoots of <i>A. halleri</i> wild-type and <i>AhNAS4</i> -RNAi plants hydroponically grown in standard medium for 10 days	42
Fig. 3.15 Fe detection in roots of hydroponically grown <i>A. halleri</i> wild-type and <i>AhNAS4</i> -RNAi plants using the Perls staining associated to Intensification by DAB	43
Fig. 3.16 Phenotype of <i>A. halleri</i> wild-type and <i>AhNAS4</i> -RNAi plant hydroponically grown in alkaline medium	44
Fig. 3.17 Fe content in roots and shoots of <i>A. halleri</i> wild-type and <i>AhNAS4</i> -RNAi plants grown in alkaline medium	45

Fig. 3.18 Zn content in roots and shoots of <i>A. halleri</i> wild-type and <i>AhNAS4</i> -RNAi plants grown in alkaline medium.....	46
Fig. 3.19 Metal content in roots and shoots of <i>A. halleri</i> wild-type and <i>AhNAS4</i> -RNAi plants grown in alkaline medium.....	47
Fig. 3.20 <i>AhNAS4</i> suppression causes Ni hypersensitivity in <i>A. halleri</i>	49
Fig. 3.21 <i>AhNAS4</i> suppression has no effect on root and shoot Ni content in <i>A. halleri</i>	50
Fig. 3.22 <i>AhNAS4</i> suppression specifically enhances Fe root-to-shoot translocation under control and Ni stress conditions	52
Fig. 3.23 <i>AhNAS4</i> suppression has no effect on root and shoot Zn content in <i>A. halleri</i> hydroponically grown for 3 weeks under control and Ni stress conditions.....	53
Fig. 3.24 <i>AhNAS4</i> suppression has no effect on tolerance towards excess Zn and Cd in <i>A. halleri</i>	54
Fig. 3.25 Phenotype of soil-grown <i>A. halleri</i> wild-type and <i>AhNAS4</i> -RNAi plants under alkaline (Fe-limiting) and alkaline + Fe (excess Fe) conditions	55
Fig. 3.26 Phenotype of normal soil-grown <i>A. halleri</i> wild-type and <i>AhNAS4</i> -RNAi plants.....	56
Fig. 3.27 Chlorophyll content of <i>A. halleri</i> wild-type and <i>AhNAS4</i> -RNAi plants grown in normal and alkaline soils	57
Fig. 3.28 Catalase activity of <i>A. halleri</i> wild-type and <i>AhNAS4</i> -RNAi plants grown in alkaline soil.....	58
Fig. 3.29 Fe content in shoots of <i>A. halleri</i> wild-type and <i>AhNAS4</i> -RNAi plants grown in normal and alkaline soils.....	59
Fig. 3.30 Mn, Zn, Mg and Ca contents in shoots of <i>A. halleri</i> wild-type and <i>AhNAS4</i> -RNAi plants grown in normal and alkaline soils	60
Fig. 3.31 PIXE images of <i>A. halleri</i> wild-type and <i>AhNAS4</i> -suppressed line leaves of plants grown in alkaline soil.....	61
Tab.3.2 Extractable metal content of soils were used for <i>A. halleri</i> cultivation.....	62
Tab.3.3 Exchangeable metal content of soils were used for <i>A. halleri</i> cultivation.....	62
Fig. 3.32 Phenotype of <i>A. halleri</i> wild-type and <i>AhNAS4</i> -RNAi plants grown in Bestwig and phenotyping soils.....	63
Fig. 3.33 Metal content in shoot of <i>A. halleri</i> wild-type and <i>AhNAS4</i> -RNAi plants grown in Bestwig and phenotyping soils	64
Fig. 3.34 Reduction of <i>AhZIP6</i> transcript level in independent RNAi lines.....	66
Fig. 3.35 Metal content in roots and shoots of <i>A. halleri</i> wild-type and <i>AhZIP6</i> -RNAi plants hydroponically grown in standard <i>A. halleri</i> 1/10 Hoagland medium.....	67
Fig. 3.36 Phenotype of <i>A. halleri</i> wild-type and <i>AhZIP6</i> -RNAi grown in Zn or Fe depletion medium or in media supplemented with sufficient or excess Zn content.....	69
Fig. 3.37 Metal content in roots and shoots of <i>A. halleri</i> wild-type and <i>AhZIP6</i> -RNAi plants grown in Zn or Fe depletion medium or in media supplemented with sufficient or Zn excess content ...	70
Fig. 3.38 Phenotype of <i>A. halleri</i> wild-type and <i>AhZIP6</i> -RNAi plants grown under Zn and Ni stress conditions	72
Fig. 3.39 Metal content in roots and shoots of of <i>A. halleri</i> wild-type and <i>AhZIP6</i> -RNAi plants grown under Zn and Ni stress conditions.....	73

Fig. 3.40 <i>AhZIP6</i> suppression enhances tolerance towards Cd in <i>A. halleri</i>	75
Fig. 3.41 Metal content in roots and shoots of <i>A. halleri</i> wild-type and <i>AhZIP6</i> -RNAi plants grown under Cd stress conditions	77
Fig. 3.42 Short-term uptake of Cd in <i>A. halleri</i> wild-type and <i>AhZIP6</i> -RNAi plants.....	78
Fig. 3.43 Phenotype of <i>A. halleri</i> wild-type and <i>AhZIP6</i> -RNAi lines grown in Bestwig and phenotyping soils.....	79
Fig. 3.44 Metal content in shoots of <i>A. halleri</i> wild-type and <i>AhZIP6</i> -RNAi lines grown in Bestwig and phenotyping soils	80
Fig. 3.45 Phenotype of <i>A. halleri</i> wild-type and <i>AhZIP6</i> -RNAi plants grown under Pb stress conditions	81
Fig. 3.46 <i>AhCAX1</i> transcript level in shoots of <i>Auby</i> and <i>C-line</i> individuals	82
Fig. 3.47 Reduction of <i>AhCAX1</i> transcript level in independent RNAi lines	83
Fig. 3.48 Sequential Cd tolerance assay in <i>A. halleri</i> wild-type and <i>Ah-CAX1</i> -RNAi plants.....	84
Fig. 3.49 Detection and quantification of H ₂ O ₂ in <i>AhCAX1</i> -RNAi roots.....	85
Fig. 3.50 Detection and quantification of NBT in <i>AhCAX1</i> -RNAi roots	86
Fig. 3.51 Reduction of <i>AhNRAMP3</i> transcript level in shoots of independent RNAi lines	87
Fig. 3.52 Cd tolerance assay in <i>A. halleri</i> wild-type and <i>AhNRAMP3</i> -RNAi plants hydroponically grown in the medium with sufficient Zn content.....	88
Fig. 3.53 Cd tolerance assay in <i>A. halleri</i> wild-type and <i>Ah-NRAMP3</i> -RNAi plants hydroponically grown in the medium with low Zn content.....	90
Fig. 3.54 Ni tolerance assay in <i>A. halleri</i> wild-type and <i>AhNRAMP3</i> -RNAi plants.....	91
Fig. 3.55 Fe deficiency assay in <i>A. halleri</i> wild-type and <i>AhNRAMP3</i> -RNAi plants.....	92
Fig. 3.56 Metal content in roots and shoots of <i>A. halleri</i> wild-type and <i>AhNRAMP3</i> -RNAi plants grown in control and Fe deficiency conditions.....	93

List of abbreviations

2,4-D	2,4-Dichlorophenoxyacetic acid
ABC	ATP-binding cassette
ADAM	Adamantan-1-amine hydrochloride
AHA2	H ⁺ -ATPASE 2
ANOVA	Analysis of variance
ATP	Adenosine triphosphate
BA	Benzylaminopurine
CAX	Cation/proton exchangers
CDF	Cation diffusion facilitator
cDNA	Complementary DNA
CDS	Coding DNA sequence
Chl a	Chlorophyll a
Chl b	Chlorophyll b
CIM	Callus induction medium
DAB	3,3'-diaminobenzidine
DW	Dry weight
EC100	100% effective concentration
EDTA	Ethylen-diamine tetraacetate
EFSA	European Food Safety Authority
FDA	Fe deficiency-induced anemia
FMOC	Fluorenylmethyl chloroformate
FRD	Ferric reductase defective
FRO	Ferric reduction oxidase
FW	Fresh Weight
gDNA	Genomic DNA
GFP	Green fluorescent protein
GSH	Glutathione
HMA	Heavy metal ATPase
HPLC	High pressure liquid chromatography
ICP-OES	Inductively-coupled plasma optical emission spectrometry

IRT	Iron-regulated transporter
LA-ICP-MS	laser ablation-inductively coupled plasma-mass spectrometry
LB	Lysogeny Broth
LC	La Calamine
LPP	Low-phosphate/low-pH
MA	Mugineic acid family
Min	Minutes
MIT	Mitochondrial iron transporter
MS	Murashige and Skoog
MTP	Metal transport protein
NA	Nicotianamine
NAA	1-Naphthaleneacetic acid
NAAT	Nicotianamine aminotransferase
NAS	Nicotianamine synthase
NBT	Nitroblue tetrazolium
NRAMP	Natural resistance-associated macrophage protein
O₂⁻	Superoxide
OD₆₀₀	Optical Density
OsLCT	<i>Oryza sativa</i> L Cd transporter
PCR	Polymerase Chain Reaction
PC	Phytochelatin
PSI	Photosystem I
PSII	Photosystem II
PTWI	Provisional tolerable weekly intake
QRT-PCR	Quantitative real time polymerase chain reaction
QTL	Quantitative trait loci
RIM	Root induction medium
RNA	Ribonucleic acid
RNAi	RNA interference
ROS	Reactive oxygen species
Rpm	Revolutions per minute s
SD	Standard deviation
SIM	Shoot induction medium
TAIR	The <i>Arabidopsis thaliana</i> Information Resource

V/V	Volume/volume
W/V	Weight/volume
WHO	World Health Organization
WT	Wild type
YEP	Yeast Extract Peptone
YSL	Yellow stripe-like
ZIF1	Zinc induced facilitator
ZIP	Zinc-regulated transporter, iron-regulated transporter-like protein
ZNT	Zinc transporter
ZRT	Zinc-regulated transporter
μPIXE	Micro Particle-induced X-ray emission

1. Introduction

1.1 Plant mineral nutrition

1.1.1 Mineral nutrients roles in plant growth and development

Plants require an assortment of inorganic mineral elements to ensure successful growth and development. These minerals are based on the relative amounts required by plants divided into two classes. The first group is called macronutrients. They are generally found in plants at concentrations between 1,000 and 40,000 $\mu\text{g g}^{-1}$ of dry tissue weight, including nitrogen (N), potassium (K), calcium (Ca), magnesium (Mg), phosphorus (P) and sulfur (S). The second group is micronutrients, which are required by plants at concentrations between 0.1 and 150 $\mu\text{g g}^{-1}$ of dry tissue weight. They include iron (Fe), zinc (Zn), manganese (Mn), copper (Cu), boron (B), chlorine (Cl), molybdenum (Mo) and nickel (Ni) (White and Brown, 2010). These minerals plus the elements carbon (C), hydrogen (H) and oxygen (O), are essential for the growth of all plants. Additional minerals, such as aluminum (Al), cobalt (Co), sodium (Na), silicon (Si) and selenium (Se) are not required by all plants but can promote plant growth and even may become essential for particular taxa but their widespread essentiality has yet to be established (Pilon-Smits et al., 2009). Amongst mineral nutrients, there are several transition metals like Iron, copper, zinc, and manganese which are essential nutrients for plants (Clemens et al., 2002; Morrissey et al., 2009; Olsen and Palmgren, 2014). These metals are associated with functionality of metal-dependent proteins (metalloproteins) which represent about one third of the proteins of a typical cell (González-Guerrero et al., 2016). According to a search of protein descriptions in The *Arabidopsis thaliana* Information Resource (TAIR) database, the largest number of proteins are functionally associated with zinc (1272), followed by copper (108), iron (106), manganese (12), and nickel (4) (Krämer et al., 2007). Following Fe, the second most widely used transition metal in living systems is Zn (Clemens, 2010). It is predicted that the Zn metalloproteome comprises around 5 to 6% of prokaryotic and about 9% of the eukaryotic proteome (Andreini et al., 2009). Zn has a key structural and catalytic role in a large number of enzymes (Hall and Williams, 2003). RNA polymerase, superoxide dismutase, alcohol dehydrogenase and carbonic anhydrase are well-known examples of Zn-dependent enzymes in plants and the structural Zn-finger domains in proteins known for their implications in the regulation of different signal transduction pathways as well as developmental processes and programmed cell death (Laity et al., 2001; Palmer and Guerinot, 2009; Li et al., 2013). Under biological conditions, as a result of its complete d-shell of electrons, Zn is redox-stable and never undergoes changes in redox state, so it cannot directly participate in electron transfer reactions, for example in electron transport chains as Fe and Cu do (Sinclair and Krämer, 2012). Fe can alternate between two oxidation states, Fe³⁺ or ferric iron and Fe²⁺ or ferrous iron, which makes it a good candidate to transfer electrons (Thomine and Vert, 2013). Fe serves as a cofactor in metal containing proteins of the photosynthetic electron transport chain and is essential for chlorophyll biosynthesis (Krämer et al., 2007; Jeong et al., 2008; Roschttardt et al., 2009; Nouet et al., 2011; Roschttardt et al., 2013; Schmidt et al., 2014). Fe is present in proteins of the photosystem I (PSI), photosystem II (PSII), the cytochrome *b₆f* complex and ferredoxin (Raven et al., 1999). Copper (Cu) and manganese (Mn) also exist in different ionic states and are suitable cofactors for redox reactions in cells (Nouet et al., 2011). Mn ions participate in photosynthetic O₂ evolution in PSII and Cu is an integral component of certain electron transfer proteins such as plastocyanin, the most abundant Cu-containing protein in plants. It transfers

Introduction

electrons from the cytochrome *b₆f* complex to PSI (Raven et al., 1999; Hall and Williams, 2003; Palmer and Guerinot, 2009).

1.1.2 Zn and Fe deficiency and toxicity in plants

Plants, like humans and any other organism, rely on sufficient Zn and Fe supply to drive cellular functions. *A. thaliana* is estimated to express approximately 2400 different Zn proteins (Broadley et al., 2007). Across nature, total cellular zinc concentration required for optimum growth is about 0.1 to 0.5 mM in bacteria, yeast, and mammalian cells and 0.3 to 3 mM in plant cells (Eide, 2006). Shoot Zn concentration in plants vary but is usually in the range of 50 to 100 $\mu\text{g g}^{-1}$ dry biomass (Broadley et al., 2007). Plants show Zn deficiency symptoms at shoot concentrations below a minimum of 15 to 20 $\mu\text{g g}^{-1}$ dry biomass (Hänsch and Mendel, 2009). Zn deficiency is the most widespread micronutrient deficiency problem in soils especially in arid and semi-arid regions, as a result of low organic matter and soil moisture as well as high levels of pH and CaCO_3 (Cakmak, 2008; Alloway, 2008). Maize, rice and wheat as the major staple cereal crops are affected by Zn deficiency. Maize is highly susceptible to Zn deficiency and Zn fertilizers have to be used routinely where the crop is grown (Brown, 2008). Most of the rice is produced in flooded soils in the paddy system in which half of it is affected by Zn deficiency (Alloway, 2008). Wheat is less sensitive to Zn deficiency than rice and maize, but it is still severely affected by Zn deficiency in calcareous soils (Cakmak et al., 1999). The most common visible symptoms of Zn deficiency in plants include reduced biomass production, poor floral fertility, leaf chlorosis, increased shoot branching, early senescence of older leaves and increased production of reactive oxygen species (Sinclair and Krämer, 2012). However, because of its strong potency in displacing other divalent metal ions from catalytic sites of enzymes plus the increased stability of Zn-ligand complexes, Zn in excess amounts is able to replace other metals or bind to undesired proteins and enzymes resulting in their inactivation and consequently inhibiting plant growth and reducing crop yield (White and Brown, 2010). Zn contamination hardly ever reach toxic levels in mammals but its toxicity is a major environmental concern in other organisms (Sinclair and Krämer, 2012). Zinc toxicity symptoms in plants usually become visible at a leaf concentration of more than 300 $\mu\text{g g}^{-1}$ Zn on a dry biomass (Deinlein et al., 2012), although some crops may even show symptoms at just over 100 $\mu\text{g g}^{-1}$ Zn (Shanmugam et al., 2011). The first symptom of Zn toxicity in plants is general chlorosis of younger leaves with necrotic lesions on leaves in severe cases and eventually entire leaf death. This chlorosis may be a secondary effect caused by an induced deficiency of Fe^{2+} or Mg^{2+} , which might be displaced by Zn^{2+} due to the similar ionic radii of these three elements. In roots, Zn toxicity is apparent as a reduction in the growth of the main root, fewer and shorter lateral roots and a yellowing of roots (Boardman and McGuire, 1990). Fe is the sixth most abundant element in the universe and the fourth most abundant in the earth's crust (López-Millán et al., 2013) but is only slightly soluble especially under alkaline and aerobic conditions. Plants grown under low Fe availability, such as in calcareous soils, often suffer from Fe deficiency, which causes decreases in vegetative growth and marked yield and quality losses (Kobayashi and Nishizawa, 2014). It is well known that Fe deficiency causes chlorosis in plants (Haydon et al., 2012). Up to 80% of the cellular Fe in Leaf cells is found in chloroplasts (Hänsch and Mendel, 2009). Fe starvation particularly affects photosystem I (PSI), which contains 12 Fe atoms per monomer and reduces the efficiency of photosynthesis. It causes chlorosis in leaves due to reduction in chlorophyll synthesis as Fe-requiring steps are indispensable in chlorophyll biosynthesis (Tottey et al., 2003). Also in plants, mitochondrial respiration rate and ATP production decrease when a shortage of Fe in respiratory complexes occurs (Nouet et al., 2011). Excessive Fe is also harmful, as ionized Fe^{2+}

Introduction

catalyzes the generation of reactive oxygen species (ROS) in the Fenton reaction where H_2O_2 is converted to highly reactive hydroxyl radicals, promoting oxidative stress (Kobayashi and Nishizawa, 2014). Reactive oxygen species react rapidly with DNA, proteins and lipids, causing oxidative damage (Ercal et al., 2001). Therefore a tightly controlled homeostatic network consisting of uptake, import, translocation and sequestration is needed in order to ensure sufficient supply to metal-requiring sites and to prevent metal accumulation at toxic levels in tissues, cells, or subcellular compartments (Clemens et al., 2002; Olsen and Palmgren, 2014).

1.2 Molecular mechanism of Zn and Fe uptake and distribution in plants

1.2.1 Zn uptake and sequestration

Transition metal ions such as Zn and Fe are essential for healthy plant growth. However, an excess of free metal ions is toxic to cells. Therefore plants have mechanisms for metal homeostasis including metal uptake, metal partitioning to plant organs and different cell types, subcellular localizations of metals and their delivery to metalloproteins, metal storage and remobilization while maintaining metals within cells or subcellular compartments below levels that cause toxic symptoms (Clemens, 2001; Clemens et al., 2002). Since the dynamic range of optimal Zn and Fe internal concentrations at which plants are unaffected by deficiency or toxicity is very narrow, the metal homeostatic network must be precise, specific and highly regulated (Krämer et al., 2007; Sinclair and Krämer, 2012). Like most other metal ions, the concentrations of Zn ions in soil are subject to major fluctuations. In soil, Zn is either bioavailable in soluble form in the soil solution and plants are able to take it up or is insoluble and either precipitated or adsorbed to clays, hydrous oxides and organic matter (Reichman, 2002). Insoluble Zn comprises more than 90% of soil Zn and is unavailable for plant uptake. The bioavailability of zinc in soil strongly depends on soil pH and with increasing pH, due to higher adsorption and precipitation of metal in alkaline environments the bioavailability of Zn decreases (Broadley et al., 2007). Because Zn ions cannot diffuse across cell membrane, root Zn acquisition from soil into the symplast of the epidermis requires an efficient plasma membrane metal transport system, which spans the membrane to facilitate the movement of Zn. Therefore, plants evolved specific zinc transporters to transport Zn into cytoplasm (Li et al., 2013). In recent years, a number of metal transporters have been identified in plants, including the P1B-ATPase family, zinc-regulated, iron-regulated transporter (ZRT-IRT)-like proteins (ZIP) family, natural resistance-associated macrophage protein (NRAMP) family, and cation diffusion facilitator (CDF) family (Hall and Williams, 2003; Krämer et al., 2007; Sinclair and Krämer, 2012; Li et al., 2013). ZIP protein family members are known to have a major role in the eukaryotic zinc transport. Most ZIP proteins have eight predicted transmembrane domains and similar predicted topologies with the N- and C-termini of the protein located on the extracellular side of the membrane. They also have a long histidine-rich cytoplasmic loop between the third and the fourth-transmembrane domain predicted to have metal binding function (Eide, 2006; Guerinot, 2000). The genome of *A. thaliana* encodes 15 ZIP transporters (Colangelo and Guerinot, 2006). The first member of the ZIP family identified in *A. thaliana* was IRT1, which primarily is described as an Fe^{2+} transporter and later complementation and uptake studies in yeast revealed that IRT1 is able to transport quite broad range of metals including Zn^{2+} , Mn^{2+} , Cd^{2+} and Co^{2+} (Eide et al., 1996; Clemens et al., 2002). The *IRT1* gene is expressed in the plasma membrane of root epidermal cells and is involved in Zn^{2+} uptake (Olsen and Palmgren, 2014). Since *irt1* plants are able to survive without the addition of excess Zn, it

Introduction

is likely that Zn is primarily taken up into the plant via other transporters. Functional expression of *A. thaliana* ZIP1, ZIP2, ZIP3, ZIP4, ZIP7, ZIP11, and ZIP12 genes in the *zrt1/zrt2* double mutant yeast showed they are all capable of mediating cellular Zn²⁺ uptake across the plasma membrane and restore zinc-limited growth fully or partially to this mutant (Clemens et al., 2002; Eide, 2006; Guerinot, 2000; Pence et al., 2000). Expression analysis revealed that the transcripts of 10 members of the ZIP family, *AtZIP1* to *AtZIP5*, *AtZIP9* to *AtZIP12*, and *AtIRT3*, were increased in response to Zn deficiency, suggest that they may enhance Zn²⁺ acquisition under Zn deficiency status in *A. thaliana* (Krämer et al., 2007). The *AtZIP4* gene in particular is strongly induced upon shortage in zinc supply (Talke et al., 2006). *AtZIP1*, *AtZIP2* and *AtZIP5* are assumed as good candidates for Zn²⁺ uptake as they localize to the plasma membrane of root epidermal cells and their transcription increases under Zn deficiency (Sinclair and Krämer, 2012). This assumption has been questioned as functional studies with plants mutated in *AtZIP1* and *AtZIP2* genes suggested a role of them in Zn²⁺ root to shoot transport (Milner et al., 2008). However, the specific role of ZIP genes and their contribution to plant Zn acquisition remain poorly understood. Zn is taken up across the plasma membrane of root cells predominantly as a free ion (Guerinot, 2000). After uptake in the cytoplasm of plant cells, neutral pH increases non-specific binding of Zn to biomolecules, which severely restricts its free mobility. To prevent non-specific cytoplasmic binding and precipitation of Zn, it is actively sequestered into vacuoles via vacuolar membrane proteins. In *A. thaliana* Zinc Induced Facilitator 1 (ZIF1), Metal Transport Protein 1 (MTP1) and MTP3 and Heavy Metal ATPase 3 (HMA3) are known vacuolar membrane proteins (Arrivault et al., 2006; Haydon and Cobbett, 2007a; Morel et al., 2009). It was hypothesized that metal chelator nicotianamine (NA) could contribute to Zn translocation by increasing the symplastic mobility of Zn²⁺ (Weber et al., 2004). Intracellularly Zn-NA complexes formation demonstrated in NAS-expressing *Schizosaccharomyces pombe* cells (Trampczynska et al., 2010) and finally, it was shown that Zn-NA complexes diffuses between root cells via plasmodesmata toward the xylem (Deinlein et al., 2012). It has been shown that ZIF1 transports NA into root cell vacuoles and overexpression of *ZIF1* in *A. thaliana* plants enhanced vacuolar accumulation of NA which leads to strongly enhanced vacuolar Zn accumulation and consequently immobilization and decrease of root-to-shoot transport of Zn (Haydon et al., 2012). This sequestration of NA and Zn in root vacuoles of *ZIF1*-overexpressing *A. thaliana* plants support the hypothesis that Zn-NA complexes in addition to neutral to slightly alkaline pH of the cytosol also exist at the acidic pH of the vacuoles (See Fig 1.1).

1.2.2 Xylem Zn loading and unloading

Zn effluxes into the xylem from the symplast for long distance transport by the heavy metal transporters AtHMA2 and AtHMA4, which localize to the plasma membrane of the root and shoot vasculature (Hussain et al., 2004). It also has been suggested that NA mediates loading of Zn into the xylem and the lower root NA synthesis results in decreased NA and Zn concentrations in xylem exudates of *A. halleri* (Cornu et al., 2015). In *A. thaliana*, *nas4x* mutant which failed in NA production, accumulated more Zn than the wild type in all root tissues and had the lower Zn concentrations in the xylem sap and in the shoots, which indicates depressed xylem loading of Zn in the *nas4x* mutant (Persson et al., 2016). How does NA mediate xylem loading and which transporters are involved in this process is not yet understood. Inside the xylem, Zn flux into the shoot is mass- flow driven. Since in the xylem pH is slightly acidic (around pH 5.5), Zn chelates to low-molecular-weight ligands to prevent Zn retention by metal-binding components of the surrounding cell walls or uptake into cells via Zn²⁺ transporters (Sinclair and Krämer, 2012). Inside

Introduction

the shoot, Zn must be taken up from the xylem across the plasma membrane of adjacent cells. However, little is known about the mechanism and proteins involved in this process.

1.2.3 Phloem Zn loading and unloading

Loading of zinc into the phloem typically takes place in leaves. The transporter proteins involved in zinc transport out of leaf mesophyll cells to the slightly alkaline phloem are not yet known. Transport proteins of the Yellow Stripe-Like (YSL) family, which presumably transport complexes of Zn-NA across membranes are assumed to play a role in transporting zinc into the phloem (Olsen and Palmgren, 2014). The mechanisms involved in phloem unloading and post-phloem movement of zinc and its distribution between cells are not well understood. Generally, metals are often compartmentalized or sequestered in photosynthetically inactive tissues, like the epidermis, or in storage tissues, such as trichomes and old leaves. Trichomes and epidermal cells, in particular, accumulate the highest Zn concentrations (Clemens et al., 2002; Lin and Aarts, 2012). However, cell vacuoles are believed to make the largest contribution to the storage of excess Zn in leaves. The remobilization of Zn from photosynthetic source tissues to sink tissues, i.e., meristems, developing leaves, inflorescences and developing seeds occurs via mass flow driven transport in the phloem. The higher pH inside the phloem sap provides optimal conditions for NA molecule to reach the highest affinity and stability (Stephan et al., 1996). Glutathione, cysteine and NA have been found in the phloem of *Brassica napus* (Mendoza-Cozatl et al., 2008) and it was shown that Zn-NA complex occurs in the phloem sap of rice (Nishiyama et al., 2012). The chelation of Zn is particularly important for long-distance transport inside the phloem (Sinclair and Krämer, 2012).

1.2.4 Fe uptake

Despite its high abundance in the soil, Fe is not readily available for plant uptake in the presence of oxygen as it precipitates in the form of insoluble ferric oxides. This process is enhanced at alkaline pH especially on calcareous soils. It is estimated that 30% of the world's arable land is too alkaline for optimal plant growth. Plants grown under low Fe availability often suffer from Fe deficiency, which reduces growth, crop yield and quality (Morrissey and Guerinot, 2009). In excessive Fe conditions, ionized Fe^{2+} catalyzes the generation of reactive oxygen species in the Fenton reaction where H_2O_2 is converted to highly reactive hydroxyl radicals, promoting oxidative stress that leads to deleterious effects such as blackening of root tips, inhibition of root growth and necrotic spots on the leaves (Pich et al., 2001; Kobayashi and Nishizawa, 2014). To acquire enough Fe while avoiding toxicity, plants tightly control uptake, utilization, and storage in response to environmental availability. Higher plants have evolved two different strategies for Fe acquisition from the rhizosphere, sequential acidification- reduction-transport strategy (strategy I) which is used by non-graminaceous plants, whereas graminaceous plants use the chelation strategy named strategy II. (Curie et al., 2001; Nozoye et al., 2011; Kobayashi and Nishizawa, 2012; Schmidt et al., 2014). These two strategies were previously considered mutually exclusive, but some exceptions are reported in which strategy II plants possess partial strategy I uptake systems and vice versa (Curie et al., 2009; Verbruggen and Hermans, 2013). The first step of Fe acquisition by non-graminaceous higher plants is rhizosphere acidification, which includes excretion of proton and phenolic compounds from the roots to the rhizosphere to help increase the solubility of ferric ions or support the reducing capacity of ferric Fe on the root surface. In *A. thaliana* (H^+ -ATPASE2) AHA2 is mainly responsible for excretion of protons to the rhizosphere and its expression is increased in Fe deficiency conditions (Palmer and

Introduction

Guerinot, 2009; Morrissey and Guerinot, 2009; Fourcroy et al., 2014). The second step of Fe acquisition by non-graminaceous plants is the extracellular reduction of ferric to ferrous iron at the root surface. In *A. thaliana* the ferric reductase (FRO2) is mainly responsible for it. The subsequent uptake of the generated ferrous ions across the root plasma membrane into epidermal cells is the final step of Fe acquisition by non-graminaceous plants and the protein mainly responsible for this process in *A. thaliana* is IRT1. (Vert et al., 2002; Krämer et al., 2007; Curie et al., 2009). IRT1 localizes to the plasma membrane of the root epidermis and is required for seedling survival and the lethal phenotype of *irt1* mutants can be rescued by addition of exogenous Fe, indicating that its primary role is in uptake of Fe (Vert et al., 2002; Henriques et al., 2002). *FRO2* and *IRT1* are upregulated in response to Fe deficiency (Vert et al., 2002; Shanmugam et al., 2011). The graminaceous strategy II is based on the solubilization of ferric precipitates through the secretion of strong Fe(III)-chelating phytosiderophores of the Mugineic Acid (MA) family (Curie et al., 2009; Nozoye et al., 2011). The MAs are synthesized through a conserved pathway from S-adenosyl-L-methionine which includes three sequential enzymatic reactions mediated by nicotianamine synthase (NAS), nicotianamine amino transferase (NAAT), and deoxymugineic acid synthase (DMAS) (Takahashi et al., 2003; Mizuno et al., 2003; Kim et al., 2005; Nozoye et al., 2011). The MAs secreted into the rhizosphere solubilize Fe(III), and the resulting Fe(III)-MA complexes are primarily taken up into root symplast by the yellow stripe 1 (YS1) and YSL transporters (Curie et al., 2001; Krämer et al., 2007; Klatte et al., 2009) (See Fig 1.1).

1.2.5 Fe Translocation

Following uptake from the soil Fe has to be distributed to plant tissues and organs by cell-to-cell and long distance transport. Due to the poor solubility and high reactivity of Fe, it is translocated in chelated forms to accomplish proper control of redox states between the ferrous and ferric forms (Hell and Stephan, 2003). Fe translocation in plants involves various steps, including radial transport across the root tissues, which must include symplastic transport to pass through the Casparian strip; xylem loading, transport, and unloading; xylem-to-phloem transfer; phloem loading, transport, and unloading; symplastic movement toward the site of demand; and re-translocation from source or senescing tissue (Kobayashi and Nishizawa, 2012). It has been shown that chelators such as citrate and NA are involved in the translocation of Fe from the root to the young leaves (Kobayashi and Nishizawa, 2012). NA has an important role in maintaining the mobility of metal ions in vascular tissues and between cells (Pich et al., 2001). NA is synthesized from three molecules of S-adenosyl-L-methionine via NAS. The genome of *A. thaliana* contains four NAS isoforms that originated from a single ancestral NAS gene. *AtNAS1* and *AtNAS4* are expressed both in roots and in shoots whereas *AtNAS2* is exclusively expressed in root tissue and *AtNAS3* only in leaves (Klatte et al., 2009). NA can form complexes with several divalent metal cations including Fe^{2+} and Zn^{2+} (Kim et al., 2005; Haydon and Cobbett, 2007b; Trampczynska et al., 2010; Clemens et al., 2013b). Citrate is the preferred Fe chelator at the typical pH values of 5.5 in xylem, while in the phloem sap with the pH value of 7, NA is supposed to be the main candidate for Fe chelation (Rellán-Alvarez et al., 2008; Grillet et al., 2014). Because the xylem and phloem consist of dead and living cells, respectively, xylem loading is assumed to require efflux transporters, whereas phloem loading would require influx transporters. In *A. thaliana* Ferric reductase defective 3 (FRD3) facilitates citrate efflux into the xylem. The *frd3* mutant shows Fe deficiency and leaf chlorosis, and despite enhanced root Fe uptake and localization to the central vascular cylinder tissues in mutant plants, Fe cannot be transported to aerial parts. The *frd3* mutant demonstrates that citrate plays a dominant role in xylem Fe transport (Green and

Introduction

Rogers, 2004; Durrett et al., 2007). Due to the neutral pH values inside the phloem the likelihood of the stable Fe-NA complex formation is very high (Reichman and Parker, 2002; Weber et al., 2006; Rellán-Alvarez et al., 2008). It is believed that NA is important in transporting Fe from the phloem to sink organs (Schuler et al., 2012). Lack of NA production in the quadruple mutant *nas4x-2* led to severe symptoms such as leaf interveinal chlorosis and sterility (Schuler et al., 2012). Phenotypes of the mutant are predominantly attributable to defects in the distribution (cell-to-cell movement and long-distance transport) of Fe and possibly because NA-mediated delivery of Fe to the growing pollen tube is defective (Schuler et al., 2012). In *A. thaliana* *YSL1*, *YSL2*, and *YSL3* are expressed in vascular bundles and are induced by Fe deficiency (Didonato et al., 2004; Schaaf et al., 2005; Curie et al., 2001, 2009). These YSL transporters presumably mediate the lateral movement of Fe-NA from the xylem and phloem and are involved in reproduction and seed Fe loading (Schuler et al., 2012).

1.2.6 Subcellular transport of Fe

Excess accumulation of Fe in the cytosol leads to cytotoxicity within the plant cells. Inside the cell, Fe mostly has been compartmentalized into different organelles, such as chloroplasts, mitochondria, and vacuoles. In most plant cell types, quantitatively the largest sinks for Fe are chloroplasts and mitochondria. Chloroplast Fe accounts for 70–90% of cellular Fe in mesophyll cells (Thomine and Vert, 2013; Roschzttardtz et al., 2013). In *A. thaliana* the FRO7 ferric chelate reductase protein is required for Fe import into the chloroplast. The *fro7* mutants show 33% less Fe content in chloroplasts compared to wild type plants and display severe chlorosis in alkaline soil (Jeong et al., 2008). *A. thaliana* *YSL4* and *YSL6* transporters control Fe release from the chloroplast and knocking out of both *YSL4* and *YSL6* led to Fe being trapped in the chloroplasts of the *ysl4 ysl6* double mutants which greatly reduces the plants ability to cope with excess Fe (Divol et al., 2013). Mitochondria represent a significant Fe sink within cells, as Fe is required for the proper functioning of respiratory chain protein complexes. Mitochondria are a site of Fe-S cluster synthesis, and possibly heme synthesis as well (Jain and Connolly, 2013). Little is known about how Fe is transported into and out of mitochondria. Ferric chelate reductase might be involved in mitochondrial Fe transport because FRO8 has been identified in the mitochondrial proteome (Nouet et al., 2011). In rice, mitochondrial Fe transporter (MIT) is responsible for Fe transport to the mitochondria and is essential for rice growth and development. The homozygous knockout of *MIT* gene resulted in a lethal phenotype, whereas the knockdown lines exhibit impaired growth despite abundant Fe accumulation in shoots but less Fe in mitochondria (Bashir et al., 2011; Vignani et al., 2015). The vacuole in plants generally functions as a metal pool to avoid toxicity. In *A. thaliana* the tonoplast membrane vacuolar Fe transporter 1 (VIT1) that effluxes Fe from the cytosol into the vacuole is responsible for vacuolar Fe storage in cells (Kim et al., 2006). The *vit1* mutant shows abolished vacuolar Fe localization especially in seeds and poor germination and seedling development in iron limiting conditions like alkaline soils (Kim et al., 2006; Roschzttardtz et al., 2009). In contrast to VIT1, AtNRAMP3 and AtNRAMP4 are metal influx transporters mediating the remobilization of Fe from vacuolar stores during germination, and their expression is upregulated under Fe starvation (Thomine et al., 2003; Lanquar et al., 2005). In Arabidopsis a double *nramp3 nramp4* mutant fails to remobilize Fe stored the vacuolar globoids and provide sufficient Fe to sustain plant growth and consequently mutants exhibit germination arrest (Lanquar et al., 2005; Roschzttardtz et al., 2009). AtNRAMP3 and AtNRAMP4 play a role in iron mobilization from vacuole at other stages in plant life (Lanquar et al., 2005).

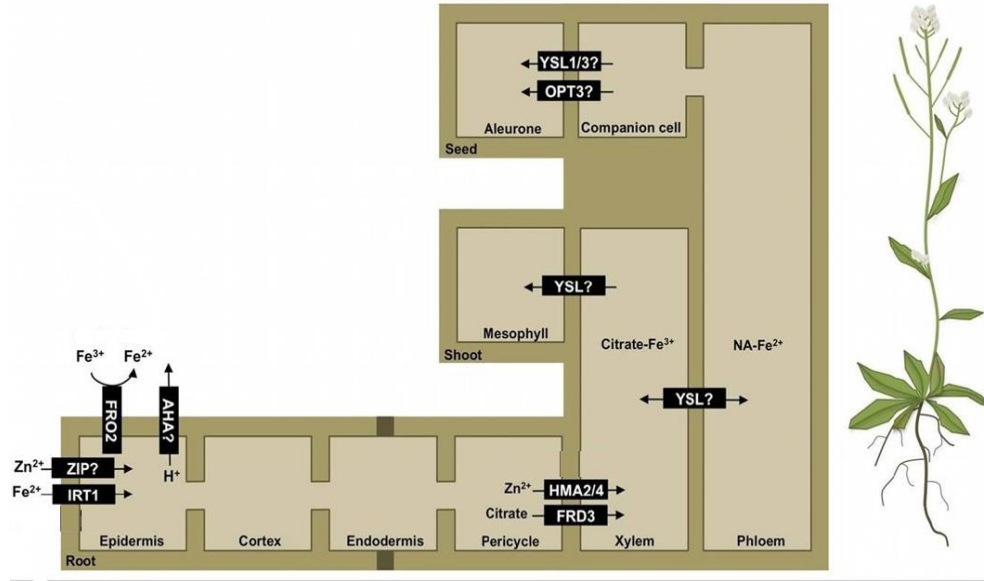


Fig. 1.1 Intercellular Zn and Fe transport in *A. thaliana*

Shown are transporters contributing to Zn and Fe homeostasis in *A. thaliana*. IRT1 and ZIP transporters mediate uptake of Fe and Zn from soil into the root symplast in the epidermis. FRO2 reduces Fe and AHA contributes to increased metal uptake by acidification of the soil. Metals can then travel through the symplastic and apoplastic paths to the vasculature, bypassing the Casparian strip on the endodermis. Transporters of the HMA family and the citrate effluxer are involved in loading Zn and Fe into the xylem. In the xylem, metals move to the shoot through the transpiration stream. YSLs protein thought to be involved in unloading metals from xylem into the shoot and translocate metals to the phloem, where they can then be delivered to the seed (Palmer and Gueriot, 2009).

1.2.7 Zn and Fe deficiency in Human

Zn deficiency is a widespread condition, an estimated 17.3% of the world's population is at risk of inadequate zinc intake (Wessells and Brown, 2012). Zn deficiency has a strong impact on public health and child mortality. Growth retardation, impaired neurology, decreased immune function and enhanced susceptibility to diarrhea are among the reported symptoms due to zinc deficiency, particularly in regions of the world where the population relies primarily on cereal diets (Das and Green, 2013; Sinclair and Krämer, 2012). Fe deficiency represents the most widespread nutritional disorder in the world and affects more than 2 billion people worldwide (Wu et al., 2002; McLean et al., 2009). Young children, pregnant and postpartum women commonly affected by Fe deficiency. According to a World Health Organization (WHO) report, Fe deficiency increases the risk of pregnancy and perinatal mortality especially in developing countries <http://www.who.int/whr/2002/en/>. In the developing world, the prevalence of phytate in the plant-based diet is believed to contribute to the high rate of Fe deficiency-induced anemia (FDA) (USA National Institute of Health, Office of Dietary Supplements, <http://ods.od.nih.gov/factsheets/Iron-HealthProfessional/>).

1.3 Nonessential toxic heavy metals uptake in plants

Heavy metals are a set of chemical elements, mostly belonging to the transition metals. They include essential and most non-essential metals as well as highly toxic elements like lead (Pb) and cadmium (Cd) (Rascio and Navari-Izzo, 2011). Among heavy metals, most toxic to humans are

Introduction

elements that resemble essential minerals, such as Hg, Pb, and Cd. Toxicity of these metals is not limited to humans or animals, but affects many organisms, including plants. During their life cycle, plants acquire essential and beneficial elements from the soil, but because their selectivity is imperfect, they can also take up nonessential elements when those elements are bioavailable (Weber et al., 2004). Some of these inadvertently accumulated elements are highly toxic, the most important ones being arsenic (As), lead (Pb), mercury (Hg), and cadmium (Cd) (Järup, 2003). Highly toxic heavy metals like Cd cause damage to plants at far lower exposure concentrations than essential metals by altering major plant physiological and metabolic processes (DalCorso et al., 2008). Most of the bioavailable Cd in the environment is of anthropogenic origin. It is generally associated with Zn and Pb mineral deposits, and extraction of these metals has been the main source of Cd pollution (Clemens et al., 2013a). Application of sewage sludge and phosphate fertilizers also resulted in Cd increase (UNEP, 2010) and consequently, the circulation of Cd through the soil and water led to an important environmental issue that involves high risks for human health (Clemens et al., 2013a). Cd is present only in inorganic form and in one oxidation state Cd^{2+} . Its bioavailability depends largely on soil conditions and because of the formation of insoluble CdS in anaerobic soils, it is more available in aerobic soils than in anaerobic soils (Clemens and Ma, 2016).

1.3.1 Cadmium toxicity in human and plants

The primary targets of Cd toxicity are not known, but its chemical similarity with essential elements, particularly Zn, Ca and Fe causes deregulating the homeostasis of these elements or displacement from proteins and therefore, it can damage different cellular structures and a variety of tissues and organs (Verbruggen et al., 2009a; Clemens and Ma, 2016). Kidney is the main organ affected by chronic Cd exposure and toxicity. Cd also increases mortality and a range of diseases, including various types of cancer and renal damage and osteoporosis (Johri et al., 2010). Cd interferes with Ca metabolism in mammals, causing Itai-itai disease upon severe exposure (Inaba et al., 2006). Cd can replace Zn in proteins and is classified as carcinogen and because of long-term bioaccumulation in the human body can cause disease even in low-dose exposure far below than the thresholds (Clemens and Ma, 2016; Person et al., 2013). In the nonsmoking general population, more than 90% of Cd exposure is due to the ingestion of cereals, vegetables, and other plant-derived food (Clemens and Ma, 2016). Worldwide data on human Cd exposure level revealed that many populations have a Cd intake above the provisional tolerable weekly intake (PTWI) levels which according to the European food safety authority (EFSA) should be lowered from 5.8 to 2.5 μg per kilogram of body weight, a level that is near the average intake around the world (Clemens et al., 2013a). Since the major sources for the Cd intake in humans are cigarettes and food, one of the most efficient ways to decrease Cd exposure would be the reduction of Cd accumulation in the tissues of the main edible plants, especially rice and wheat. Mechanistic understanding of the pathways of Cd accumulation can aid the development of crop plants with strongly reduced toxic element content, thereby limiting human health risks (Clemens and Ma, 2016). Due to the high solubility in water, Cd distributes rapidly in the environment which prompts its accessibility for plant root uptake and transport to reproductive organs (DalCorso et al., 2010; DalCorso et al., 2008). Root uptake of Cd prominently depends on soil pH, the rhizosphere and presence of organic acids. For instance, it has been reported that Cd uptake in corn was lower in acid soils with high organic matter content (DalCorso et al., 2008). As Cd enters roots, it causes damage in nucleoli and inhibition of RNA synthesis and consequently roots are likely to experience damage. Cd also inhibits the nitrate reductase activity in the shoots and reduces the absorption of nitrate and its transport from roots to

Introduction

shoots (Hernandez et al., 1996). It inhibits the root ferric reductase enzyme leading to ferrous Fe deficiency which seriously affects photosynthesis (di Toppi and Gabbrielli, 1999). Cd toxicity symptoms have been investigated more than any other metal toxicity symptoms in plenty of plant systems under various conditions. In many studies an extremely high Cd²⁺ concentrations has been applied and therefore, the documented symptoms of toxicity are consequences of acute Cd stress (di Toppi and Gabbrielli, 1999). The evident symptoms of high Cd toxicity in plants are leaf rolling and chlorosis, water uptake imbalance and stomatal closure (Clemens, 2006b), reduction in growth of roots and stems, dehydration and necrosis (Verbruggen and Hermans, 2013). Cd causes damage in the photosynthetic apparatus, in particular the light harvesting complex II, the photosystems II and I and decrease in total chlorophyll and carotenoid content (di Toppi and Gabbrielli, 1999). In several plant species, Cd toxicity at cellular level causes chromosomal abnormalities and alteration of cell cycle and division. High mutation rate and deformed embryos have been observed in *A. thaliana* plants exposed to Cd (DalCorso et al., 2010).

1.3.2 Cadmium toxicity at the cellular level

At cellular and molecular levels, Cd inactivate or denature proteins by direct interaction with them or displacement of essential metal ions from specific binding sites of proteins, led to chromosomal aberrations, alterations of the cell cycle and cell division (Schutzendubel and Polle, 2002; Villiers et al., 2011; Chen et al., 2015). Because of similarity of Cd with essential elements, in particular Zn, but also Ca and Fe, it displaces other metals from protein active sites (e.g. Fe, Zn, Ca) or binds sulfhydryl groups of structural proteins and enzymes, leading to misfolding and inhibition of their activity (DalCorso et al., 2008; Villiers et al., 2011). It is suggested that displacement of Ca²⁺ by Cd²⁺ in calmodulin, an important protein in cellular signaling, might result to the inhibition of calmodulin-dependent phosphodiesterase activity which led to toxicity during the early phases of radish seed germination (Rivetta et al., 1997). Cd²⁺ ions by substituting Zn in Zn-dependent and Zn-binding molecules affect many metabolic enzymes, transcription factors and many Zn-dependent processes (Qu and Zhu, 2006). As an indirect evidence it was shown that presence of Cd²⁺ led to up-regulation of putative Zn²⁺ uptake genes (Weber et al., 2004). Heavy metals can enter into the nucleus, bind to nucleic acids, and modify both transcription and DNA replication; they can also affect microtubule assembly–disassembly, thereby arresting cell division (Gamalero et al., 2009). It has been shown that Cd inactivates DNA mismatch repair by blocking the ATPase activity of proteins in yeast cells (Banerjee and Flores-rozas, 2005) and it was suggested that the same mechanisms may also act in plants (Verbruggen et al., 2009a). Cd aggravates the production of reactive oxygen species (ROS), which are extremely harmful to cells at high concentrations and can pose a threat to cells by causing peroxidation of lipids, oxidation of proteins, damage to nucleic acids, enzyme inhibition, activation of programmed cell death pathway and ultimately leading to death of the cells (Petrov et al., 2015). It is well known that high concentrations of heavy metal ions can stimulate ROS bursts inside the cell (Hossain et al., 2012). Since Cd has a high affinity for thiol groups (R-SH), it reacts with glutathione molecules, which are the major cellular antioxidant in plants (Jozefczak et al., 2012). The reduced form of the glutathione molecule, GSH, has an important role in handling Cd stress because of its tripartite role in metal detoxification as a metal chelator, a cellular antioxidant, and as a ROS signaling component (Lin and Aarts, 2012). Among heavy metals Cu can directly generate ROS, whereas Cd is a redox inactive metal and can only generate ROS indirectly by inducing the expression of lipoxygenases in plant and increasing oxidation of polyunsaturated fatty acids (Cho and Seo, 2005). Accumulation of ROS inside the cell leads to alteration of the plant nutrient and

Introduction

water status and reduction of plasma membrane H⁺-ATPase activity (Gamalero et al., 2009). Higher plants always produce ROS during different metabolic processes mainly in cellular organelles like chlorophyll, mitochondria, and peroxisomes (Faller et al., 2005; Sharma et al., 2012). In chloroplasts, the main sources of ROS production are the PSI and PSII. Cd replaces the Ca²⁺ and Mn²⁺ ions in the PS II reaction center, thereby inhibiting the reaction of PS II leads to the disconnection of the electron transport in the chlorophyll. It also inhibits the electron flow on the reducing side of PS I. Thereby, decrease of the NADP supply occurring limits the CO₂ fixation rate by blocking the Calvin cycle, reduces electron coupling efficiency and lead to the formation of superoxide anion O₂^{•-} from O₂ (Sharma et al., 2012). After accumulation of ROS in these organelles, it react with lipids, proteins, nucleic acids and pigments causing toxic effects and oxidative eruption (Cuypers et al., 2010).

1.4 Molecular mechanism of Cd uptake, chelation, sequestration and translocation in plants

1.4.1 Cd uptake

Cd is a toxic element with no biological functions in plants and therefore; it is assumed plants have no specific mechanisms to take it up from soil. In plants, Cd uptake occurs through essential or beneficial elements transporters (Clemens, 2006b). It was suggested that in *A. thaliana*, IRT1 mediates Cd uptake from the environment. According to one study, after growing plants for 8 days in the presence of 20 μm Cd²⁺, root Cd content in *irt1* mutants was 5-fold lower than the wild type plants (Vert et al., 2002). The functional complementation analysis in yeast showed that ZNT1 in *Noccea caeruleascens*, a homolog of *AtZIP4*, mediates high affinity Zn²⁺ uptake as well as low affinity Cd²⁺ uptake (Pence et al., 2000). In rice, OsIRT1 and OsIRT2 are among the major Fe²⁺ transporters induced under Fe deficiency. Functional complementation analysis in yeast showed their Cd uptake activity in low Fe conditions (Nakanishi et al., 2006). OsNRAMP1 is a rice plasma membrane protein and its overexpression resulted in a slight increase in Cd content of rice leaves (Takahashi et al., 2011). The *OsNRAMP5* constitutively expresses in the roots of rice and encodes a plasma membrane protein in the distal side of exodermis and endodermis cells. OsNRAMP5 has been identified as the major Cd uptake transporter in rice. Knockout of *OsNRAMP5* resulted in the lower Cd content in root and shoot, corresponding with a 5-fold lower short-term roots Cd uptake compared to the wild-type plants (Sasaki et al., 2012). It is suggested that OsNRAMP5 is responsible for most of the rice Cd uptake under different Fe supply conditions and OsIRTs and OsNRAMP1 play only a minor role in Cd uptake from the soil (Sasaki et al., 2012) (See Fig 1.2).

1.4.2 Cd chelation and sequestration

Inside the cell, Cd must be detoxified. The strategy for detoxification of Cd is the synthesis of high-affinity binding sites to suppress binding of Cd²⁺ ions to physiologically important functional groups. Because the high reactivity of Cd²⁺ ions with thiol groups (-SH), the Cys-containing peptides glutathione (GSH) and phytochelatins (PCs) (Clemens, 2006a), when Cd enters plant cells, it forms stable complexes with GSH, PCs and MTs (Verbruggen et al., 2009a). PCs are synthesized from GSH by PC synthase, an enzyme ubiquitously present in plants (Clemens, 2001). Cytosolic PC–Cd complexes are subsequently sequestered into vacuoles by ATP-binding cassette (ABC) transporters, ABCC1 and ABCC2, which can enhance Cd tolerance and accumulation through vacuolar

Introduction

sequestration of PC–Cd (Park et al., 2012; Lin and Aarts, 2012). A defect in PC synthesis is tantamount to a loss of cytosolic buffering and causes strong hypersensitivity to Cd as shown in *A. thaliana cad1* mutants, which contains wild-type levels of GSH yet are PC deficient and consequently Cd hypersensitive (Clemens, 2001). It was shown that root Cd is largely bound by PC and other thiols (Clemens et al., 2013a). While most Cd is chelated before its transport to the vacuole, Cd²⁺ can possibly be also directly transported into the vacuoles by cation/proton transporters. Cation/proton exchangers (CAXs) are a class of secondary energized ion transporter that primarily efflux Ca²⁺ from the cytosol into the vacuole (Cheng et al., 2005). Some CAX isoforms have broad substrate specificity, providing the ability to transport trace metal ions such as Cd²⁺ (Pittman and Hirschi, 2016). AtCAX2 and AtCAX4 have Cd/H⁺ antiport activity, and overexpression of them in tobacco enhance Cd transport into root tonoplast and Cd accumulation in roots of plants exposed to Cd (Korenkov et al., 2007). The *A. thaliana* HMA3 is located in the vacuolar membrane and over expression of a the functional HMA3 in *A. thaliana* increases Cd tolerance and leaf Cd accumulation 2 to 4-fold (Morel et al., 2009). It was shown that HMA3 is the major locus responsible for the variation in leaf Cd accumulation among world-wide *A.thaliana* accessions and reduced function of HMA3 caused by a nonsense mutation and polymorphisms elevated leaf Cd accumulation (Chao et al., 2012). In rice, functional OsHMA3 specifically limits translocation of Cd from the roots to the seeds and leaves by selectively sequestering Cd into the root vacuoles (Ueno et al., 2010). In *A. thaliana* Cd can be released from the vacuole into the cytosol by AtNRAMP3 and AtNRAMP4 (Thomine et al., 2003; Oomen et al., 2009). AtNRAMP3 disruption as well as AtNRAMP3 and AtNRAMP4 over expression in *A. thaliana* mildly alter Cd sensitivity without modifying the total Cd content (Lanquar et al., 2004; Thomine et al., 2000). The double *nramp3 nramp4* mutant exhibits hypersensitivity to Cd (Oomen et al., 2009), presumably as a result of a general defect of metal remobilization from the vacuole, which may be required for Cd tolerance. Zinc or Cd hypersensitivity was not observed in single *nramp3* or *nramp4* mutants In *A. thaliana* (Thomine et al., 2000). *A. thaliana* transgenic plants overexpressing AtNRAMP6 were hypersensitive to Cd, although plant Cd content remained unchanged. Consistently, a null allele of AtNRAMP6, named *nramp6-1*, was more tolerant to Cd toxicity (Cailliatte et al., 2009).

1.4.3 Cd translocation

As soon as Cd enters the roots, due to its high mobility and water solubility, it can reach the xylem via an apoplastic and symplastic pathway, in its free or complexed forms (Salt et al., 1995). Since efflux of metal cations (including Cd²⁺) into the xylem occurs against the plasma membrane potential, it needs to be energized (Clemens and Ma, 2016). However, no Cd-specific efflux transporter has been found in plants, which indicates that Cd efflux always accompanies the transport of other metals by action of efflux transporters with higher affinities for other metals than Cd (Lin and Aarts, 2012). In both *A. thaliana* and *A. halleri* the prominent Zn efflux transporters HMA2 and HMA4 are mainly responsible for the xylem loading of Cd (Hanikenne et al., 2008; Kum et al., 2009). The transport form of Cd in the xylem is generally ionic Cd (Clemens and Ma, 2016). Once loaded into the xylem, Cd spreads throughout the entire plant following the water flow (DaCorso et al., 2008). How Cd is loaded into the phloem is not totally clear especially in dicots, and the responsible transporters have not been identified (Khan et al., 2014). In rice OsLCT1 is a strong candidate mediating the intervascular transfer of Cd into the phloem. The *OsLCT1* is strongly expressed in nodes during grain ripening and RNAi-mediated knockdown of *OsLCT1* resulted in 50% less Cd in grains without affecting the concentration of essential micronutrients or grain yield

Introduction

(Uraguchi et al., 2011). Overall, the molecular mechanisms underlying the Cd distribution in dicots are unknown (Clemens and Ma, 2016) (See Fig 1.2).

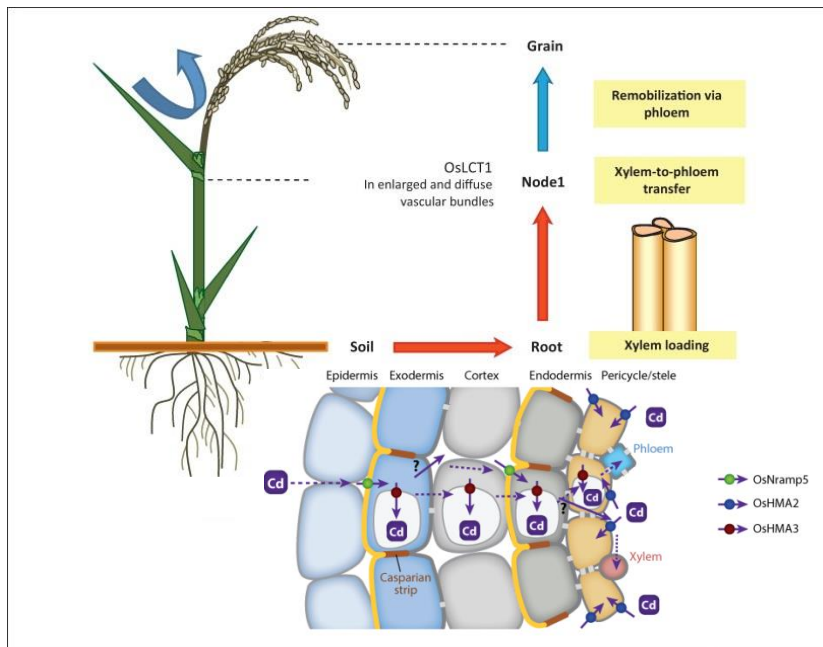


Fig. 1.2 Mechanisms underlying Cd uptake and translocation in rice

Shown are transporters involved in uptake and root to shoot translocation of Cd in rice roots. OsNrap5 is responsible for the transport of Cd from the apoplast into the root cells. OsHMA3 sequesters Cd into vacuoles, and OsHMA2 is hypothesized to facilitate Cd translocation via the phloem. Dashed arrows indicate possible passive diffusion of Cd. The Cd transporter OsLCT1 mediates xylem-to-phloem transfer in node 1. Blue arrows indicate the remobilization of Cd to the grain through the phloem. Modified from (Clemens et al, 2013a; Clemens and Ma, 2016).

1.5 Metal hyperaccumulation and hypertolerance in plants

Unlike humans and animals, plants cannot move from heavy metal contaminated areas and therefore they must evolve ways to deal with the heavy metal contamination in their direct environment (Lin and Aarts, 2012). On metal contaminated soils, a range of plants have evolved physiological mechanisms which enable them not only to survive in metal rich soils but to sequester and store exceptionally high levels of metals and metalloids in their above-ground tissues. These plants are called hyperaccumulators (Baker, 1981; Baker and Brooks, 1989). The tolerance towards high levels of metals apparently enables metal hyperaccumulator plants to colonize metalliferous soils which either naturally are metal-rich, or have been contaminated by human activities (Baker and Brooks, 1989). Metal hyperaccumulators are able to accumulate exceptionally high concentration of metals or metalloids such as Ni, Zn, Cd, Se, As, Mn, and Pb, in their leaves without showing metal toxicity symptoms. Different suggested thresholds for hyperaccumulation for each respective accumulated metal are listed in table 1 (Krämer, 2010). Hyperaccumulators are able to accumulate high concentrations of trace element in the shoot even when the concentration in the soil is low, with the consequence of a shoot/root concentration ratio above one (Verbruggen et al., 2013). The strategy most commonly associated with metal tolerance in plants is metal exclusion

Introduction

strategy that restricts soil metal availability via complex formation and limits metal movement into shoots (Baker, 1981; Audet and Charest, 2008; Krämer, 2010). Excluder plants secrete organic acids such as oxalate, malate and citrate in the rhizosphere to prevent the uptake of toxic metals like Cd in roots despite their elevated concentration in the soil (Pinto et al., 2008; Zhu et al., 2011). The second strategy is the tolerance strategy, which relies on quarantine and detoxification of metals in a controlled way, which allow plants not just to survive high metal exposure but also to accumulate metals to extremely high concentrations (Lin and Aarts, 2012). Plants using tolerance strategy either take up metals and accumulate them in the roots and are called heavy metal-tolerant non-hyperaccumulator, or accumulate exceptional concentrations of trace elements and preferentially transport them to the above-ground parts which are called heavy metal-hypertolerant hyperaccumulator plants (Jaffre et al., 1976; Pollard et al., 2002). Figure 1.1 summarizes the four types of plant responses to Zn and Cd exposure.

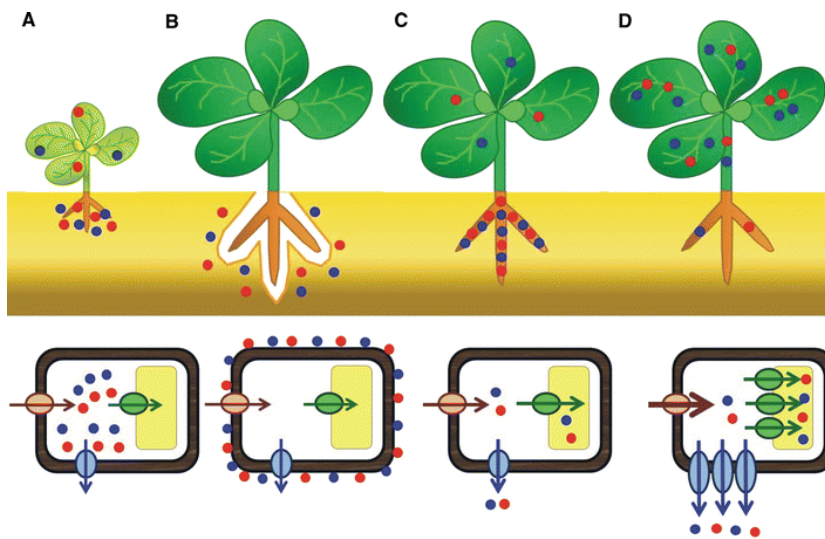


Fig. 1.3 Plants differently respond to Zn and Cd exposure

(A) Heavy metal-sensitive plants cannot keep metals out of their roots or prevent transport to the shoot and suffer from the toxic effects of metals. (B) Heavy metal-resistant excluder plants keep metals outside the roots or take care of rapid efflux in case toxic metals have entered root cells. (C) Heavy metal-tolerant non-hyperaccumulator plants can sequester heavy metals into root vacuoles, preventing translocation to shoots. (D) Heavy metal-hypertolerant hyperaccumulator plants actively take metals up through the root and largely load into xylem, translocate from root to shoot and safely sequester them in vacuoles of aerial parts. Modified from (Lin and Aarts, 2012).

1.5 .1 Metal hypertolerant and hyperaccumulator species

Hyperaccumulation is found in a rare class of plants (approximately 450 plant species, representing 0.2 % of the angiosperms) table 1 (Krämer, 2010; Verbruggen et al., 2009b). So far, ca. 390 taxa of Ni hyperaccumulators have been reported in 42 families (Verbruggen et al., 2009b) About 15 plant taxa possess the remarkable ability to accumulate Zn in their aboveground tissues to levels of 100-fold higher than normally found in plants or any other organism in nature (Kramer, 2010). Cd hyperaccumulation has been reported in 5 taxa to date. Zn and Cd hyperaccumulation are reported in the Brassicaceae, in particular in the genus *Thlaspi*, *Noccaea* section and the species *A. halleri* (Verbruggen et al., 2009b). *A. halleri* is a perennial, self-incompatible and highly outcrossing ,

Introduction

stoloniferous plant with a highly disjunctive distribution between Europe and the Far East (Wasowicz et al., 2016). It is able to both colonize zinc- and cadmium-polluted sites and concentrate large amounts of these metals in foliar tissues (Pauwels et al., 2012; Meyer and Verbruggen, 2012). It is a pseudometallophyte species that is able to grow on both metal-polluted and non-polluted soils (Bert et al., 2002). *A. halleri* and its nontolerant and non-accumulator sister species *A. thaliana* diverged 3.5–5.8 million years ago and still share 94% sequence identity within coding regions (Becher et al., 2004). *A. halleri* is a model plant for Zn/Cd hyperaccumulation studies, and because of its close phylogenetic relationship with *A. thaliana*, it has been successfully used in molecular investigation of metal hyperaccumulation and hypertolerance. Dissection of molecular mechanisms involved in metal hyperaccumulation may provide suitable information for several biotechnological aspects. Decontamination of metal polluted soils using plants, i.e. phytoremediation (Kim et al., 2005), and the engineering of staple crops to accumulate additional nutrients in edible parts, i.e. biofortification are among the interesting plant biotechnological aspects (Clemens et al., 2002; Chiang et al., 2006; Palmgren et al., 2008; Zhao and McGrath, 2009). The major part of the available data on Zn and Cd hyperaccumulation mechanisms originated from microarray analysis, molecular genetics and genomic analyses, collected using this species and *N. caerulea* (Hanikenne et al., 2011; Krämer, 2010; Verbruggen et al., 2009b). The *Auby* and *Langelsheim* are two *A. halleri* metallicolous populations originate from France and Germany respectively. They have been the only populations that were used for molecular studies. So far *Agrobacterium*-mediated stable transformation, as a key-tool for functional analysis of candidate genes has been applied only in individuals from Langelsheim population that were collected from the Harz mountains in Germany (Deinlein et al., 2012; Hanikenne et al., 2008).

Element	Critical deficiency level ($\mu\text{g g}^{-1}$)	Critical toxicity level ($\mu\text{g g}^{-1}$)	Hyperaccumulation concentration criterion ($\mu\text{g g}^{-1}$)		Taxa (No.)	Families (No.)
			To date	Newly suggested		
Lead	n. r.	0.6-28	>1,000	-	14	7
Cadmium	n. r.	6-10	>100	-	5	2
Zinc	15-20	100-300	>10,000	>3,000	15	6
Manganese	10-20	200-3,500	>10,000	-	10	6
Nickel	0.002-0.004	10-50	>1,000	-	390	342
Copper	1-5	20-30	>1,000	>300	35	15

Table 1.1 Hyperaccumulation of trace elements in land plants

The critical concentrations for deficiency and toxicity represent the concentrations in which the maximum dry matter yield is decreased by more than 10% (Bouma, 1983; Ohki, 1984). n.r.: no known requirement Modified from Krämer (2010).

1.5.2 Molecular mechanisms of metal hyperaccumulation and hypertolerance

Metal hyperaccumulators show differences in aspects of their metal homeostasis compared to *A. thaliana*. The common set of changes include, (i) enhanced metal uptake in roots, (ii) efficient symplastic metal transport towards the vasculature together with reduced vacuolar sequestration in roots, (iii) increased rate of root-to-shoot metal transport, and (iv) efficient metal distribution mechanisms and high vacuolar storage capacity in shoots (Maestri et al, 2010; Hanikenne and

Introduction

Nouet, 2011). These physiological changes in metal hyperaccumulators are associated with an altered expression of sets of genes involved in the transport and homeostasis of the metals. Various aspects can be changed: increases in the expression level of genes, expression of genes in a new tissue or at different developmental stages, or copy number variation for metal transporter genes (Talke et al., 2006; Hanikenne et al., 2008; Suryawanshi et al., 2016). Combination of transcriptomic, genetic and functional approaches allowed the identification of a set of metal transporter and metal chelator biosynthesis genes, which constitutively are more highly expressed in *A. halleri* and *N. caerulescens* compared to their non-accumulator relative *A.thaliana*. They are listed in table 1.2 (Hanikenne and Nouet, 2011). The metal transporter genes more highly expressed in hyperaccumulators encode predominantly ZIPs, HMAs, MTPs, and NRAMPs proteins. Enhanced Zn root uptake may be driven by overexpression of members of the ZIP family (Krämer et al., 2007). Several member of the ZIP family genes are overexpressed in *A. halleri* and *N. caerulescens* (Becher et al, 2004; Talke et al., 2006; van de Mortel et al., 2006; Weber et al., 2004, 2006). High endogenous TcZNT1 expression is associated with increased Zn uptake in the roots of *N. caerulescens* (Pence et al., 2000). Enhanced Zn uptake into root cells of *A. halleri* is possibly driven by ZIP4 and to some extent by IRT1, ZIP3, ZIP9, and ZIP10. Yet the contribution of individual members to the Zn uptake from the soil solution to the root has not been determined (Verbruggen et al., 2009b). Enhanced root metal uptake mediated by the ZIP family proteins is likely to be a factor necessary but not sufficient for hyperaccumulation (Krämer et al., 2007). Overexpression of *IRT3* and *ZIP4* in roots of *A. halleri*, seems to be a secondary consequence of increased HMA4 activity and related to the root sensing of Zn starvation due to efficient loading of Zn into the xylem (Hanikenne et al., 2008). Different from several other members of the ZIP family, in *A. thaliana* *ZIP6* transcript level is not upregulated under Zn deficiency (Becher et al., 2004; Talke et al., 2006; Filatov et al., 2006). Compared to *A. thaliana*, *ZIP6* is more highly expressed in the shoots and roots of *A. halleri* under low and high Zn conditions. *ZIP6* expression is predominant in the shoots of *A.halleri*, where it is believed to be involved in xylem unloading and cellular uptake of the metals Zn and Fe (Becher et al., 2004; Talke et al., 2006; van de Mortel et al., 2006; Weber et al., 2004, 2006). In *A. halleri*, *ZIP6* appears to be a duplicated gene with no metal-dependent transcript regulation (Becher et al., 2004; Talke et al., 2006). In a microarray study comparing *A. halleri*, *A. lyrata* and Zn-accumulating and non-accumulating F3 progeny of a cross between these two species, the data filtering procedure combined with the lack of Zn-dependent transcriptional regulation of *ZIP6* resulted in identification of *ZIP6* as a candidate gene for Zn hyperaccumulation (Filatov et al., 2006). The quantitative trait locus (QTL) analysis in *A. halleri* under conditions of Cd excess using an interspecific *A. halleri* x *A. lyrata* F2 population suggested the peaks of one of the Zn accumulation responsible QTLs, Znconc-3, colocalized exactly with genetic markers defined within the coding sequence of *ZIP6*, suggesting its role in Zn hyperaccumulation (Willems et al., 2010). A yeast complementation study showed that *AtZIP6* is only able to transport Mn and failed to complement Fe, Zn and Cu uptake mutants (Milner et al., 2013). Expression of the *N. caerulescens* accession La Calamine (LC) ortholog of the *AtZIP6* gene, *TcZNT6-LC*, in *A. thaliana* specifically enhanced the Cd sensitivity with shorter root length in transgenic plants without changing metal profiles in roots and shoots, *zip6* T-DNA insertion loss-of-function mutant showed no phenotype (Wu et al., 2009).

Introduction

Name	Protein family	Putative substrate	<i>A. halleri</i>	<i>N. caerulescens</i>
Cellular uptake				
<i>ZIP4</i>	ZIP	Zn, (Cu?)	Root	Root-shoot
<i>ZIP6</i>	ZIP	Zn	Root-shoot	Shoot
<i>ZIP9</i>	ZIP	Zn	Root	Root
<i>ZIP10</i>	ZIP	Zn	Root	Root
<i>IRT3</i>	ZIP	Zn, Fe	Root	Root-shoot
Xylem loading/unloading				
<i>HMA4</i>	P-type ATPase	Zn, Cd	Root-shoot	Root-shoot
<i>FRD3</i>	MATE	Citrate	Root-shoot	Root
Vacuolar sequestration				
<i>HMA3</i>	P-type ATPase	Zn, Cd	Root-shoot	Root-shoot
<i>MTP1</i>	CDF	Zn	Root-shoot	Root-shoot
<i>MTP8</i>	CDF	Mn	Root-shoot	Root
Remobilization from the Vacuole				
<i>NRAMP3</i>	NRAMP	Fe, Mn, Cd	Root-shoot	Root
Endomembrane transport				
<i>MTP11</i>	CDF	Mn	Shoot	Shoot
Transport of metal chelates				
<i>YSL3</i>	YSL	NA-metal	-	Root-shoot
<i>YSL5</i>	YSL	NA-metal	-	Root-shoot
<i>YSL6</i>	YSL	NA-metal	Shoot	-
<i>YSL7</i>	YSL	NA-metal	-	Root-shoot
Synthesis of metal ligands				
<i>NAS1</i>	NAS	SAM	Root-shoot	Shoot
<i>NAS2</i>	NAS	SAM	Root	Root
<i>NAS3</i>	NAS	SAM	Shoot	-
<i>NAS4</i>	NAS	SAM	Root-shoot	Shoot

Table 1.2 Metal homeostasis genes that are highly expressed in *A. halleri* and *N. caerulescens*

Common set of metal homeostasis genes that are more highly expressed in both *A. halleri* and *N. caerulescens* compared to non-accumulator relatives. Adapted from Hanikenne and Nouet (2011). Bold identifies genes that are the focus of this thesis.

Among the vacuolar metal transporters, *MPT1*, *MTP8* and *HMA3* expression in the roots and shoots of *A. halleri* and *N. caerulescens* is higher than *A. thaliana* suggesting they may be important for heavy metal homeostasis and tolerance (Talke et al., 2006; Verbruggen et al., 2009b; Ueno et al., 2011). The *MTP1* is believed to be responsible for detoxification of Zn and partially for the Zn hypertolerance trait in *A. halleri* (Dräger et al., 2004; Shahzad et al., 2010). Little is known about the proteins encoded by *MTP8* of *A. halleri* or *N. caerulescens*. *MTP8* does not appear to be Zn-responsive in either species, but is upregulated in response to Cd and Cu in roots and to Cu in shoots of *A. halleri* (Talke et al., 2006; van de Mortel et al., 2006). AhHMA3 is able to confer partial Zn tolerance to a Zn-sensitive yeast strain, suggesting it might be involved in regulation of cellular Zn status in *A. halleri* (Talke et al., 2006). *NRAMP3* displays constitutively high expression in *A. halleri* compared to *A. thaliana* (Weber et al., 2004). Microarray data indicated that, in *N. caerulescens*,

Introduction

NRAMP3 expression is generally higher than in *A. thaliana* (van de Mortel et al., 2006). Expression of *TcNRAMP3*, the closest homologues to *AtNRAMP3* in *N. caerulescens*, in Cd and Zn hypersensitive *A. thaliana nramp3nramp4* mutants fully restored the sensitivity to Zn and Cd to the wild-type levels (Oomen et al., 2009). It remains to be investigated whether the NRAMP3 transporter highly expressed in *A. halleri* has a direct role in Zn or Cd hyperaccumulation or ensures the maintenance of Fe or Mn homeostasis (See Fig 1.4).

NAS genes are among those genes showing constitutively higher expression in *A. halleri* compared to *A. thaliana*. So far four *A. halleri* orthologs of the *A. thaliana* *NAS* genes have been identified (Weber et al., 2004). *AhNAS1* and *AhNAS4* are expressed in both roots and leaves, while *AhNAS2* is expressed predominantly in roots and *AhNAS3* almost exclusively in leaves (Deinlein et al., 2012). Transcript levels of *AhNAS2*, *AhNAS3*, and *AhNAS4* are substantially higher in *A. halleri* compared to *A. thaliana* (Becher et al., 2004; Talke et al., 2006; Weber et al., 2004). Similar results were reported for *N. caerulescens* in which *NAS1*, 3 and 4 are more expressed than in *A. thaliana* (van de Mortel et al., 2006). Constitutively high expression of *AhNAS2* in *A. halleri* roots which is associated with elevated NA concentrations (Weber et al., 2004), regardless of metal accumulation ability of different populations is a species-wide trait (Deinlein et al., 2012). Suppression of *AhNAS2* expression by RNAi resulted in reduced root NA concentrations which correlated with a significant reduction of root-to-shoot Zn translocation (Deinlein et al., 2012). Speciation analysis showed that NA is a major Zn(II) ligand in *A. halleri* roots besides thiols which enhances symplastic mobility of Zn(II) and is therefore a key molecule for the translocation of Zn within plants (Deinlein et al., 2012). Suppression of *AhNAS2* expression by RNAi had no effect on Zn and Cd tolerance but rendered plants Ni-hypersensitive (Cornu et al., 2015). *AhNAS4* expression in roots is much lower than that of *AhNAS2*. However, that might be due to a more localized expression only in particular root cells. There are indications that *AhNAS4* is up-regulated at low Zn conditions (Talke et al., 2006). *A. thaliana* *NAS4* is up-regulated in roots under conditions of Fe deficiency (Long et al., 2010). The effect of *AhNAS4* on metal hyperaccumulation has to be investigated. A key gene in metal hyperaccumulation overexpressed in *A. halleri* is *HMA4* (Courbot et al., 2007; Talke et al., 2006). In *A. halleri*, *HMA4* was hypothesized to be explaining major QTLs of Zn and Cd tolerance (Courbot et al., 2007; Willems et al., 2007) and of Zn and Cd hyperaccumulation (Willems et al., 2010). Suppression of *AhHMA4* in *A. halleri* resulted in loss of the Zn/Cd hypertolerance and hyperaccumulation ability, including increased sensitivity to high Zn and Cd exposure and reduced root to shoot translocation efficiency. These phenotypes demonstrated that elevated expression of *AhHMA4* is indeed essential for Zn hyperaccumulation and Zn hypertolerance (Hanikenne et al., 2008). The *FRD3* gene also is highly expressed in roots of *A. halleri* relative to *A. thaliana* (Talke et al., 2006). *A. thaliana* *FRD3* facilitates root-to-shoot Fe transport and apoplastic Fe distribution in leaves (Durrett et al., 2007; Green and Rogers, 2004). In *A. halleri*, *FRD3* may have a similar function or contributes to the hyperaccumulation of Zn or Cd, or even mediate the homeostasis of a different metal. Members of the YSL proteins are highly expressed in *A. halleri* and *N. caerulescens* and it is believed they are involved in the long-distance transport of metals through and between vascular tissues (Talke et al., 2006; Gendre et al., 2006). So far, there is no direct evidence for their contribution to the metal hyperaccumulation. In a F2 population derived from an *A. lyrata* x *A. halleri* cross three QTLs for Cd hypertolerance were detected (Courbot et al., 2007). The major QTL co-localized with the *HMA4* gene, whose contribution to Cd hypertolerance was directly shown in RNAi lines with reduced *AhHMA4* transcript levels (Hanikenne et al., 2008). Recently, the second major QTL for Cd tolerance, *Cdtol2*, was fine-mapped and *AhCAX1* was identified as a candidate gene. Interestingly, *Cdtol2* is Ca-dependent and only is detectable in the presence of low Ca²⁺

Introduction

concentrations (Baliardini et al., 2015). Experiments with *A. thaliana* showed that CAX1 can indeed contribute to Cd tolerance (Baliardini et al., 2015). However, direct evidence for the involvement of CAX1 in *A. halleri* Cd hypertolerance is missing.

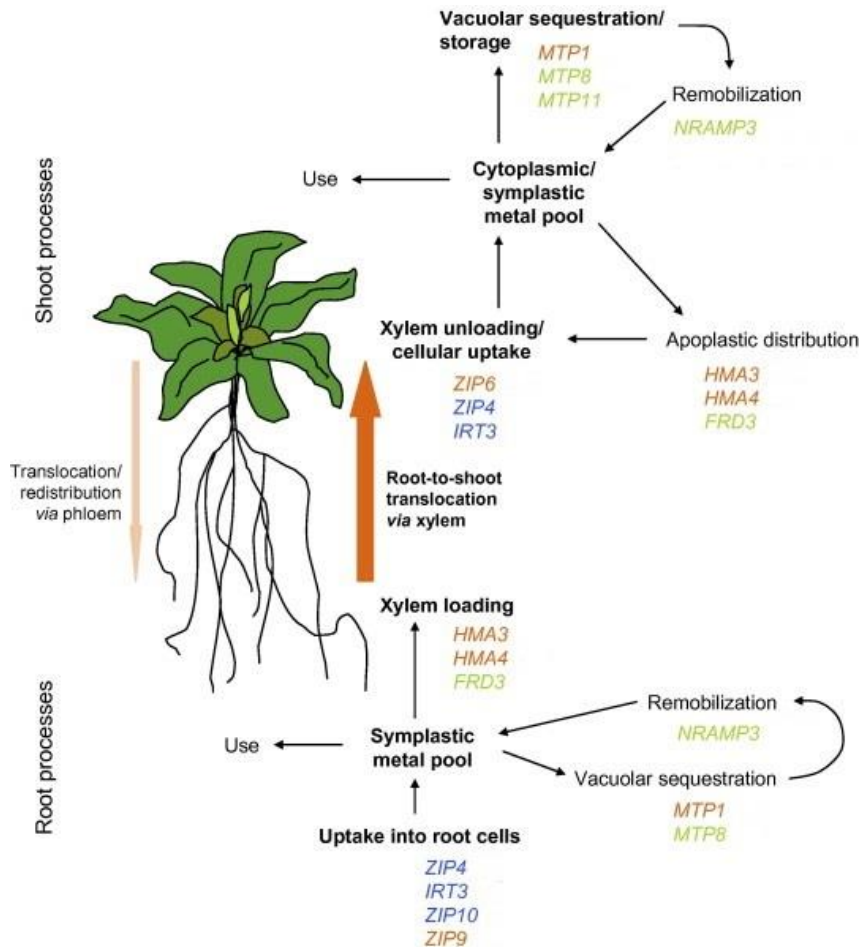


Fig. 1.4 The common core set of metal transporter genes highly expressed in *A. halleri* and *N. caerulescens* and their role in hyperaccumulation and hypertolerance

Shown are genes with significantly higher transcript levels in both *A. halleri* and *N. caerulescens* than in a related non-accumulator species and their putative physiological functions for the encoded transporter proteins. Blue color denotes Zn-responsive genes with increased transcript levels upon Zn deficiency; orange color denotes Zn homeostasis genes with mainly constitutive expression; green color denotes genes that are more likely to be involved in the homeostasis of metal ions other than Zn. Modified from Krämer et al., (2007).

1.6 The aim of this study

The aim of this thesis is the characterization of the roles of the candidate genes *NAS4*, *ZIP6*, *CAX1* and *NRAMP3* in heavy metal hyperaccumulation and hypertolerance in *A. halleri*. RNA interference technology is used for silencing each of these genes separately. Generated RNAi lines are characterized using Q-RT PCR technique. Since no knockout mutant collections are available for hyperaccumulator *A. halleri*, analysis of RNAi lines provides a direct tool for dissecting the molecular mechanisms of hyperaccumulation and hypertolerance. Initially, the RNAi lines were hydroponically cultivated in defined media supplemented with different metal concentrations and depending on

Introduction

the gene, which was suppressed; different RNAi plants were grown in normal soil, alkaline soil or metalliferous and non-metalliferous soils. Elemental profiles of roots and shoots of RNAi plants were compared with wild-type and the role of each gene in metal hyperaccumulation and hypertolerance in *A. halleri* was characterized.

2. Materials and methods

2.1. Generation of *A. halleri* RNAi lines

2.1.1 Generation of *AhNAS4*, *AhZIP6*, *AhNRAMP3* and *AhCAX1* RNAi constructs

In order to generate the *A. halleri* RNAi lines, the gateway-compatible binary vectors bearing RNAi constructs were generated with short Polymerase Chain Reaction (PCR) fragments of *AhZIP6*, *AhNRAMP3*, *AhCAX1* and *AhNAS4*. The RNA was extracted from homogenized leaf or root material of *A. halleri* wild-type with Trizol (Life Technologies GmbH, Darmstadt) according to the manufacturer's instructions. 500 ng of DNase-treated RNA was used for cDNA synthesis with PrimeScript RT Master Mix (TaKaRa BIO INC, Shiga, Japan). For generation of the RNAi constructs, a short fragment (263-417 bp) of cDNA of the gene of interest, from more specific and conserved region of gene, was PCR-amplified using the corresponding primers are listed in table (2:1). Primers were designed by using Primer 3 online tool (<http://primer3.sourceforge.net/>). Each fragment was cloned into pENTR/D-Topo (Invitrogen) using the Gateway LR Clonase enzyme mix (Invitrogen) and the fragment was subcloned into pHELLSGATE8 (Helliwell et al., 2002). The *A. tumefaciens* strain (GV3101) was transformed with *A. halleri* RNAi constructs and used to transform wild-type plants.

Gene	Forward-Primer (5'-3')	Reverse-Primer (5'-3')	Amplicon Length
<i>AhZIP6</i>	TACCGGAAGCGTTTGAGTCT	caccTGCAGCAATCAAAGGTCAATG	398 bp
<i>AhNRAMP3</i>	ACGACAGAAATACCGAGTTCAAG	caccTACCAGTAATAGTGCTGCTTTG	263 bp
<i>AhCAX1</i>	GATCGAGTAGAGAACTGAGACTTG	caccCTGTCAAAAAGCTGACTCG	286 bp
<i>AhNAS4</i>	TAATTTGGTAGCAGCTCGTTTGG	caccGAACAGTTACTCGAGATCCG	417 bp

Table 2.1 Primers were used for RNAi constructs of *AhNAS4*, *AhZIP6*, *AhNRAMP3* and *AhCAX1*

2.1.2 *A. halleri* transformation

For transfer into sterile culture cuttings with 4 to 6 leaves were washed with distilled water. Surface sterilization was achieved by sequential dipping into 70% (v/v) ethanol for 10 seconds, in 0.5% H₂O₂ solution for 3 minutes and finally in 3% H₂O₂ solution for 1 min. Cuttings were then rinsed with distilled water for 30 seconds, gently blotted dry and placed on MS medium in transparent plastic boxes. Before the preparation of explants, plants were grown for 6 to 8 weeks with a standard photoperiod at 25°C. For callus induction fragments of leaves, stems or roots were placed on callus induction medium (CIM) according to (Vera-Estrella et al., 2009). (MS medium + 10 mg l⁻¹ thiamine hydrochloride, 0.5 mg l⁻¹ nicotinic acid, 0.5 mg l⁻¹ pyridoxine hydrochloride, 1 mg l⁻¹ 2,4-dichlorophenoxy D, 0.05 mg l⁻¹ 6-benzylaminopurine) and incubated for 3 to 4 weeks in darkness at room temperature before selection of friable calli for transformation. *A. tumefaciens* strain GV3101 transformed with the constructs described above was grown in liquid (LB) medium supplemented with selection antibiotics as a first culture and subsequently 750 µl of this culture was transferred to

Materials and methods

50 ml (YEP) medium supplied with selective antibiotics as second culture. The second cultures harvested and re-suspended in MS medium. *A. tumefaciens* cells and calli were co-incubated for 10 min. After removal of *A. tumefaciens* suspension, blotting and 5 minutes of drying, calli were placed back onto CIM and incubated for 3 more days in darkness at room temperature. Calli were then transferred onto shoot induction medium (SIM; MS medium + 1 mg l⁻¹ 6-benzylaminopurine, 0.5 mg l⁻¹ α -naphthaleneacetic acid) (Hanikenne et al., 2008) with 125 mg l⁻¹ ticarcillin disodium/clavulanate potassium (Duchefa) to suppress *A. tumefaciens* growth and incubated at 25°C with 16 h light (45 μ mol m⁻² s⁻¹)/ 8 h dark. After 7 days, selection of transgenic cells was initiated with the addition of kanamycin to 25% of the final concentration (50 mg l⁻¹). Each week calli were transferred to fresh plates. Selection strength was augmented by increasing the kanamycin concentration to 50%, then 75% and finally 100% in week 5. Ticarcillin disodium/clavulanate potassium concentration was maintained at 125 mg l⁻¹ throughout. Shootlets were appeared on calli after 2 to 4 weeks, were allowed to grow until they were big enough to be cut from the remaining callus, and were placed on fresh SIM. Surviving shootlets with a single apical meristem were transferred onto root induction medium (RIM; MS medium + 1 mg l⁻¹ indole-3-acetic acid) with 125 mg l⁻¹ ticarcillin disodium/clavulanate potassium and 50 mg l⁻¹ kanamycin (Hanikenne et al., 2008). After root formation the transgenic lines were transferred to soil pots and cultivated with a standard photoperiod at 25 °C. Covers to maintain high humidity were removed after 2 weeks. The construct was used for establishing the transformation protocol, was according to Mustroph et al., (2009) 35S:FLAG-GFP-RPL18. The RNAi constructs that were used for the generation of the *AhNAS4*-RNAi, *AhNRAMP3*-RNAi, *AhZIP6*-RNAi and *AhCAX1*-RNAi, also were used for the stable transformation of *A. halleri*.

2.1.2.1 Optimal density of *Agrobacterium tumefaciens*

To establish the optimal density of *Agrobacterium* for *A. halleri* stable transformation, fresh *Agrobacterium* suspension in liquid (LB) medium supplemented with selection antibiotics were grown to log phase (OD₆₀₀ of 1.6) or to stationary phase (OD₆₀₀ of 3). The second culture was grown in (YEP) medium to reach three different OD₆₀₀ of 0.5, 1.6 or 5. After harvesting, second cultures re-suspended in MS medium and co-incubated with calli.

2.1.2.2 Acetosyringone effect on *A. halleri* transformation

In order to analysis the effect of acetosyringone on transformation efficiency, acetosyringone was added to the co-cultivation medium at a final concentration of 150 μ M and compared with the suspension with no additional acetosyringone.

2.1.2.3 Effect of genotype on *A. halleri* transformation

To assess the possible effects of genotype on transformation efficiency in *A. halleri*, individuals from different populations belonging to separate biogeographical regions according to (Koch and Matschinger, 2007) were selected for testing genotype influence on transformation (Fig. 2.1).



No.	Population	Short form	GPS Coordinates
1	<i>Auby</i>	<i>Auby</i>	50.40568°, 003.08385°
2	<i>Stutenkamm</i>	<i>Stut</i>	50.41014°, 011.55604°
3	<i>Čenkov</i>	<i>Lita</i>	49.7714722°, 014.0063889°
4	<i>Golino</i>	<i>Goli</i>	46.1774000°, 008.7182833°
5	<i>Miasteczko Śląskie</i>	<i>Mias</i>	50.5035278°, 018.9357500°
6	<i>Lgota</i>	<i>Lgot</i>	50.1989722°, 019.5400278°

Fig. 2.1: Origin of the individuals selected for the assessment of variation in transformation competence.

An individual from *Auby* and individuals from five sites sampled by Stein et al. (2017) were tested using the protocol established here for the transformation of vegetatively propagated *A. halleri* plants. Upper panel is a map indicating the positions of the populations (red labels: metalliferous sites, green labels: non-metalliferous sites). Lower panels list of populations and GPS coordinates.

2.2. GFP analysis by florescent and confocal microscopy

Putative transgenic calli on kanamycin-containing medium were monitored for GFP expression by fluorescence microscopy (Axiophoto microscope, Carl Zeiss, Jena, Germany). Roots of each putatively transgenic line were subjected to fluorescent microscopy (Leica MZFLIII, Leica Microsystem, Wetzlar, Germany) and then positive lines were analyzed via confocal laser scanning microscopy (Leica TCS SP5, Leica Microsystem, Wetzlar, Germany) with excitation at 488 nm. Green fluorescence of GFP was detected between 490nm and 510 nm. Digital images were recorded using the confocal operating system software.

2.3 Transcript analysis

Transcript analysis was performed essentially as described in (Deinlein et al., 2012). Briefly, RNA from homogenized *A. halleri* leaf or root material was extracted with Trizol (Life Technologies

Materials and methods

GmbH, Darmstadt) according to the manufacturer's instructions. 500 ng of DNase-treated RNA was used for cDNA synthesis with PrimeScript RT Master Mix (TaKaRa BIO INC, Shiga, Japan). Real time qPCR reactions were performed with a Bio-Rad iCycler MyiQ detection System (Bio-Rad, Munich), using SYBR® Green (Eurogentec, Köln). Three technical replicates were run per cDNA and primer pair combination. Data were analyzed using iQ5 Optical System software version 2.0 (Bio-Rad). Relative expression values were determined by the $\Delta\Delta C_T$ method. *EF1a* served as the reference gene. Its suitability had been validated before (Deinlein et al., 2012; Talke et al., 2006).

2.4 Plant material and growth conditions

2.4.1 Hydroponic cultures

For initial characterization of genotypes, plants were grown hydroponically in the standard *A. halleri* 1/10 Hoagland medium. [0.0871 mM $(\text{NH}_4)_2\text{HPO}_4$, 0.4 mM $\text{Ca}(\text{NO}_3)_2$, 0.6 mM KNO_3 , 0.2 mM MgSO_4 , 5 μM of a complex of Fe(III) and N,N'-di-(2-hydroxybenzoyl)-ethylenediamine-N,N'-diacetate (HBED), 4.63 μM H_3BO_3 , 0.032 μM CuSO_4 , 0.915 μM MnCl_2 , 0.011 μM MoO_3 and 0.077 μM ZnSO_4], pH 5.7 supplemented with 10 μM Zn^{2+} . Concentrations of Zn^{2+} , Cd^{2+} or Ni^{2+} were changed as indicated in experiments. Depending on experiment, the medium was changed either every week or twice a week.

For hydroponically growth in alkaline conditions as described by (Schmid et al., 2014) 1/10 Hoagland medium was buffered with 2.5 mM MES (2-morpholino-ethane-sulphonic acid) and adjusted with KOH to pH 7.2.

Hydroponic cultivation of *AhCAX1*-RNAi plants was carried out in modified MS medium as described by (Baliardini et al., 2015). In order to achieve comparability MS medium with: K_2SO_4 (0.88 mM), KH_2PO_4 (0.25 mM), NaCl (10 mM), MgSO_4 (1 mM), Fe-ethylenediamine-N,N-bis(2-hydroxyphenylacetic acid; 20 mM), H_3BO_3 (10 mM), ZnSO_4 (1 mM), MnSO_4 (0.6 mM), CuSO_4 (0.1 mM), and $(\text{NH}_4)_6\text{Mo}_7\text{O}_{24}$ (0.01 mM), 0.25 mM 2-(N-morpholino) ethanesulfonic acid, pH 5.7 was used. The Ca^{2+} concentrations in media were 0.5 as low concentration or 2 mM as moderate concentration.

The low-phosphate/low-pH (LPP) medium was prepared as described by Fischer et al., (2014) (10 μM $(\text{NH}_4)_2\text{HPO}_4$, 90 μM NH_4NO_3 , 200 μM MgSO_4 , 280 μM $\text{Ca}(\text{NO}_3)_2$, 600 μM KNO_3 , 5 μM Fe-HBED, 1% (w/v) sucrose, 5 mM MES, pH 5.0).

2.4.2 Short-term uptake experiment

To examine the effect of *AhZIP6* suppression on transport activity for Cd in *A. halleri*, a short-term (15 and 30 minutes) uptake experiment was performed using intact plants of the wild-type, 35S-GFP control line and two *AhZIP6*-suppressed lines 7-2 and 11-1 as described in (Sasaki et al., 2012). The cuttings (2 weeks old) were exposed to a 1/10 Hoagland medium without Cd for 2 weeks and then subjected to the uptake media containing 2 μM Cd^{2+} and 5 μM Cd^{2+} at 25 and 4°C. After 15 or 30 min, the roots were washed three times with 5 mM CaCl_2 and two times with deionized water

Materials and methods

and then were separated from the shoots. The roots were dried and metal content measured via ICP-OES.

Standard growth conditions for hydroponic cultivation were a 16h light ($90 \mu\text{mol m}^{-2} \text{s}^{-1}$)/8h dark photoperiod and a temperature cycle of 23°C (day)/18°C (night).

2.4.3 Plant culture on soil

For maintenance and vegetative propagation, *A. halleri* wild-type and all *Ah*-RNAi lines grown on normal soil a mixture of 3:3:1 (v/v) standard soil type GS90 (Unit Werkverband, Sinntal-Jossa), compost (Okohum, Herbertingen) and vermiculite (vermiculite German dam material GmbH) respectively. Metal hyperaccumulation and tolerance assays depending on *Ah*-RNAi lines carried out in four different soil types. Plants were grown on non-metalliferous normal soil or on soil that was alkalized by addition of CaO resulting in a pH of 7.8 (Kim et al., 2006). Plants were grown on an artificially slightly Zn and Cd contaminated phenotyping soil according to (Stein et al., 2016). phenotyping soil contained of 2:1 loamy soil: sand mix amended with 300 mg Zn kg⁻¹ (added as ZnS) and 5mg of Cd Kg⁻¹ (added as CdCl₂ x H₂O). Finally, for metal tolerance assays plants were cultivated in a metalliferous soil collected from native *A. halleri* site from Bestweig in Germany (N 51° 18.525' E 008° 24.578'). Standard growth conditions for plants were a 16h light ($90 \mu\text{mol m}^{-2} \text{s}^{-1}$)/8h dark photoperiod and a temperature cycle of 23°C (day)/18°C (night).

2.5 Elemental Analysis

2.5.1 ICP-OES Analysis

For elemental analysis, leaves were harvested, rinsed with Millipore water, and blotted dry. Roots of hydroponically grown plants were washed for 10 minutes in ice-cold water following by ice-cold 0.2 mM CaCl₂ and 10 mM EDTA, then rinsed and blotted dry. Plant material was digested in HNO₃ (65%, w/w) in the microwave oven using a temperature step gradient (maximum of 210°C). Digests were, if necessary, diluted with HNO₃ (2%, w/w), filtered, and the concentrations of Ca, Cd, Fe, Mn, Mg, Ni and Zn in the plant digest were assayed by ICP-optical emission spectroscopy (ICP-OES; iCAP 6500 Series; Thermo- Fisher, Waltham, MA, USA). The validity and accuracy of the procedure were checked against a certified sample of tomato leaves (NIST-SRM 1573a).

In order to determine the extractable metal content in soil samples, 1 gram of dried and sieved (2 mm mesh) soil was extracted with 10 ml of 0.1 M HCl incubated overnight at room temperature with gentle shaking. Suspension centrifuged for 10 min at 3000 g and then filtered through Whatman cellulose filter n° 595½ (GE Healthcare Life Sciences, Solingen, Germany) and 1 ml of HNO₃ 65% added to each sample tube and volume was adjusted to 10 mL with HNO₃ 2% and concentration of metals were measured by ICP-OES. Exchangeable metal was determined similarly with 10 ml of 10 mM BaCl₂.

2.5.2 Perls staining of Fe coupled to DAB intensification

In order to stain Fe in roots of *AhNAS4* RNAi plants, roots were separated from shoots and were desorbed for 10 min each in ice-cold solutions of 0.1M CaCl₂ and 10mM EDTA, then rinsed and stained according to (Meguro et al, 2007; Roschztardt et al, 2009). Roots were vacuum infiltrated with equal volumes of 4% (v/v) HCl and 4% (w/v) K-ferrocyanide (Perls stain solution) which was prepared immediately prior to use for 15 minutes and incubated for 30 minutes at room temperature. After washing with MilliQ water for three times, roots were incubated in a methanol solution containing 0.01 M NaN₃ and 0.3% (v/v) H₂O₂ for 2 hours, and then washed with 0.1 M phosphate buffer (pH 7.4). For the intensification reaction the roots were incubated for 10 min in a 0.1 M phosphate buffer (pH 7.4) solution containing 0.025% (w/v) diaminobenzidine (DAB) (Sigma), 0.005% (v/v) H₂O₂, and 0.005% (w/v) CoCl₂ (intensification solution). The reaction was stopped by rinsing with distilled water three times. Perls stained roots were investigated under the stereomicroscope and after fixation, thin sections (7 μm) were made using the microtome. The sections were viewed under the microscope (Leica DM1000, camera DFC420 series) and photos were processed using the Leica Application (Suite version. 3.3.1).

2.5.3 Quantitative mapping of elements by Particle-Induced X-ray Emission (μPIXE)

The elemental mapping of whole-mount leaves was performed in alkaline soil-grown *A. halleri* plants, young and mature leaves were detached from the plant, wrapped in Al foil and rapidly frozen in propane that was cooled with liquid nitrogen (Vogel-Mikus et al., 2008). Dr. Katarina Vogel-Mikus from university of Ljubljana performed the μPIXE imaging of plants.

2.6 Determination of leaves chlorophyll content

Chlorophyll contents were measured after the extraction of chlorophyll from leaf material with methanol. Briefly, after harvesting, leaves were grinded in liquid nitrogen and 20 mg of frozen powder was used for total chlorophyll (Tchl) extraction upon the addition of 2 mL 100% (v/v) methanol. Suspensions were incubated at 70 °C for 15 min with 10 s of shaking in every 5 minutes. Subsequently they were incubated on ice for 5 minutes. Samples were covered with aluminum foil during the incubation and were exposed to light as little as possible during the extraction. An aliquot of 100% (v/v) methanol was incubated and used as the blank. Samples were centrifuged at 14,000 rpm at 4 °C for 1 min, and 200 μL of the supernatant was used to record the absorbance at 652 nm and 665 nm (Porra et al., 1989) in a microplate reader spectrophotometer (SPECORD® 200 Plus, Jena, Germany). Chlorophyll *a*, chlorophyll *b* and total chlorophyll concentrations were determined in μg mL⁻¹ and converted into mg g FW⁻¹ using the following calculations:

$$\text{Chlorophyll a} = \{[(16.29 \cdot A_{665}) - (8.54 \cdot A_{652})] \cdot \text{mL MetOH}\} / \text{mg FW}$$

$$\text{Chlorophyll b} = \{[(30.66 \cdot A_{652}) - (13.58 \cdot A_{665})] \cdot \text{mL MetOH}\} / \text{mg FW}$$

$$\text{Total Chlorophyll} = \{[(22.12 \cdot A_{652}) + (2.71 \cdot A_{665})] \cdot \text{mL MetOH}\} / \text{mg FW}$$

2.7 Determination of catalase activity

Catalase activity in leaves of plants grown in lab soil and alkaline soil was measured using a UV spectrophotometric method as described by Ghasemi et al., (2009). Frozen samples were homogenized in liquid nitrogen and 100 mg of frozen powder transferred into a pre cooled 2 ml Eppendorf tube. Soluble proteins were extracted by adding 200 μ l of freshly prepared extraction buffer containing (50 mM Tris-HCl, pH 7.0, 1 mM EDTA, 0.2 % (v/v) Triton X-100, and 0.1 mM Pefa-Block proteases inhibitor), following vortex for 30 seconds and incubation on ice for 5 minutes. Samples were centrifuged at 14000g at 4°C for 15 minutes, and the supernatants were used for measurement of enzyme activities. Proteins concentration was determined using the Bradford protein assay (Bradford, 1976). For measuring catalase activity, same amount of protein for all samples added to the reaction solution contained 5 mm H₂O₂ in 50 mm potassium phosphate buffer, pH 7. The reaction was started by adding 100 μ l protein extract to 900 μ l reaction solution. The reduction in absorbance at 240 nm was monitored and catalase activity was calculated using an absorbance coefficient for H₂O₂ of 0.039 mm⁻¹ cm⁻¹. One unit of catalase is defined as the amount of enzyme that is needed for the decomposition of 1 μ mol of H₂O₂ in 1 min at 25°C. Decrease in absorption at 240 nm was negligible in the absence of H₂O₂ or in the absence of protein extract in the reaction solution.

2.8 ROS detection and quantification

In situ detection of hydrogen peroxide and superoxide radical in *A. halleri* roots was performed by 3,3'-diaminobenzidine (DAB) and nitroblue tetrazolium (NBT) staining, respectively, according to (Daudi et al., 2012) and (Ramel et al., 2009). Briefly, roots were infiltrated under gentle vacuum with DAB staining solution (1 mg mL⁻¹ DAB containing Tween 20 (0.05 % v/v) and 10 mM sodium phosphate buffer (pH 7.0)) or NBT staining solution (3.5 mg mL⁻¹ NBT containing 10 mM KH₂PO₄ and 10 mM NaN₃). Infiltrated roots were incubated in the dark at room temperature for 4 h with shaking at 100 rpm. Staining reaction was terminated by immersing roots twice in ethanol/glycerol/acetic acid (3:1:1) bleaching solution for 30 minutes at room temperature with shaking at 100 rpm. To quantify the H₂O₂ content, samples were frozen in liquid nitrogen, ground to a powder, resuspended in 0.2 M HClO₄, and centrifuged for 10 minutes at 12.000g at 4°C. The absorbance at 450 nm was measured and compared to a standard curve obtained with known amounts of H₂O₂ was resuspended in 0.2 M HClO₄ (Ramel et al., 2009). For NBT quantification, samples were homogenized in liquid nitrogen and resuspended in 2 M KOH-DMSO (1:1.16 v/v). After centrifugation for 10 minutes at 12.000g at 4°C, the absorbance at 630 nm was measured and the NBT content determined based on a standard curve.

2.9 Determination of NA content

NA was extracted by according to a modified protocol from Klatte et al., (2009). Amount of 0.1 g fresh root materials and 0.25 g of fresh shoot materials were grinded to a fine powder in liquid nitrogen and extracted with 500 μ l of H₂O incubated for 20 min at 80 °C with 600 rpm shaking, followed by sonification for 15 min in a water bath (Bandelin, Berlin, Germany). Cell debris was removed by two times centrifugation for 20 minutes at 15000g. 25 μ L of the resulting supernatant was diluted with 75 μ L of 0.5 M sodium-borate buffer (pH 7.7) containing 50 mM EDTA and

Materials and methods

derivatized for 45 seconds by the addition 50 μ L of 12 mM 9fluorenylmethyl chloroformate (FMOC, Sigma). Excess of FMOC was precipitated by the addition of 50 μ L 40 mM adamantan-1-amine hydrochloride (ADAM, Sigma) in acetone: water (3:1, v/v) and removed by two centrifugation steps for 30 min at 15,000g at 4 °C. The derivatisation-assay (10 μ l) was injected on a Nucleosil 100-5 C18, 250/4 column (Macherey-Nagel, Düren, Germany) that was connected to a Waters 600E HPLC system. After equilibration of the column for 8 min in buffer A (20 % (v/v) acetonitrile in 50 mM sodium acetate buffer pH 4.2), nicotianamine was separated by using the following binary gradient with a flow rate of 1 mL per minute: 0-5 min (0 % B), 5-15 min (20 %B, linear), 15-20 min (100 % B, linear), 20-22 min (100 % B). 80 % (v/v) acetonitrile in 50 mM sodium acetate buffer pH 4.2 served as buffer B. Fluorescence of FMOC-derivatives was detected by using a fluorescence detector (Jasco FP 920, excitation: 263 nm, emission: 313 nm, Gain: 10, Response: Fast) and quantified by external NA standards (T. Hasegawa Co., Tokyo, Japan). Data were collected and processed with the Millenium32 software (Waters). The identity of nicotianamine was evidenced by spiking of chemically synthesized nicotianamine to plant samples.

2.10 Determination of soil pH

Soil pH was determined according to the method was described by Stein et al., (2016). The amount of 3 g soil was mixed with 7.5 ml of 0.01 M CaCl₂ in a 15-ml round-bottom polypropylene screw- cap tube using an overhead shaker at 150 rpm at room temperature overnight. Samples were centrifuged at 2000 g at room temperature and pH was determined in the supernatant using a pH meter (MP220, Mettler- Toledo GmbH, Schwerzenbach, Switzerland).

2.11 Statistical Analysis

The one-way analysis of variance and Tukey tests were performed with SigmaPlot 11.0.

3. Results

3.1 Optimization the *Agrobacterium*-mediated transformation of *A. halleri*

3.1.1 Media for callus induction and shoot regeneration

A. halleri transformation has been established previously based on a seed-dependent in vitro culture and regeneration protocol (Deinlein et al., 2012; Hanikenne et al., 2008) that used roots as a source of explants. In another attempt callus induction and shoot regeneration were established by using leaflets as explants (Vera-Estrella et al., 2009). In this study modifications of the established transformation protocol (Deinlein et al., 2012; Hanikenne et al., 2008) were explored that would allow transformation of vegetatively propagated plants, i.e. independent of crossing and seed production. For this, plants collected at the Langelsheim site in the Harz region were employed which are known to be transformation-competent. In *A. halleri* transformation protocol that established by Hanikenne et al., (2008) and Deinlein et al., (2012), 0.5 mg/l of 2,4-D and 0.5 mg/l of kinetin were used for inducing callus from root explants. Later 1 mg/l of BA and 0.5 mg/l of NAA were used in shoot induction medium (SIM) to regenerate shoots from calli. However in the protocol developed by (Vera-Estrella et al., 2009) the double amount of 2,4-D (1 mg/l) and 0.05 BA instead of (1 mg/l) kinetin were applied for callus induction medium (CIM), while for regeneration of shoots 0.5 mg/l 2,4-D and 0.1 mg/l BA were used in SIM.

In order to obtain higher rates of callus induction and shoot regeneration after transformation, both protocols and a combination of them were tested in parallel in preliminary experiments. During the callus induction phase big differences were detected in response to application of two different callus induction regimes. Soft, quickly growing and pale or green-yellow fresh calli appeared by using CIM as described by (Vera-Estrella et al., 2009) after 3 to 4 weeks of incubation. Application of 0.5 mg/l 2,4-D and 0.5 mg/l Kinetin in callus induction medium as described by (Deinlein et al., 2012; Hanikenne et al., 2008) led to a lower number of calli with reduced size. The percentage of regenerated shoots from transformed calli after application of shoot induction medium as described in these protocols was vice versa: the number of shoots generated using SIM described by (Vera-Estrella et al., 2009) was lower than shoot formation from transformed calli on SIM described by (Deinlein et al., 2012; Hanikenne et al., 2008). Based on these observations, concentrations of 0.05 mg/l BA and 1 mg/l of 2,4-D were chosen for the callus inducing medium and 1.0 mg/l of BA with 0.5 mg/l of NAA for the shoot inducing medium.

3.1.2 *A. halleri* regeneration steps

A. halleri plants were regenerated from leaflet and petiole explants via a three-step procedure is shown in Fig. 3.1, callus induction, shoot induction and root development. Leaflets and petioles as explants were initially incubated in CIM as described in materials and methods (Fig. 3.1 A, B). Callus formation was observed in all explants within 2 weeks of culturing in CIM in darkness. After 3 to 4 weeks calli had grown, were friable, fresh, and ready to be transformed (Fig. 3.1 C and D).

Results

No statistically significant differences in callus formation were observed between the two different sources of explants (Table. 3.1). 3 to 4 weeks-old calli from induction medium were subjected to transformation with a construct containing GFP as reporter under control of the constitutive 35S promoter. For that calli were inoculated with *Agrobacterium tumefaciens* carrying the respective plasmid. 2 weeks following transfer to shoot induction medium supplemented with kanamycin, adventitious shoots began to grow from the calli (Fig. 3.1 E). Shoots were cut out from calli and directly placed in touch with SIM for an extra 2 weeks, then transferred to root induction medium (RIM). After 4 weeks, strong and abundant root systems had formed (Fig. 3.1 F). Finally, regenerated plants were transferred to soil pots (Fig. 3.1 G).

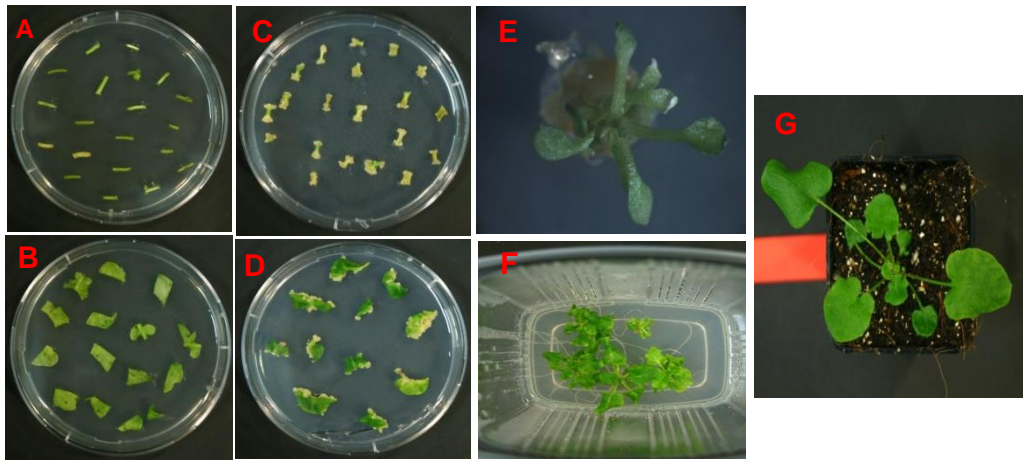


Fig. 3.1 A. *halleri* regeneration steps

Shown in (A and B) are leaflet and petiole explants. (C and D) are developed calli from leaflet and petiole explants on callus induction medium. Shown in (E) is regeneration of *A. halleri* transgenic plant on shoot induction medium supplemented with a selective agent (kanamycin), (F) is rooting shoots on root induction medium supplemented with a selective agent (kanamycin) and (G) is transgenic plant after transfer to soil.

3.1.3 Analysis of plants stably transformed with GFP

The construct was used for establishing the transformation protocol was 35S:FLAG-GFP-RPL18 (Mustroph et al., 2009). After selection for two months with kanamycin in shoot and root induction media, resistant plants were transferred to soil pots and grown as mother plants. From each mother plant, at least three clonal replicates were made and hydroponically rooted. GFP served as a reporter to detect transformed plants based on presence of a GFP signal in roots as detected by fluorescence and confocal microscopy. No GFP activity was detected in root tissues from wild-type plants (Fig. 3.2 A), indicating that the green fluorescent signal was specific to GFP (Fig. 3.2 B, C).

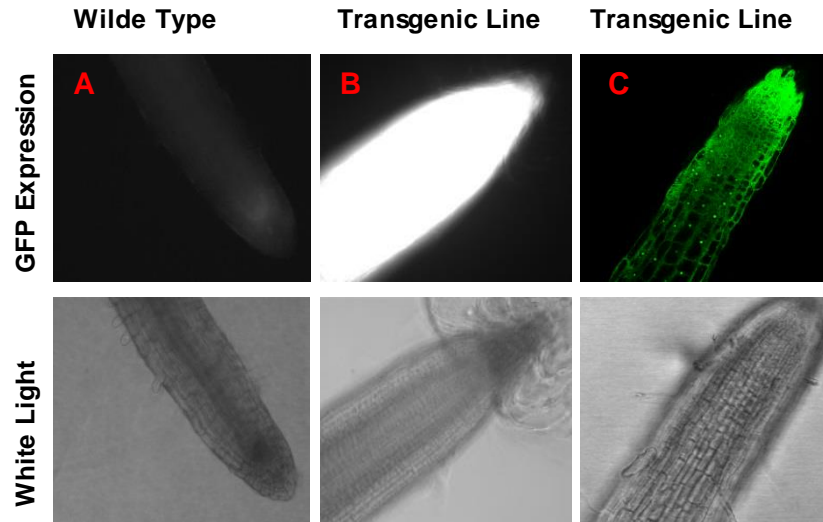


Fig. 3.2 GFP expression in root tips of *A. halleri*

Shown in (A) is root tip of wild-type and in (B and C) are two independent transgenic lines. Top panels show GFP fluorescence and bottom panels show the corresponding bright field image. Images are representative of at least 12 replicates.

3.1.4 Effect of *A. tumefaciens* density on *A. halleri* transformation efficiency

To establish the optimal density of *Agrobacterium* for *A. halleri* stable transformation, the first culture of *Agrobacterium* in liquid (LB) medium was grown to log phase (OD_{600} of 1.6) or to stationary phase (OD_{600} of 3) and the second culture (YEP) medium was then grown to OD_{600} of 0.5, 1.6 or 5. Four days after inoculation with *Agrobacterium*, the percentage of positive GFP signal was observed in calli was not correlated with *Agrobacterium* preculture LB density. The highest percentage of about 8% was observed in calli inoculated with (LB=3 & YEP=5), (LB=1.6 & YEP=5), and (LB=1.6 & YEP=1.6). In contrast, when density of the inoculation medium (YEP) decreased to its lowest level, GFP positive signal in calli decreased to 3% regardless of preculture LB density (LB=3 & YEP=0.5) and (LB=1.6 & YEP=0.5) (Fig. 3.3). In all tested conditions, the highest percentage of GFP positive signal was detectable in calli one week after transformation and decreased weekly (Fig. 3.3). The highest rates of transformed plants with positive GFP signal were achieved when *Agrobacterium* density was (LB=3 & YEP=5) (about 8%) and the second positive signal rates were observed when *Agrobacterium* density was (LB=1.6 & YEP=5) (about 4%), indicating that final density had a major impact on transformation (Fig. 3.3).

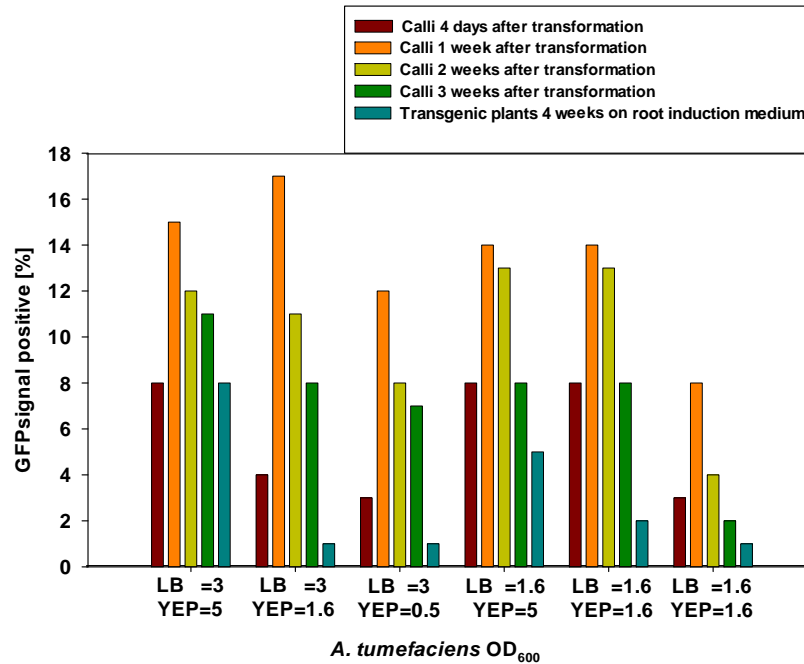


Fig. 3.3 Effect of *A. tumefaciens* density on *A. halleri* transformation efficiency

Transformation efficiency expressed in percentage of calli and regenerated plants with positive GFP signal. Data are representing 100 Calli grown in 10 petri dishes in each treatment. Values for LB and YEP stand for density of *Agrobacterium* in preculture medium LB and final inoculation YEP medium.

3.1.5 Effect of acetosyringone on *A. halleri* transformation efficiency

In *Agrobacterium* the transfer of T-DNA is mediated by the virulence genes and in vitro induction of them can be achieved by cultivation of *Agrobacterium* in media containing molecules such as acetosyringone (Gelvin, 2003; Pitzschke, 2013). The acetosyringone is widely utilized to enhance transformation efficiency for both dicotyledonous and monocotyledonous plants (Pitzschke and Hirt, 2010; Păcurar et al., 2011). In order to test the possible effect of acetosyringone on transformation efficiency in *A. halleri*, the acetosyringone was added to the *Agrobacterium* co-cultivation MS medium at a final concentration of 150 μ M and transformation efficiency was compared to the same suspension without acetosyringone. In both conditions *Agrobacterium* preculture density of (LB=3 & YEP=5) and (LB=1.6 & YEP=5) were used. Results showed a positive effect of acetosyringone on transformation efficiency regardless of *Agrobacterium* preculture density (Fig. 3.4). For the preculture density of (LB=3 & YEP=5) with no acetosyringone 8% positive GFP signal in roots of transgenic plants after 4 weeks of growth on RIM was detectable while adding acetosyringone to the same medium enhanced the percentage of GFP positive signal to 14%.

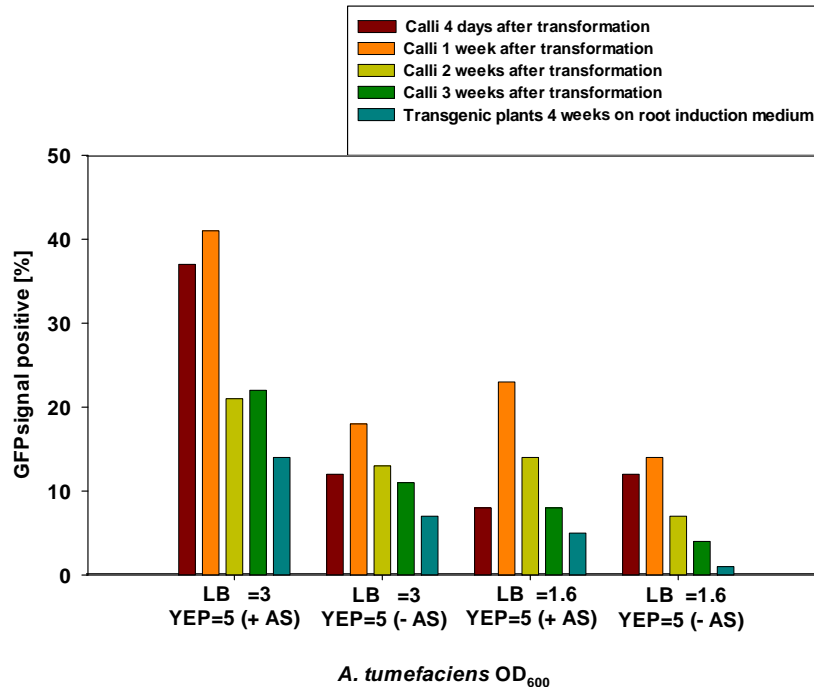
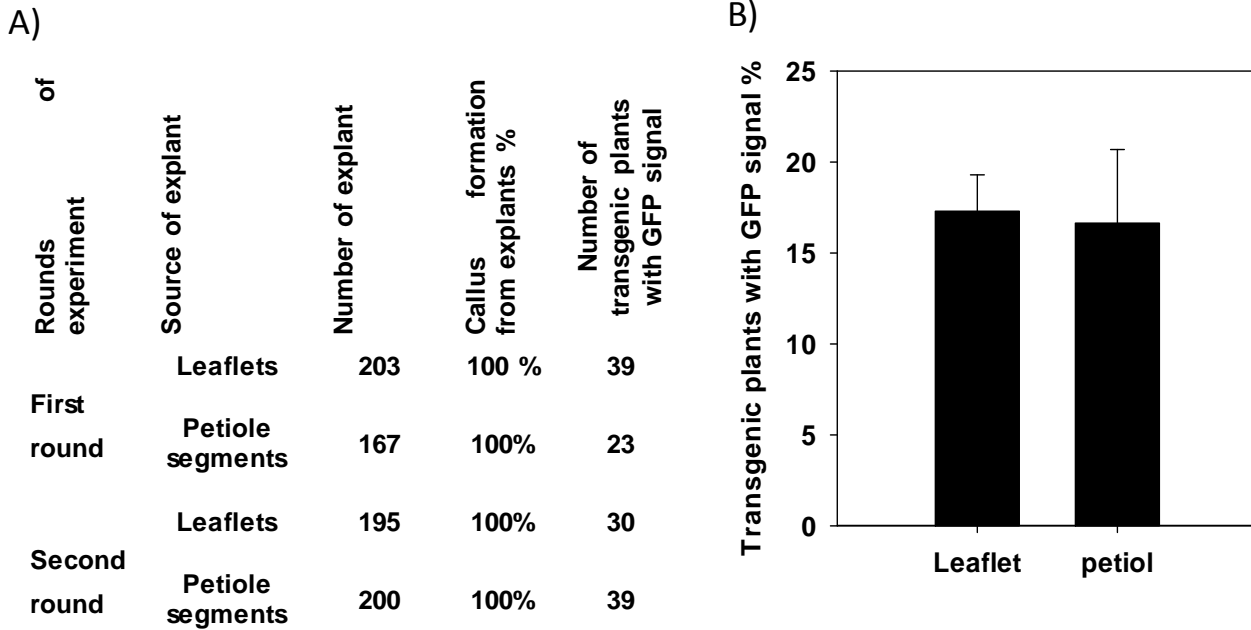


Fig. 3.4 Effect of acetosyringone on *A. halleri* transformation efficiency

Transformation efficiency is expressed in percentage of calli and regenerated plants that show GFP signal. Numbers are derived from 100 calli (grown in 10 petri dishes) per treatment.

3.1.6 Effect of source of explants on *A. halleri* transformation efficiency

To investigate the possible effect of the source of explants on *A. halleri* transformation efficiency, leaf blade and petiole segments of young plants were used as explants for callus induction and further transformation. *Agrobacterium* density of (LB=3 & YEP=5) with additional 150 μ M of acetosyringone in MS co-cultivation medium was used for transformation in two independent rounds. Results shown in Tab. 3.1 and Fig. 3.5 suggested that, the ratio of callus formation from both petiole segments and leaflet explants was 100% in two independent rounds. The ratio of regenerated plants with positive GFP signal in their roots from calli originated from both types of explants was on average comparable (Fig. 3.5), suggesting that both type of explants successfully could be used for transformation of *A. halleri*.



Tab. 3.1 and Fig. 3.5 Effect of source of explants on *A. halleri* transformation efficiency

Leaflets and petiole segments of young *A. halleri* wild-type plants were used in two independent rounds of stable *Agrobacterium*-mediated transformation with 35S-GFP construct. Shown in (A) are number of explants were used in callus formation, percentage of callus formation, number of transgenic plants show positive GFP signal in their roots. Shown in (B) is the percentage of transgenic plants with positive GFP signal derived from leaflet and petiole segment explants in two independent rounds.

3.1.7 Effect of *A. halleri* genotype on transformation efficiency

To assess the possible effects of genotype on transformation efficiency in *A. halleri*, individuals from different populations belonging to separate biogeographical regions according to Koch and Matschinger (2007), were selected for testing genotype influence on transformation (Fig. 2.1). Results suggested that explants from various ecotypes clearly differ in their competence of callus formation after 3 weeks of induction in CIM as shown in Fig. 3.6. Explants originating from individuals of the populations *Lita*, *Stut*, *Golino* and *Mias* produced fragile, fresh, pale yellow calli at the edge of explants and their leaflet explants were green with no signs of browning as an indication of phenolic compounds accumulation. In contrast, explants derived from the *Lgot* individual turned brown and their calli were darker and compacted as a result of phenolic compound accumulation. Explants derived from the *Auby* individual did not show any visible callus induction and explants turned yellow and further incubation on CIM led to darker explants with less viability and no improvement of callus formation (Fig. 3.6). As shown in Fig. 3.7, calli derived from individuals of different populations of *A. halleri* show varying competence of shoot regeneration after incubation on SIM for 4 weeks. Individuals of the populations (*lita*, *Stut*, *Golino* and *Mias*) regenerated shoots from their calli within 4 weeks of incubation on SIM. Individuals of the populations (*Lita* and *Stut*); shoots regenerated after 2 weeks of calli incubation on SIM. Individuals of the populations (*Auby* and *Lgot*) were not able to regenerate any shoots from their calli after incubation on (SIM) for 8 weeks.

Results

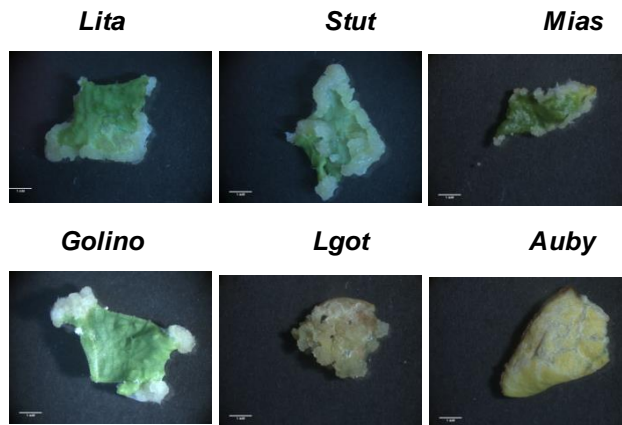


Fig. 3.6 Effect of *A. halleri* genotype on callus induction

Explants of *A. halleri* individuals from different populations (*Lita*, *Auby* and *Stut*); (*Golino*) and (*Lgot* and *Mias*) belonging to different biogeographical regions (3), (12) and (11) respectively; according to (Koch and Matschinger, 2007) after 3 weeks of incubation on callus induction medium. Photos are representative of at least 100 calli. Scale bars represent 1mm.

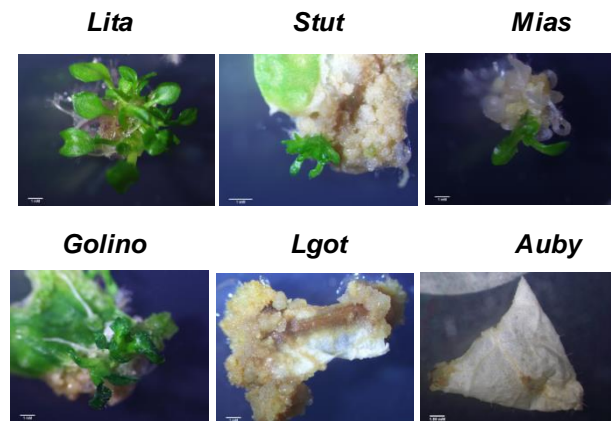


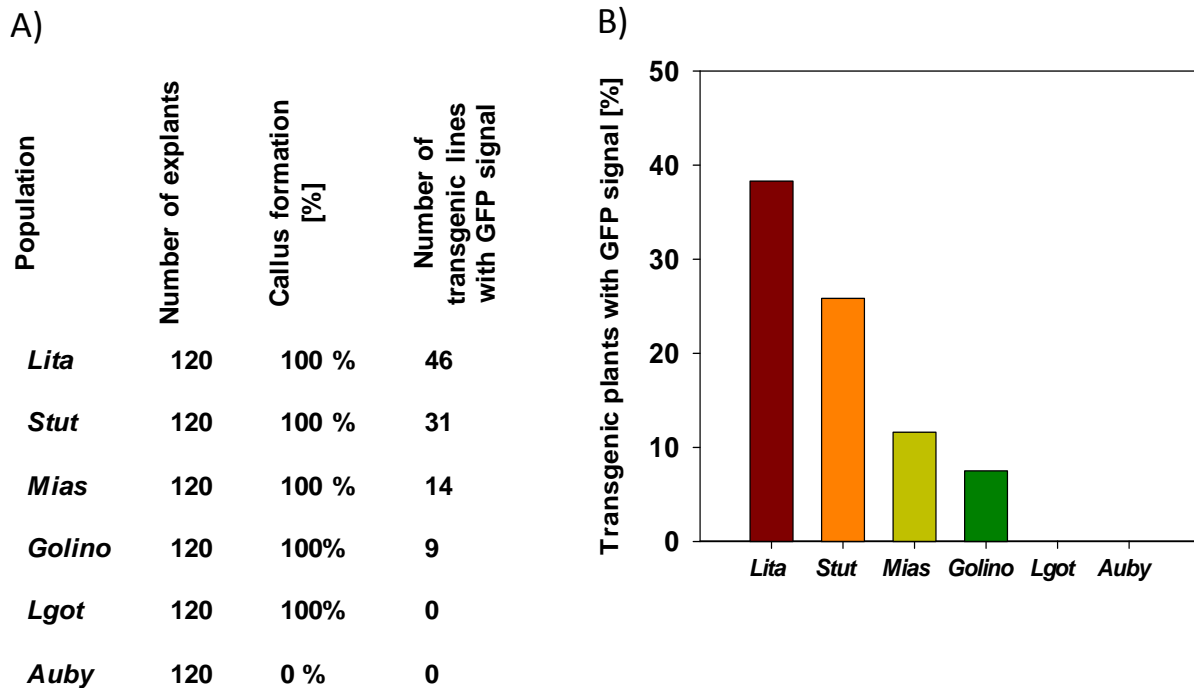
Fig. 3.7 Effect of *A. halleri* genotype on shoot regeneration

Regenerated shoots from transformed calli of different populations of *A. halleri* after incubation on SIM for 4 weeks. Photos are representative of at least 100 calli. Scale bars represent 1mm.

In order to study the influence of *A. halleri* genotype on transformation efficiency 120 explants, i.e. leaflet and petiole segments from young plants of each of the individual of selected populations shown in Fig. 3.6 were used for callus formation, transformation with GFP construct and shoot regeneration in parallel. Results suggested that among all six chosen populations; only explants derived from *Auby* are incompetent to induce callus, while other populations regardless of their biogeographical origin have induced 100% calli after 4 weeks of incubation on CIM. Various populations were different in their ability to regenerate shoots from their transformed calli on SIM. Highest rate of transformation was observed in individuals from *Lita* and *Stut* populations, 38.3% and 25.83%, respectively, followed by *Mias* 11.6% and *Golino* 7.5%. Although *Lgot* population successfully produced 100% calli, transformed calli from this ecotype were unable to regenerate

Results

shoots, and finally explants derived from *Auby* population were unable to induce callus or regenerate shoots (Tab. 3.2 and Fig. 3.8). Results suggested that, there was no correlation between biogeographical origin of populations and their transformation competence. *Lgot* and *Mias* come from contaminated sites of the very same region and still *Lgot* was untransformable. In addition, *Auby*, *Stut* and *Lita* come from the same biogeographical region yet *Lita* and *Stut* showed highest rate of transformation success while *Auby* did not give rise to callus usable for transformation (Tab. 3.2 and Fig. 3.8).



Tab. 3.2 and Fig. 3.8 Effect of *A. halleri* genotype on transformation efficiency

A. halleri individuals (*lita*, *Auby* and *Stut*); (*Golino*) and (*Lgot* and *Mias*) belong to different biogeographical regions (3), (12) and (11) respectively; according to (Koch and Matschinger, 2007) transformed with GFP construct. Shown in (A) are number of explants were used for callus induction, rate of callus induction and number of regenerated plants with positive GFP signals in their roots. Shown in (B) is the transformation efficiency in different populations.

3.2 The physiological role of *NAS4* in *A. halleri*

3.2.1 Confirmation of *AhNAS4*-RNAi lines with real-time PCR

To investigate the potential role of *NAS4* in metal hyperaccumulation and Fe homeostasis in *A. halleri*, *AhNAS4*-RNAi lines were generated from a wild-type individual called *C-line* collected at the Langelsheim site in the Harz region in Germany. Quantitative real time RT-PCR analyses using specific primers were performed in order to quantify transcript levels of the *NAS4* gene. Out of 10 independent *AhNAS4*-RNAi lines which initially were analyzed, one line which displayed a relative transcript level similar to the wild-type was chosen as transgenic control and two which showed significantly reduced transcript levels relative to the wild-type were selected as strong RNAi lines for further study (Fig. 3.9).

The *NAS4* transcript levels in the three independent *NAS4*-RNAi lines were analyzed in shoots of soil-grown plants in growth chamber and compared to the wild-type in two independent rounds. Results showed that, there was no significant reduction in transcript level in line 11-2 in comparison to the wild-type while two strong RNAi lines 1 and 2 had reductions of 90% and 93% respectively (Fig. 3.9).

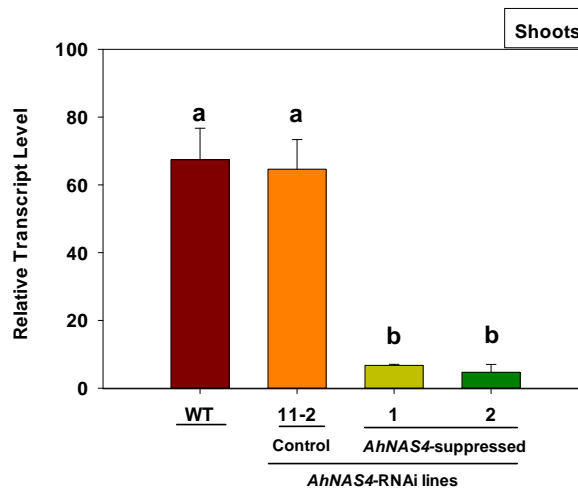


Fig. 3.9 Reduction of *AhNAS4* transcript level in independent RNAi lines

Transcript level of *NAS4* was analyzed in shoots of soil-grown *A. halleri* wild-type plant, control transformant, and two *AhNAS4*-RNAi lines. Tissues were harvested after 6 weeks of cultivation in normal soil and transcript level was analyzed by real-time RT-PCR. Transcript abundance was expressed relative to *EF1α*. Values are means ± SD of n = 2 independent experiments (Six replicate clones per genotype were pooled for each data point). Different characters above the bars indicate statistically significant differences detected in a one-way ANOVA, followed by Tukey test. (P < 0.01 significance level between (a) and (b)).

Previous studies had shown that *A. halleri* carries orthologs of the four *NAS* genes known from *A. thaliana* (Deinlein et al., 2012). To investigate specificity of the RNAi as well as potential effects of *NAS4* suppression on transcript abundance of other *NAS* genes in *NAS4*-RNAi lines, transcript levels of all four *NAS* homologs were analyzed in leaves and roots of hydroponically grown *A. halleri* wild-type plant, control transformant, and the two *AhNAS4*-RNAi lines in standard *A. halleri* 1/10 Hoagland medium for 10 days. Results confirmed the tissue specific expression pattern of *NAS*

Results

orthologs known from *A. thaliana*. *NAS1* and *NAS4* are expressed in roots and leaves, while expression of *NAS2* is detected only in roots and expression of *NAS3* is restricted to shoots (Figure 10). Our results suggested that *A. halleri* roots and leaves expressed dominantly *NAS2* and *NAS4* respectively (Fig. 3.10). No significant changes in transcript abundance relative to the wild-type were detected in *NAS1*, *NAS2* and *NAS3* in suppressed *NAS4-RNAi* lines in comparison to the wild-type and control transformant. As found before transcript abundances of *NAS4* were strongly reduced in strong *NAS4-RNAi* lines 1 and 2 (93% and 89%, respectively) in roots (Fig. 3.10 A) and (94% and 92% respectively) in leaves (Fig. 3.10 B) in comparison to the wild-type. Transcript levels of *NAS4* in control transformant line 11-2 were similar to the wild-type in roots and shoots (Fig. 3.10 A, B). It was concluded that the selected lines were suitable for addressing the effects of silencing of *NAS4* expression on metal hyperaccumulation and homeostasis in *A. halleri*.

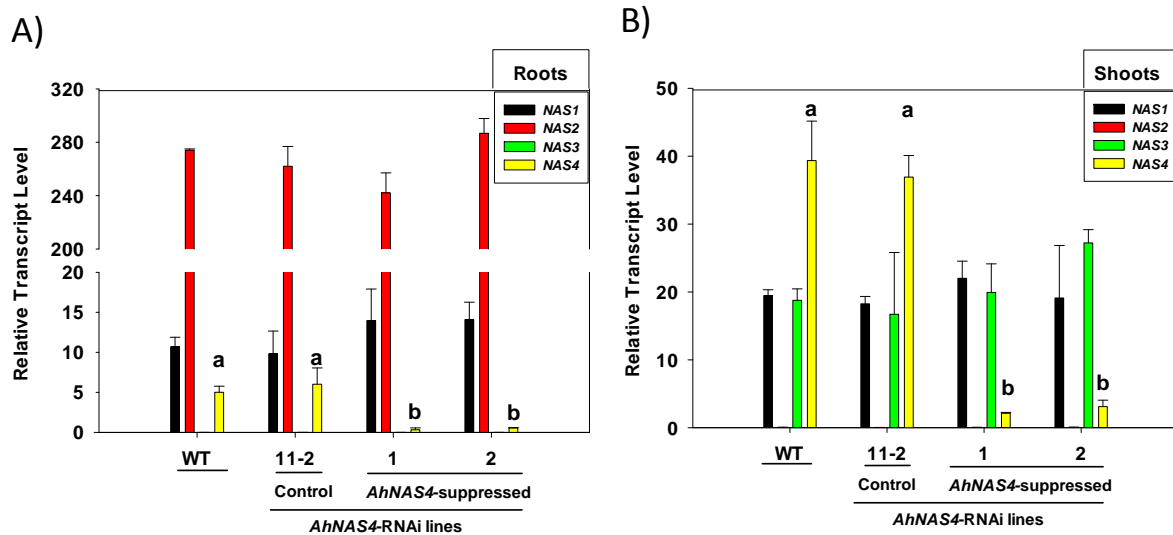


Fig. 3.10 Effect of *AhNAS4* suppression on *NAS1*, *NAS2*, *NAS3* and *NAS4* transcript abundance in roots and shoots of *A. halleri*

Transcript levels of *NAS1* (Black bars), *NAS2* (Red bars), *NAS3* (Green bars), and *NAS4* (Yellow bars) were analyzed in roots (A) and leaves (B) of hydroponically grown *A. halleri* wild-type plant, control transformant, and the two *AhNAS4-RNAi* lines hydroponically grown in standard 1/10 Hoagland medium for 10 days. After harvest, transcript abundance was analyzed by real-time RT-PCR relative to *EF1 α* . Values are means \pm SD of $n = 2$ independent experiments (Six replicate clones per genotype were pooled for each data point). Different characters above the bars indicate statistically significant differences detected in a one-way ANOVA, followed by Tukey test A: $P < 0.05$ significance level between (a) and (b), B: $P < 0.01$ significance level between (a) and (b).

3.2.1.1 Suppression of *AhNAS4* results in reduced root NA content in *A. halleri* grown in standard medium for 10 days

To assess the consequences of altered *NAS4* expression on root and shoot NA content, the selected *NAS4*-suppressed lines, *C-line* wild-type plant, and the control transformant line were grown hydroponically in standard *A. halleri* 1/10 Hoagland medium for 10 days. This medium has an identical concentration to those applied in previous studies on *A. halleri* metal hyperaccumulation to ensure Zn sufficiency (Hanikenne et al., 2008; Deinlein et al., 2012). As shown in Fig 3.11, root NA contents of the two *NAS4*-suppressed lines were significantly lower than those of wild-type and

Results

control transformant plants, whereas no significant changes in shoot NA content were observed upon altered *NAS4* transcript level (Fig. 3.11).

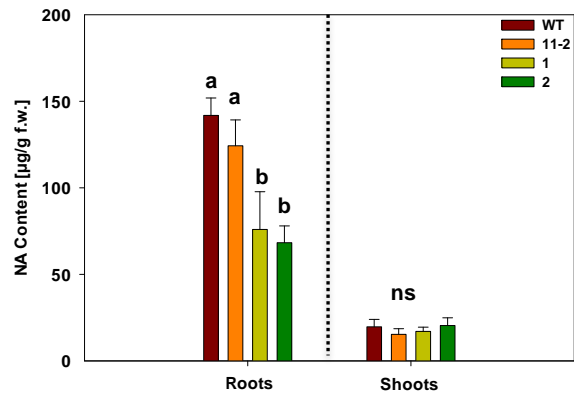


Fig 3.11 NA content in root and shoot of hydroponically grown *A. halleri* wild-type and *AhNAS4*-RNAi plants

Plants were cultivated in standard *A. halleri* 1/10 Hoagland medium. Tissues were harvested after 10 days, roots and shoots separated and NA was extracted with water, derivatized with Fmoc-Cl, and quantified by HPLC. All values are arithmetic means \pm SD, $n = 4$ independent experiments (Six replicate clones per genotype were pooled for each data point). Different characters above the bars indicate statistically significant differences detected in a one-way ANOVA, followed by Holm-Sidak method: $P < 0.001$ significance level between (a) and (b).

3.2.2 Elemental profiling of *AhNAS4*-RNAi lines hydroponically grown in standard *A. halleri* 1/10 Hoagland medium for 10 days

3.2.2.1 Suppression of *AhNAS4* slightly disturb Zn translocation in *A. halleri* grown in standard medium for 10 days

To assess the consequences of altered *NAS4* expression on metal content, the selected *NAS4*-suppressed lines, *C-line* wild-type plant, and the control transformant line were grown hydroponically in standard *A. halleri* 1/10 Hoagland medium for 10 days. After harvesting plants, metal content in root and shoot material were measured via inductively coupled plasma–optical emission spectroscopy (ICP-OES). Root Zn contents of the two *NAS4*-suppressed lines were significantly higher than those of wild-type and control transformant plants (Fig. 3.12 A). While shoot Zn content of *NAS4*-suppressed line 2 was significantly increased compared to the wild-type and control lines, this increase was not significant in shoots of *NAS4*-suppressed line 1 compared to the wild-type and control transformant lines (Fig. 3.12 B). Shoot: Root Zn ratio was significantly reduced in two *NAS4*-suppressed lines in comparison to the wild-type, while this reductions was not significant in comparison to control transformant line 11-2 (Fig. 3.12 C).

Results

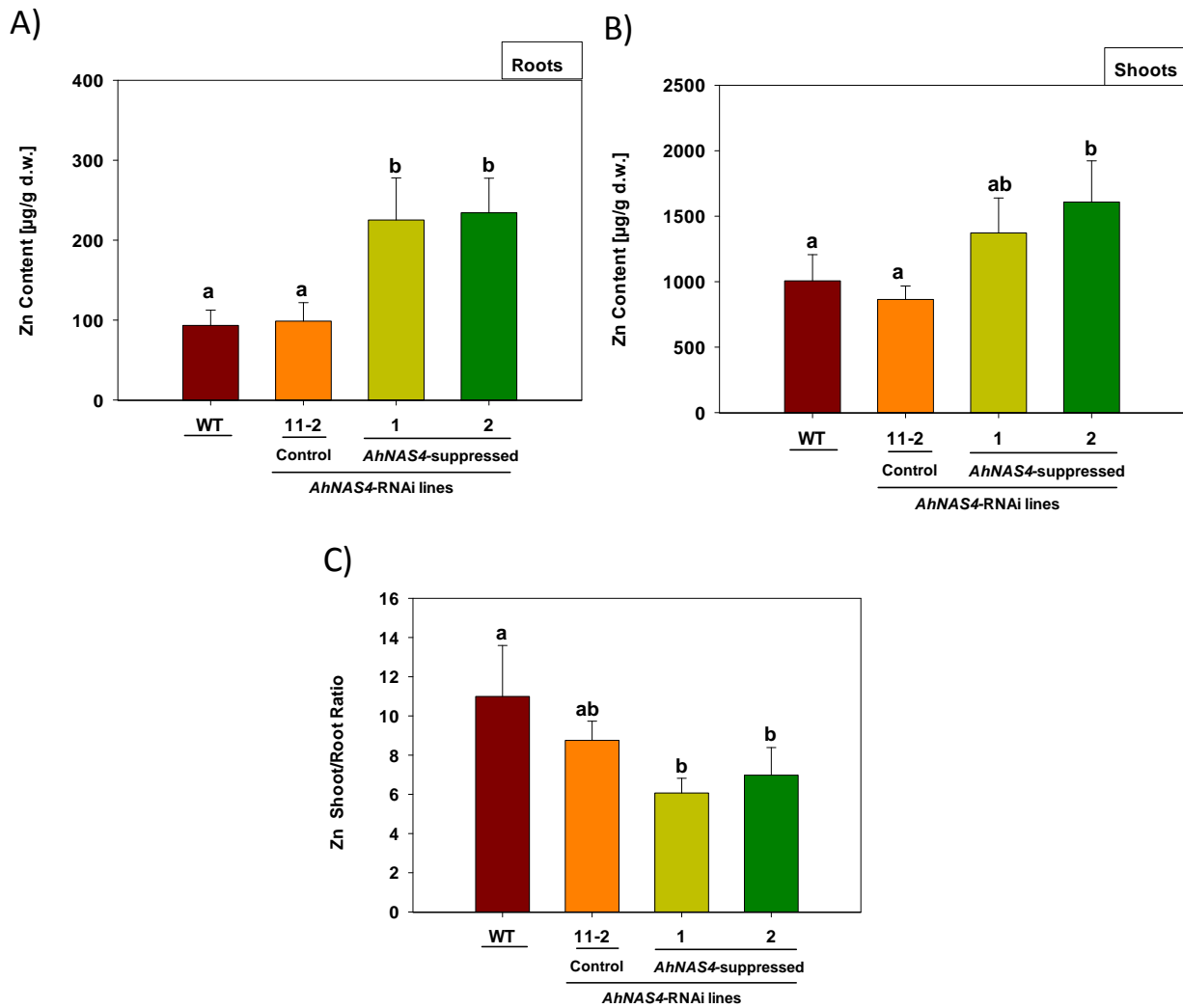


Fig. 3.12 Zn accumulation in *A. halleri* wild-type and *AhNAS4*-RNAi plants hydroponically grown in standard medium for 10 days

Plants were cultivated in standard *A. halleri* 1/10 Hoagland medium. Tissues were harvested after 10 days, digested and analyzed by ICP-OES. Shown in (A) and (B) are values for roots and shoots, respectively. For (C), shoot: root Zn ratio was calculated from data shown above. All values are arithmetic means \pm SD, $n = 16$ replicate clones per genotype from four independent experiments. Different characters above the bars indicate statistically significant differences detected in a one-way ANOVA, followed by Tukey test. A: $P < 0.01$ significance level between (a) and (b), B: $P < 0.05$ significance level between (a) and (b), C: $P < 0.05$ significance level between (a) and (b).

3.2.2.2 Silencing of *AhNAS4* results in more efficient root-to-shoot translocation specifically of Fe in *A. halleri* grown in standard medium for 10 days

Root Fe content of the two *NAS4*-suppressed lines was strongly reduced compared to the wild-type and control transformant plants (Fig. 3.13 A). An opposite effect was observed in shoot where Fe contents in *NAS4*-suppressed lines were increased in comparison to the wild-type and control transformant lines (Fig. 3.13 B). The shoot: root Fe ratio was approximately 4-fold increased in two *NAS4*-suppressed lines in comparison to the wild-type and control transformant plants (Fig. 3.13 C).

Results

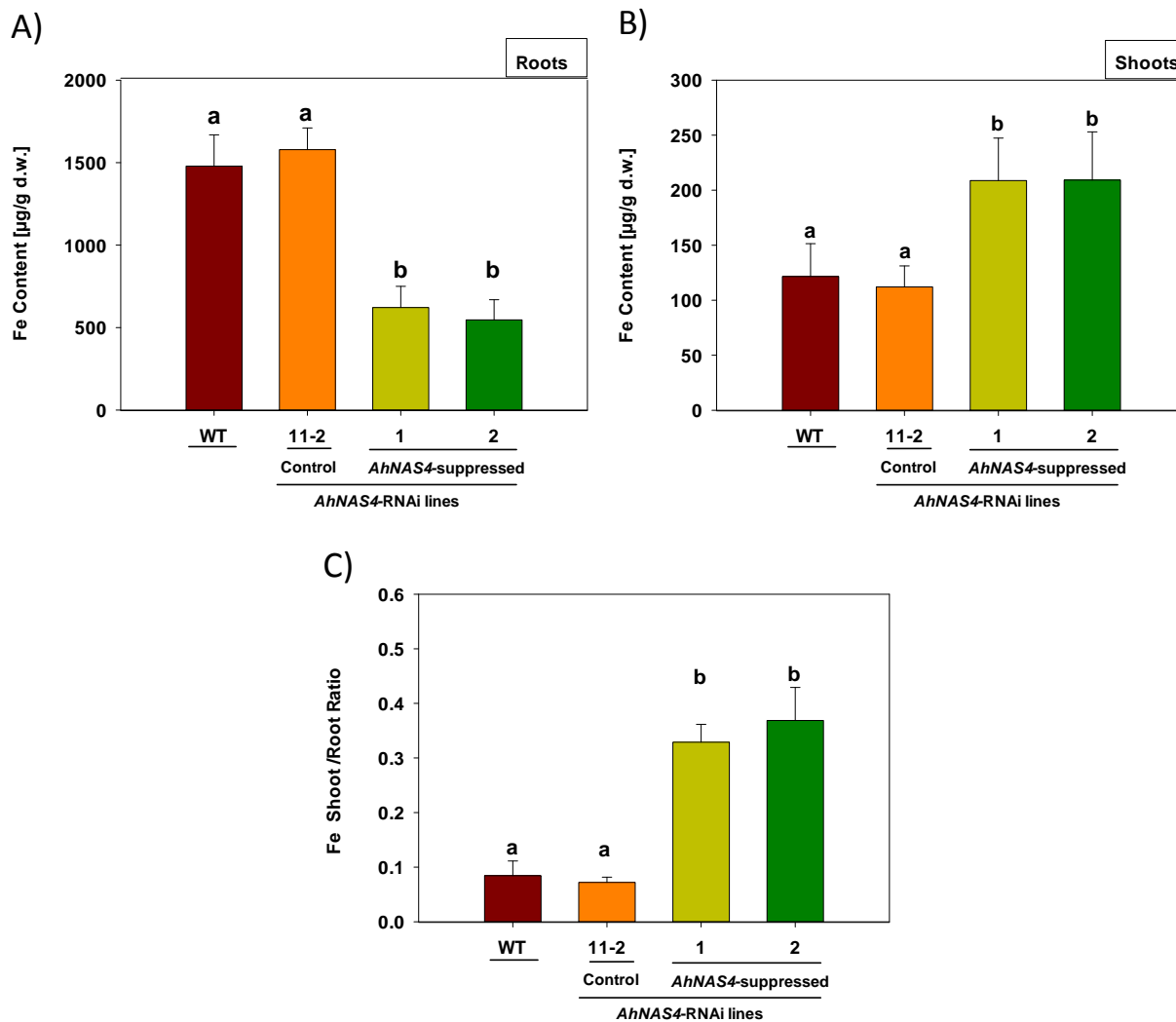


Fig. 3.13 Fe content in roots and shoots of *A. halleri* wild-type and *AhNAS4*-RNAi plants hydroponically grown in standard medium for 10 days

Plants were cultivated in standard *A. halleri* 1/10 Hoagland medium. Tissues were harvested after 10 days, digested and analyzed by ICP-OES. Shown in (A) and (B) are values for root and shoot Fe contents respectively. For (C), shoot: root Fe ratio was calculated from data shown above. All values are arithmetic means \pm SD, $n = 16$ replicate clones per genotype from four independent experiments. Different characters above the bars indicate statistically significant differences detected in a one-way ANOVA, followed by Tukey test A: $P < 0.001$ significance level between (a) and (b), B: $P < 0.05$ significance level between (a) and (b), C: $P < 0.001$ significance level between (a) and (b).

3.2.2.3 *AhNAS4* suppression results in no change in root and shoot contents and root-to-shoot translocation of Mn, Ca and Mg

Besides Zn and Fe, NA is able to form stable complexes with Mn^{2+} , Cu^{2+} and Co^{2+} (Benes et al., 1983). In order to test whether *NAS4* suppression affects distribution of these metals and other elements like Ca and Mg, ICP-OES data were analyzed. Results suggest that *AhNAS4* suppression has no effect on root and shoot contents of Mn, Ca and Mg. Cu and Co contents were under the detection limit (Fig. 3.14 A, B and C).

Results

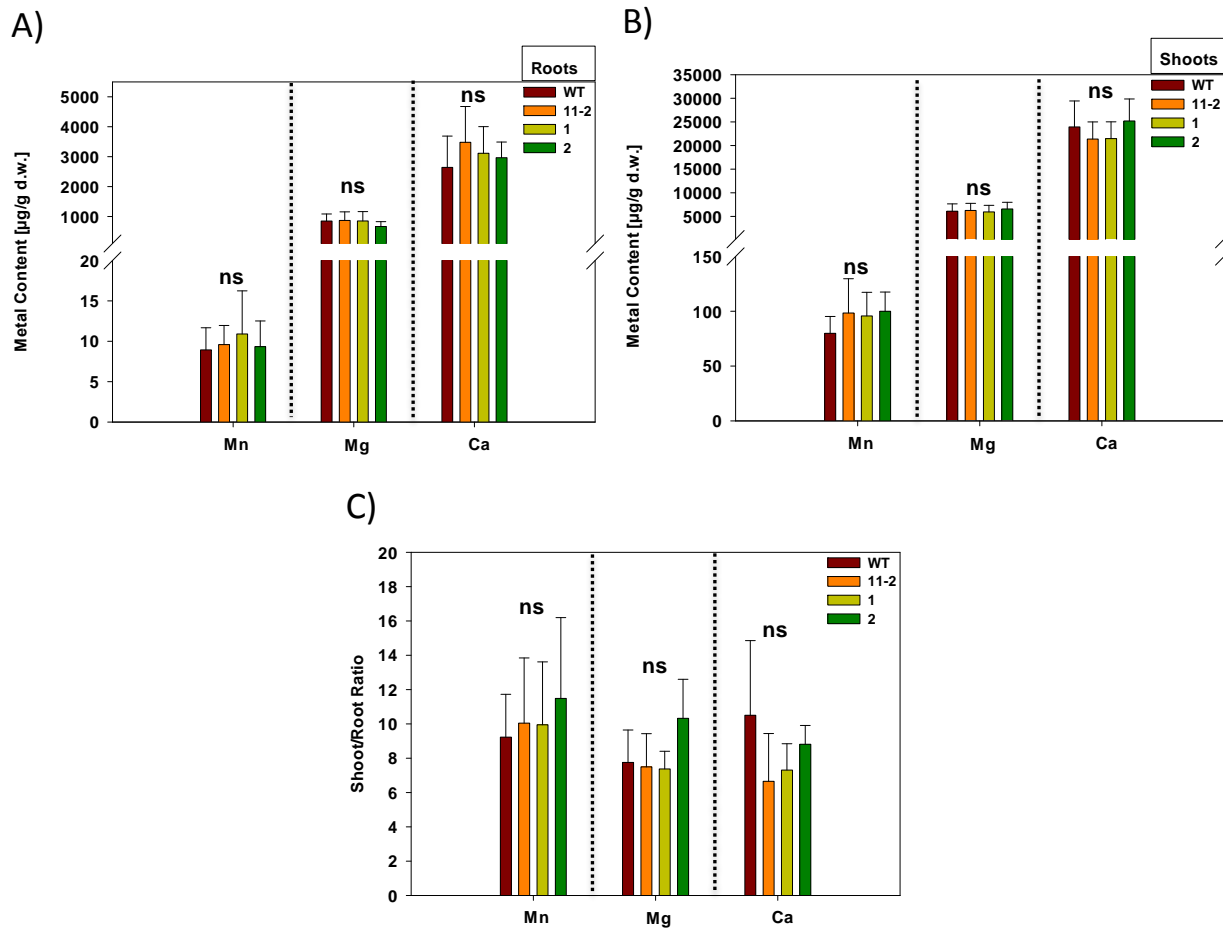


Fig. 3.14 Mn, Mg and Ca contents in roots and shoots of *A. halleri* wild-type and *AhNAS4*-RNAi plants hydroponically grown in standard medium for 10 days

Plants were cultivated in standard *A. halleri* 1/10 Hoagland medium. Tissues were harvested after 10 days, digested and analyzed by ICP-OES. Shown in (A) and (B) are values for roots and shoots, respectively. For (C), shoot: root ratios of Mn, Mg and Ca were calculated from contents shown above. All values are arithmetic means ± SD, n = 16 replicate clones per genotype from four independent experiments. There was no statistically significant differences detection between genotypes regarding each element in a one-way ANOVA, followed by Tukey test, ns: not significant.

3.2.2.4 *AhNAS4* suppression results in change in Fe localization pattern in roots

The ICP-OES data showed a strong reduction in bulk root Fe content upon *NAS4* suppression (Fig. 3.13 A). It was interesting to find out whether Fe localization also changes in roots of *A. halleri* upon *NAS4* suppression or not. To investigate that, root tissues of wild-type, control transformant and two *AhNAS4*-RNAi lines grown in standard *A. halleri* 1/10 Hoagland medium for 10 days were subjected to Perls staining with DAB intensification based on (Meguro et al., 2007; Roschztardt et al., 2009). Roots of two *AhNAS4* suppressed lines showed less stained and patchy distribution of Fe in comparison to the wild-type and control transformant line 11-2 (Fig. 3.15 A). In order to identify the possible differences in Fe distribution in root cell types among lines, cross sections of Perls stained roots were processed. Results showed that Fe was not distributed evenly along the roots

Results

and within cross sections, stained and non-stained sections were found, but overall a clear difference in Fe distribution pattern between two *AhNAS4* suppressed lines compared to the wild-type and control line was observed. Fe mainly was accumulated in the epidermis layer of wild-type and control lines, while in two *AhNAS4* suppressed lines Fe distribution was evenly among different cell types of roots and no outer layer Fe plaque formation was observed (Fig. 3.15 B).

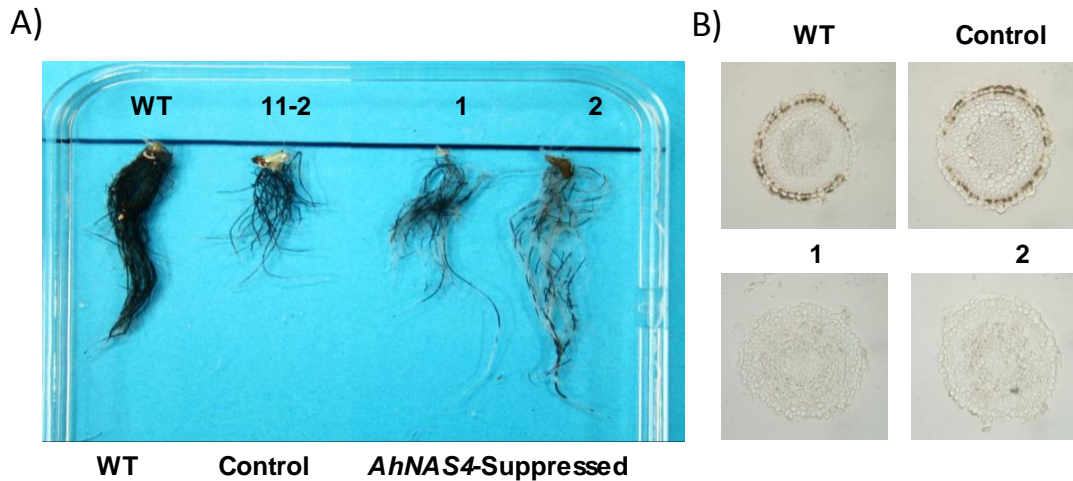


Fig. 3.15 Fe detection in roots of hydroponically grown *A. halleri* wild-type and *AhNAS4*-RNAi plants using the Perl's staining associated to intensification by DAB

Plants were cultivated in standard *A. halleri* 1/10 Hoagland medium and harvested after 10 days. Roots were subjected to Fe staining using the Perl's staining method associated to intensification by DAB. Photos represent roots of plants from three independent experiments. Shown in (A) are roots after Perl's staining associated to intensification by DAB. Shown in (B) are cross sections (7 μ m) of root tips after Perl's staining and intensification by DAB.

3.2.3. Silencing of *AhNAS4* increases tolerance towards Fe deficiency in *A. halleri* grown in alkaline medium

In order to assess the effect of *NAS4*-suppression in *A. halleri* under Fe limiting conditions, two *NAS4*-suppressed lines, wild-type and the control transformant line 11-2 were grown in alkaline (pH=7.2) 1/10 Hoagland medium for 3 weeks in growth chamber under controlled conditions. After 3 weeks of cultivation, *A. halleri* wild-type and control transformant line showed chlorosis in young leaves while *A. halleri* *NAS4*-suppressed lines had green young leaves with no detectable sign of chlorosis (Fig. 3.16). Regardless of plant genotypes, old leaves in all plants grown in alkaline medium were green and not suffering from Fe deficiency (Fig. 3.16).

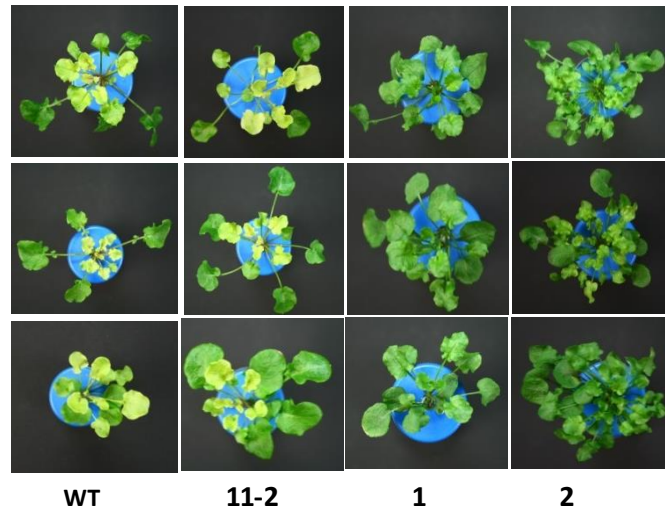


Fig. 3.16 Phenotype of *A. halleri* wild-type and *AhNAS4*-RNAi plant hydroponically grown in alkaline medium

Plants were cultivated in alkaline 1/10 Hoagland medium (pH=7.2) and photos were taken after 3 weeks of cultivation. All photographs of *AhNAS4*-RNAi and wild-type lines are representative of n =15 replicate clones per genotype from three independent experiments.

3.2.3.1 Silencing of *AhNAS4* results in more efficient root-to-shoot translocation specifically of Fe in *A. halleri*

Results suggested that root Fe contents of the two *NAS4*-suppressed lines were strongly reduced compared to the wild-type and control transformant plants. *AhNAS4*-suppressed line 1 had 52% and 55% lower root Fe content in comparison to the wild-type and control transformant line respectively. *AhNAS4*-suppressed line 2 had 49% and 53% lower root Fe content in comparison to the wild-type and control transformant line respectively (Fig. 3.17 A). Fe content in young leaves of both *AhNAS4*-suppressed lines was between 45% to 47% higher compared to the wild-type and control line. Results showed the Fe content differences between genotypes were bigger in their young leaves than in old leaves. Two *AhNAS4*-suppressed lines had between 19.5% and 30% higher Fe content compared to the wild-type and control line and total shoot Fe content in both *AhNAS4*-suppressed lines was between 21% to 35% higher compared to the wild-type and control transformant line (Fig. 3.17 B). Shoot: root Fe ratio was approximately 2.7 to 3.5-fold increased in two *NAS4*-suppressed lines in comparison to the wild-type and transformant control line (Fig. 3.17 C). These results emphasize that suppression of *NAS4* in *A. halleri* increases root to shoot translocation of Fe.

Results

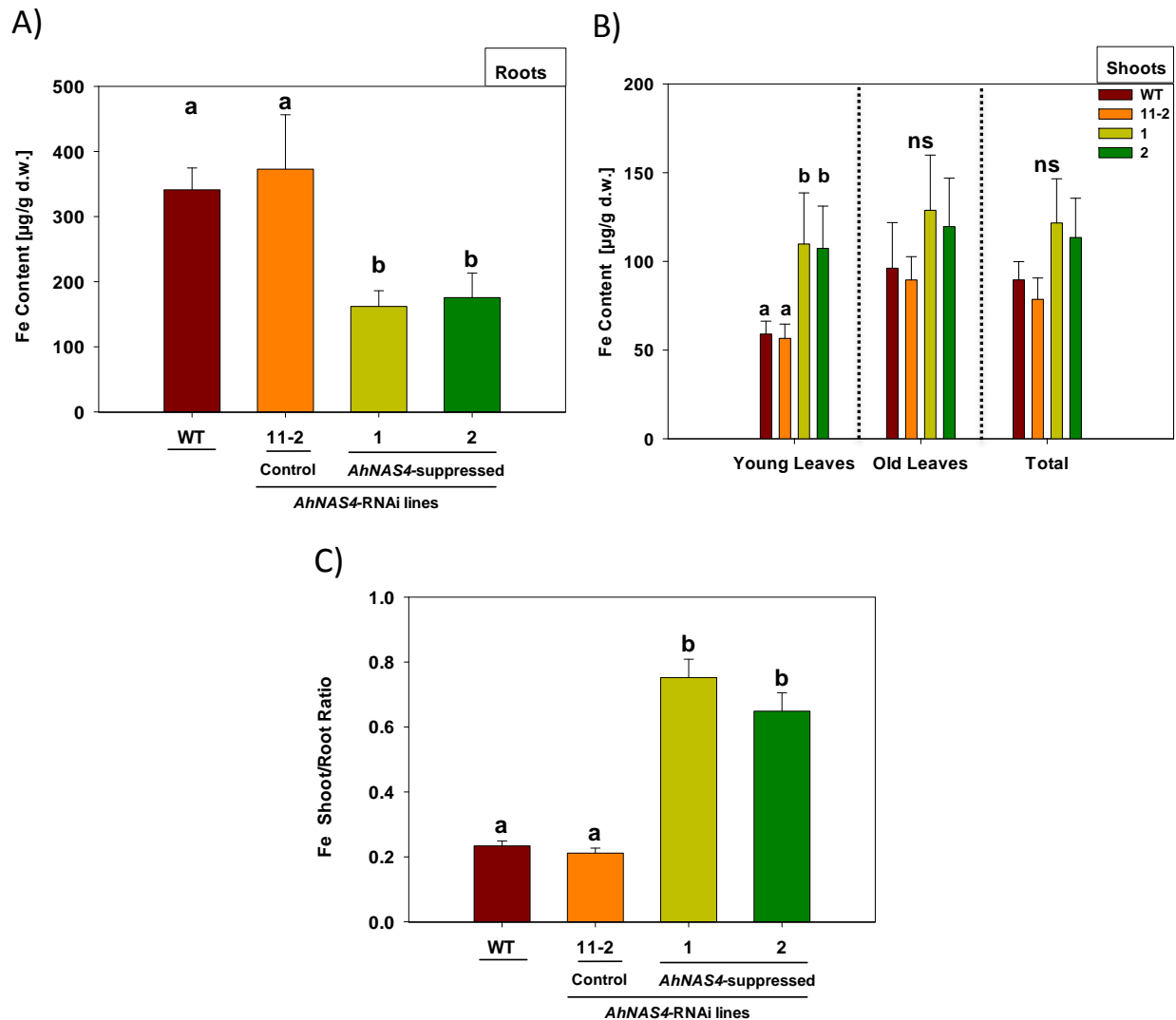


Fig. 3.17 Fe content in roots and shoots of *A. halleri* wild-type and *AhNAS4*-RNAi plants grown in alkaline medium

Plants were cultivated in alkaline (pH=7.2) 1/10 Hoagland medium. Tissues were harvested after 3 weeks, digested and analyzed by ICP-OES. Shown in (A) are values for roots and (B) are values for separated young and old leaves and total shoot Fe content. For (C), shoot: root Fe ratio was calculated from data shown above. All values are arithmetic means \pm SD, $n = 15$ replicate clones per genotype from three independent experiments. Different characters above the bars indicate statistically significant differences detected in a one-way ANOVA, followed by Tukey test A: $P < 0.05$ significance level between (a) and (b), B: $P < 0.05$ significance level between (a) and (b), C: $P < 0.001$ significance level between (a) and (b), ns: not significant.

3.2.3.2 Silencing of *AhNAS4* does not change root-to-shoot translocation of Zn in *A. halleri* plants grown in alkaline medium

In plants hydroponically grown in alkaline (pH=7.2) medium, two *NAS4*-suppressed lines had similar root Zn content compared to the wild-type and transformant control line (Fig. 3.18 A). In young leaves there was an insignificant slight reduction in Zn content in *NAS4*-suppressed lines compared to the wild-type and control plants, which was vice versa in old leaves and *NAS4*-suppressed lines

Results

had slightly insignificant higher Zn content compared to the wild-type and control line. There was a trend that suppression of *AhNAS4* slightly and not significantly increases Zn accumulation in total leaves in comparison to the wild-type and control plants (Fig. 3.18 B). Root-to-shoot translocation of Zn seems also slightly but not significantly increased in *AhNAS4* suppressed lines (Fig. 3.18 C).

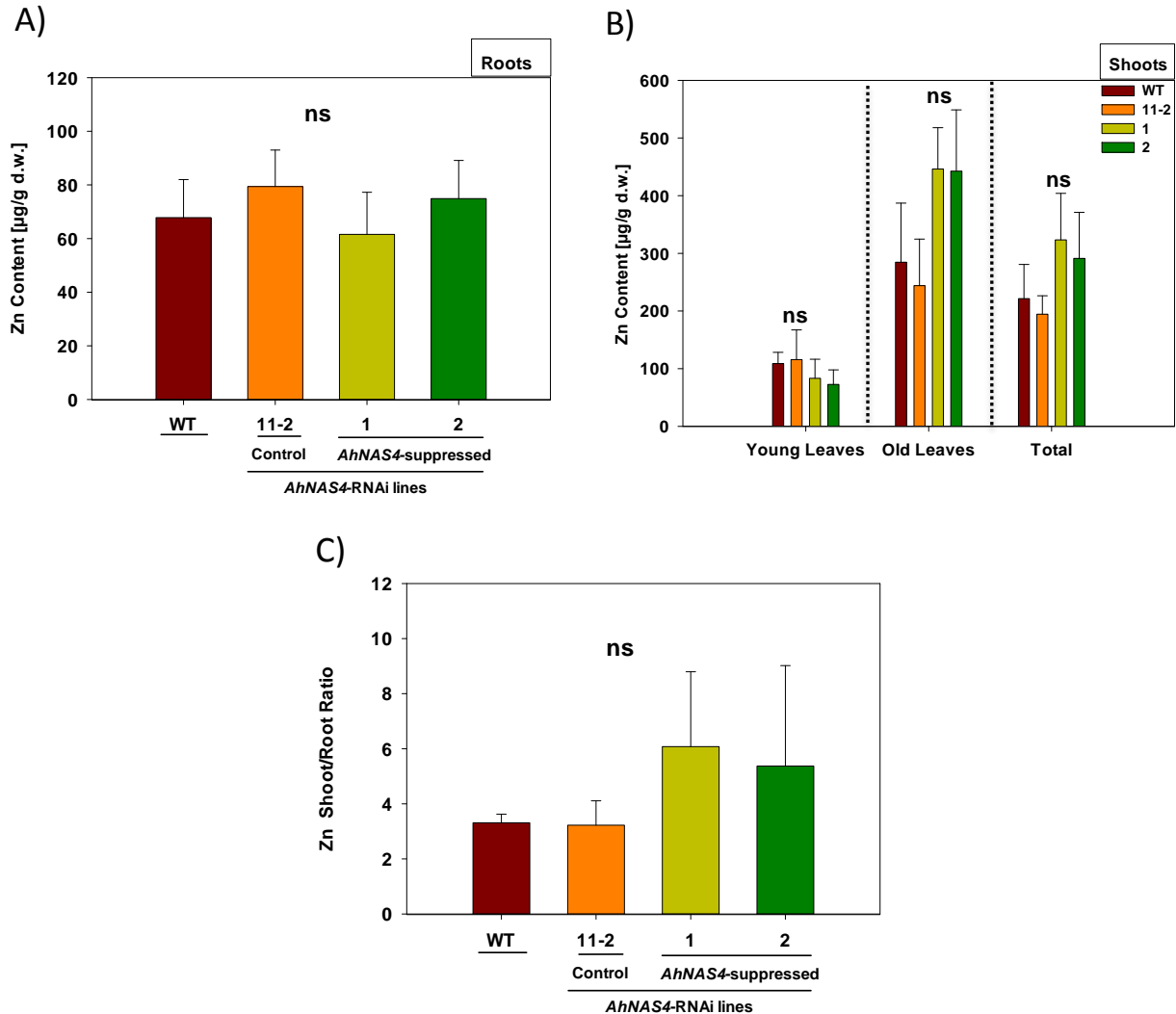


Fig. 3.18 Zn content in roots and shoots of *A. halleri* wild-type and *AhNAS4*-RNAi plants grown in alkaline medium

Plants were cultivated in alkaline (pH=7.2) 1/10 Hoagland medium. Tissues were harvested after 3 weeks, digested and analyzed by ICP-OES. Shown in (A) are values for roots and (B) are values for separated young and old leaves and total shoot Zn content. For (C), shoot: root Zn ratio was calculated from data shown above. All values are arithmetic means \pm SD, $n = 15$ replicate clones per genotype from three independent experiments. ns: not significant.

Results

3.2.3.3 Silencing of *AhNAS4* does not change root and shoot Mn, Mg and Ca contents in *A. halleri* plants grown in alkaline medium

AhNAS4 suppression had no effect on of Mg and Ca contents in roots of *A. halleri* plants grown in alkaline medium (Fig. 3.19 A). There was a non- significant trend that *AhNAS4*-suppressed lines had more Mn in roots than the wild-type and transgenic control lines (Fig. 3.19 A). In young leaves (Fig. 3.19 B), old leaves (Fig. 3.19 C) and total shoots of plants grown in alkaline medium conditions, there were no significant differences between genotypes regarding Mn, Mg and Ca contents.

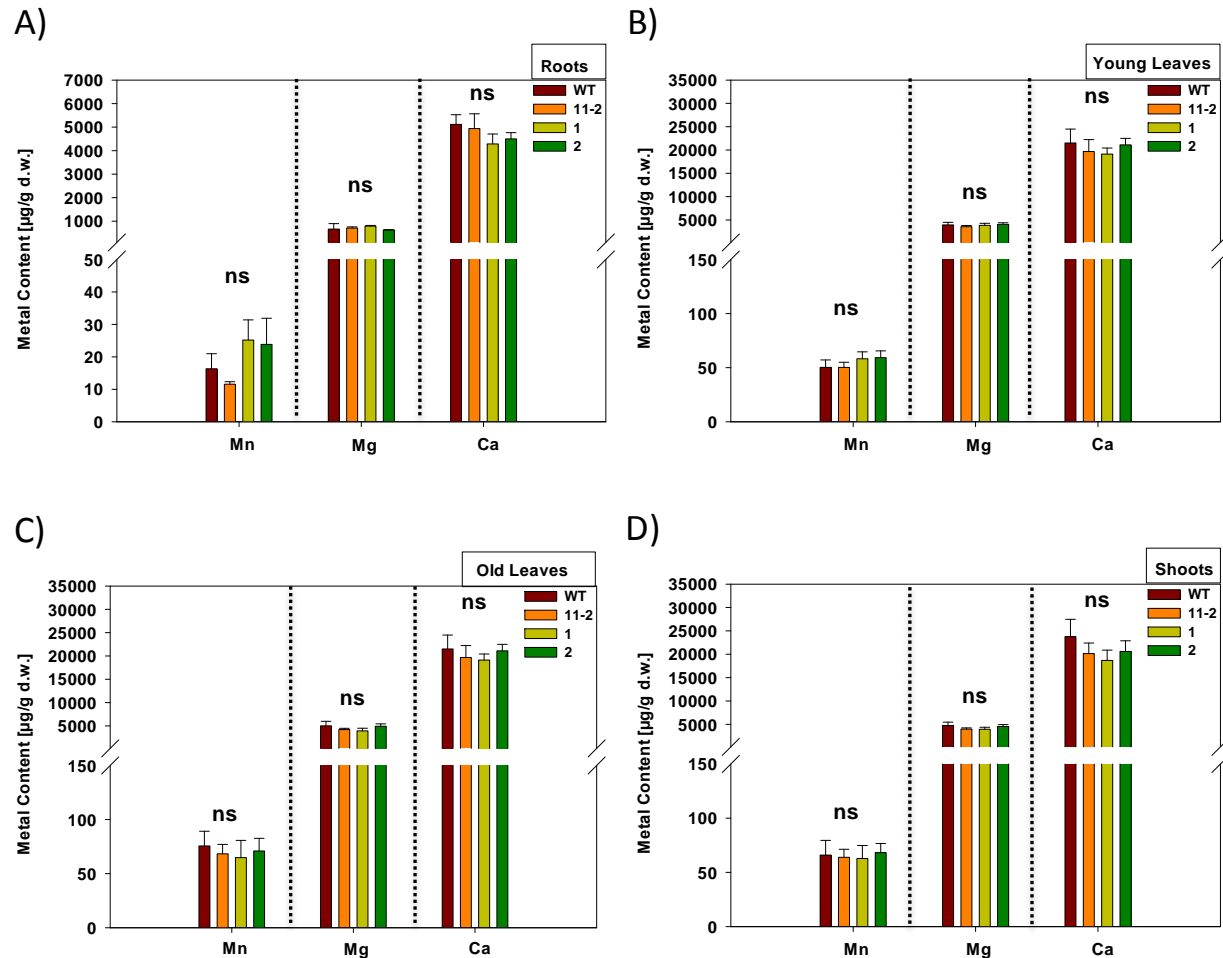


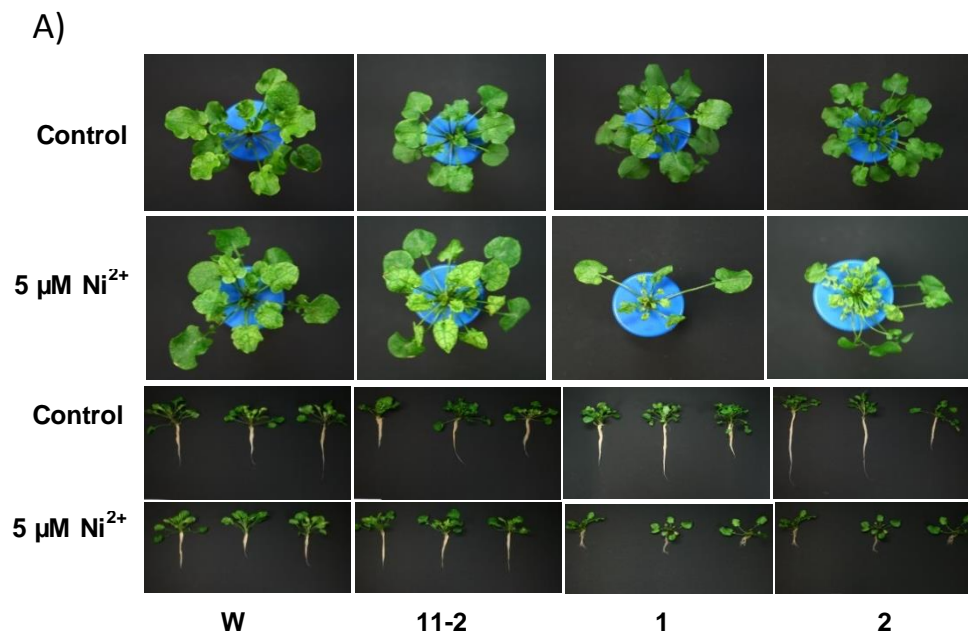
Fig. 3.19 Metal content in roots and shoots of *A. halleri* wild-type and *AhNAS4*-RNAi plants grown in alkaline medium

Plants were cultivated in alkaline (pH=7.2) 1/10 Hoagland medium. Tissues were harvested after 3 weeks, digested and analyzed by ICP-OES. Shown in (A) are values for roots (B) are values for separated young and (C) old leaves and (D) total shoot metal content. All values are arithmetic means \pm SD, n = 15 replicate clones per genotype from three independent experiments. ns: not significant .

Results

3.2.4. *AhNAS4* suppression causes Ni hypersensitivity in *A. halleri*

It has been shown that increasing NA synthesis led to Ni tolerance in *A. thaliana* or tobacco (Douchkov et al., 2005; Kim et al., 2005). The *A. thaliana nas4-1* mutants, which are unable to produce *NAS4* transcript, are sensitive to excess level of Ni and suffer from severe growth defects in comparison to the wild-type when grown on soil with extra Ni (Klatte et al., 2009; Palmer et al., 2013). In *A. halleri*, *AhNAS2*-RNAi lines, which have reduced amounts of root NA level, also showed Ni hypersensitivity. These strong *AhNAS2*-RNAi lines when grown hydroponically in 1/10 Hoagland medium supplemented with extra 5 μM Ni^{2+} showed severe reduction in root elongation and a slightly stronger reduction in root biomass than the wild-type (Cornu et al., 2015). In order to test the effects of *AhNAS4* suppression on Ni tolerance, wild-type, control *AhNAS4*-RNAi line 11-2 and two strong *AhNAS4*-RNAi line 1 and 2 were grown hydroponically under control conditions and with additional 5 μM Ni^{2+} as described in (Cornu et al., 2015). There were no detectable differences in root growth and plant biomass between lines under control conditions (Fig. 3.28 A). Upon addition of 5 μM Ni^{2+} , wild-type and control line showed interveinal and whole-leaf chlorosis which are known symptoms of Ni toxicity in plants (Ghasemi et al., 2009). No significant reduction in root length and biomass and shoot biomass was detected in wild-type and control transgenic line upon addition of 5 μM Ni^{2+} (Fig. 3.20 A). By contrast, upon addition of 5 μM Ni^{2+} to the growth medium, two strong RNAi lines 1 and 2 showed a severe reduction in root elongation and a slightly stronger reduction in root biomass compared to the wild-type and control RNAi line 11-2 (Fig. 3.20 B and C). Two strong *AhNAS4*-RNAi lines also showed significantly reduced shoot biomass in comparison to control lines (Fig. 3.20 D), which was not detectable in for *Ah-NAS2*-RNAi lines as reported by (Cornu et al., 2015).



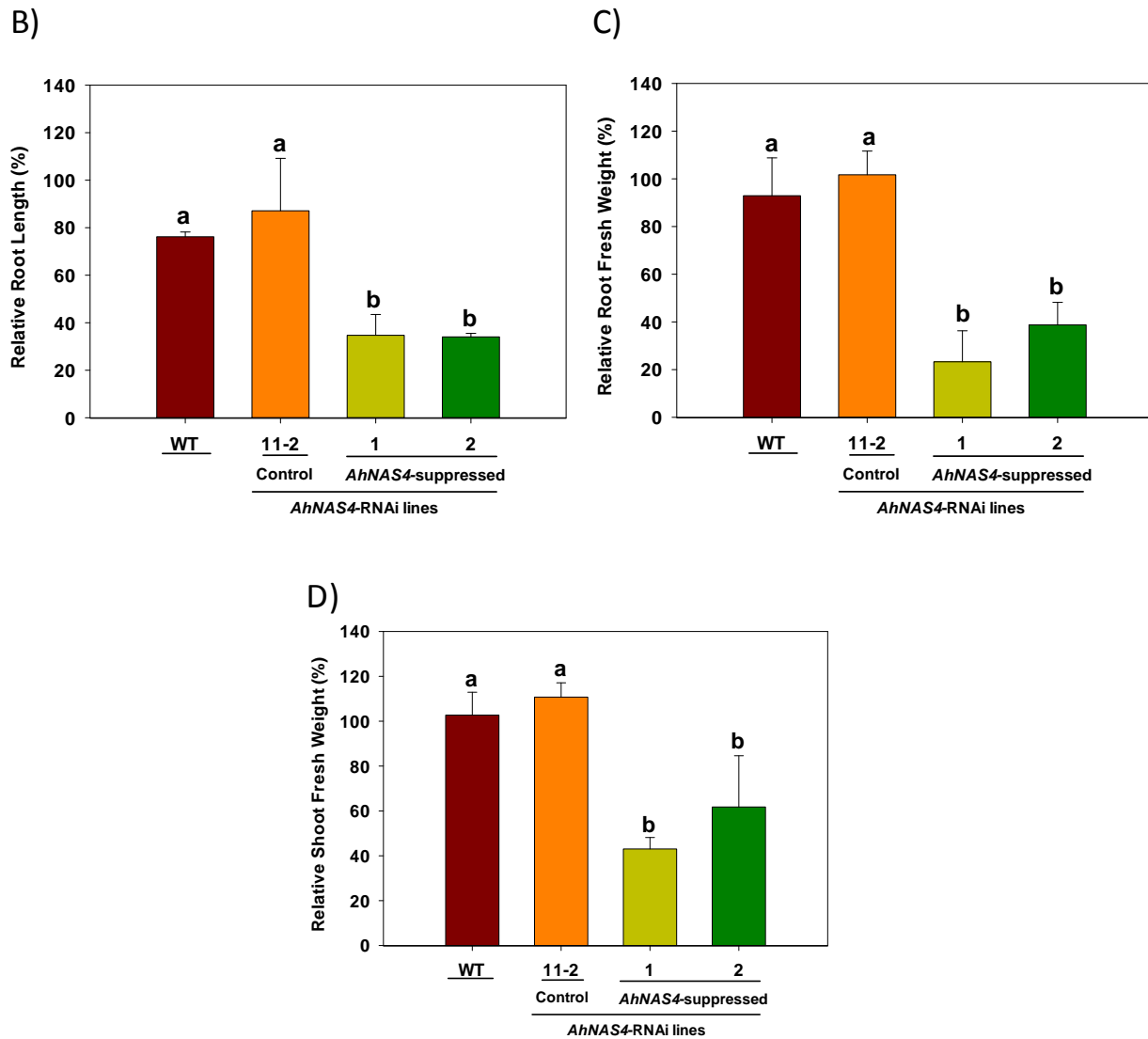


Fig. 3.20 *AhNAS4* suppression causes Ni hypersensitivity in *A. halleri*

Shown in (A) are photographs of representative wild-type, control transformant *AhNAS4*-RNAi line 11-2 and two *AhNAS4*-suppressed line 1 and 2; three individuals each in three independent runs were grown hydroponically in 1/10 Hoagland medium with no additional metal ions as control and with additional 5 μM Ni^{2+} for 3 weeks. Upper part is top view and down part is longitude view of plants. Shown in (B, C and D) summaries of relative root length (B) relative root fresh weight (C) and relative shoot fresh weight (D), expressed as a percentage of growth in control medium. All values are arithmetic means \pm SD, $n = 9$ replicate clones per genotype from three independent experiments. Different characters above the bars indicate statistically significant differences detected in a one-way ANOVA, followed by Tukey test. B: $P < 0.05$ significance level between (a) and (b), C: $P < 0.01$ significance level between (a) and (b), D: $P < 0.05$ significance level between (a) and (b).

Results

3.2.4.1. *AhNAS4* suppression has no effect on root and shoot Ni content in *A. halleri*

To analyze possible effects of *AhNAS4* suppression on Ni root–shoot partitioning in hydroponically grown plants, elemental profiling was performed for roots and shoots via ICP-OES. With a non-significant trend of reduction in root Ni contents of *AhNAS4* suppressed lines compared to the wild-type and control transformant lines, Ni content in roots and shoots of all genotypes was comparable (Fig. 3.21 A and B). Therefore, Ni shoot: root ratio was comparable in two strong RNAi lines in comparison to the wild-type and control transgenic line (Fig. 3.21 C).

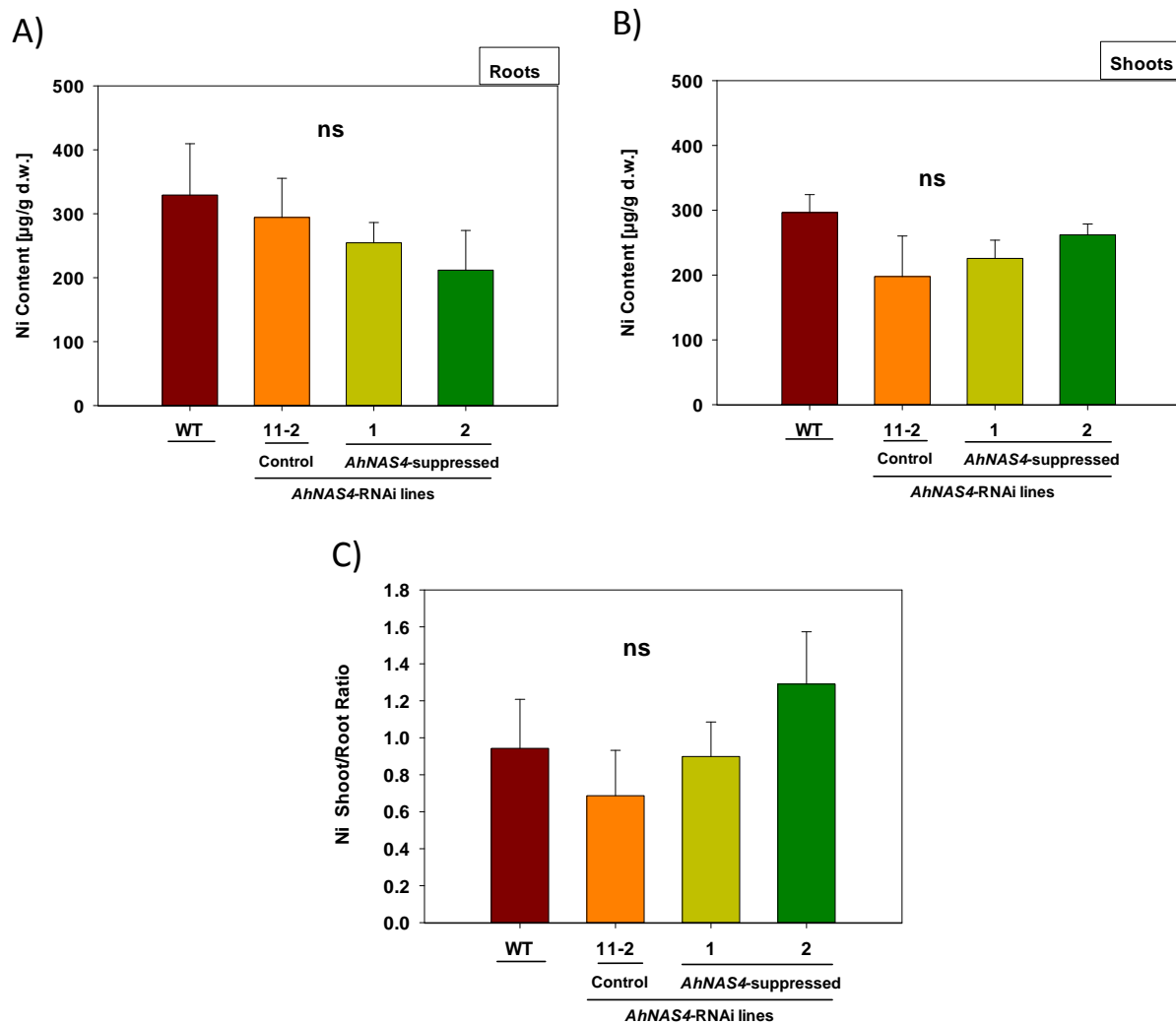


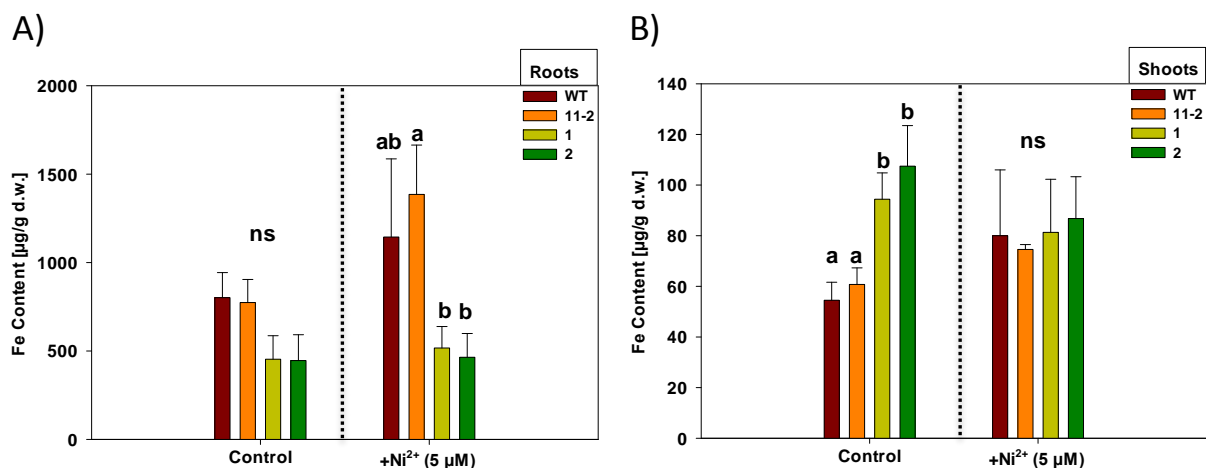
Fig. 3.21 *AhNAS4* suppression has no effect on root and shoot Ni content in *A. halleri*

Plants were cultivated in 1/10 Hoagland medium supplemented with additional 5 μM Ni^{2+} . Tissues were harvested after 3 weeks, digested and analyzed by ICP-OES. Shown in (A) and (B) are values for root and shoot Ni content respectively. For (C), shoot: root ratio of Ni was calculated from data shown above. All values are arithmetic means \pm SD, $n = 9$ replicate clones per genotype from three independent experiments. ns: not significant, indicate statistically not significant differences detected in a one-way ANOVA, followed by Tukey test.

Results

3.2.4.2. *AhNAS4* suppression specifically enhances Fe root-to-shoot translocation under control and Ni stress conditions

In control conditions there was a non-significant 42% to 44% reduction in root Fe contents of two *NAS4*-suppressed lines compared to the wild-type and control transformant plants respectively (Fig. 3.22 A). Analysis of plants grown in medium supplemented with 5 μM Ni^{2+} showed higher, but not significant reduction in root Fe contents of *NAS4*-suppressed lines compared to the wild-type. *NAS4*-suppressed line 1 and line 2 showed respectively 54% to 59% reduction in root Fe content compared to the wild-type and significantly 62% to 66% reduction in root Fe contents of *NAS4*-suppressed line 1 and line 2 compared to the control transformant 11-2 plants (Fig. 3.22 A). In plants grown in control medium both *NAS4*-suppressed lines showed higher shoot Fe content in comparison to the wild-type and control transformant 11-2 plants. *NAS4*-suppressed line 1 had 35% of higher Fe content in shoot compared to the control line and to 42% of higher Fe content in comparison to the wild-type plants. *NAS4*-suppressed line 2 showed 43% to 49% higher shoot Fe content compared to the control line and wild-type respectively (Fig. 3.22 B). There was no detectable differences between genotypes regarding shoot Fe content after growth in medium supplemented with 5 μM Ni^{2+} (Fig. 3.22 B). Fe shoot: root ratio was increased under both control and Ni stress conditions in *AhNAS4*-suppressed lines compared to the wild-type and control lines. In control conditions, *AhNAS4*-suppressed line 1 had 2.59 to 3.13-fold higher Fe shoot: root ratio compared to control line 11-2 and wild-type respectively and *AhNAS4*-suppressed line 2 had 3.29 to 3.97-fold higher Fe shoot: root ratio compared to control line 11-2 and wild-type respectively (Fig. 3.22 C). In medium supplemented with 5 μM Ni^{2+} , *AhNAS4*-suppressed line 1 showed 2.67 to 3.23-fold higher Fe shoot: root translocation in comparison to the wild-type and control RNAi line 11-2 respectively and *AhNAS4*-suppressed line 2 had 2.99 to 3.62-fold higher Fe shoot: root ratio compared to control RNAi line and wild-type respectively (Fig. 3.22 C).



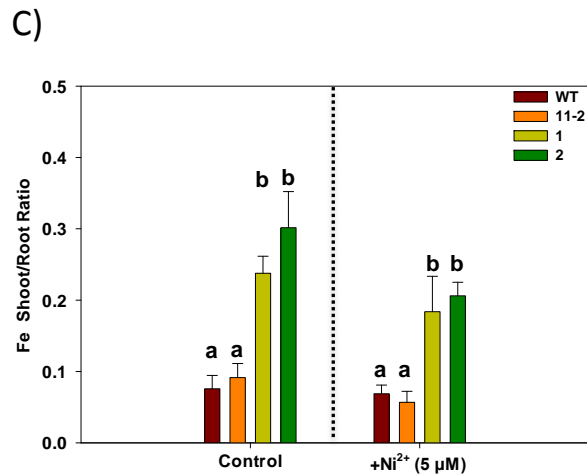


Fig. 3.22 *AhNAS4* suppression specifically enhances Fe root-to-shoot translocation under control and Ni stress conditions

Plants were cultivated in 1/10 Hoagland medium as control or in medium supplemented with additional 5 µM Ni²⁺. Tissues were harvested after 3 weeks, digested and analyzed by ICP-OES. Shown in (A) and (B) are values for roots and shoots in both conditions respectively. For (C), shoot: root Fe ratio was calculated from data shown above. All values are arithmetic means ± SD, n= 9 replicate clones per genotype from three independent experiments. Different characters above the bars indicate statistically significant differences detected in a one-way ANOVA, followed by Tukey test. A: P < 0.05 significance level between (a) and (b), B: P < 0.05 significance level between (a) and (b), C: P < 0.01 significance level between (a) and (b), ns: not significant.

3.2.4.3. *AhNAS4* suppression has no effect on root and shoot Zn content in *A. halleri* hydroponically grown for 3 weeks under control and Ni stress conditions

It has been shown that suppression of *AhNAS2* as a major responsible gene for root nicotianamine synthesis led to a reduction of Zn root to shoot translocation in plants grown in medium with extra 5 µM Ni²⁺ (Cornu et al., 2015). Results suggested that Zn content in root and shoot of plants grown in control medium or in the medium with extra 5 µM Ni²⁺ were comparable in all tested lines (Fig. 3.23 A, C) and consequently, Zn shoot : root ratio was comparable in two strong RNAi lines in comparison to the wild-type and control transgenic line 11-2 (Fig. 3.23 C).

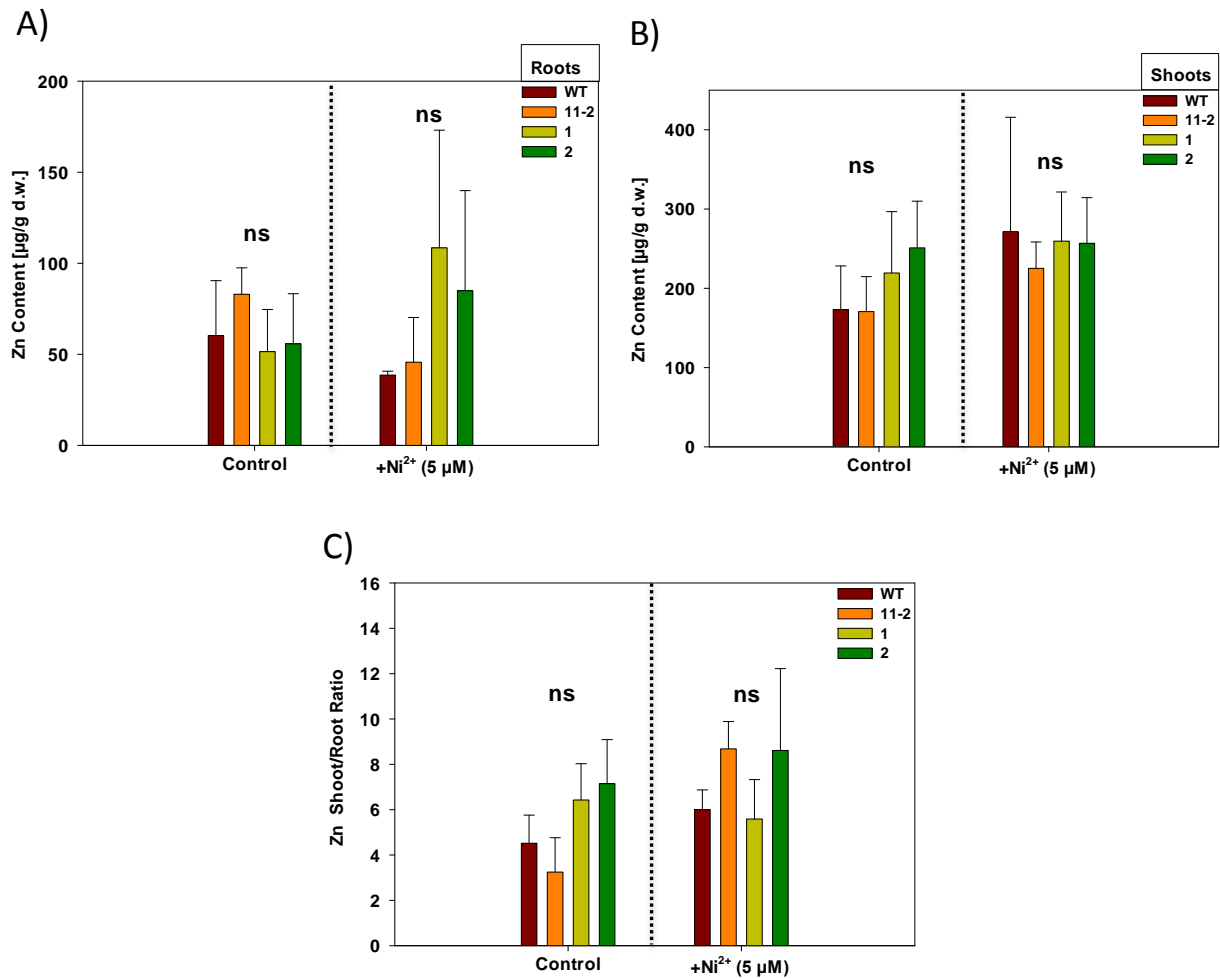


Fig. 3.23 *AhNAS4* suppression has no effect on root and shoot Zn content in *A. halleri* hydroponically grown for 3 weeks under control and Ni stress conditions

Plants were cultivated in 1/10 Hoagland medium as control or in medium supplemented with additional 5 µM Ni²⁺. Tissues were harvested after 3 weeks, digested and analyzed by ICP-OES. Shown in (A) and (B) are values for roots and shoots in both conditions, respectively. For (C), shoot: root Fe ratio was calculated from data shown above. All values are arithmetic means ± SD, n = 9 replicate clones per genotype from three independent experiments. ns: not significant.

3.2.5. *AhNAS4* suppression has no effect on excess Zn and Cd tolerance in *A. halleri*

To analyze possible effects of *AhNAS4* suppression on excess Zn and Cd tolerance in *A. halleri*, wild-type plants, control *AhNAS4*-RNAi line 11-2 and two *AhNAS4*-suppressed lines 1 and 2 hydroponically grown in control 1/10 Hoagland medium or in media supplemented with additional 10 µM Cd²⁺ or 300 µM Zn²⁺ in 1.5 liter pots in growth chamber for 3 weeks. There were no detectable differences between genotypes in root length, root and shoot biomass in control conditions (Fig. 3.24). Likewise, in excess Zn conditions there were no significant phenotypical differences between genotypes (Fig. 3.24). Upon addition of 10 µM Cd²⁺, plants showed reduced root and shoot biomass, indicating toxicity of the metal excess. Surprisingly *AhNAS4*-suppressed line 2

Results

showed severe reduction in root length root biomass and shoot biomass compared to control lines and even to the other *AhNAS4*-suppressed line 1. However, no significant differences between the control lines and *AhNAS4*-suppressed line 2 were observed (Fig. 3.24).

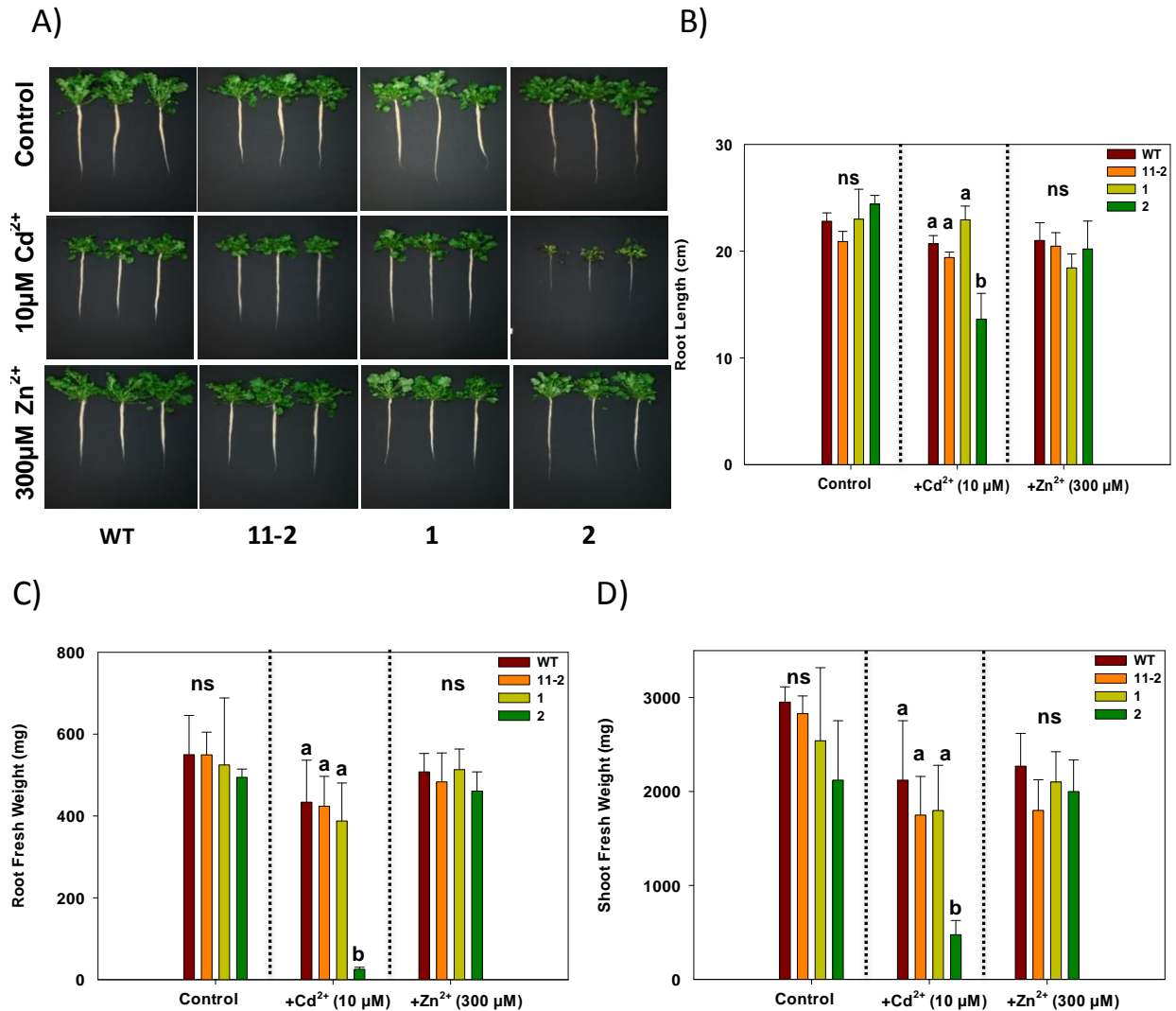


Fig. 3.24 *AhNAS4* suppression has no effect on tolerance towards excess Zn and Cd in *A. halleri*

Shown in (A) are photographs of representative wild-type, control transformant *AhNAS4*-RNAi line 11-2 and two *AhNAS4*-suppressed line 1 and 2 plants grown hydroponically for 3 weeks in control 1/10 Hoagland medium or in media supplemented with additional 10 μM Cd²⁺ or 300 μM Zn²⁺. Shown in (B, C and D) are root length (B) root fresh weight (C) and shoot fresh weight (D). All values are arithmetic means ± SD, n = 3 replicate clones per genotype. Different characters above the bars indicate statistically significant differences detected in a one-way ANOVA, followed by Tukey test. B: P < 0.01 significance level between (a) and (b), C: P < 0.01 significance level between (a) and (b), D: P < 0.05 significance level between (a) and (b), ns: not significant.

Results

3.2.6 Silencing of *AhNAS4* increases tolerance towards Fe deficiency in *A. halleri* grown in alkaline soil

It has been shown that in *A. thaliana*, *NAS4-1* mutants are very sensitive to Fe deficiency and upon growth in alkaline soil, they show reduced size and interveinal chlorosis (Palmer et al, 2013). To test the effect of *NAS4* suppression on *A. halleri* grown in alkaline soil, two *NAS4*-suppressed lines, wild-type and the control transformant line 11-2 were grown in normal and alkaline soils in parallel for 6 weeks in growth chamber under controlled conditions. After 6 weeks of cultivation on alkaline soil, surprisingly *A. halleri* wild-type and control transformant line showed chlorosis in all leaves produced after transferring cuttings to the soil, while leaves of *A. halleri* *NAS4*-suppressed lines were green and had no detectable sign of chlorosis (Fig. 3.25 A). Chlorosis in *A. halleri* wild-type and control transformant lines grown in alkaline soil could be rescued by application of exogenous Fe as described by Palmer et al., (2013) via watering plants growing in alkaline soil with 500 μM FeEDDHA (Fig. 3.25 B). Wild-type and control transformant line 11-2 grown in alkaline soil showed significantly reduced shoot biomass in comparison to *AhNAS4*-suppressed lines (Fig. 3.25 C).

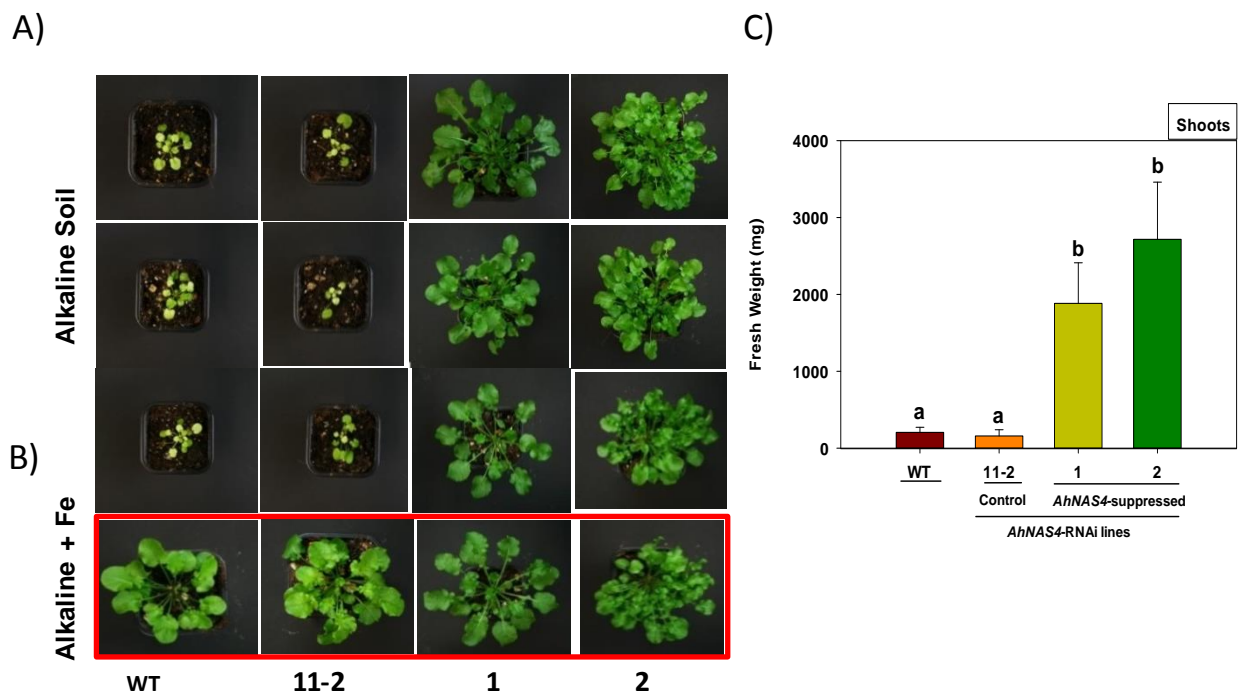


Fig. 3.25 Phenotype of soil-grown *A. halleri* wild-type and *AhNAS4*-RNAi plants under alkaline (Fe-limiting) and alkaline + Fe (excess Fe) conditions

Photographs of *A. halleri* wild-type and *AhNAS4*-RNAi plants cultivated in alkaline soil (pH=7.8) (A) or alkaline soil +Fe (B) after 6 weeks. Shown in (C) are values for shoot fresh biomass of plants harvested after 6 weeks of cultivation. All photographs of *AhNAS4*-RNAi and wild-type lines are representative of $n = 15$ replicate clones per genotype from three independent experiments. Different characters above the bars indicate statistically significant differences detected in a Kruskal-Wallis One Way Analysis of Variance on, C: $P < 0.001$ significance level between (a) and (b).

Wild-type plants, control line 11-2 and two *AhNAS4*-suppressed lines grown in normal soil were green and healthy with no sign of chlorosis or visible differences between genotypes (Fig. 3.26 A).

Results

Results suggested that there was no difference in shoot fresh biomass among plants from different genotypic backgrounds (Fig. 3.26 B).

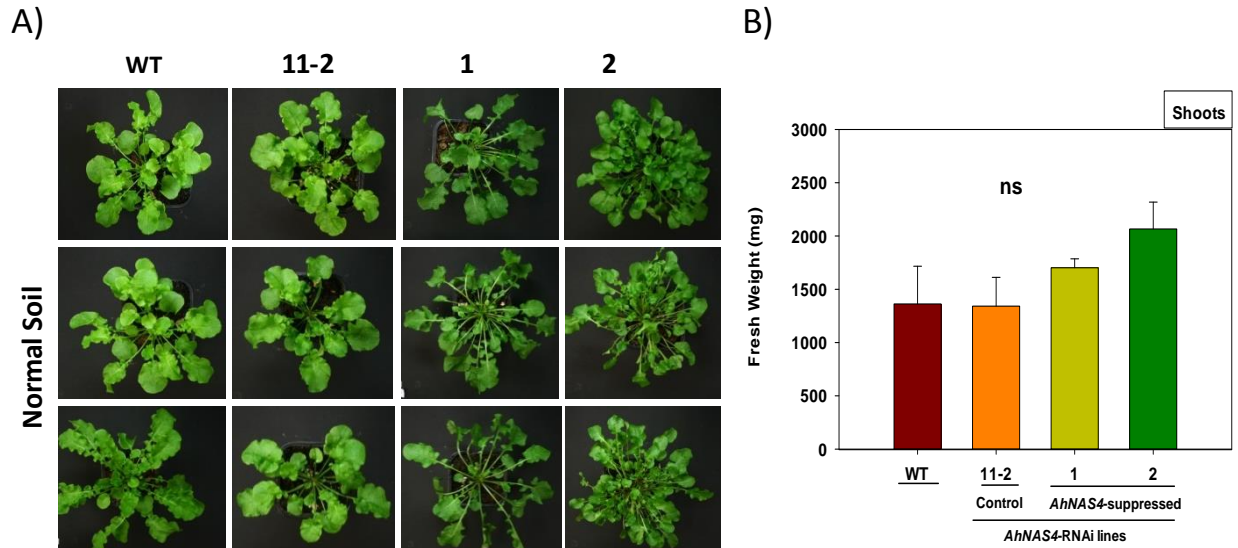


Fig. 3.26 Phenotype of normal soil-grown *A. halleri* wild-type and *AhNAS4*-RNAi plants

Photographs of *A. halleri* wild-type and *AhNAS4*-RNAi plants cultivated in normal soil (A) or alkaline soil (pH=7.8) after 6 weeks. (B) Shoot fresh biomass of plants was harvested after 6 weeks of cultivation. All photographs of *AhNAS4*-RNAi and wild-type lines are representative of $n = 15$ replicate clones per genotype from three independent experiments. There were no statistically significant differences between genotypes in a one-way ANOVA, followed by Tukey test, ns: not significant.

3.2.6.1 Silencing of *AhNAS4* results in higher chlorophyll content in leaves of *A. halleri* in alkaline soil

In planta, Fe serves as a cofactor in the photosynthetic electron transport chain and is essential for chlorophyll biosynthesis. Fe deficient plants often show decreased levels of chlorophyll (Cornu et al., 2015; Palmer et al., 2013). Chlorophyll a, b and total chlorophyll levels in plants grown on alkaline and normal soils were measured. Results showed that in plants grown in normal soil, there were no significant differences in chlorophyll a, chlorophyll b and total chlorophyll content between genotypes (Fig. 3.27 A). In plants grown in alkaline soil, chlorophyll a content in two *NAS4*-suppressed lines was between 123% to 163% higher than those of wild-type and control transformant plants. Chlorophyll b content in both *NAS4*-suppressed lines was between 142% to 144% higher for line 2 and more than 100% higher for line 1 than those of wild-type and control transformant plants respectively. Total chlorophyll content in both *NAS4*-suppressed lines was higher than those of wild-type and control transformant plants, between 2.5 to 2.75-fold for line 2 and 2.17 to 2.34-fold for line 1 respectively (Fig. 3.27 B).

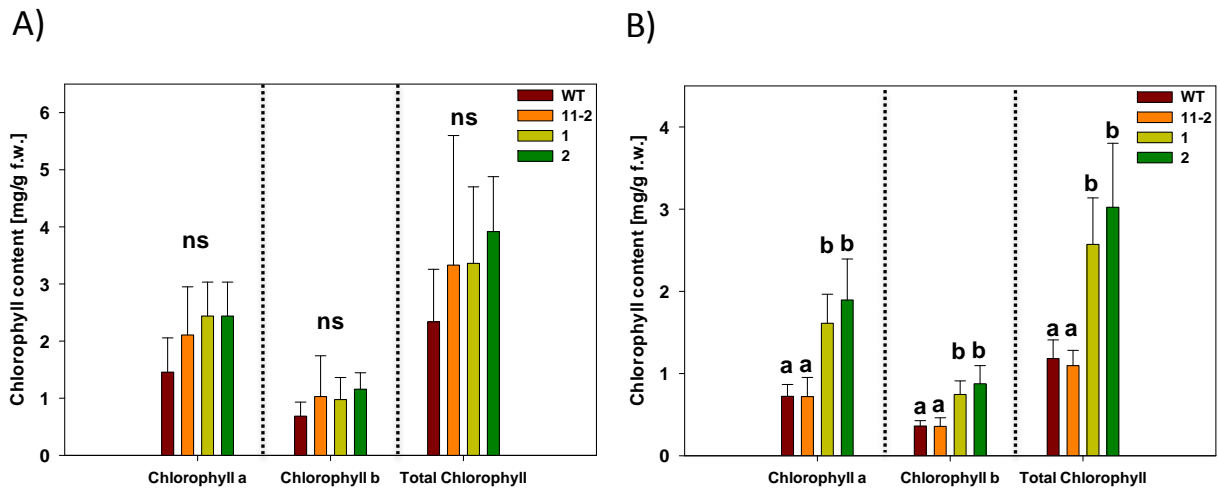


Fig. 3.27 Chlorophyll content of *A. halleri* wild-type and *AhNAS4*-RNAi plants grown in normal and alkaline soils

Plants were cultivated in normal or alkaline (pH=7.8) soils. Tissues were harvested after 6 weeks and chlorophyll levels measured. Shown in (A) and (B) are chlorophyll a, b and total chlorophyll levels of plants grown in normal and alkaline soils respectively. All values are arithmetic means \pm SD, n = 15 replicate clones per genotype from three independent experiments. Different characters above the bars indicate statistically significant differences detected in a one-way ANOVA, followed by Tukey test B: P < 0.05 significance level between (a) and (b), ns: not significant.

3.2.6.2 Silencing of *AhNAS4* results in higher catalase activity in leaves of *A. halleri* grown in alkaline soil

Fe has a critical role in abundant proteins of photosynthesis and respiration, as well as in antioxidant activities (Ghasemi et al., 2009). Catalases are the primary enzymatic detoxifiers of H₂O₂ in most plant tissues (Anderson, 2002). In stress conditions plants increase the activity of several group of antioxidant enzymes including Fe dependent enzymes such as catalases to cope with ROS (Jozefczak et al., 2014). Since catalase enzymes are Fe dependent, catalase activity measurement could be an index of Fe status in plants (Bernal et al., 2012), therefore to determine effect of *AhNAS4* suppression on the catalase activity, *A. halleri* wild-type and *AhNAS4*-RNAi plants grown on alkaline soil were used for determination of catalase activity. Results showed that there is a trend of increase in catalase activity of *AhNAS4* suppressed lines in comparison to the wild-type and control transformant lines (Fig. 3.28).

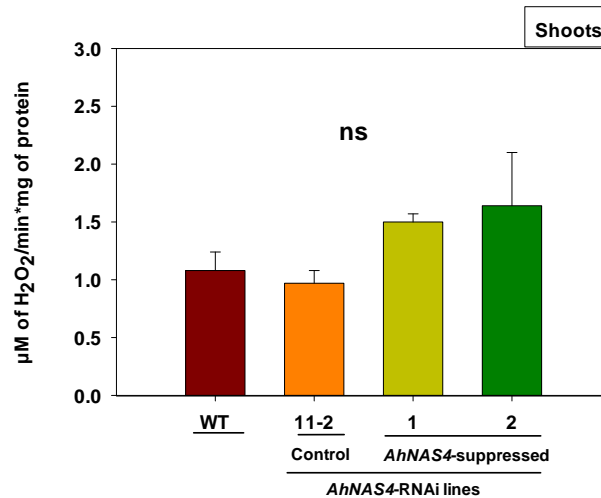


Fig. 3.28 Catalase activity of *A. halleri* wild-type and *AhNAS4*-RNAi plants grown in alkaline soil

Plants were cultivated in alkaline soil (pH=7.8), Tissues were harvested after 6 weeks and catalase activity was measured in leaves. All values are arithmetic means \pm SD, n = 3 independent experiments (Five replicate clones per genotype were pooled for each data point). There were no statistically significant differences between genotypes in a one-way ANOVA, followed by Tukey test, ns: not significant.

3.2.6.3. Fe content in shoots of *A. halleri* plants grown in normal and alkaline soils

AhNAS4-suppressed lines cultivated alongside wild-type and control plants in both normal and alkaline soils had higher Fe content than wild-type and control transformant lines. In normal soil, shoot Fe content of *AhNAS4*-suppressed line 1 was 50% and 26% higher than wild-type and control transformant line respectively. *AhNAS4*-suppressed line 2 had 55% and 32% more shoot Fe content than wild-type and control transformant line respectively. In alkaline soil, differences were more visible, where shoot Fe content of *AhNAS4*-suppressed line 1 was 47% and 45% higher than wild-type and control transformant line respectively. *AhNAS4*-suppressed line 2 had 56% and 54% more shoot Fe content than wild-type and control transformant line respectively (Fig. 3.20 A and B). Although *AhNAS4*-suppressed lines had higher Fe content compared to the wild-type and control transformant lines, due to high deviation in their Fe content levels no significant differences detected in a one-way ANOVA, followed by Tukey test (Fig. 3.29 A and B). Interestingly, Fe content of all plants regardless of their genotypes was comparable in both alkaline and normal soil conditions (Fig. 3.29 A and B).

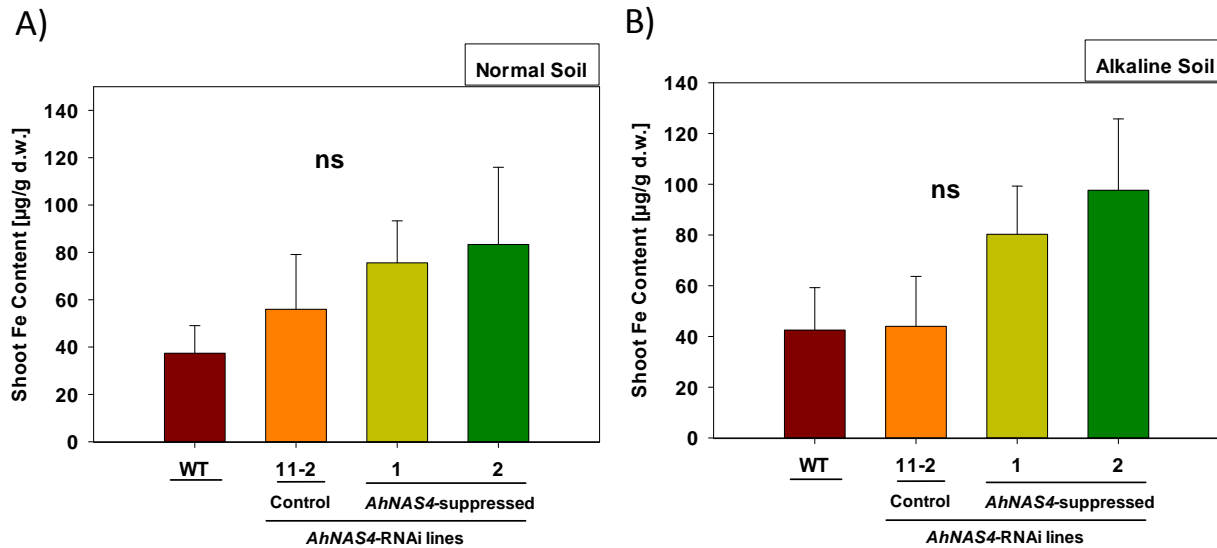


Fig. 3.29 Fe content in shoots of *A. halleri* wild-type and *AhNAS4*-RNAi plants grown in normal and alkaline soils

Plants were cultivated in normal or alkaline (pH=7.8) soils. Tissues were harvested after 6 weeks, digested and analyzed by ICP-OES. Shown in (A) and (B) are values for Fe content in shoots of plants grown in normal or alkaline soil respectively. All values are arithmetic means \pm SD, n = 15 replicate clones per genotype from three independent experiments. ns: not significant, indicate statistically not significant differences detected in a one-way ANOVA, followed by Tukey test.

3.2.6.4 *AhNAS4* suppression decreases shoot Mg content of alkaline soil grown plants

AhNAS4 suppression had no effect on Mn and Zn contents in shoot of *A. halleri* plants grown in normal and alkaline soils (Fig. 3.21 A and B). In plants grown in normal soil, Ca content in *AhNAS4* suppressed line 1 was significantly lower than wild-type, but similar to control transformant line 11-2, *AhNAS4* suppressed line 2 had no difference in Ca content in comparison to the other genotypes (Fig. 3.30 A). There were no significant differences in Ca content between genotypes grown in alkaline soil. Both *AhNAS4* suppressed lines grown in normal soil had lower amount of Mg in comparison to the wild-type and control transformant line (Fig. 3.30 A). However, in alkaline soil suppression of *AhNAS4* led to 41% and 29% reduction in Mg content compared to the wild-type and control line 11-2 respectively (Fig. 3.30 B). Exogenous Fe treatment rescued chlorosis phenotype in wild-type and control plants grown in alkaline soil without altering shoot Mg content (data are not shown).

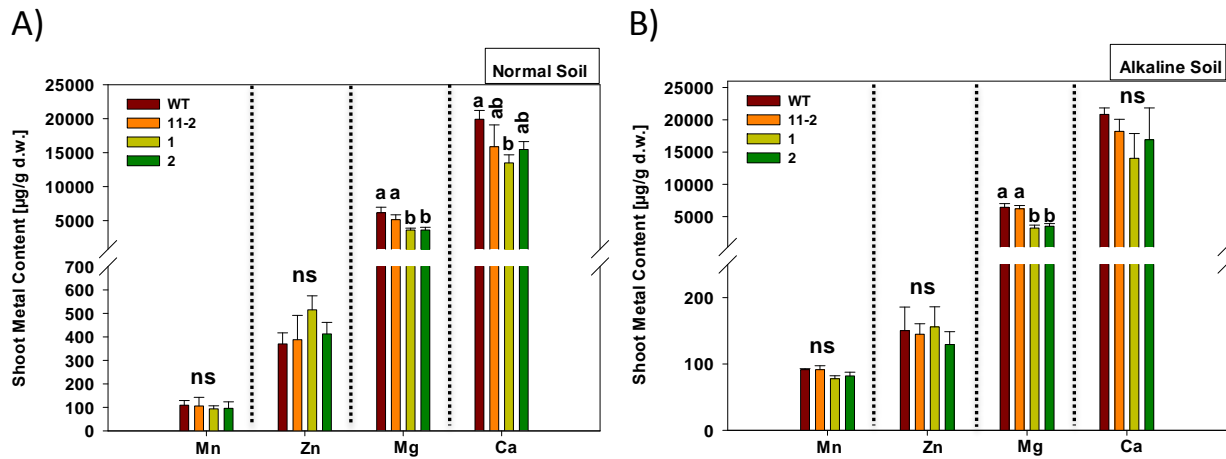


Fig. 3.30 Mn, Zn, Mg and Ca contents in shoots of *A. halleri* wild-type and *AhNAS4*-RNAi plants grown in normal and alkaline soils

Plants were cultivated in normal soil, alkaline (pH=7.8) or in alkaline soil +Fe, Tissues were harvested after 6 weeks, digested and analyzed by ICP-OES. Shown in (A), (B) and (C) are values for Fe content in shoot of plants grown in normal and alkaline soils. All values are arithmetic means \pm SD, n = 15 replicate clones per genotype from three independent experiments. Different characters above the bars indicate statistically significant differences detected in a one-way ANOVA, followed by Tukey test A: P < 0.05 significance level between (a) and (b), B: P < 0.01 significance level between (a) and (b), ns: not significant.

3.2.6.5 PIXE imaging of the whole leaves of *A. halleri* wild-type and *AhNAS4*-RNAi plants grown in normal and alkaline soils

When studying *NAS4* suppressed lines grown in alkaline soil, it was noted that the strength of leaf chlorosis phenotypes differed in young and old leaves. We hypothesized that perhaps the accumulation and localization of Fe in *NAS4* suppressed lines leaves varied with age. To study this aspect further, young and aged leaves of alkaline soil-grown *A. halleri* wild-type and *AhNAS4* suppressed lines were separated and subjected to the Particle-induced X-ray emission (PIXE) imaging as described by (Vogel-Mikus et al., 2008). Results suggested that there were clear differences in the leaf element distribution patterns between the wild-type and the *NAS4* suppressed line, irrespective of the leaf age, however the differences were much more pronounced in the mature leaves as seen from the cluster analysis of the Z scaled element concentrations measured in the whole leaves. The young leaves formed a distinct cluster that was separated from the *NAS4* suppressed line and the wild-type old leaves. The mature as well as young leaves of *NAS4* suppressed lines accumulated more Fe, Mn and Zn compared to the wild-type leaves of the same age (Fig. 3.31). The wild-type leaves showed patchy Fe distribution with some "hot spots" seen at the vicinity of the main vein (young leaves) and the leaf tip (the old leaves), with a depletion in the mesophyll part, that was especially prominent in the old leaves (Fig. 3.31). Fe distribution pattern was correlated well with the development of leaf chlorosis, which was especially prominent in the mesophyll part between the main and the lateral veins in the wild-type. The highest Fe concentration was seen in the old leaves of *NAS4* suppressed line, where slightly higher Fe concentration was seen in the leaf mesophyll compared to the other leaf parts. In the young as well as old leaves, Mn and Zn were distinctly localized on the leaf edge in the wild-type. In the *NAS4*

Results

suppressed line, the highest contents of Mn were seen on the leaf tip, while Zn content gradually increased from the main vein towards the mesophyll and the leaf edge (Fig. 3.31). Similarly as for Fe, distinct amounts of Zn were seen in the leaf mesophyll of the *NAS4* suppressed line leaves when compared to the wild-type (Fig. 3.31).

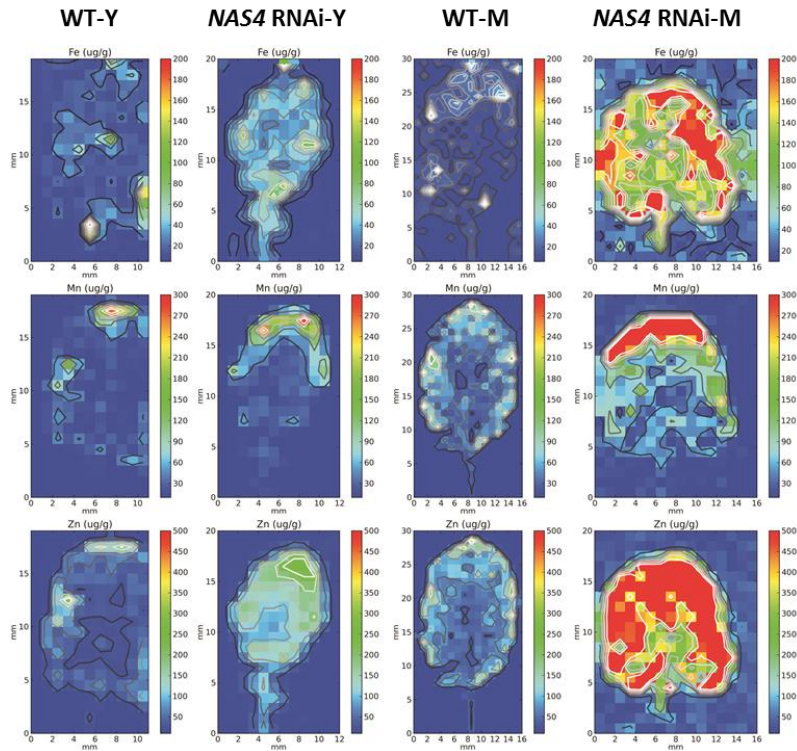


Fig. 3.31 PIXE images of *A. halleri* wild-type and *AhNAS4*-suppressed line leaves of plants grown in alkaline soil

Plants were cultivated in alkaline (pH=7.8) soil and leaves harvested after 6 weeks and subjected to PIXE imaging. WT-Y (wild-type young), *NAS4*-Y (*AhNAS4*-suppressed line young), WT-M (wild-type mature), *NAS4*-M (*AhNAS4*-suppressed line mature).

3.2.7. Characterization of *AhNAS4*-RNAi lines on phenotyping and Bestwig soils

To test whether results obtained from controlled hydroponic experiments are transferable to near-natural conditions, soil characterization of *AhNAS4*-RNAi lines carried out via growing wild-type and *A. halleri* *NAS4*-RNAi plants in heavily or slightly contaminated soils. For tolerance test on heavily contaminated soil, plants were cultivated in a metalliferous soil hosting a native *A. halleri* population collected from a highly a contaminated site from Bestwig in Germany (N 51° 18.525' E 008° 24.578'). In order to investigate metal accumulation in *AhNAS4*-RNAi plants in slightly contaminated soil, the phenotyping soil, an experimental soil mix consisting of 2 : 1 loamy soil: sand mix amended with 300 mg Zn kg⁻¹ (added as ZnS) and 5 mg Cd kg⁻¹ (added as CdCl₂ × H₂O) of dry weight (Stein et al., 2016) was chosen. Extractable (Table. 3.2) and exchangeable (Table. 3.3) metal content of soils showed that Bestwig soil contains several-fold higher levels of Zn, Pb and Cd compared to normal soil, alkaline and phenotyping soils, which makes it suitable for growth tolerance test, on the other

Results

hand phenotyping soil contain enough Zn and Cd content to be used for metal accumulation test. By the end of the cultivation period of 6 weeks, in non-metalliferous phenotyping soil there were no significant differences in shoot fresh weight between genotypes and all plants had grown normally (Fig. 3.32 B and C). In plants grown in Bestwig soil, there were no sign of toxicity in leaves of all plants and regardless of their genotype all were green and healthy (Fig. 3.32 A). Soil shoot fresh weight of two *AhNAS4*- suppressed lines was reduced in comparison to the wild-type and control line 11-2, but the differences only were significant compared to control line 11-2 (Fig. 3.32 C).

Tab.3.2 Extractable metal content of soils were used for *A. halleri* cultivation

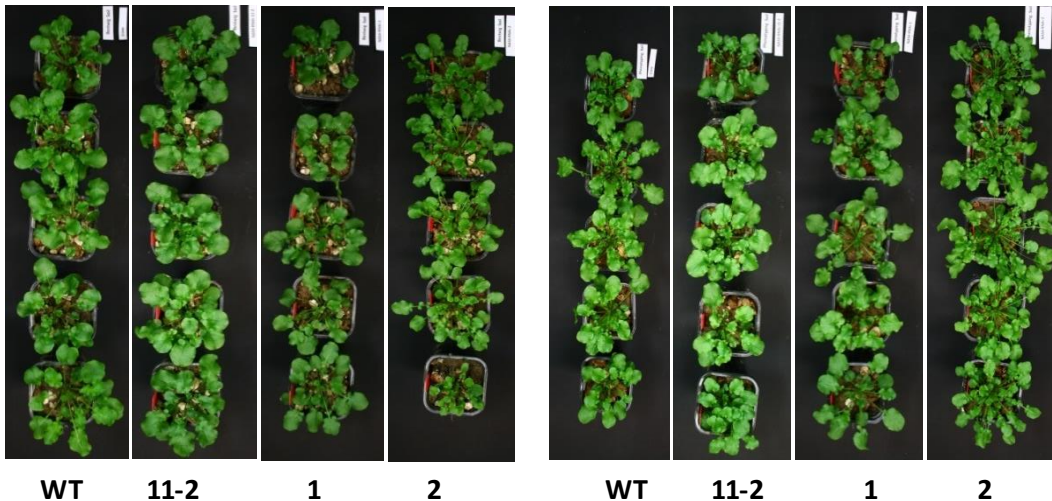
HCL extractable metal content ($\mu\text{g g}^{-1}$)						
Soil Type	Fe	Zn	Mn	Pb	Cd	pH
Normal	513.5 \pm 12.4	13.3 \pm 0.11	80 \pm 0.27	0 \pm 0	0.0 \pm 0.0	6.3 \pm 0.1
Alkaline	18.6 \pm 12.5	8.6 \pm 2.16	78.8 \pm 1.71	0 \pm 0	0.0 \pm 0.0	8.0 \pm <0.1
Phenotypig	717.8 \pm 17	238 \pm 6.34	205.7 \pm 6.4	6.2 \pm 0.0	4.06 \pm 0.12	7.6 \pm <0.1
Bestwig	804.9 \pm 218	4257 \pm 105	537 \pm 11.15	3384 \pm 47	8.44 \pm 0.25	6.8 \pm <0.1

Tab.3.3 Exchangeable metal content of soils were used for *A. halleri* cultivation

BaCl ₂ exchangeable metal content ($\mu\text{g g}^{-1}$)						
Soil Type	Fe	Zn	Mn	Pb	Cd	pH
Normal	6.45 \pm 0.14	0.33 \pm 0.02	1.71 \pm 0.22	0.05 \pm 0.02	0.0 \pm 0.0	6.3 \pm 0.1
Alkaline	1.56 \pm 0.01	0.56 \pm 0.03	3.2 \pm 0.35	0.01 \pm 0.0	0.0 \pm 0.0	8.0 \pm <0.1
Phenotypig	0.54 \pm 0.07	0.1 \pm 0.0	21.6 \pm 0.78	0.08 \pm 0.0	0.01 \pm 0.0	7.6 \pm <0.1
Bestwig	2.29 \pm 0.45	57.78 \pm 6.81	1.38 \pm 0.14	1.94 \pm 0.44	0.51 \pm 0.05	6.8 \pm <0.1

A) Bestwig Soil

B) phenotyping Soil



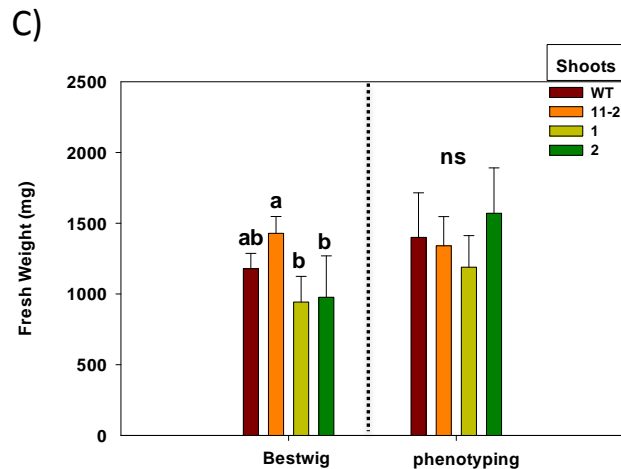


Fig. 3.32 Phenotype of *A. halleri* wild-type and *AhNAS4*-RNAi plants grown in Bestwig and phenotyping soils

Shown in (A) and (B) are photographs of representative wild-type, control transformant *AhNAS4*-RNAi line 11-2 and two *AhNAS4*-suppressed line 1 and 2 grown in Bestwig and phenotyping soils respectively. Shown in (C) is shoot fresh weight. All values are arithmetic means \pm SD, n=5 replicate clones per genotype. Different characters above the bars indicate statistically significant differences detected in a one-way ANOVA, followed by Tukey test C: $P < 0.05$ significance level between (a) and (b), ns: not significant.

Shoot metal profiles of the Bestwig soil-grown plants showed highly significant increase in Fe content in *AhNAS4*-suppressed plants compared to the wild-type and control line 11-2 (Fig. 3.33 A) which was similar and more pronounced to previous experiments on normal and alkaline soils (Fig. 3.20). In phenotyping soil Fe content was slightly increased in suppressed lines compared to the wild-type but was similar to control transgenic line 11-2 (Fig. 3.33 A). Results suggested a slightly but non-significant increase in shoots Zn content of *AhNAS4*-suppressed lines compared to the wild-type and significantly increase compared to control line 11-2 (Fig. 3.33 B). There were no differences in Zn content of plants grown in phenotyping soil (Fig. 3.33 A). In plants grown in Bestwig and phenotyping soils there were no significant differences in leaves Cd content among genotypes (Fig. 3.33 C). Surprisingly two *AhNAS4*-suppressed line grown in Bestwig and phenotyping soil showed strong reduction in shoots Mn content compared to the wild-type and control line 11-2 (Fig. 3.33 D). There were no differences in Ca content of plants grown in phenotyping and Bestwig soils (Fig. 3.33 E) and finally while there were no significant differences in Mg content between plants grown in Bestwig soil, two *AhNAS4*-suppressed lines showed lower amount of shoot Mg content compared to the wild-type and control transformant line (Fig. 3.33 F).

Results

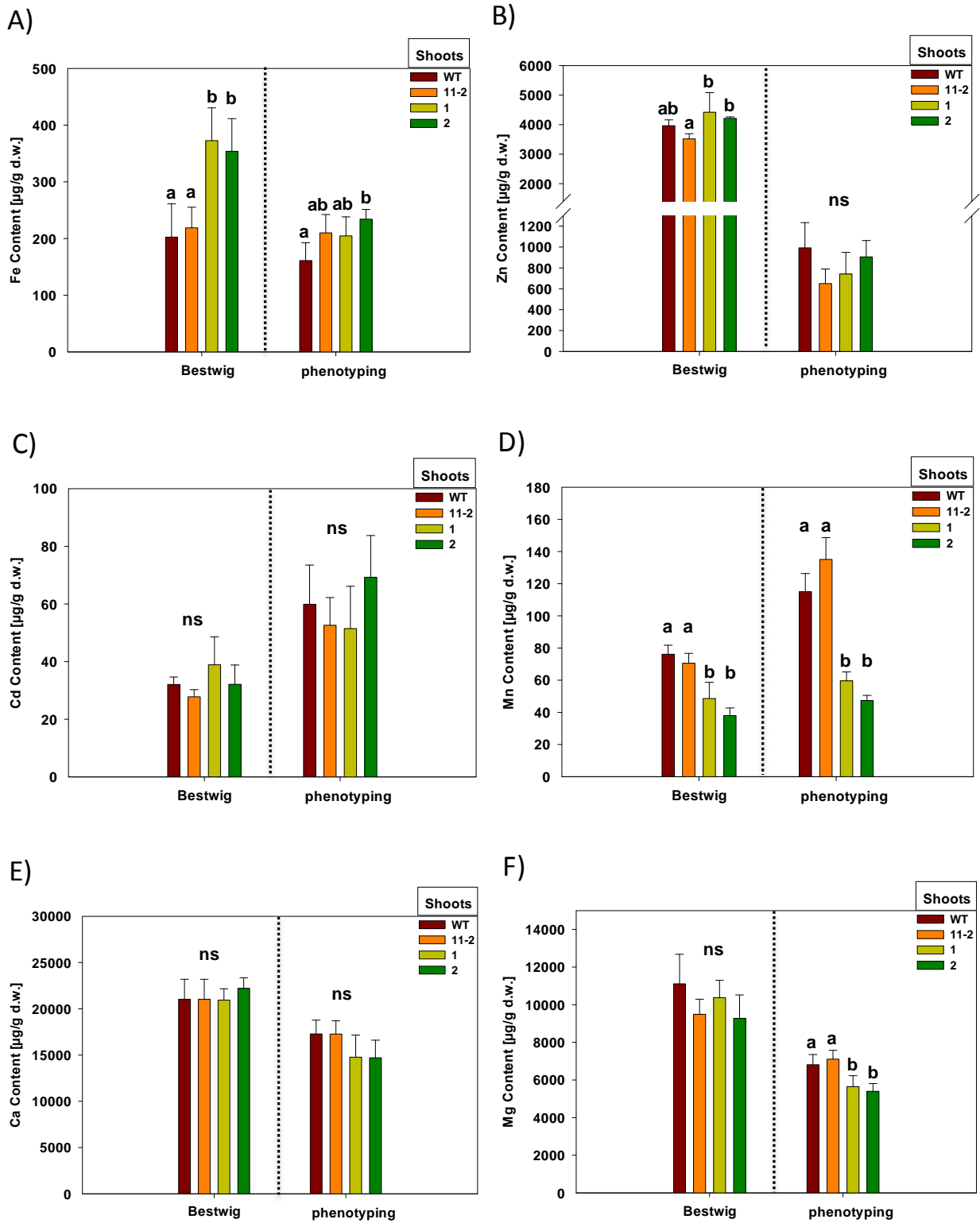


Fig. 3.33 Metal content in shoot of *A. halleri* wild-type and *AhNAS4*-RNAi plants grown in Bestwig and phenotyping soils

Wild-type, *AhNAS4*-RNAi control line 11-2 and two *AhNAS4*-suppressed lines 1 and 2 were cultivated in Bestwig and phenotyping soils. Shoots were harvested after 6 weeks, digested and analyzed by ICP-OES. Fe content (A), Zn

Results

content (B), Cd content (C), Mn content (D), Ca content (E) and Mg content (F) are shown respectively. All values are arithmetic means \pm SD, n =5 replicate clones per genotype. Different characters above the bars indicate statistically significant differences detected in a one-way ANOVA, followed by Tukey test. A: P < 0.05 significance level between (a) and (b), B: P < 0.05 significance level between (a) and (b), D: P < 0.001 significance level between (a) and (b), F: P < 0.01 significance level between (a) and (b), ns: not significant.

3.3 The physiological role of ZIP6 in *A. halleri*

3.3.1 Confirmation of *AhZIP6*-RNAi lines with real-time PCR

The heavy metal hyperaccumulator *A. halleri* has higher transcript abundance of *ZIP6* gene in roots and especially in shoots compared to the non-hyperaccumulator *A. thaliana* (Becher et al., 2004; Talke et al., 2006), which makes it an interesting candidate gene in the metal accumulation process. It has been shown, based on predicted amino acid sequences analysis, that in *A. thaliana* *ZIP6* is more distantly related to the other ZIP family members (Wu et al., 2009). The coding sequence of *A. halleri* *ZIP6* has been cloned and submitted to the Gene bank (AJ580315.1) (Becher et al., 2004). Since the whole genome of *A. halleri* is not fully sequenced, at this stage the early release *A. halleri* genome on Phytozome (<https://phytozome.jgi.doe.gov>) does not have the similar sequence to the Gene bank submitted *A. halleri* *ZIP6* (AJ580315.1). Pairwise predicted amino acid sequences comparison of *A. halleri* *ZIP6* to the *ZIP6* of other Brassicaceae family members via (http://www.ebi.ac.uk/Tools/psa/emboss_needle/), revealed that *A. halleri* *ZIP6* is 97.4 % identical to *A. thaliana* and *A. lyrata* *ZIP6*, 93.3 % identical to *C. sativa* *ZIP6*, 93.5 % identical to *C. rubella* *ZIP6* and 91.5 % identical to *B. oleracea* *ZIP6*. It has been shown that more than one gene copy is present in the *A. halleri* genome for the *ZIP6* (Talke et al., 2006; Suryawanshi et al., 2016). Querying the early release *A. halleri* genome on Phytozome (<https://phytozome.jgi.doe.gov>) showed genes with high similarity to some members of the *ZIP* family in *A. thaliana*, including *AtZIP1* (Araha.3837s0009.1), *AtZIP2* (Araha.7283s0002.1), *AtZIP4* (Araha.11242s0018.1), *AtZIP7* (Araha.17510s0004.1), *AtZIP9* (Araha.24726s0001.1), *AtZIP10* (Araha.10595s0008.1) and *AtZIP12* (Araha.17932s0003.1).

To elucidate the role of *ZIP6* in metal hyperaccumulation and homeostasis in *A. halleri*, *ZIP6*-RNAi lines generated from the wild-type individual *C-line*. Quantitative real time RT-PCR analyses using specific primers were performed in order to quantify transcript levels of the *AhZIP6* gene. Initially 31 independent *AhZIP6*-RNAi lines were analyzed and all showed transcript reduction for the *AhZIP6* gene. The *ZIP6* transcript abundance was analyzed in shoots of soil-grown 13 independent *AhZIP6*-RNAi in two independent rounds and compared to the wild-type. There was no transgenic line with the same *AhZIP6* transcript level as wild-type as transgenic control line (Fig. 3.34 A). The *A. halleri* expressing GFP under the control of 35S promoter was chosen as a control line, since this line went through the same process of transformation and GFP has no effect in metal accumulation process. Two lines 7-2 and 11-1, which showed 88% reduced *ZIP6* transcript level in comparison to the wild-type were selected as strong RNAi lines for further study (Fig. 3.34 B).

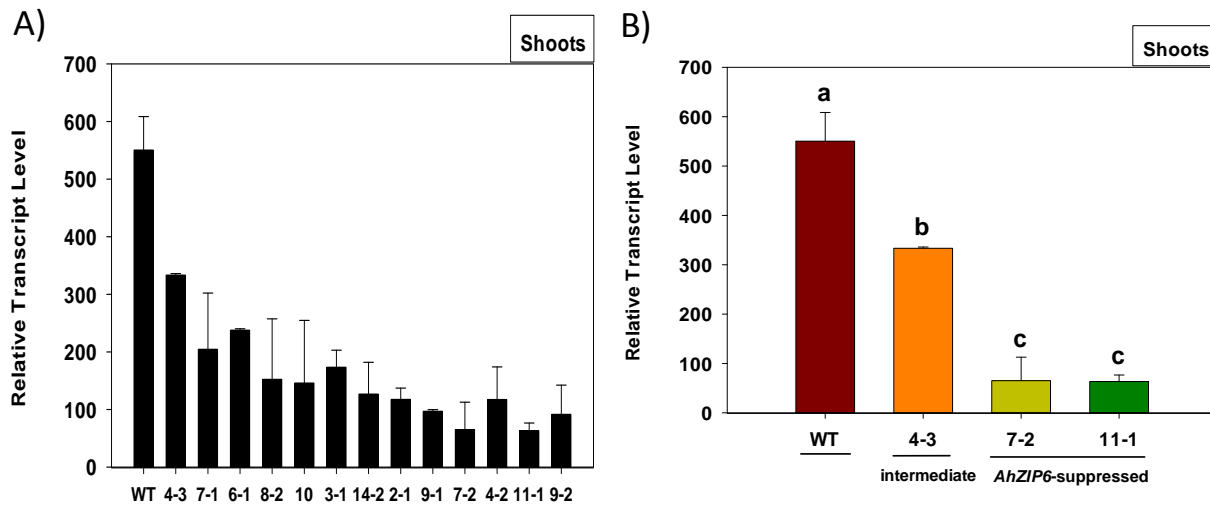


Fig. 3.34 Reduction of *AhZIP6* transcript level in independent RNAi lines

Transcript levels of *ZIP6* were analyzed in shoots of *A. halleri* wild-type and *AhZIP6*-RNAi plants grown in normal soil. Tissues were harvested after 6 weeks of cultivation and analyzed by real-time RT-PCR. Transcript abundance was expressed relative to *EF1 α* . Values are means \pm SD of $n = 2$ independent experiments (Six replicate clones per genotype were pooled for each data point). Different characters above the bars indicate statistically significant differences detected in a one-way ANOVA, followed by Tukey test, B $P = 0.016$ significance level between (a) and (b), $P < 0.001$ significance level between (a) and (c) and $P = 0.08$ significance level between (b) and (c).

3.3.2 Elemental profiling of *AhZIP6*-RNAi lines

3.3.2.1 Elemental profiling of *AhZIP6*-RNAi lines hydroponically grown in standard *A. halleri* 1/10 Hoagland medium

To assess the consequences of altered *ZIP6* expression on metal content, wild-type plant, the intermediate RNAi line 4-3 and the selected *ZIP6*-suppressed lines were grown hydroponically in standard *A. halleri* 1/10 Hoagland medium for 3 weeks. After harvesting roots and shoots, metal contents were measured via ICP-OES. Root Zn, Mn and Fe contents of the two *ZIP6*-suppressed lines were similar to the wild-type and *ZIP6*-intermediate lines (Fig. 3.35 A). The same effect was observed in leaves, i.e. metal content of *ZIP6*-suppressed lines was comparable to the wild-type and line 4-3 (Fig. 3.35 B). Our results suggested that in *A. halleri* suppression of *ZIP6* has no detectable effect in Zn, Fe and Mn accumulation in plants grown in medium with sufficient Zn supply.

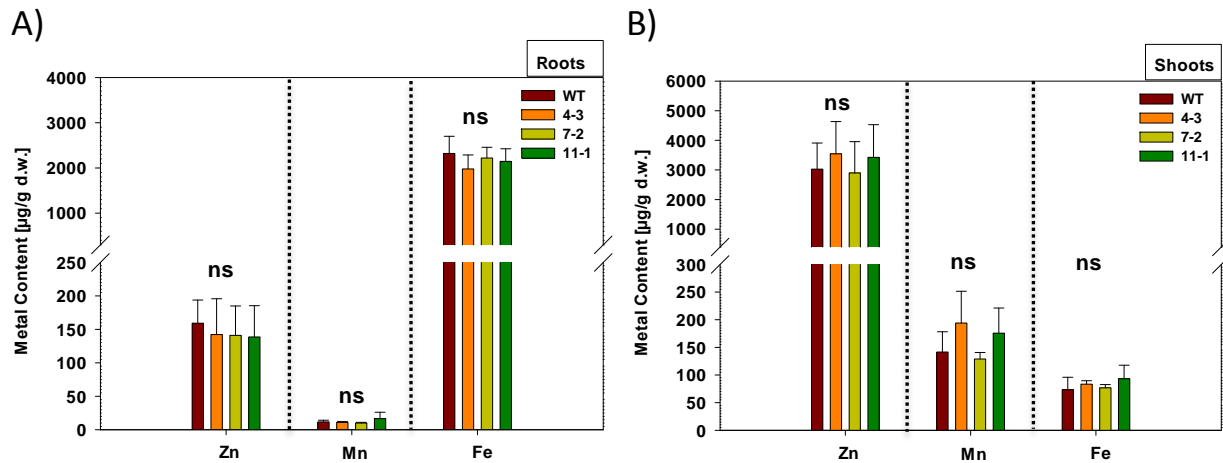


Fig. 3.35 Metal content in roots and shoots of *A. halleri* wild-type and *AhZIP6*-RNAi plants hydroponically grown in standard *A. halleri* 1/10 Hoagland medium

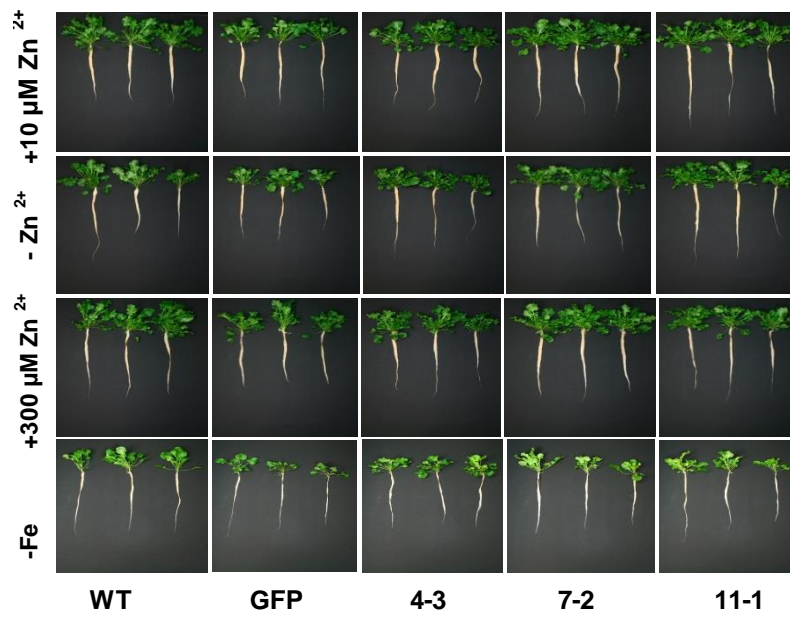
Plants were cultivated in standard *A. halleri* 1/10 Hoagland medium. Tissues were harvested after 3 weeks, digested and analyzed by ICP-OES. Shown in (A) and (B) are values for roots and shoots respectively. All values are arithmetic means \pm SD, n = 3 replicate clones per genotype. ns: not significant.

3.3.2.2 *AhZIP6* suppression results in no phenotypic change in *A. halleri* plants grown under Zn and Fe depletion or in medium with sufficient or Zn excess content

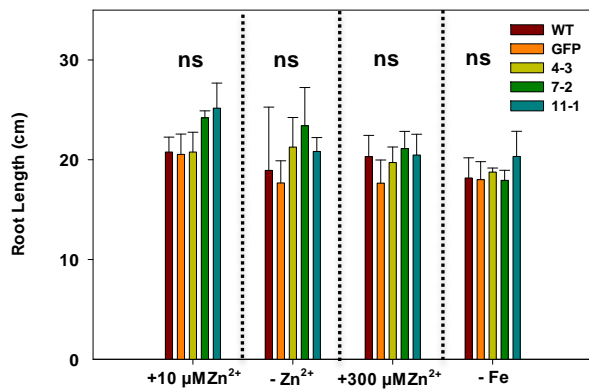
So far, there were no detectable effects of *AhZIP6* suppression on plants grown in sufficient Zn condition (Fig. 3.35). To address whether *AhZIP6* suppression affects plants in Zn depletion, Zn excess or Fe depletion conditions, the wild-type, 35S-GFP transgenic lines as control, *AhZIP6* line 4-3 as intermediate RNAi line and two *AhZIP6* -suppressed lines 7-2 and 11-1 were hydroponically grown for 4 weeks in 1.5 liter pots in 1/10 Hoagland media with different Zn and Fe regimes. During the first week of cultivation all plants were grown in standard *A. halleri* 1/10 Hoagland medium and then plants were transferred for another 3 weeks in medium with no Zn, medium with no Fe, medium supplemented with sufficient Zn and finally medium supplemented with extra 300 μ M Zn²⁺ as Zn excess medium in parallel in growth chamber. Results showed that there were no detectable differences between genotypes in all treatment regimes (Fig. 3.36 A). Root length (Fig. 3.36 B), root fresh weight (Fig. 3.36 C) and shoot fresh weight (Fig. 3.36 D) of *ZIP6*-suppressed lines 7-2 and 11-1 were comparable to those have seen in wild-type, GFP line and *AhZIP6* -intermediate line 4-3 in all treatment conditions.

Results

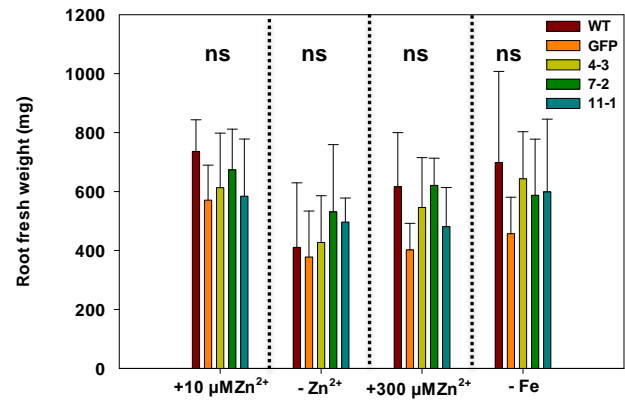
A)



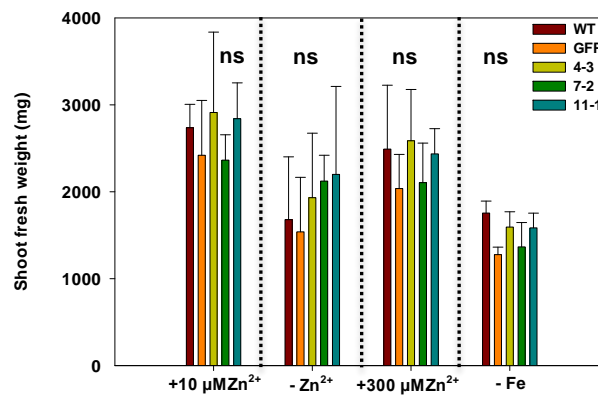
B)



C)



D)



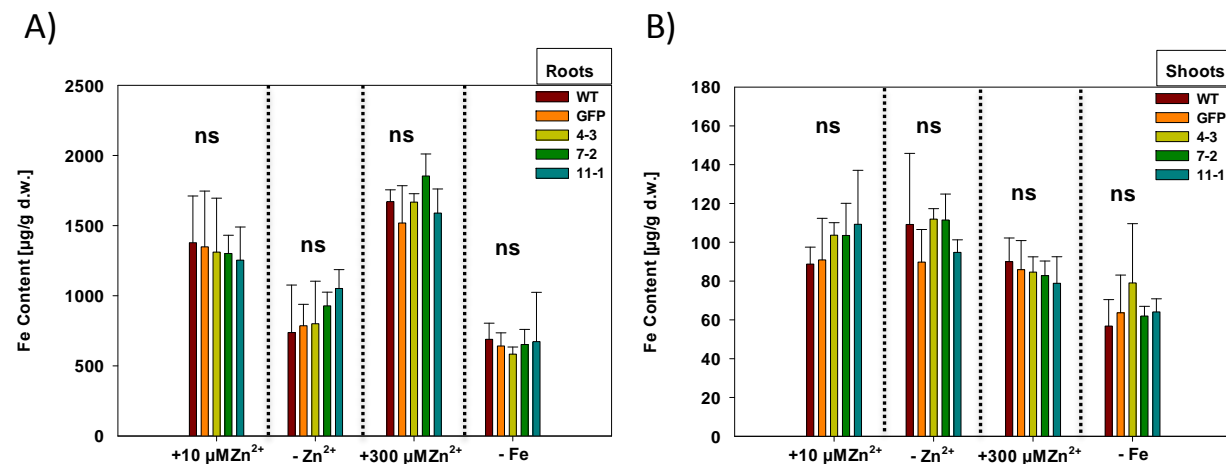
Results

Fig. 3.36 Phenotype of *A. halleri* wild-type and *AhZIP6*-RNAi grown in Zn or Fe depletion medium or in medium supplemented with sufficient or excess Zn content

Plants were cultivated in standard *A. halleri* 1/10 Hoagland medium a week prior to the experiment. Then for another 3 weeks were grown in medium with no Zn, medium with no Fe, medium supplemented with sufficient Zn content and finally medium supplemented with extra 300 μM Zn^{2+} as Zn excess content. Shown in (A) are Photographs of representative wild-type and 35S-GFP as control, *AhZIP6* line 4-3 as intermediate RNAi lines and two *AhZIP6*-suppressed lines 7-2 and 11-1. Shown in (B) are values for roots length, (C) and (D) are values for roots and shoots fresh weight respectively. All values are arithmetic means \pm SD, $n = 6$ replicate clones per genotype. ns: not significant.

3.3.2.3 *AhZIP6* suppression does not change root and shoot metal content of *A. halleri* plants grown in Zn and Fe depletion or in medium with sufficient or Zn excess content

Elemental profiling of plants grown in Zn and Fe depletion or in media with sufficient or Zn excess content showed that, root and shoot Fe contents in plants grown under Fe depletion medium were lower compared to the plants grown in other regimes with sufficient Fe (Fig. 3.37 A and B). Root Fe content of two *ZIP6*-suppressed lines 7-2 and 11-1 was similar compared to the wild-type, GFP and *ZIP6*-intermediate line 4-3 in all treatment regimes (Fig. 3.37 A). The same effect was observed in leaves, i.e. metal contents of *ZIP6*-suppressed lines were comparable to those seen in wild-type, GFP and *ZIP6*-intermediate line 4-3 (Fig. 3.37 B). Regardless of their genotypes, root and shoot Zn contents in plants grown in Zn depletion medium were lower compared to the plants grown in medium with sufficient Zn (Fig. 3.37 C and D). Root and shoot Zn contents in plants grown in excess Zn content were higher compared to plants grown in other regimes (Fig. 3.37 C and D). Root and shoot Zn contents of the two *ZIP6*-suppressed lines were comparable to the wild-type, GFP and *ZIP6*-intermediate line 4-3 in all treated regimes (Fig. 3.37 C and D). Root and shoot Mn contents in plants grown in Fe depletion conditions were slightly higher compared to plants grown in other regimes (Fig. 3.37 E and F). There were no significant differences between genotypes in their root and shoot Mn contents upon cultivation in media with different Zn and Fe regimes (Fig. 3.37 E and F). These results suggest in *A. halleri*, suppression of *ZIP6* has no detectable effect in Zn, Fe and Mn accumulation in plants.



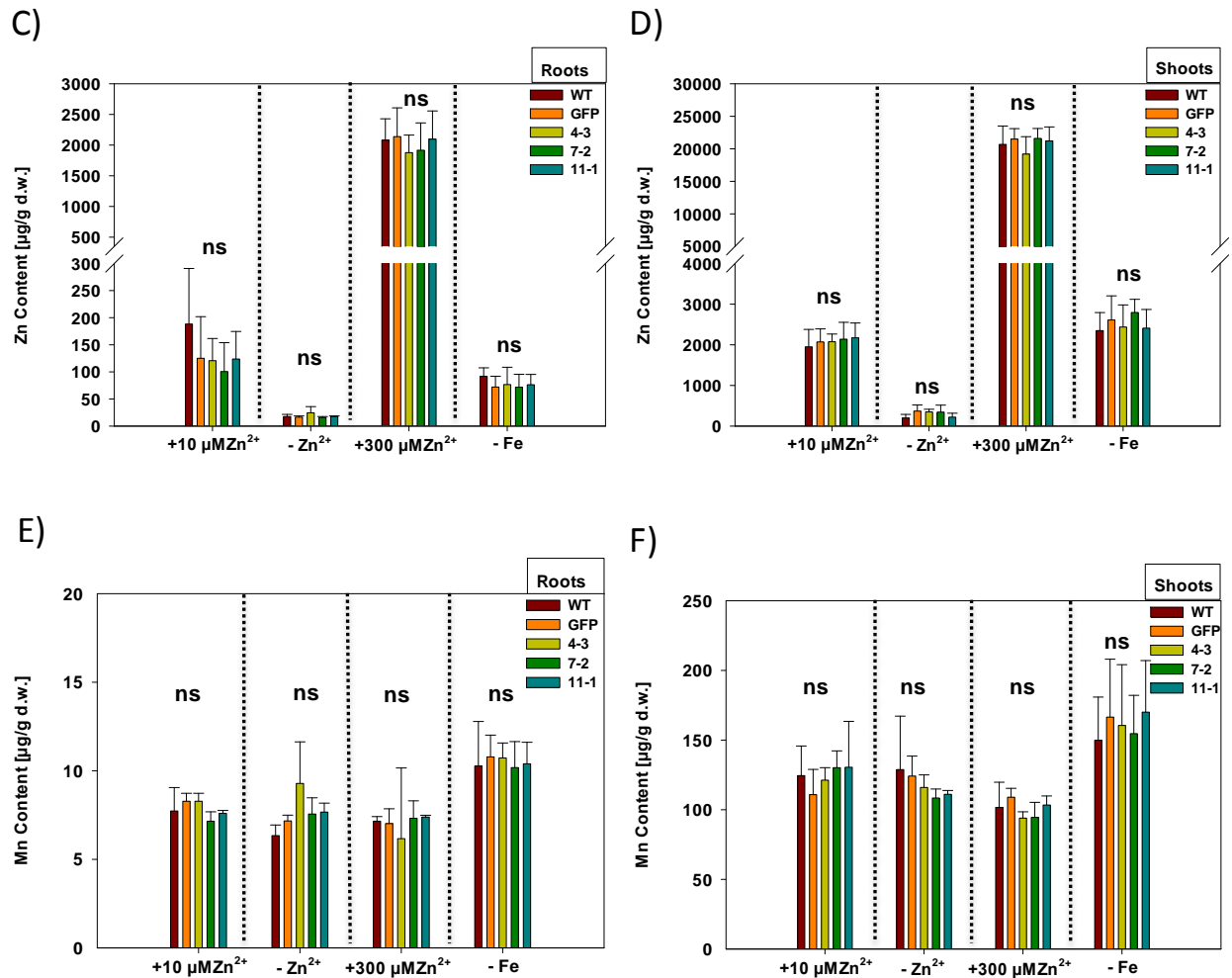


Fig. 3.37 Metal content in roots and shoots of *A. halleri* wild-type and *AhZIP6*-RNAi plants grown in Zn or Fe depletion medium or in medium supplemented with sufficient or Zn excess content

Plants were cultivated in standard *A. halleri* 1/10 Hoagland medium a week prior to the experiment. For another 3 weeks plants were grown in medium with no Zn, medium with no Fe, medium supplemented with sufficient Zn content and finally medium supplemented with extra 300 $\mu\text{M Zn}^{2+}$ as Zn excess content, and then tissues were harvested, digested and analyzed by ICP-OES. Shown in (A) and (B) are values for root and shoot Fe content respectively. Shown in (C) and (D) are values for root and shoot Zn content respectively and finally (E) and (F) are values for root and shoot Mn content respectively. All values are arithmetic means \pm SD, n = 3-6 replicate clones per genotype. ns: not significant.

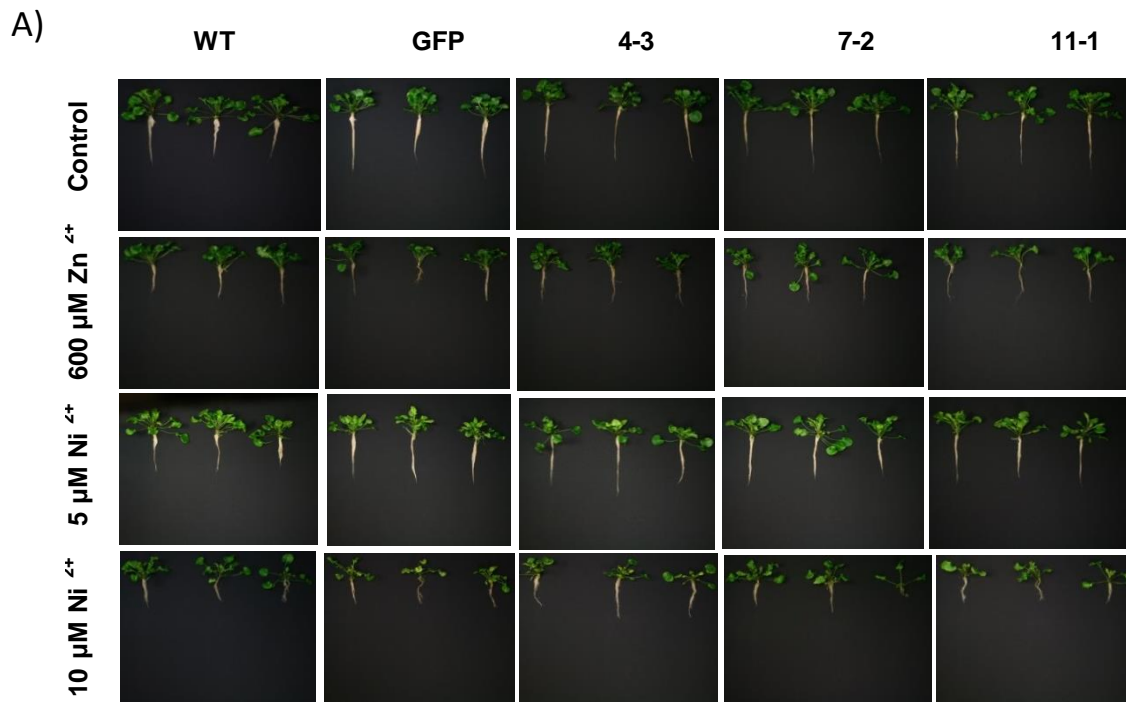
3.3.3 Tolerance assay of *AhZIP6*-RNAi lines

3.3.3.1 Suppression of *AhZIP6* has no effect on Ni and Zn tolerance in *A. halleri*

To analyze the possible effects of altered *ZIP6* on *A. halleri* tolerance towards Zn and Ni, wild-type, 35S-GFP transgenic plants and *AhZIP6*-RNAi lines were grown hydroponically in control 1/10 Hoagland medium, in medium supplemented with 600 $\mu\text{M Zn}^{2+}$ and in media supplemented with extra 5 or 10 $\mu\text{M Ni}^{2+}$ as Ni stress conditions, for 3 weeks. All plants were grown in parallel in 50-ml

Results

falcon tubes in growth chamber and media were changed twice a week. The wild-type and 35S-GFP transgenic plants exposed to medium supplemented with additional 600 μM Zn^{2+} showed 34% to 48% reduction in their root length (Fig. 3.38 A), 49% to 72% reduction in their root fresh (Fig. 3.38 B) weight and 20% to 40% reduction in their shoot fresh weight (Fig. 3.38 C), compared to the control conditions. The wild-type and 35S-GFP transgenic plants exposed to medium supplemented with additional 10 μM Ni^{2+} showed 44% to 53% reduction in their root length (Fig. 3.38 A), 71% to 84% reduction in their root fresh weight (Fig. 3.38 B) and 43% to 60% reduction in their shoot fresh weight (Fig. 3.38 C) compared to the control conditions. The wild-type and 35S-GFP transgenic plants grown in medium supplemented with additional 5 μM Ni^{2+} showed 10% to 27% reduction in their root fresh weight compared to the control conditions, indicating a slight toxicity (Fig. 3.38 B). The control transformant *AhZIP6*-RNAi line 4-3 and two *AhZIP6*-suppressed lines 7-2 and 11-1 also responded similarly with no significant differences towards Zn and Ni stresses conditions compared to the wild-type and 35S-GFP transgenic plants (Fig. 3.38 A). The control transformant *AhZIP6*-RNAi line 4-3 and two *AhZIP6*-suppressed lines 7-2 and 11-1 showed similar reduction in their root length (Fig. 3.38 B), root biomass (Fig. 3.38 C), and shoot biomass (Fig. 3.38 D) compared to the wild-type and 35S-GFP transgenic plants upon Zn and Ni stress conditions.



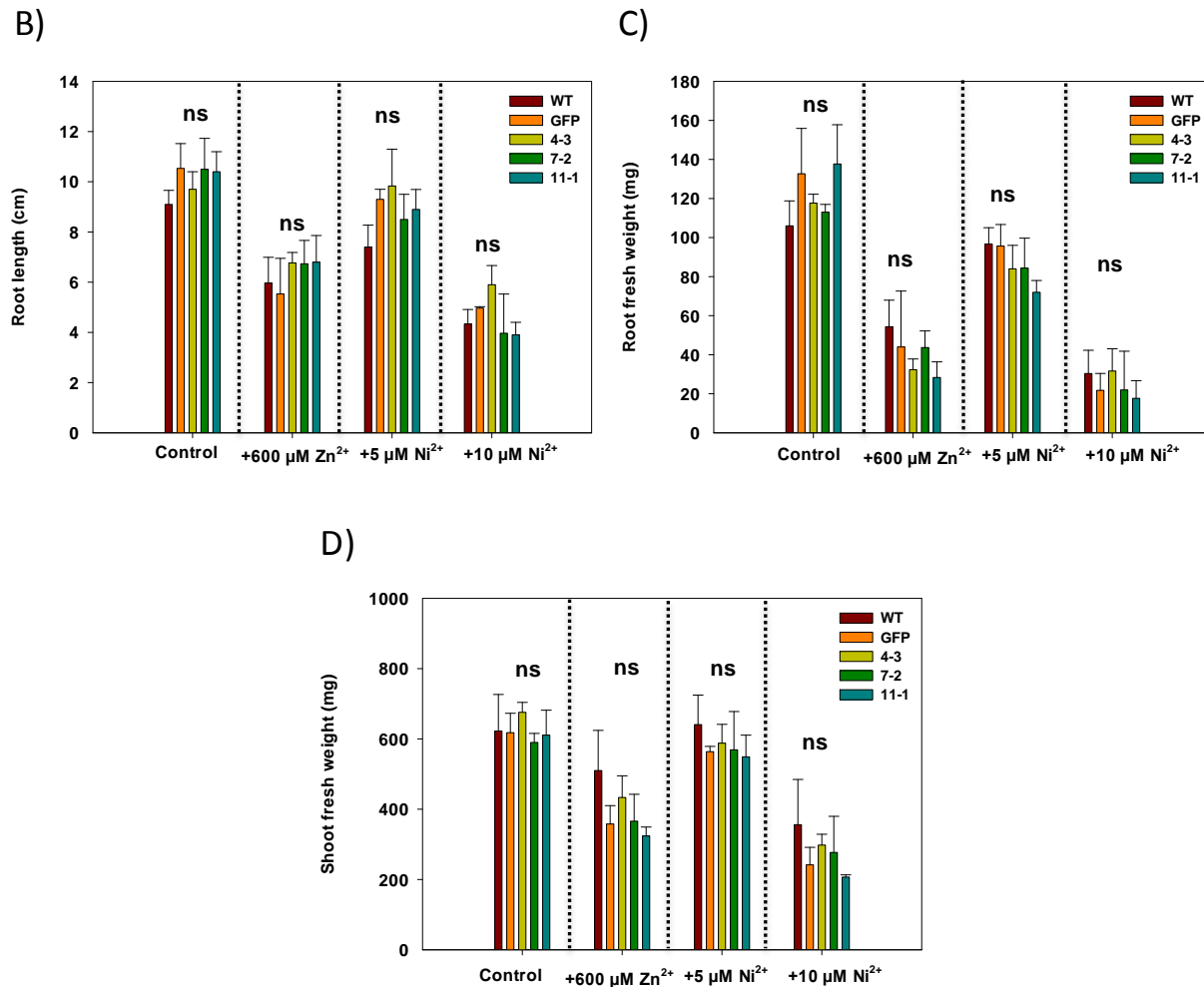


Fig. 3.38 Phenotype of *A. halleri* wild-type and *AhZIP6*-RNAi plants grown under Zn and Ni stress conditions

Plants were cultivated in 1/10 Hoagland medium as control, medium supplemented with extra 600 $\mu\text{M Zn}^{2+}$ and media supplemented with extra 5 $\mu\text{M Ni}^{2+}$ or 10 $\mu\text{M Ni}^{2+}$. Shown in (A) are photographs of representative wild-type and 35S-GFP transgenic lines as control, *AhZIP6* line 4-3 as intermediate RNAi line and two *AhZIP6*-suppressed lines 7-2 and 11-1. Shown in (B) are values for root length, (C) and (D) are values for root and shoot fresh weight respectively. All values are arithmetic means \pm SD, n = 3 replicate clones per genotype. ns: not significant.

3.3.3.2 Suppression of *AhZIP6* has no effect on root and shoot metal content in *A. halleri* plants under Ni and Zn stress conditions

There were no significant differences in root and shoot Fe contents between *AhZIP6*-suppressed and control lines in Zn and Ni stress conditions (Fig. 3.39 A and B). The same observation was found regarding Zn and Ni contents, i.e. there were no detectable differences in root and shoot Zn (Fig. 3.39 C and D) and Ni contents (Fig. 3.39 E and F) between all genotypes in both Ni and Zn stress conditions. Regardless of their genotype, plants exposed to media supplemented with additional 5 and 10 $\mu\text{M Ni}^{2+}$ showed higher root Fe content, while Fe content increased in shoots of all

Results

genotypes at the presence of $10 \mu\text{M Ni}^{2+}$. Overall, there was no evidence that suppression of *AhZIP6* changes root and shoot metal content in *A. halleri* plants under Ni and Zn stress conditions.

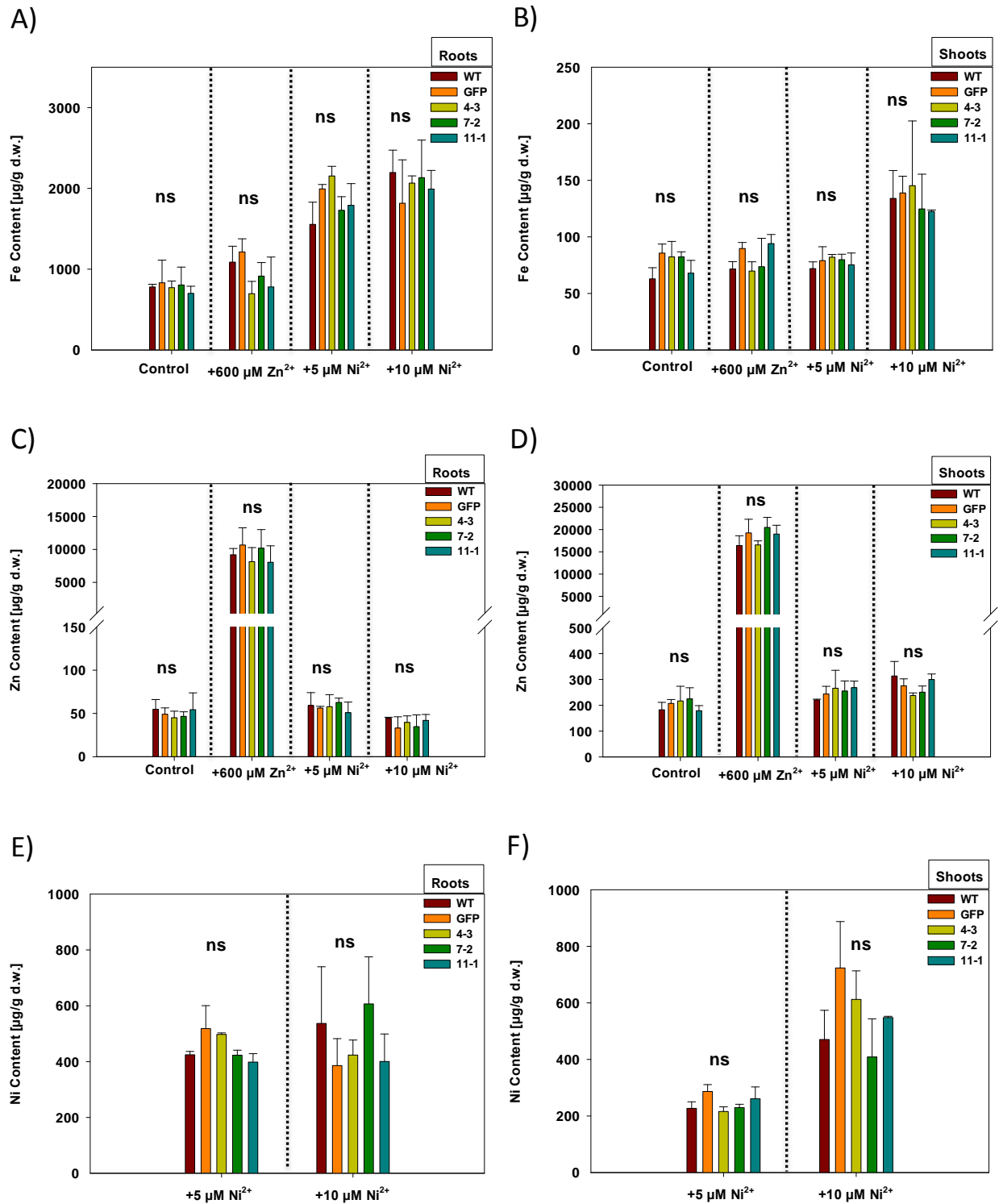


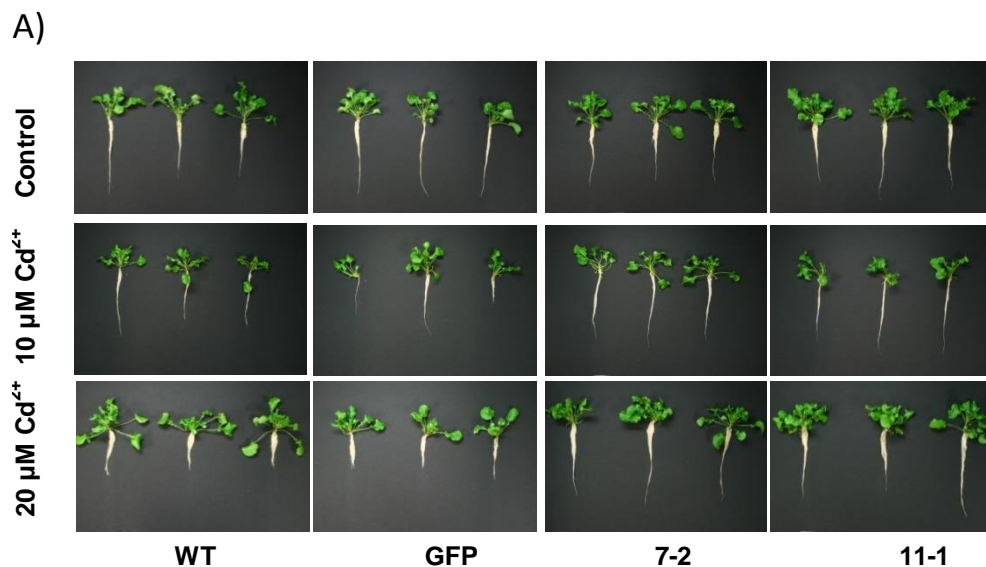
Fig. 3.39 Metal content in roots and shoots of *A. halleri* wild-type and *AhZIP6*-RNAi plants grown under Zn and Ni stress conditions

Results

Plants were cultivated in 1/10 Hoagland medium as control, medium supplemented with extra 600 μM Zn^{2+} and media supplemented with extra 5 μM Ni^{2+} or 10 μM Ni^{2+} . Tissues were harvested after 3 weeks, digested and analyzed by ICP-OES. Shown in (A) and (B) are values for root and shoot Fe content respectively. (C) and (D) are values for root and shoot Zn content respectively and finally (E) and (F) are values for root and shoot Ni content respectively. All values are arithmetic means \pm SD, $n=3$ replicate clones per genotype. ns: not significant.

3.3.3.3 Suppression of *AhZIP6* specifically enhances tolerance towards Cd in *A. halleri*

To investigate the possible effects of *AhZIP6* suppression on Cd tolerance in *A. halleri*, the wild-type and 35S-GFP transgenic lines as control and two *AhZIP6*-suppressed lines 7-2 and 11-1 were grown hydroponically for 3 weeks in 1/10 Hoagland medium as control and in media with additional 10 or 20 μM Cd^{2+} . Phenotypic analysis of plants showed that, there were no differences in root growth and plant biomass between lines under control conditions (Fig. 3.40 A). Upon Cd stress, the wild-type and 35S-GFP transgenic line showed a severe reduction in root elongation, while two *AhZIP6*-suppressed lines 7-2 and 11-1 suffered less from Cd toxicity. At the presence of 10 μM Cd^{2+} , the *ZIP6*-suppressed line 7-2 showed 22.8 % to 30 % of less reduction in relative root length compared to the wild-type and GFP lines respectively and *AhZIP6*-suppressed line 11-1 showed 29 % to 37 % of less reduction in relative root length compared to the wild-type and GFP line respectively. These phenotypes were more pronounced when plants grown in medium with extra 20 μM Cd^{2+} , i.e. the two *AhZIP6*-suppressed lines 7-2 and 11-1 showed 50 % and 46 % of less reduction in relative root length compared to the wild-type and GFP line respectively (Fig. 3.40 B). At the presence of 10 μM Cd^{2+} , the two *AhZIP6*-suppressed lines 7-2 and 11-1 showed less, but not significant, reduction in relative root fresh weight compared to the wild-type and GFP plants (Fig. 3.40 C). At the presence of 20 μM Cd^{2+} , *AhZIP6*-suppressed line 7-2 showed 30 % to 39 % of less reduction in relative roots fresh weight compared to the wild-type and 35S-GFP transgenic line respectively. The *AhZIP6*-suppressed line 11-1 showed 27 % to 36 % of less reduction in relative roots fresh weight compared to the wild-type and 35S-GFP transgenic line respectively (Fig. 3.40 C). The different responses towards Cd stress between genotypes were limited to roots and no significant differences in shoot biomass between genotypes were detected (Fig. 3.40 B).



Results

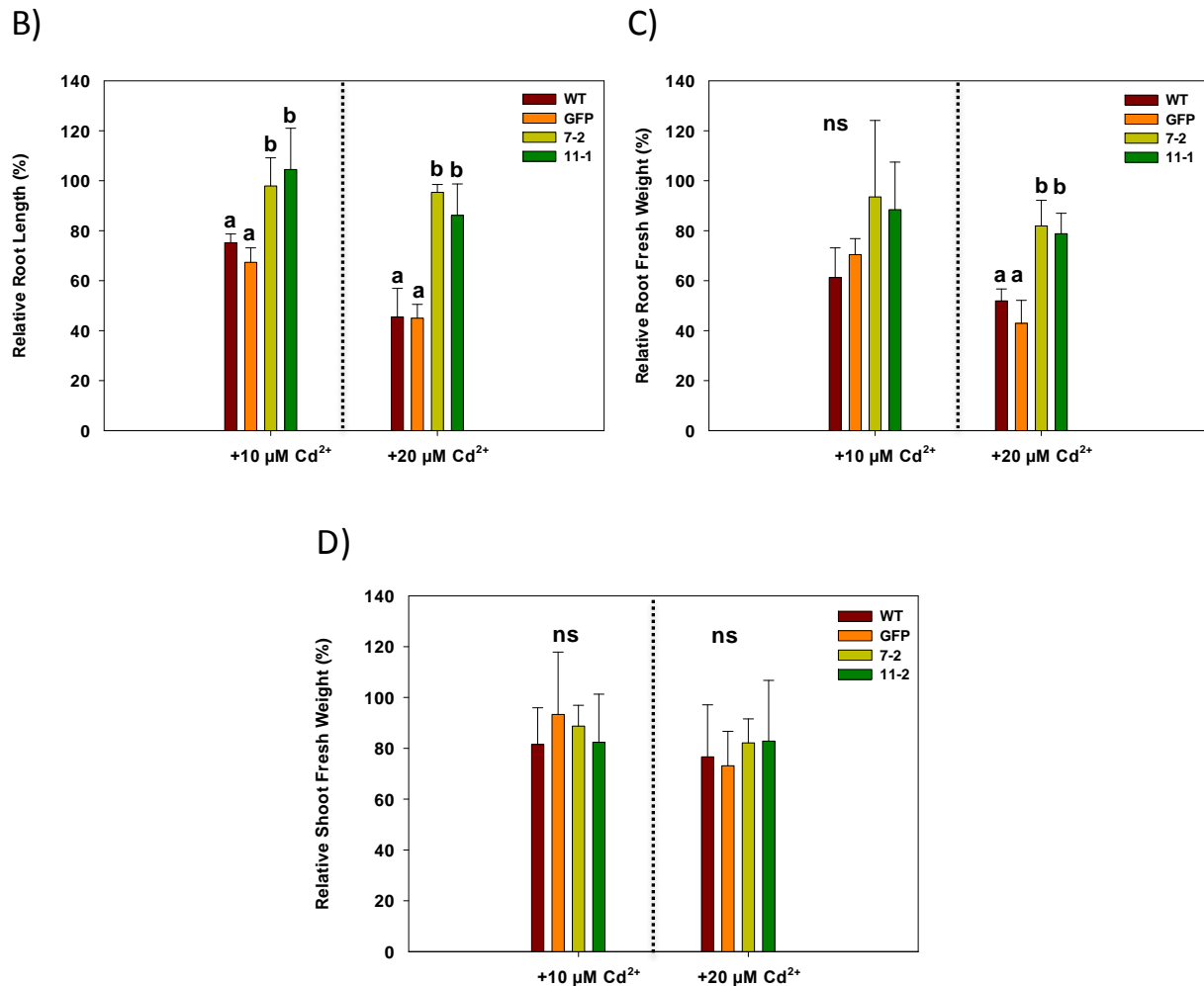


Fig. 3.40 *AhZIP6* suppression enhances tolerance towards Cd in *A. halleri*

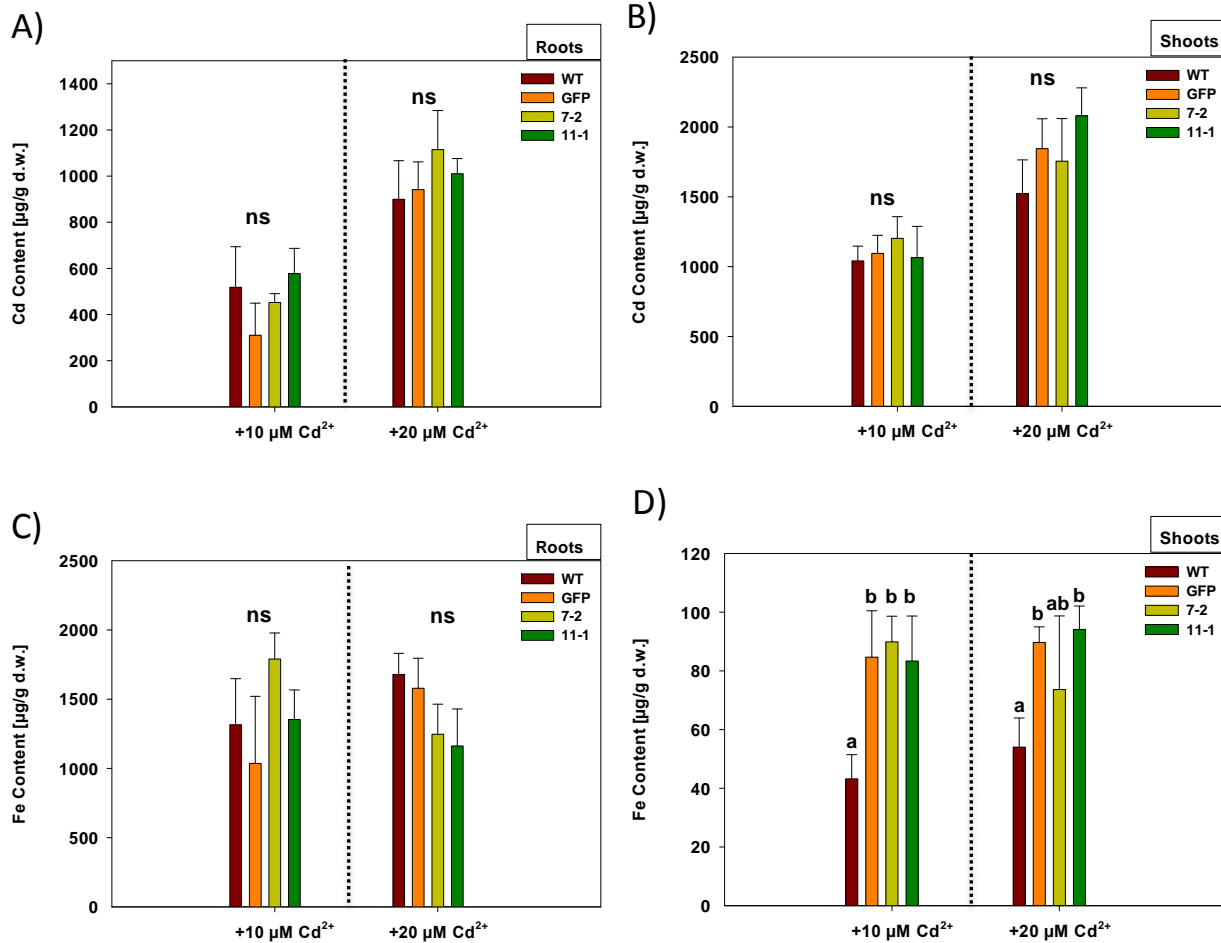
Shown in (A) are photographs of representative wild-type, 35S-GFP transgenic line and two *AhZIP6*-suppressed lines 7-2 and 11-1; plants were grown hydroponically for 3 weeks in 1/10 Hoagland medium as control and in media supplemented with additional 10 or 20 $\mu\text{M Cd}^{2+}$. Summaries of relative root length (B) relative root fresh weight (C) and relative shoot fresh weight (D) expressed as a percentage of growth in control medium. All values are arithmetic means \pm SD, $n = 12$ replicate clones per genotype from three independent experiments. Different characters above the bars indicate statistically significant differences detected in a one-way ANOVA, followed by Tukey test. B: $P < 0.05$ significance level between (a) and (b), C: $P < 0.01$ significance level between (a) and (b), ns: not significant.

3.3.3.4 Suppression of *AhZIP6* has no effect on metal content in *A. halleri* grown under Cd stress conditions for 3 weeks

Regardless of their genotypes, plants grown in the medium supplemented with additional 20 $\mu\text{M Cd}^{2+}$ showed higher root and shoot Cd content compared to the plants grown in medium with extra 10 $\mu\text{M Cd}^{2+}$. There were no significant differences in root and shoot Cd content between *AhZIP6*-suppressed and control lines in both Cd stress conditions after 3 weeks of cultivation (Fig. 3.41 A and B). Similar observations were made for Zn content, as there were no detectable differences in root

Results

and shoot Zn content between all genotypes in both Cd stress conditions (Fig. 3.41 E and F). There were no significant differences in root Fe content between *AhZIP6*-suppressed and control lines in both Cd stress conditions after 3 weeks of cultivation (Fig. 3.41 C). When plants grown in medium with extra 10 $\mu\text{M Cd}^{2+}$ the wild-type had significantly lower Fe content in shoot compared to *AhZIP6*-Suppressed lines and also control line (Fig. 3.41 D). At the presence of extra 20 $\mu\text{M Cd}^{2+}$, the wild-type had significantly lower Fe content in shoot compared to *AhZIP6*-Suppressed line 11-1 and 35S-GFP transgenic lines control line.



Results

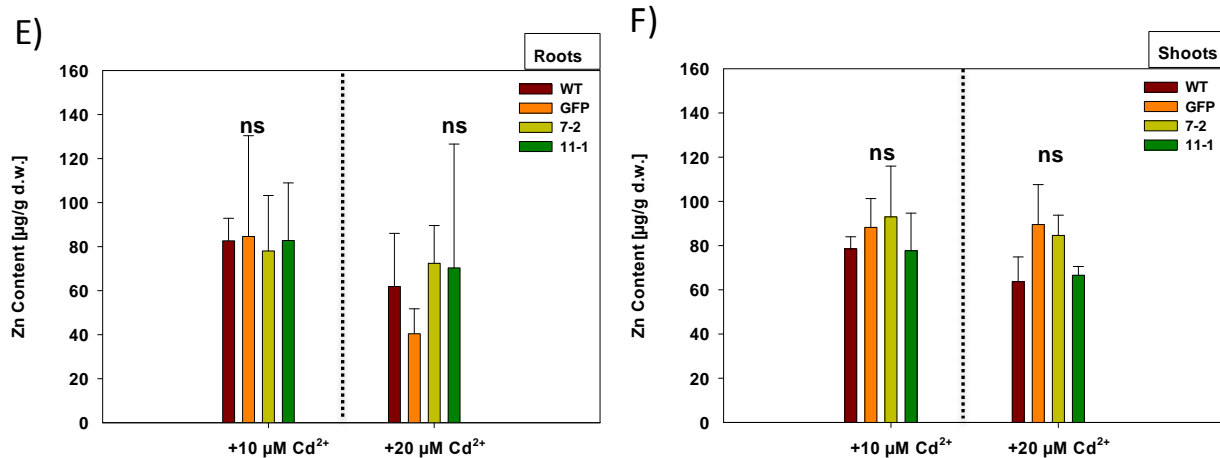


Fig. 3.41 Metal content in roots and shoots of *A. halleri* wild-type and *AhZIP6*-RNAi plants grown under Cd stress conditions

Plants were cultivated in 1/10 Hoagland medium as control, media supplemented with extra 10 μM or 20 μM Cd²⁺. Tissues were harvested after 3 weeks, digested and analyzed by ICP-OES. Shown in (A) and (B) are values for root and shoot Cd content respectively. Shown in (C) and (D) are values for root and shoot Fe content respectively and finally (E) and (F) are values for root and shoot Zn content respectively. All values are arithmetic means ± SD, n = 12 replicate clones per genotype from three independent experiments. Different characters above the bars indicate statistically significant differences detected in a one-way ANOVA, followed by Tukey test. D: P < 0.05 significance level between (a) and (b), ns: not significant.

3.3.3.5 Suppression of *AhZIP6* decreases roots short-term uptake of Cd in *A. halleri*

The higher tolerance towards Cd in *AhZIP6*-suppressed lines could be due to lower root Cd uptake. Since no significant differences were detected in root Cd content between *AhZIP6*-suppressed lines and control plants after 3 weeks of exposure to the Cd (Fig. 3.42 A), a short-term (15 and 30 minutes) uptake experiment using intact roots of wild-type, 35S-GFP transgenic line and two *AhZIP6*-suppressed lines 7-2 and 11-1 was performed. Roots were exposed to 2 or 5 μM Cd²⁺ at 4°C and room temperature. The 4°C and room temperature were chosen as indicator of non-active precipitation of metals in root surface and active root metal uptake temperatures respectively. Regardless of their genotypes, the Cd uptake at 4°C was similar in the roots of all plants in both short term conditions (15 and 30 minutes) in the presence of 2 μM Cd²⁺ (Fig. 3.41 A) or 5 μM Cd²⁺ (Fig. 3.41 B). In the presence of 2 μM Cd²⁺ at room temperature *AhZIP6* suppressed line 11-1 showed 30% reduction in root Cd uptake activity compared to the wild-type after 15 minutes of uptake and 33% reduction in root Cd content compared to the 35S-GFP transgenic line after 30 minutes of uptake (Fig. 3.42 A). In the presence of 5 μM Cd²⁺ at room temperature, after 15 minutes of uptake assay *AhZIP6* suppressed line 7-2 showed 24% and 28% reduction in Cd uptake activity in comparison to the wild-type and 35S-GFP lines respectively (Fig. 3.42 B). In the very same conditions, *AhZIP6* suppressed line 11-1 showed 20% and 24% reduction in Cd uptake activity compared to the wild-type and 35S-GFP lines respectively (Fig. 3.41 A). Reduction in root Cd uptake activity in *AhZIP6* suppressed lines was more pronounced after 30 minutes of activity test. In the presence of 5 μM Cd²⁺ at room temperature, after 30 minutes of uptake assay, *AhZIP6* suppressed line 7-2 showed 50% and 54% reduction in Cd uptake activity compared to the wild-type and 35S-

Results

GFP line respectively. *AhZIP6* suppressed line 11-1 showed 39% and 44% reduction in Cd uptake activity compared to the wild-type and 35S-GFP line respectively (Fig. 3.42 B). These results represent the first direct evidence for the role of *AhZIP6* in Cd uptake in *A. halleri*.

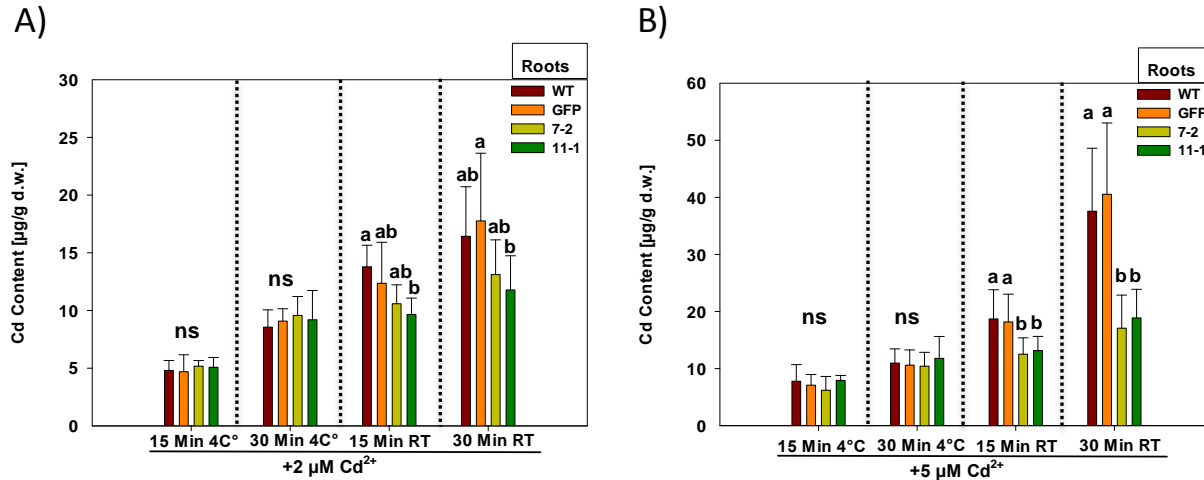


Fig. 3.42 Short-term uptake of Cd in *A. halleri* wild-type and *AhZIP6*-RNAi plants

Plants were cultivated in 1/10 Hoagland medium for 2 weeks and then subjected to the uptake media containing 2 µM and 5 µM Cd²⁺ at 25°C and 4°C. Roots were digested and metal content was analyzed by ICP-OES. Shown in (A) and (B) are values for root Cd content of plants exposed to 2 µM and 5 µM Cd²⁺ respectively. All values are arithmetic means ± SD, n = 12-15 replicate clones per genotype from three independent experiments. Different characters above the bars indicate statistically significant differences detected in Kruskal-Wallis One Way Analysis of Variance on Ranks A: P < 0.05 significance level between (a) and (b), B: P < 0.05 significance level between (a) and (b), ns: not significant.

3.3.3.6. Characterization of *AhZIP6*-RNAi lines on phenotyping and Bestwig soils

To investigate the possible effects of altered *AhZIP6* on metal accumulation and metal tolerance in near-natural conditions, the wild-type and 35S-GFP transgenic lines and two *AhZIP6*-suppressed lines 7-2 and 11-1 were grown in Bestwig soil as a highly contaminated soil and phenotyping soil as a standard soil for Cd and Zn hyperaccumulation assay. At the end of the cultivation, no sign of metal toxicity were detected in leaves of plants grown in both Bestwig and phenotyping soils and all genotypes had green leaves (Fig. 3.43 A and B). There were no significant differences in shoot fresh weight between genotypes grown in both soil conditions (Fig. 3.43 C).

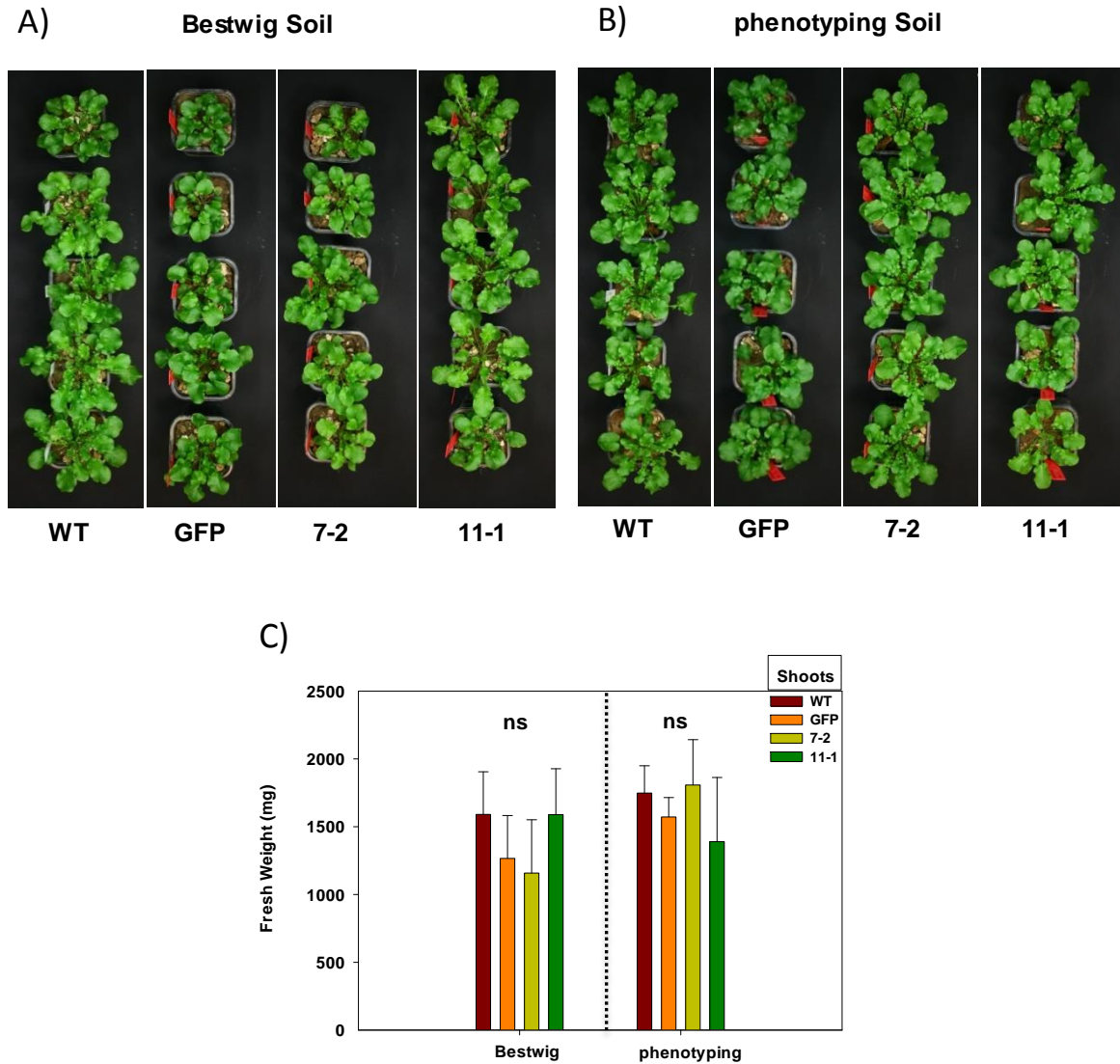


Fig. 3.43 Phenotype of *A. halleri* wild-type and *AhZIP6*-RNAi lines grown in Bestwig and phenotyping soils

Shown in (A) and (B) are photographs of representative wild-type, control transformant *GFP* line and two *AhZIP6*-suppressed lines 7-2 and 11-1 grown in Bestwig and phenotyping soils respectively. Shown in (C) is shoot fresh weight of plants grown for 6 weeks. All values are arithmetic means \pm SD, n =5 five replicate clones per genotype. ns: not significant.

3.3.3.6 Suppression of *AhZIP6* has no effect on shoot metal content of soil-grown *A. halleri*

There were no significant differences in shoot Fe content of two *AhZIP6*-suppressed lines compared to the wild-type and 35S-*GFP* control line (Fig. 3.44 A), Although plants grown in Bestwig soil generally accumulated higher amount of Zn compared to those grown on phenotyping soil, there were no differences between genotypes in their shoot Zn content (Fig. 3.44 B). Plants grown in phenotyping soil accumulated higher amounts of Mn (Fig. 3.44 C) and Cd (Fig. 3.44 D) regardless of

Results

their genotype, but with no detectable differences between shoot content of two *AhZIP6*-suppressed lines compared to the wild-type and control 35S-GFP transgenic line. Overall, based on these results, one could conclude that the suppression of *AhZIP6* had no effect on shoot metal content of *A. halleri* grown in Bestwig and phenotyping soils.

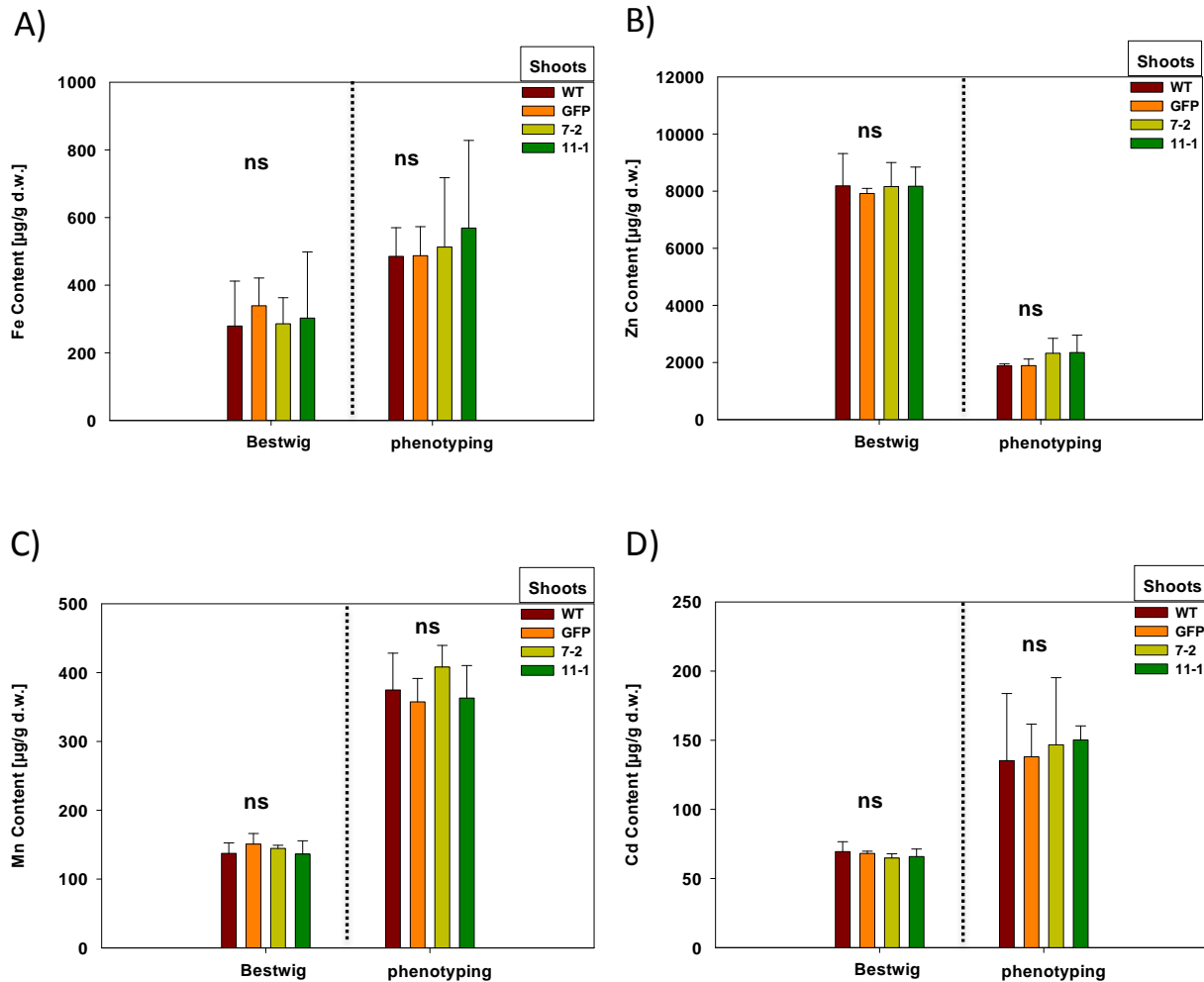


Fig. 3.44 Metal content in shoots of *A. halleri* wild-type and *AhZIP6*-RNAi lines grown in Bestwig and phenotyping soils

Plants were cultivated in Bestwig or phenotyping soils. Shoots were harvested after 6 weeks, digested and analyzed by ICP-OES. Fe content (A), Zn content (B), Mn content (C) and Cd content (D) are shown respectively. All values are arithmetic means \pm SD, $n=5$ replicate clones per genotype. ns: not significant.

3.3.3.7 Suppression of *AhZIP6* has no effect on lead (Pb) tolerance in *A. halleri*

It has been shown that, *A. halleri* is capable of accumulating above $1000 \mu\text{g g}^{-1}$ Pb in leaf dry biomass when it grows naturally in Pb-contaminated sites (Stein et al., 2016). To assess the effect of *AhZIP6* suppression on tolerance towards Pb in *A. halleri*, the wild-type plants, 35S-GFP transgenic line and *AhZIP6*-suppressed lines were hydroponically grown in LPP medium as control or in LPP medium supplemented with extra 2 and 5 $\mu\text{M Pb}^{2+}$ as Pb stress conditions as described in (Fischer et al.,

Results

2014). Regardless of their genotypes, *A. halleri* plants exposed to media with additional 2 μM Pb^{2+} and especially 5 μM Pb^{2+} showed shorter root length compared to the control conditions (Fig. 3.45 A). This reduction was less pronounced when root biomass was measured (Fig. 3.45 B) and was not detectable in shoot biomass (Fig. 3.45 C), indicating that Pb exposure is predominantly affecting root elongation in *A. halleri*. Results suggested that there were no significant differences in root length (Fig. 3.45 A), fresh root biomass (Fig. 3.45 B) and shoot biomass (Fig. 3.45 C) between genotypes in Pb stress conditions.

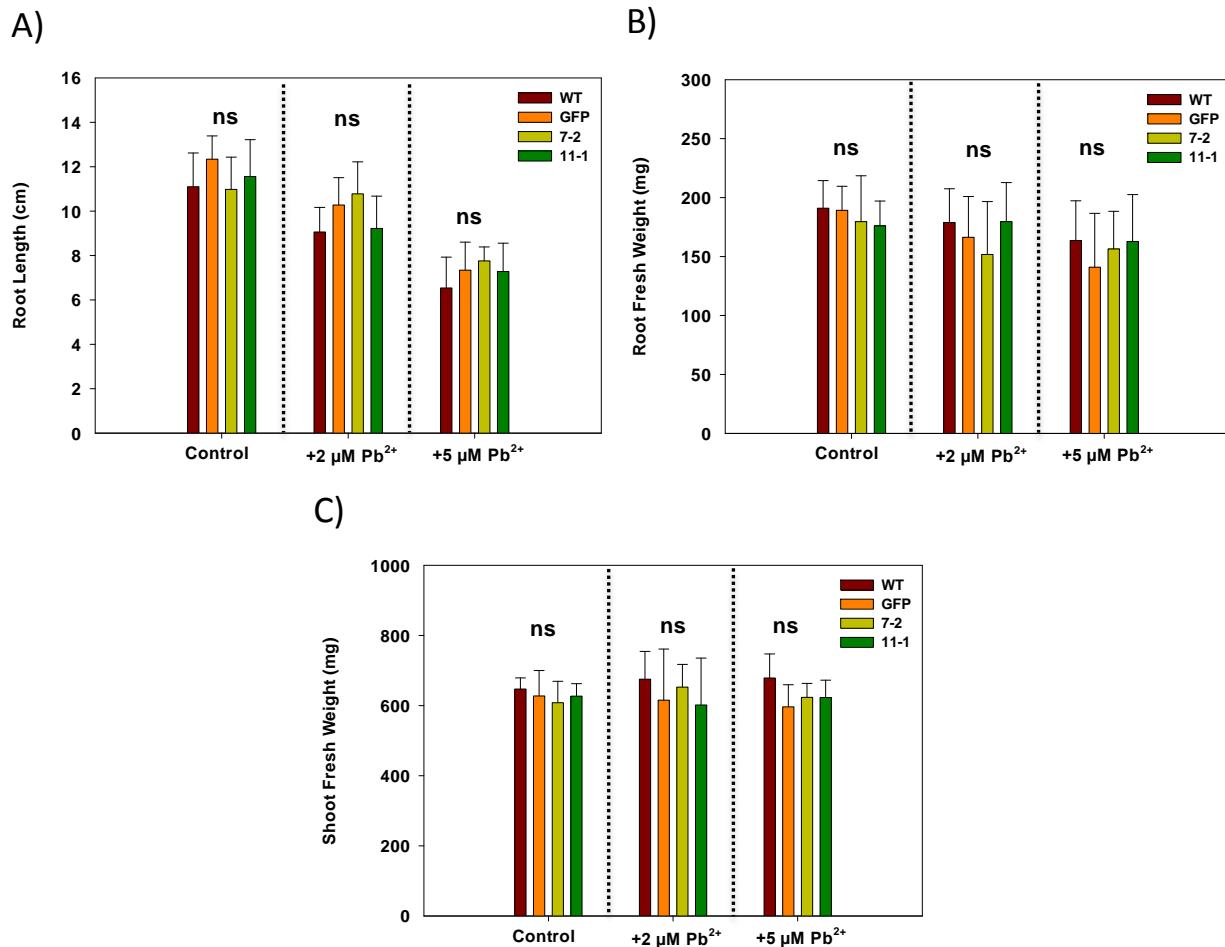


Fig. 3.45 Phenotype of *A. halleri* wild-type and *AhZIP6*-RNAi plants grown under Pb stress conditions

Plants were cultivated in 1/10 Hoagland LPP medium as control, medium supplemented with extra 2 and 5 μM Pb^{2+} . Shown in (A) are values for root length, (B) and (C) are values for root and shoot fresh weight respectively. All values are arithmetic means \pm SD, $n = 5$ replicate clones per genotype. ns: not significant.

3.4 The physiological role of *CAX1* in *A. halleri*

3.4.1 Comparison of *CAX1* expression in *A. halleri* C-line and *Auby* individuals

Geographic origin of the *A. halleri* individual crossed with *A. lyrata* to generate the population used for mapping the Cdtol QTLs was *Auby* in Northern France (Courbot et al., 2007). Because of the

Results

apparent lack of competence in plants from *Auby* (Figs. 3.7 and 3.8), *AhCAX1*-RNAi lines were generated via transformation of an individual from Langelsheim, so-called *C-line*. The populations in the Harz mountains in Germany and in Northern France are closely related (Pauwels et al., 2012). In order to compare *AhCAX1* expression between *Auby* and *C-line* individuals, four clonal replicates of each individual were grown for 3 weeks in 1.5 liter pots containing 1/10 Hoagland medium in parallel in growth chambers. Shoots were harvested and analyzed by real-time RT-PCR. Results suggested that, relative transcript level of *AhCAX1* in shoots of *C-line* and *Auby* individuals were similar, which confirmed that *C-line* is suitable individual in order to test whether *AhCAX1* is indeed the gene explaining Cdtol2 QTL or not (Fig. 3.46).

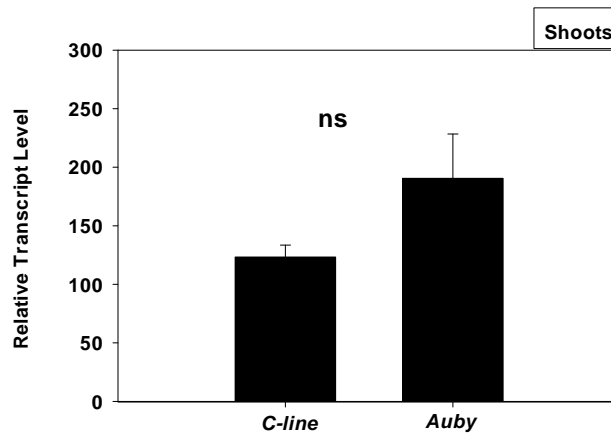


Fig. 3.46 *AhCAX1* transcript level in shoots of *Auby* and *C-line* individuals

Transcript level of *CAX1* was analyzed in shoots of hydroponically grown *A. halleri* *C-line* and *Auby* individuals. Tissues were harvested after 3 weeks of cultivation in 1.5 liter pots containing 1/10 Hoagland medium and analyzed by real-time RT-PCR. Transcript abundance expressed relative to *EF1 α* . Values are means \pm SD of four replicate clones in one cultivation round. ns: not significant, indicate statistically not significant differences detected in in Kruskal-Wallis One Way Analysis of Variance on Ranks test.

3.4.2 Confirmation of *AhCAX1*-RNAi lines with real-time PCR

To investigate the potential role of *CAX1* in Cd tolerance in *A. halleri*, *AhCAX1*-RNAi lines were generated from the wild-type individual *C-line*. Quantitative real time RT-PCR analyses using specific primers were performed in order to quantify transcript level of the *CAX1* gene. Out of 14 independent *AhCAX1*-RNAi lines which initially were analyzed, One line that showed the transcript level similar to the wild-type, was selected as transgenic control line and two lines which showed significantly reduced transcript levels relative to the wild-type were selected as strong RNAi lines for further study. The relative transcript abundance of *CAX1* was analyzed in shoots of soil-grown *AhCAX1*-RNAi lines under control conditions in two independent rounds and compared the wild-type plants. Results showed that, there was no significant reduction in transcript level in line 19-1 in comparison to the wild-type while two strong RNAi lines 17-1 and 18 had reductions of 89% and 95% respectively (Fig. 3.47).

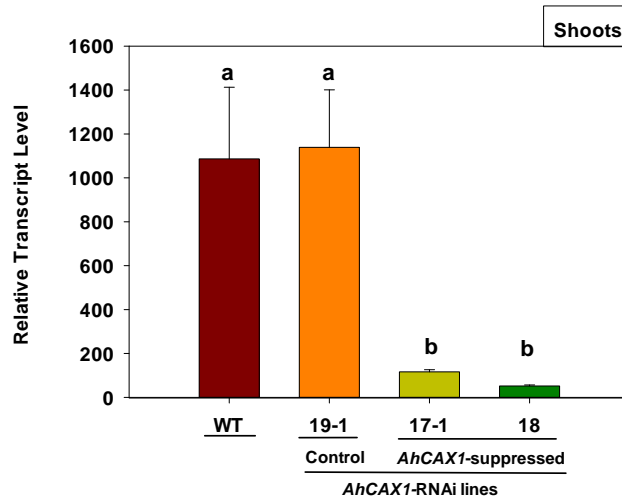


Fig. 3.47 Reduction of *AhCAX1* transcript level in independent RNAi lines

Transcript level of *AhCAX1* was analyzed in shoots of soil-grown *A. halleri* wild-type plant and *AhCAX1*-RNAi lines. Tissues were harvested after 6 weeks of cultivation in normal soil and transcript level was analyzed by real-time RT-PCR. Transcript abundance was expressed relative to *EF1α*. Values are means \pm SD of $n = 2$ independent experiments (Six replicate clones per genotype were pooled for each data point). Different characters above the bars indicate statistically significant differences detected in a one-way ANOVA, followed by Tukey test. $P < 0.05$ significance level between (a) and (b).

3.4.2 Tolerance assay of *AhCAX1*-RNAi lines

3.4.2.1 Suppression of *AhCAX1* has no effect on *A. halleri* biomass under Cd stress condition

Cd tolerance was assessed in *A. halleri* wild-type and *AhCAX1*-RNA lines according to (Courbot et al., 2007). Four clonal replicates of each line were grown hydroponically for 4 weeks in 1.5 liter pots containing a modified Murashige and Skoog (MS) medium. In order to test Cd tolerance, plants sequentially were transferred to a regime of weekly increasing Cd exposure with a range of 50, 100, 150, and 200 μM Cd. Tolerance was determined based on the relative fresh weight changes of plants following exposure to Cd, compared to their fresh weight before Cd exposure. At the end of each week, plants gently were taken out of medium and after gentle dry blotting, were weighted and taken back to the medium. The exact same procedure implicated after Cd exposure at the end of each week and plants fresh weight was measured. Results suggested that all genotypes responded similarly with no significant differences in plant biomass towards Cd stress (Fig. 3.48 A). Regardless of their genotypes, plants continued their growth after 2 weeks of exposure to additional 50 and 100 μM Cd²⁺ and there were no visible signs of toxicity in their leaves (Fig. 3.48 B). At the end of third week of Cd exposure, plants exposed to additional 150 μM Cd²⁺ showed chlorosis and appearance of curly shape growth in their leaves indicated high Cd toxicity (Fig. 48 B). While biomass of the wild-type plants was not increasing, control transformant line 19-1 and two *AhCAX1*-suppressed lines 17-1 and 18 showed minor increases in their relative fresh weight after the third week of Cd exposure (Fig. 3.48 A). At the end of fourth week of Cd exposure, all plants already

Results

reached their (EC100), i.e. the lowest content at which no new growth was observed and all plants showed reduction in their relative fresh weight (Fig. 3.48 A and B).

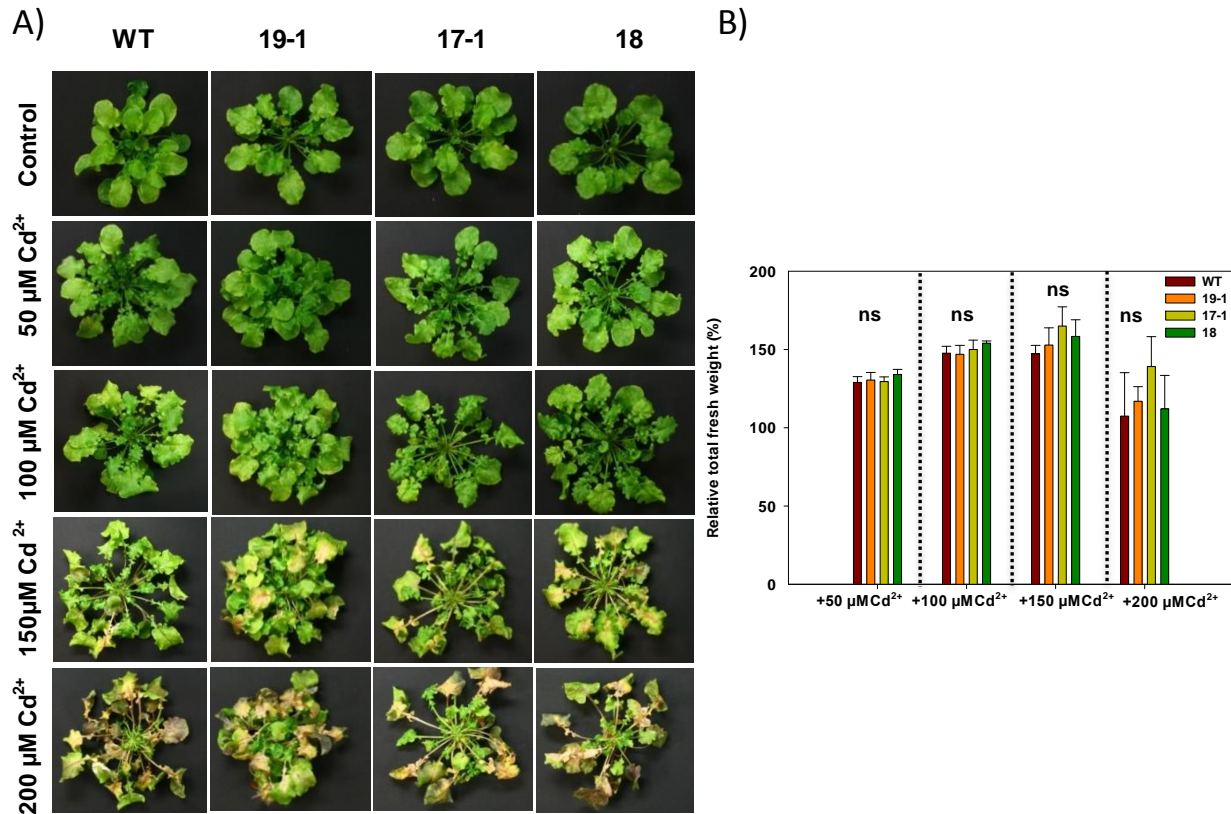


Fig. 3.48 Sequential Cd tolerance assay in *A. halleri* wild-type and *AhCAX1*-RNAi plants

Plants were hydroponically grown in a modified MS medium (Courbot et al., 2007) in 1.5 liter pots for 4 weeks. Later, they were transferred to a regime of weekly increasing Cd exposure with a range of 50, 100, 150, and 200 μM Cd. Shown in (A) are photographs of representative wild-type, control transformant line 19-1 and two *AhCAX1*-suppressed lines 17-1 and 18. Shown in (B) are values for plants relative fresh weight following exposure to 50, 100, 150 and 200 μM Cd compared to their fresh weight before Cd treatment. ns: not significant, indicate statistically not significant differences detected in a one-way ANOVA, followed by Tukey test.

3.4.3 ROS detection and quantification in *AhCAX1*-RNAi lines

3.4.3.1 Suppression of *AhCAX1* increase H₂O₂ accumulation following Cd treatment in *A. halleri*.

It has been shown that *A. thaliana* *CAX1* mutants show dramatically enhanced concentration of reactive oxygen species in roots while differences in root growth between wild-type and *CAX1* plants upon Cd²⁺ exposure were minimal (Baliardini et al., 2015). Therefore, analogous experiments were performed with the *A. halleri* *CAX1*-RNAi lines and ROS production quantified in control and Cd²⁺-treated plants. At the selected Cd²⁺ concentration of 10 μM, which does not cause growth inhibition, the roots of wild-type and control RNAi plants did not show an increase in H₂O₂ accumulation relative to untreated plants, while in *AhCAX1*-suppressed plants H₂O₂ accumulation was about 4-fold

Results

higher upon Cd^{2+} exposure (Fig. 3.49 A and B). Interestingly, this increase was completely absent when plants were treated with Cd^{2+} in medium with the higher Ca^{2+} concentration (Fig. 3.49 B).

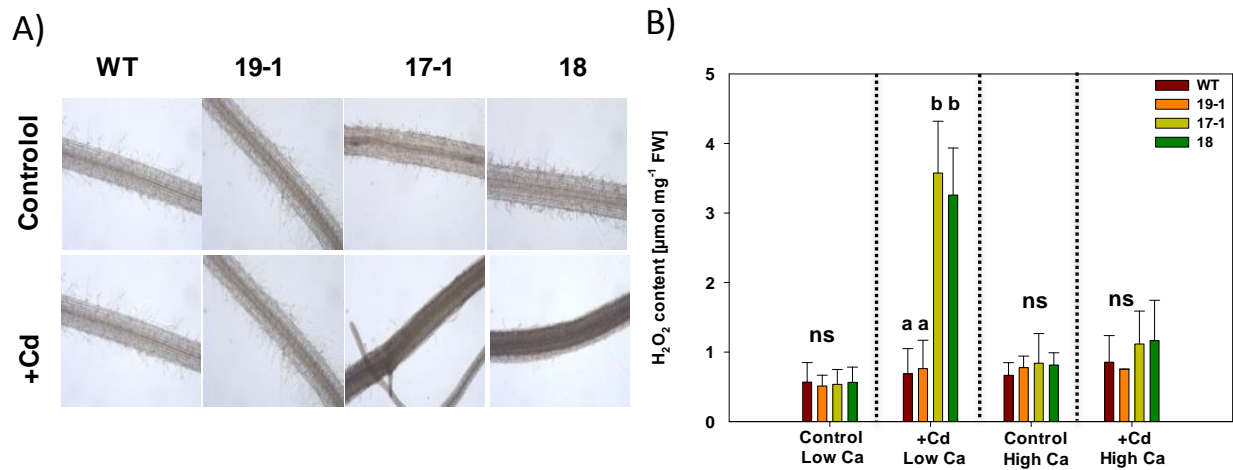


Fig. 3.49 Detection and quantification of H_2O_2 in *AhCAX1*-RNAi roots

Shown in (A) are photographs of *A. halleri* wild-type plant and *AhCAX1*-RNAi lines roots stained with DAB reagent in control conditions or after 24h of treatment with $10 \mu\text{M CdSO}_4$ in MS medium with low Ca content. Shown in (B) are values for root H_2O_2 content of plants grown in hydroponic solution with low or moderate Ca without CdSO_4 as control or with additional $10 \mu\text{M CdSO}_4$. Quantification of H_2O_2 content was achieved using a standard curve prepared with known amounts of DAB. All values are arithmetic means \pm SD, $n = 3$ with three replicate clones per genotype pooled per experiment. Different characters above the bars indicate statistically significant differences detected in a one-way ANOVA, followed by Tukey test, $P < 0.001$ significance level between (a) and (b), ns: not significant.

3.4.3.2 Suppression of *AhCAX1* increases superoxide accumulation following Cd treatment in *A. halleri*

Cd^{2+} -triggered generation of superoxide radical was assayed in a similar fashion, and quantification by NBT staining showed a strongly Ca^{2+} dependent and highly significant increase only in root of the plants with reduced *AhCAX1* transcript level (Fig. 3.50 A and B). Wild-type and control RNAi plants did not show enhanced superoxide radical accumulation when exposed to Cd^{2+} (Fig. 3.50 B).

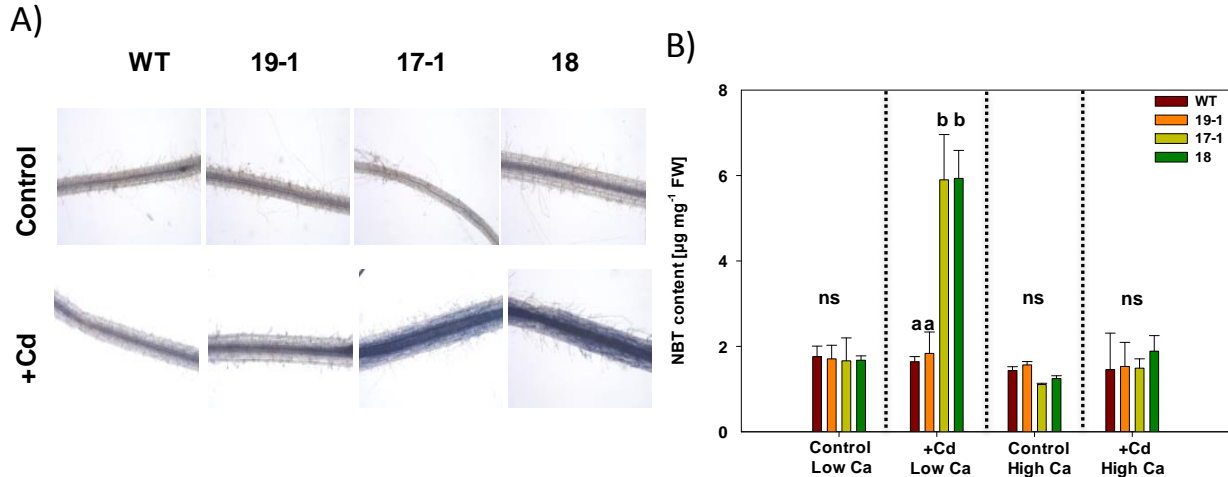


Fig. 3.50 Detection and quantification of NBT in *AhCAX1*-RNAi roots

Shown in (A) are photographs of *A. halleri* wild-type plant and *AhCAX1*-RNAi lines roots stained with NBT reagent in control conditions or after 24h of treatment with 10 μ M CdSO₄ in MS medium with low Ca content. Shown in (B) are values for root NBT content of plants grown in hydroponic solution with low or moderate Ca without CdSO₄ as control or with additional 10 μ M CdSO₄. Quantification of NBT content was achieved using a standard curve prepared with known amounts of NBT. All values are arithmetic means \pm SD, n = 3 with three replicate clones per genotype pooled per experiment. Different characters above the bars indicate statistically significant differences detected in a one-way ANOVA, followed by Tukey test, P<0.001 significance level between (a) and (b), ns: not significant.

3.5 The physiological role of *NRAMP3* in *A. halleri*

3.5.1 Confirmation of *AhNRAMP3*-RNAi lines with real-time PCR

In the heavy metal hyperaccumulator *A. halleri* the *NRAMP3* gene is expressed in roots and shoots at higher level in comparison to the non-hyperaccumulator *A. thaliana* (Weber et al., 2004 and Talke et al., 2006). Most characterized NRAMP proteins are able to transport a broad range of metal ions such as Mn, Zn, Fe, Cd and Ni (Nevo and Nelson, 2006) and it has been shown that the *NRAMP3* protein is associated with the homeostasis of Fe and Mn in *A. thaliana* (Thomine et al., 2000; Lanquar et al., 2005). In *A. halleri* *NRAMP3* protein may contribute to the Zn or Cd tolerance and hyperaccumulation or it may play roles in Zn homeostasis. In order to investigate the role of *NRAMP3* in metal hyperaccumulation and homeostasis in *A. halleri*, *AhNRAMP3*-RNAi lines were generated from wild-type plants. It has been shown in *A. thaliana* that *AtNramp3* and *AtNramp4* are most closely related sharing 75% conserved amino acid sequences (Thomine et al., 2000). The partially sequenced *A. halleri* genome (<https://phytozome.jgi.doe.gov>) revealed *A. halleri NRAMP3* (Araha.28176s0001.1) and *NRAMP4* (Araha.1484s0004.1) sequences. The pairwise predicted amino acid sequences comparison of *NRAMP3* and *NRAMP4* via (http://www.ebi.ac.uk/Tools/psa/emboss_needle/) revealed 86.4% of similarity and only 74.8% of identity in amino acid sequence between these two genes. Quantitative real time RT-PCR using specific primers was performed in order to analyze transcript levels of *AhNRAMP3* gene. Transcript level of *NRAMP3* in shoots of 11 independent soil-grown *AhNRAMP3*-RNAi transformants was analyzed in one round and compared to the wild-type plants. Among these lines, there was only line 31 with an *AhNRAMP3* transcript level similar to the wild-type plants, and all other lines showed

Results

different levels of reduction in *NRAMP3* transcript levels (Fig. 3.51 A). Line 31 was chosen as the transgenic control line and two *AhNRAMP3* lines 4-1 and 7 with 89% reduction in *AhNRAMP3* transcript levels compared to the wild-type were selected as strong RNAi lines for further experiments (Fig. 3.51 B).

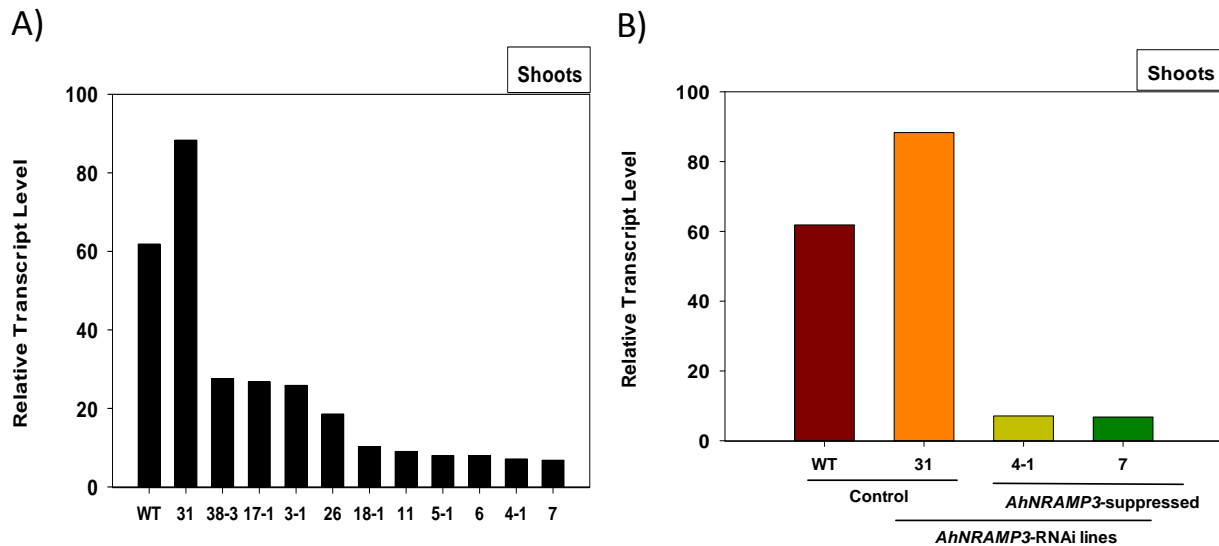


Fig. 3.51 Reduction of *AhNRAMP3* transcript level in shoots of independent RNAi lines

Transcript level of *AhNRAMP3* was analyzed in shoots of soil-grown *A. halleri* wild-type plant and 11 *AhNRAMP3*-RNAi lines (A). Shown in (B) are wild-type, control transformant line 31 and two strong RNAi lines 4-1 and 7 that were selected for further experiments. Tissues were harvested after 6 weeks of cultivation in normal soil and analyzed by real-time RT-PCR. Transcript abundance was expressed relative to *EF1 α* . Values are for one round experiment in which leaves of five replicate clones per genotype were pooled for each data.

3.5.2 Elemental profiling of *AhNRAMP3*-RNAi lines

3.5.2.1 *AhNRAMP3* suppression has no effect on *A. halleri* tolerance towards Cd

To assess the possible effects of *AhNRAMP3* suppression on Cd tolerance in *A. halleri*, wild-type, control transformant line 31 and two *AhNRAMP3*-suppressed lines 4-1 and 7 were grown hydroponically in 1.5 liter pots in *A. halleri* standard 1/10 Hoagland medium as control or in media supplemented with additional 10 μ M, 30 μ M and 50 μ M Cd²⁺. All plants were grown in parallel in growth chamber for 3 weeks and media were changed weekly. There were no detectable differences in root length and root and shoot biomass between genotypes in control conditions (Fig. 3.52 A to D). At the presence of 10 μ M Cd²⁺, there were no reduction in root length and root and shoot biomass, while at the presence of 30 and especially 50 μ M Cd²⁺, plants showed reduced root length and root and shoot biomass, indicating toxicity of the excess Cd with no significant differences between genotypes (Fig. 3.52 A to D). This experiment was conducted as an initial Cd tolerance test, and since there was extra 10 μ M Zn²⁺ in all stress media, Cd tolerance assay was also conducted in medium with low Zn content in order to minimize possible interference of Zn with Cd tolerance.

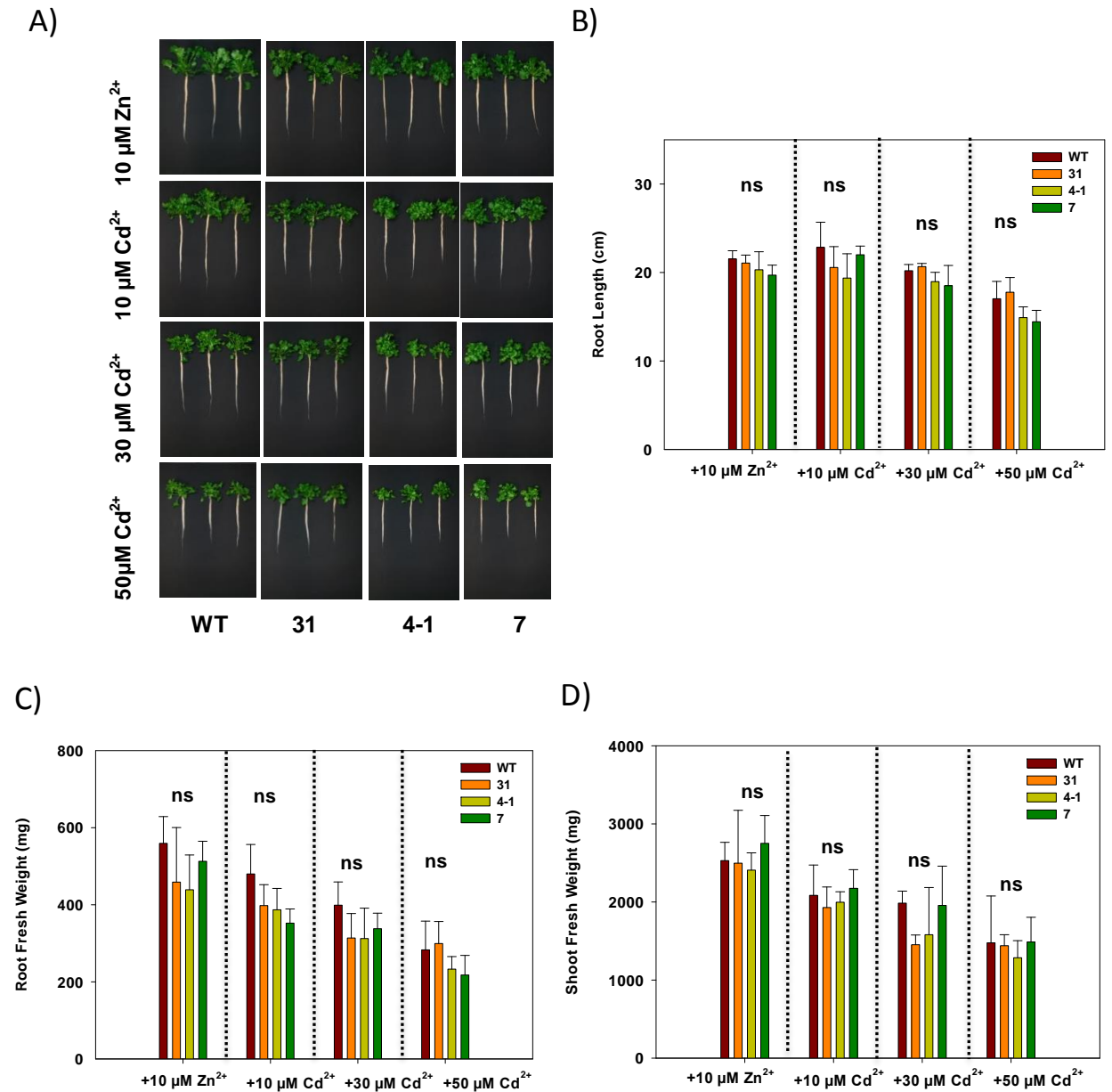


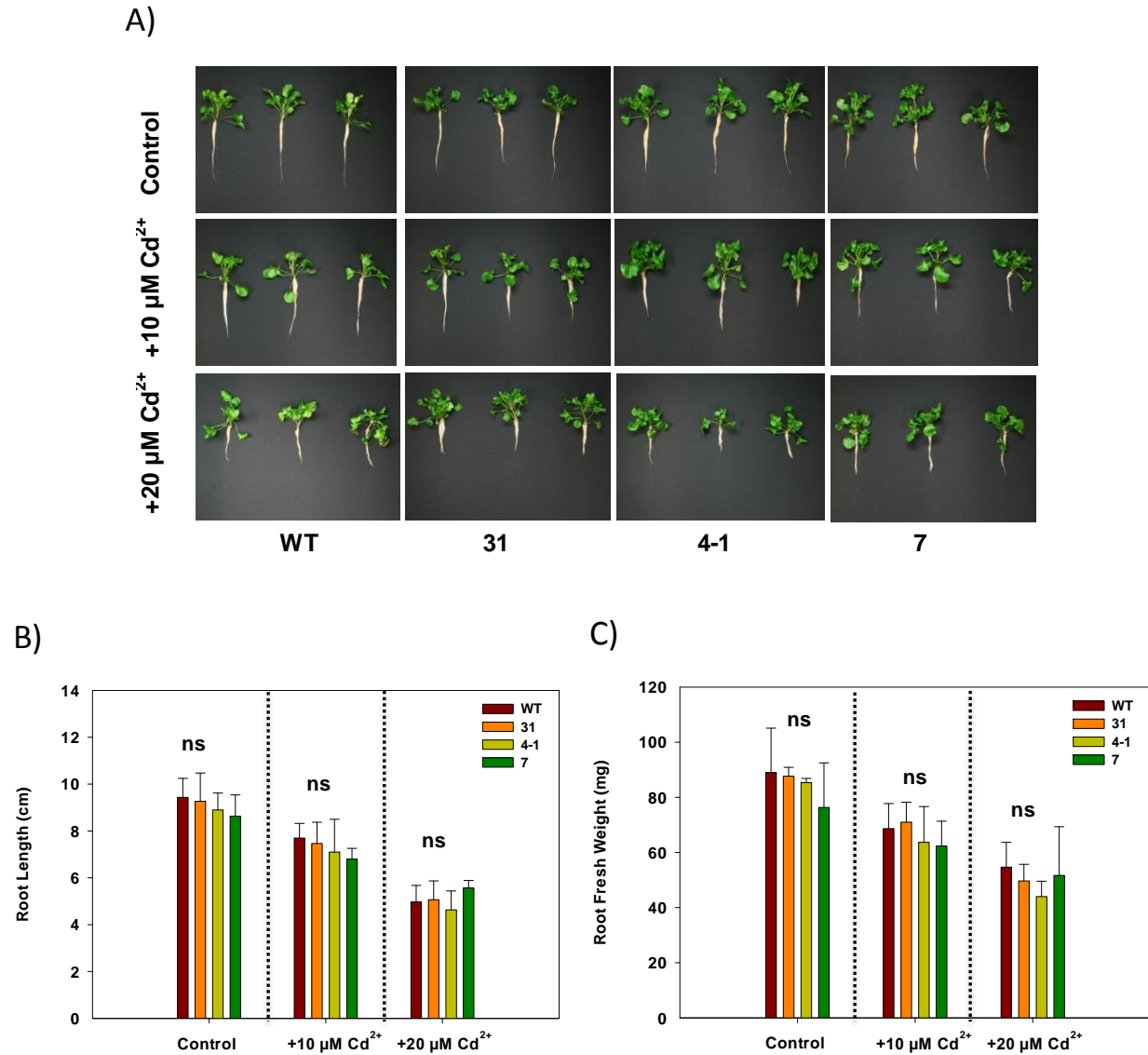
Fig. 3.52 Cd tolerance assay in *A. halleri* wild-type and *AhNRAMP3*-RNAi plants hydroponically grown in the medium with sufficient Zn content

Shown in (A) are photographs of representative wild-type, control transformant *AhNRAMP3*-RNAi line 31 and two *AhNRAMP3*-suppressed lines 4-1 and 7. Three individuals each in one round grown hydroponically for 3 weeks in 1.5 liter pots in *A. halleri* standard 1/10 Hoagland medium as control and in standard 1/10 Hoagland supplemented with additional 10 μM, 30 μM and 50 μM Cd²⁺. Values are for roots length (B) roots fresh weight (C) and shoots fresh weight (D) of plants after harvest. All values are arithmetic means ± SD, n = 3 replicate clones per genotype. ns: not significant.

A. halleri wild-type plants, control transformant *AhNRAMP3*-RNAi line 31 and two *AhNRAMP3*-suppressed lines 4-1 and 7 were also grown hydroponically for 3 weeks in 1/10 Hoagland medium as low Zn content control and in media with additional 10 or 20 μM Cd²⁺. There were no detectable differences in root length and root and shoot biomass between genotypes in control conditions (Fig.

Results

3.52 A). Upon Cd stress, regardless of their genotype, all plants showed reduction in root elongation (Fig. 3.53 A and B) and roots fresh weight (Fig. 3.53 A and C), while there was no reduction in plants shoot fresh weight in response towards Cd stress (Fig. 3.53 A and D).



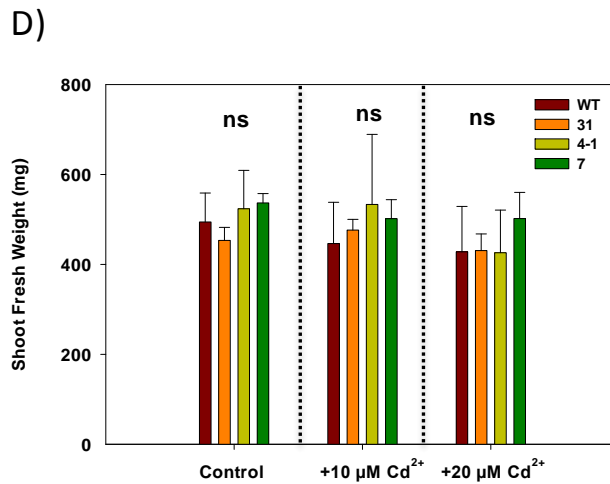
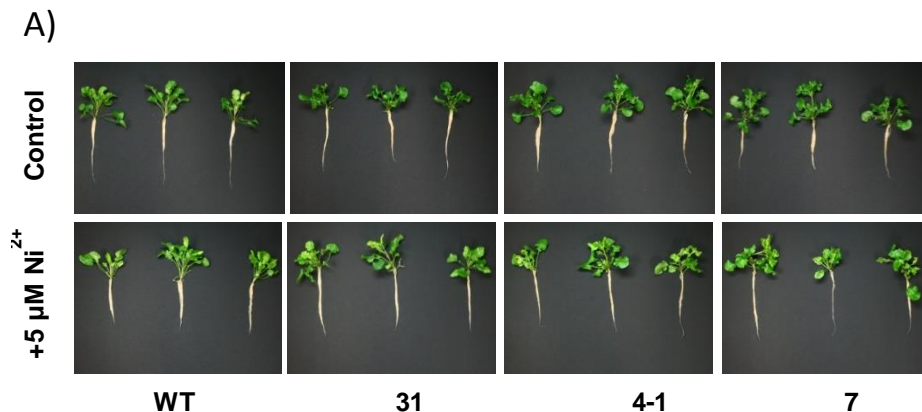


Fig. 3.53 Cd tolerance assay in *A. halleri* wild-type and *Ah-NRAMP3*-RNAi plants hydroponically grown in the medium with low Zn content

Shown in (A) are photographs of representative wild-type, control transformant line 31 and two *AhNRAMP3*-suppressed lines 4-1 and 7. Three individuals each in one round were grown hydroponically for 3 weeks in 1/10 Hoagland medium as control and in media with additional 10 or 20 µM Cd²⁺. Values are for root length (B) root fresh weight (C) and shoot fresh weight (D) respectively. All values are arithmetic means ± SD, n =3 replicate clones per genotype. ns: not significant.

3.5.2.3 *AhNRAMP3* suppression has no effect on Ni tolerance in *A. halleri*

To investigate the possible effects of *AhNRAMP3* suppression on tolerance towards Ni in *A. halleri*, wild-type, control transformant line 31 and two *AhNRAMP3*-suppressed lines 4-1 and 7 were grown hydroponically for 3 weeks in 1/10 Hoagland medium as control and in medium supplemented with additional 5 µM Ni²⁺. There were no detectable differences in root length and root and shoot biomass between genotypes in control and upon Ni stress conditions (Fig. 3.54 A to D). Although there was no reduction in plants shoot fresh weight in response towards Ni stress, but leaves of all plants regardless of their genotypes showed chlorosis as an indication of Ni toxicity (Fig. 3.54 A). These results demonstrated that suppression of *NRAMP3* gene has no effect on Ni tolerance in *A. halleri*.



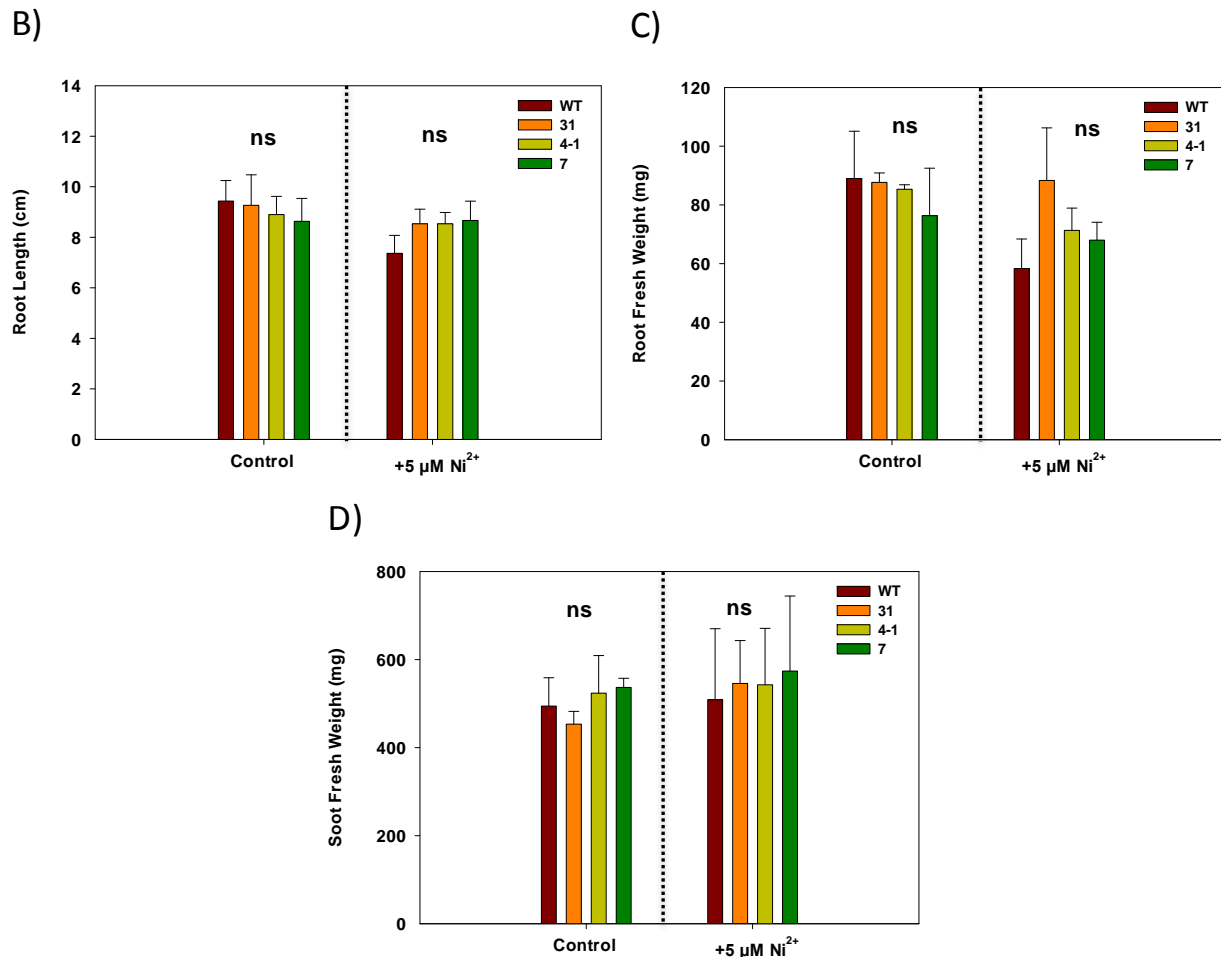


Fig. 3.54 Ni tolerance assay in *A. halleri* wild-type and *AhNRAMP3*-RNAi plants

Shown in (A) are photographs of wild-type, control transformant line 31 and two *AhNRAMP3*-suppressed lines 4-1 and 7. Three individuals each in one round grown hydroponically for 3 weeks in 1/10 Hoagland medium as control and in medium with additional 5 $\mu\text{M Ni}^{2+}$ as Ni stress conditions. Values are for root length (B) root fresh weight (C) and shoot fresh weight (D) respectively. All values are arithmetic means \pm SD, n =3 replicate clones per genotype. ns: not significant.

3.5.2.4 *AhNRAMP3* suppression has no effect on tolerance towards Fe deficiency in *A. halleri*

To assess the possible effects of *AhNRAMP3* suppression on tolerance towards Fe deficiency in *A. halleri*, wild-type, transformant control line 31 and two *AhNRAMP3*-suppressed lines 4-1 and 7 were grown hydroponically for 3 weeks in 1.5 liter pots in control 1/10 Hoagland. In parallel, all lines were also subjected to the Fe depleted medium in third week of their cultivation. In control conditions, as expected all plants were green and no signs of Fe deficiency were detectable, while plants subjected to the Fe depletion, regardless of their genotype showed leaf chlorosis (Fig. 3.55 A). There were no differences in root length, root and shoot biomass under control and upon Fe deficiency conditions between genotypes (Fig. 3.55 A to D).

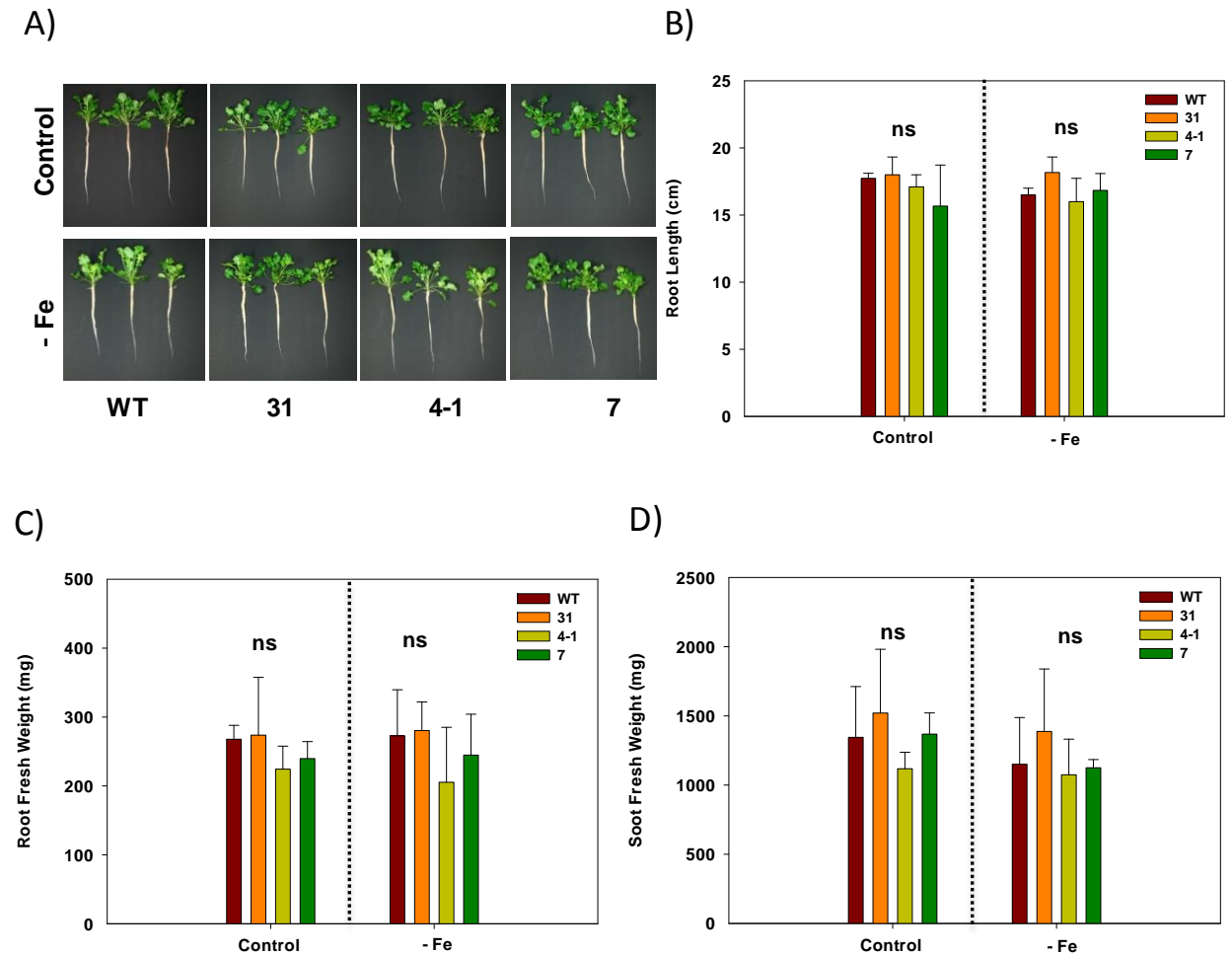


Fig. 3.55 Fe deficiency assay in *A. halleri* wild-type and *AhNRAMP3*-RNAi plants

Shown in (A) are photographs of the wild-type, control transformant line 31 and two *AhNRAMP3*-suppressed lines 4-1 and 7. Three individuals each in one round were grown hydroponically for 3 weeks in 1/10 Hoagland medium as control and in same medium for 2 weeks followed by one week growth in 1/10 Hoagland medium without Fe supply as Fe depletion conditions. Values are for root length (B) root fresh weight (C) and shoot fresh weight (D) respectively. ns: not significant.

3.5.2.5. Silencing of *AhNRAMP3* has no effect on root and shoot metal content of *A. halleri* plants hydroponically grown in control or Fe depleted medium

There were no significant differences in root and shoot Fe content (Fig. 3.56 A and B), Zn content (Fig. 3.56 C and D) and Mn content (Fig. 3.56 F and E) between two *AhNRAMP3* suppressed lines and control plants grown in control and Fe depleted conditions. These results suggested that in *A. halleri*, suppression of *AhNRAMP3* has no detectable effect in Zn, Fe and Mn accumulation under control or Fe depleted conditions.

Results

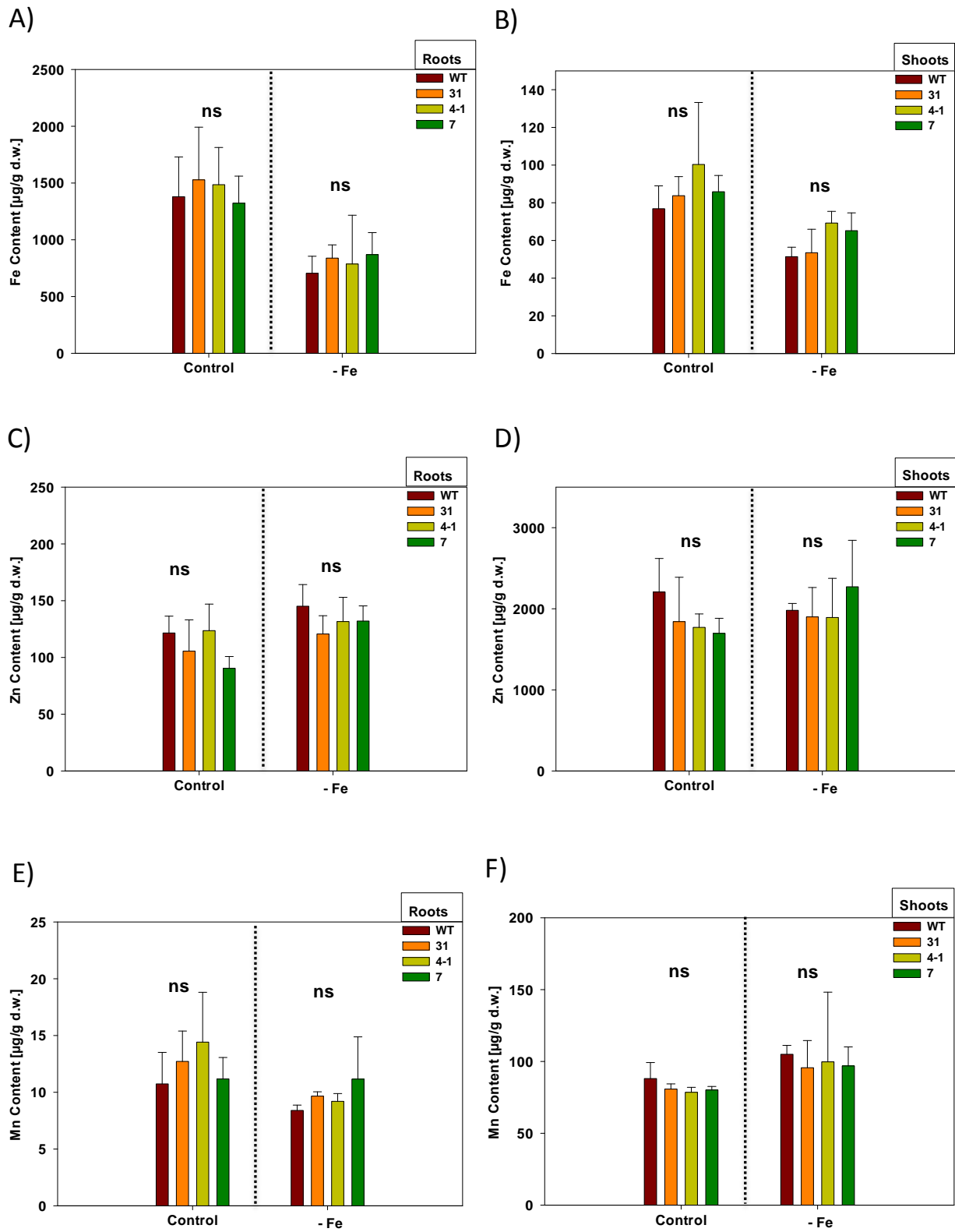


Fig. 3.56 Metal content in roots and shoots of *A. halleri* wild-type and *AhNRAMP3*-RNAi plants grown in control and Fe deficiency conditions

Results

Plants were grown hydroponically for 3 weeks in 1.5 liter pots in 1/10 Hoagland medium as control and in same medium for 2 weeks followed by one week growth in the same medium without Fe supply as Fe depletion conditions. Tissues were harvested, digested and analyzed by ICP-OES. Shown in (A and B) are values for root and shoot Fe content, (C and D) are values for root and shoot Zn content and finally (E and F) are values for root and shoot Mn content respectively. All values are arithmetic means \pm SD, n =3 replicate clones per genotype. ns: not significant.

4. Discussion

4.1 Optimized protocol for *Agrobacterium*-mediated transformation of *A. halleri*

The ability to successfully perform genetic manipulations is essential to enable reverse genetic studies in *A. halleri* aiming at dissecting molecular aspects of heavy metal hyperaccumulation and hypertolerance. Therefore, developing a successful and highly efficient method for *A. halleri* transformation and in vitro regeneration is highly appreciated. The previously established protocol for *A. halleri* transformation (Deinlein et al., 2012; Hanikenne et al., 2008), was seed-dependent and used roots as the source of explants. Although there was an attempt of callus induction and shoot regeneration by using leaflets as explants (Vera-Estrella et al., 2009), stable transformation was not explored. In order to obtain an efficient protocol that would allow transformation of vegetatively propagated plants, i.e. independent of crossing and seed production, modifications of the established transformation protocol (Deinlein et al., 2012; Hanikenne et al., 2008) were explored. In this study, callus induction and vigorous callus proliferation were achieved by incubating *A. halleri* leaflet and petiole explants on CIM (Vera-Estrella et al., 2009), and after transformation adventitious shoots formed on SIM (Deinlein et al., 2012; Hanikenne et al., 2008). The combination of CIM (Vera-Estrella et al., 2009) and SIM protocol (Deinlein et al., 2012; Hanikenne et al., 2008) resulted in optimal chemical form and concentrations of auxin and cytokinin for callus induction and subsequently for shoot regeneration. There was no difference in callus formation competency between leaf blade and petiole segments of young plants and callus formation reached 100% in two independent rounds (Table. 3.1) and (Fig. 3.5). This observation was in agreement with callus formation rates achieved by (Vera-Estrella et al., 2009). Given the large number of factors that potentially affect the transformation efficiency, primary focus was on the effects of initial culture and inoculation density of *A. tumefaciens* on transformation efficiency.

It is known that optimal *A. tumefaciens* density for transformation is dependent on *Agrobacterium* strain and plant species (Amoah et al., 2001; Mondal et al., 2001). Therefore, exploring the optimal density for a specific transformation system is essential. Since it was unknown to what extent culture density would affect or interact with inoculation density, the range between log phase and stationary phase was considered in cultures. The optimal density of *A. tumefaciens* for *A. halleri* stable transformation was achieved when the initial culture and the inoculation culture were grown until *A. tumefaciens* reached stationary phase with an OD₆₀₀ of 3 and 5 respectively. This led to an 8% rate of successful transformation (Fig. 3.3). It is documented that recalcitrant explants or species need higher density of *A. tumefaciens* for successful transformation, especially when inoculation time is short (Zhao et al., 2000; 2001; Gnasekaran et al., 2014). The comparatively short inoculation time of calli with *A. tumefaciens* in this study of 10 minutes, might explain why transformation was more efficient when inoculation culture reached its stationary phase. It was shown that acetosyringone in a final concentration of 150 µM in co-cultivation MS medium enhanced the interaction between *A. tumefaciens* and *A. halleri* cells, which led to an increase in positive stable transformation rates from 7% in those transformed without acetosyringone to 14% in plants were transformed by help of acetosyringone (Fig. 3.4). The effect of acetosyringone on *Agrobacterium*-mediated transformation efficiency is known to vary according to the plant species. Generally in monocots, addition of phenolic compounds such as acetosyringone during co-cultivation supports

Discussion

the gene transfer (Kumlehn et al., 2006; He et al., 2010) and James et al., (1993) showed that acetosyringone enhances *Agrobacterium*-mediated transformation of apple.

It has been shown that there is remarkable natural variation in the capacity of Zn and Cd accumulation between *A. halleri* individuals collected from different populations of various sites or within a specific population (Stein et al., 2016). Therefore, the ability to successfully transform particular *A. halleri* accessions would be beneficial for characterizing the functions of hyperaccumulation candidate genes in different accessions. In this study, the influence of genotype on transformation efficiency in *A. halleri* individuals from different populations belonging to separate biogeographical regions according to (Koch and Matschinger, 2007) was investigated. The explants from various individuals clearly differed in their competence of callus formation. While explants derived from *Auby* were incompetent to induce callus, individuals from other populations regardless of their biogeographical origin showed 100% callus induction. Various individuals had different ability of shoot regeneration from transformed calli, with no correlation between biogeographical origin of individuals and their transformation competence (Tab 3.2 and Fig. 3.8). It is known that within *A. thaliana* and tomato various cultivars or ecotypes show different degrees of susceptibility to tumorigenesis by *Agrobacterium* (Nam et al., 1997; Van Roekel et al., 1993) Furthermore, only a few genotypes in maize, chickpea and citrus (Sidorov et al., 2006; Bhattacharjee et al., 2010; Manjul et al., 2009) are competent for stable *Agrobacterium*- mediated transformation. In the present study, we developed an efficient protocol for *A. tumefaciens*-mediated stable transformation of vegetatively propagated *A. halleri* plants, i.e. independent of seed production.

4.2 *NAS4* plays an important role in Fe homeostasis in *A. halleri*

4.2.1 *AhNAS4* is not a Zn and Cd hyperaccumulation and hypertolerance gene in *A. halleri*

In order to gain insight into the molecular mechanisms underlying metal hyperaccumulation and hypertolerance in *A. halleri*, it is necessary to determine the contribution of putative candidate genes known to be involved in plant metal homeostasis. The ability to generate RNAi-mediated knockdown lines in *A. halleri* allowed to directly assess the role of *HMA4* and *NAS2* genes in metal hyperaccumulation (Hanikenne et al., 2008; Deinlein et al., 2012; Cornu et al., 2015). The initial hypothesis based on the comparative transcriptome analysis between *A. halleri* and *A. thaliana* was that, *AhNAS4* might play a role in metal hyperaccumulation in *A. halleri*. In this study, knockdown RNAi lines of *A. halleri* in which transcript level of *AhNAS4* was significantly reduced, were used to dissect the direct role of the *AhNAS4* gene in metal hyperaccumulation. It was confirmed that the suppression of *NAS4* did not change transcript abundance of *NAS1*, *NAS2* and *NAS3* in suppressed *NAS4-RNAi* lines (Fig. 3.10). The tissue specific expression patterns of four known *AhNAS* homolog genes were consistent with the pattern known for *A. halleri* (Deinlein et al., 2012) and *A. thaliana* (Klatte et al., 2009). Suppression of *AhNAS4* resulted in reduced root NA content in *A. halleri* grown in sufficient Zn conditions (Fig. 3.11). Despite the fact that *AhNAS4* is predominantly expressed in the shoots of *A. halleri*, surprisingly no significant changes in shoot NA content were observed upon altered *NAS4* transcript level (Fig. 3.11). It has been shown that suppression of *AhNAS2* in *A. halleri* resulted in a 5-fold reduction in Zn shoot: root ratio when plants were hydroponically grown in Zn sufficient conditions (Deinlein et al., 2012). In the similar conditions, there was a slight reduction in

Discussion

Zn shoot: root ratio of two *NAS4*-suppressed lines compared to the wild-type, but this reduction was not significant when compared to control transformant line 11-2 (Fig. 3.12 C). It has been shown that suppression of *AhNAS2* as a major responsible gene for root NA synthesis also led to a reduction of Zn root to shoot translocation in plants grown in Ni stress conditions (Cornu et al., 2015). Suppression of *NAS4* had no effects in root, shoot and consequently root-to-shoot translocation of Zn in *A. halleri* when hydroponically grown in media with low Zn (Fig. 3.22), with excess Zn, with additional Ni and Cd (Fig. 3.22 and 3.24) and in alkaline conditions (Fig. 3.18). It also had no effects in root and shoot Cd content and consequently root-to-shoot translocation of Cd in *A. halleri* when hydroponically grown under Cd stress conditions (Fig. 3.24). In addition, when plants were grown in Zn and Cd contaminated Bestwig and phenotyping soils, there were no significant changes in shoot Cd content of plants upon suppression of *AhNAS4* (Fig. 3.34 C). These results clearly show that *AhNAS4* does not have an important contribution to Zn and Cd hyperaccumulation in *A. halleri*. It has been shown that suppression of *AhNAS2* has no effects on tolerance towards Zn and Cd in *A. halleri* (Cornu et al., 2015; Deinlein et al., 2012). It was shown that the suppression of *AhNAS4* also had no significant effects in root and shoot biomass of *A. halleri* plants upon Zn and Cd excess conditions (Fig. 3.24). In addition, *A. halleri* cultivation in slightly Zn and Cd contaminated phenotyping soil or heavily Zn and Cd contaminated Bestwig soil confirmed that suppression of *NAS4* has no effects on Zn and Cd tolerance in *A. halleri* (Fig. 3.33). One could conclude from these data that *AhNAS4* does not have a measurable contribution to tolerance towards Zn and Cd in *A. halleri*. It was also shown that suppression of *AhNAS4* resulted in a severe reduction in root elongation, root and shoot biomass in *A. halleri* upon Ni stress conditions (Fig. 3.28). The Ni sensitivity symptoms caused by NA deficiency in *AhNAS2*-suppressed lines (Cornu et al., 2015) and *A. thaliana* *NAS4-1* mutants (Klatte et al., 2009; Palmer et al., 2013) were restricted to root elongation and root biomass reduction. Cornu et al., (2015) suggested that NA mediates trapping of Ni in root tissue and the formation of Ni-NA complexes in root cells suppress the interaction of reactive Ni²⁺ cations with cytosolic components and consequently leads to less toxicity in plants. Since *NAS4* is expressed in roots and shoots of *A. halleri* and *NAS2* expression is restricted to roots, the shoot biomass reduction in strong *NAS4*-RNAi lines upon additional Ni might be related to altered expression of *AhNAS4* in shoots of suppressed lines.

4.2.2 Suppression of *AhNAS4* enhances root-to-shoot translocation of Fe and consequently tolerance towards Fe deficiency

It is known that *NAS* genes evolved as a gene family in *A. thaliana* and *A. halleri* with overlapping and specific functions in metal homeostasis as well as differential gene regulation in response to metals (Klatte et al., 2009; Schuler and Bauer, 2011; Deinlein et al., 2012). It was shown that suppression of *NAS4* in *A. halleri* resulted in both similar and distinct phenotypes compared to what was observed upon *NAS2* suppression. *NAS4* suppression in *A. halleri* similar to *NAS2*-knockdown resulted in Ni susceptibility, slightly enhanced trapping of Zn in roots with no changes in tolerance towards Cd and Zn. One of the major finding of our study was that suppression of *NAS4* resulted in specifically enhanced root-to-shoot translocation of Fe in *A. halleri* when plants hydroponically grown in media with low Zn content, with sufficient Zn, with additional Ni or in alkaline conditions. In all conditions while root Fe content was strongly reduced, shoot Fe content in *NAS4*-suppressed lines was increased and consequently the Fe shoot: root ratio in two *NAS4*-suppressed lines was 2 to 4-fold higher compared to the wild-type and control plants (Fig. 3.13, 3.17 and 3.25). In addition, suppression of *AhNAS4* in *A. halleri* increased tolerance towards Fe deficiency. In Fe limiting

Discussion

conditions, while the wild-type and control plants suffered from Fe deficiency and showed interveinal chlorosis especially in their young leaves with a reduction in shoot biomass and chlorophyll content, two *AhNAS4*-suppressed lines did not show any sign of Fe deficiency (Fig. 3.16 and 3.25). These results are totally opposite to what has been reported for *A. thaliana*. The *A. thaliana nas4* single T-DNA insertion lines had similar NA content as the wild-type (Klatte et al., 2009), did not show increase in shoot Fe content when grown in normal or alkaline soils, were sensitive to Fe deficiency and exhibited reduced size and interveinal chlorosis when grown in alkaline soil (Palmer et al., 2013). In *A. thaliana* transcript levels of Fe uptake machinery genes including *AHA2*, *IRT1*, *IRT2* and *FRO2* were increased in Fe deficiency conditions (Vert et al., 2002; Palmer and Guerinot, 2009; Morrissey and Guerinot, 2009; Shanmugam et al., 2011; Fourcroy et al., 2014). *A. halleri* apparently did not involve changes in transcript levels of Fe uptake machinery genes, as their expression in *A. halleri* has been shown to be lower than in *A. thaliana* under both Fe-sufficient and Fe-deficient conditions (Shanmugam et al., 2011). The contradictory responses towards Fe deficiency in *A. halleri* compared to the non-hyperaccumulator *A. thaliana* suggest a distinct Fe homeostasis mechanism. It has been shown that citrate is the preferred Fe chelator at the typical acidic pH of xylem, while in the phloem sap at more neutral and alkaline pH values NA is the main Fe chelator (Rellán-Alvarez et al., 2008). The importance of citrate for xylem-mediated root-to-shoot translocation of Fe has been shown in the *A. thaliana frd3* mutant with a nonfunctional citrate transporter gene. This mutant had 40% less citrate in the xylem compared to the wild-type and accumulated Fe in the root central cylinder and showed symptoms of Fe deficiency (Green and Rogers, 2004; Durrett et al., 2007; Schuler et al., 2012). NA has been observed in the phloem sap of different plant species and is suggested as the Fe chelator involved in phloem-based partitioning of Fe after unloading from the xylem (Wirén et al., 1999; Schmidke et al., 1999; Krüger et al., 2002; Rellán-Alvarez et al., 2008). Schuler et al., (2012) showed that NA is required for remobilization of Fe from the phloem to the sinks. In *A. thaliana nas4x-2* quadruple mutant, bask Fe in leaves was similar to wild-type plants. However, insufficient amounts of Fe reached the chloroplasts in the interveinal cells of the young leaves, leading to chlorosis. Schuler et al., (2012) proposed that there is a crosstalk between NA and citrate-mediated Fe translocation to leaves and plants compensate the lack of citrate or NA in roots by promoting the synthesis of the other chelator. They showed that in *A. thaliana frd3* mutant *NAS4* was induced 4-fold and *frd3* mutant had a 2-fold increase in NA levels. Schuler et al., (2012) also showed that *FRD3* was induced 12-fold in roots of *nas4x-2* mutant compared to the wild-type *A. thaliana* and *nas4x-2* xylem sap showed a 4-fold increase in citrate concentrations compared with the wild-type plants. They showed that changes in gene expression levels in both mutants were confined to roots. We speculate that in Zn and Cd hyperaccumulator *A. halleri* the higher transcript level of *NAS* genes could be an adaptation to efficiently translocate more Zn and Cd from roots to shoots. Therefore, suppression of *AhNAS2* as a major responsible gene for root NA synthesis decreased Zn and Cd root to shoot translocation while it had no effect on Fe root and shoot content (Cornu et al., 2015; Deinlein et al., 2012). Furthermore, we assume that *AhNAS4* down regulation might increase synthesis and efflux of organic acids like citrate and malate into the xylem in *A. halleri*, which consequently would increase Fe translocation from roots to the shoot. Xylem sap analysis of *AhNAS4*-suppressed lines and wild-type plants in further studies might help to determine the nature and status of organic acids and their role in Fe homeostasis upon suppression of *AhNAS4*. The μ PIXE images of leaves of alkaline soil-grown plants confirmed that the young and old leaves of *AhNAS4*-suppressed line have accumulated more Fe compared to the wild-type leaves of the same age (Fig. 3.31). The Fe distribution pattern was well correlated with the development of leaf chlorosis and was especially prominent in the

mesophyll part between the main and the lateral veins in the wild-type. The interveinal chlorosis in the young leaves of *A. halleri* wild-type plants seen in Fe limiting conditions was intensified with age. We assume that suppression of *NAS4* in *A. halleri* activates loading of citrate into xylem sap leads to an increase in Fe transport across the xylem parenchyma to the phloem of adjacent leaf tissues in *NAS4* suppressed lines. Therefore, there would be higher amount of Fe in young and especially old leaves of *NAS4* suppressed lines compared to the wild type plants. The μ PIXE images confirmed more efficient Fe distribution in leaves of *NAS4* suppressed lines compared to the patchy Fe distribution in the wild-type leaves, which confirmed that the interveinal chlorosis was attributable to the decreased Fe concentration in the interveinal mesophyll area (Fig. 3.31). Schuler et al., (2012) proposed that lateral transport route for Fe from xylem to leaf parenchyma may rely on citrate rather than NA and in *A. thaliana* *frd3 nas4x-2* mutants, which are unable to load citrate into the xylem; old leaves that rely on a citrate-dependent xylem pathway for obtaining adequate levels of Fe would not recover after aging. In addition, it has been suggested that YSLs in dicots contribute to Fe distribution within the plant (Curie et al., 2009). It also has been shown that in *A. thaliana* YSLs mainly express in the xylem parenchyma of the leaf veins and act as Fe-NA transporters (Didonato et al., 2004; Le Jean et al., 2005; Schaaf et al., 2005). An up regulation in YSL genes was shown in *A. thaliana nas4x-1* mutants in Fe limited conditions by Klatt et al., (2009). We speculate that suppression of *NAS4* might also affect the expression of YSL genes, which needs to be analyzed in further experiments. The Fe Perls staining with DAB intensification of roots of *A. halleri* plants hydroponically grown in sufficient Zn conditions showed less staining with a patchy distribution in roots of two *AhNAS4* suppressed lines. Furthermore, Fe mainly was accumulated in the epidermis layer of wild-type and control line, while in two *AhNAS4* suppressed lines Fe distribution was uniform among different cell types of roots and no outer layer Fe plaque formation was observed (Fig. 3.15). When Persson et al., (2016) grew wild-type *A. thaliana* and *nas4x* quadruple mutants hydroponically under low Zn conditions, the elemental imaging of plant root cross sections by laser ablation-inductively coupled plasma-mass spectrometry (LA-ICP-MS) showed the similar pattern of Fe distribution to what we have seen in *AhNAS4* suppressed lines. In *A. thaliana nas4x* quadruple mutant no epidermal Fe accumulation was detected while in wild-type *A. thaliana* plants a clear Fe ring was detected. At this stage, the nature of this outer layer Fe plaque is not clear and the contribution of *NAS* genes to this phenotype is not clear. We recommend in further studies the root Fe distribution in *A. halleri NAS2*-suppressed lines as well all *A. thaliana NAS* single mutant be analyzed to reveal the specificity of this phenotype for *AhNAS4*.

4.3 ZIP6 plays a role in root Cd uptake in in *A. halleri*

4.3.1 *AhZIP6* is not a metal hyperaccumulation gene in *A. halleri*

The initial hypothesis based on the comparative transcriptome analysis between *A. halleri* and *A. thaliana* was that *AhZIP6* is a Zn hyperaccumulation candidate gene in *A. halleri*. In order to investigate the direct role of the *ZIP6* gene in *A. halleri* metal hyperaccumulation and hypertolerance, knockdown RNAi lines of *A. halleri* with significantly reduced transcript were generated in this study. It had been shown that *ZIP6* is expressed at higher levels in roots and especially in shoots of *A. halleri* compared to *A. thaliana*. It was suggested that it might play a role in storage or detoxification of Zn or in maintaining homeostasis of other metals like Fe or Mn (Becher et al., 2004; Talke et al., 2006; Wu et al., 2009). It was clearly shown in our study that

Discussion

suppression of *ZIP6* has no effects in root and shoots metal content of *A. halleri* plants grown hydroponically in medium with sufficient Zn, in Zn and Fe depletion media or in media with excess Zn, Cd or Ni. In all conditions Zn, Fe and Mn uptake and root-to-shoot translocation in two *ZIP6*-suppressed lines were comparable to those of wild-type and control plants (Fig. 3.36, 3.38, 3.40, 3.42 and 3.45). Evaluation of the effects of altered *ZIP6* in *A. halleri* tolerance towards Zn, Ni and Pb confirmed that *AhZIP6*-suppressed and control plants responded similarly to excess Zn, Ni and Pb with no detectable differences in root length and shoot biomass (Fig. 3.39, 3.44 and 3.46). These results clearly showed that *AhZIP6* contribution to metal hyperaccumulation is undetectable. One could speculate that the contribution of other members of the ZIP transporter family to metal hyperaccumulation redundantly diminishes the contribution of *AhZIP6*. So far, the contribution of specific ZIP transporters to Zn uptake has not been determined even in *A. thaliana*.

4.3.2 Suppression of *AhZIP6* specifically enhances tolerance towards Cd in *A. halleri*

In this study, it was shown that the suppression of *AhZIP6* in *A. halleri* enhances tolerance towards Cd specifically restricted to roots. In the presence of 10 and especially 20 μM Cd^{2+} , two *ZIP6* suppressed lines showed less reduction in their relative root length and relative root fresh weight compared to the wild-type and control plants (Fig. 3.41). The *AhZIP6* suppression had no significant effect in shoots of *A. halleri* plants grown in highly Zn and Cd contaminated Bestwig soil (Fig. 3.44) which indicates that tolerance response is limited to the roots. Interestingly no significant differences in root and shoot Cd content between *AhZIP6*-suppressed lines and control plants were detected when plants were either hydroponically grown in Cd stress conditions or grown in Bestwig and phenotyping soils (Fig. 3.42 and 3.45).

4.3.4 Suppression of *AhZIP6* decreases short-term uptake of Cd in *A. halleri* roots

It has been suggested that in *A. thaliana* IRT1, the well-known member of the ZIP transporter family, non-selectively mediates the uptake of Cd^{2+} into the root symplasm (Vert et al., 2002; Besson-Bard et al., 2009). It was shown that in the presence of 20 μM Cd^{2+} in medium after 8 days of growth, the *irt1-1* mutant had 5-fold lower root Cd content compared to the wild type plants (Vert et al., 2002). In rice, OsNRAMP5 has been identified as the major Cd uptake transporter and responsible for most of the rice Cd uptake (Sasaki et al., 2012). It has been shown that the knockout of OsNRAMP5 resulted in a 5-fold lower short-term roots Cd uptake compared to the wild-type plants (Sasaki et al., 2012). In this study, we showed the very first evidence for the role of the *AhZIP6* gene in root Cd uptake in *A. halleri*. The exposure of *A. halleri* plants to 5 μM Cd^{2+} at room temperature for 15 and 30 minutes showed that the two *AhZIP6*-suppressed lines took up 20% to 54% less Cd in their roots compared to the wild-type and control plants (Fig. 3.43). While the expression level of *IRT1* in *A. halleri* is much lower than in *A. thaliana* even under excess Zn (Shanmugam et al., 2011), other members of the ZIP transporter family like *AhZIP4*, *AhZIP10* and *IRT3* are highly expressed in roots of *A. halleri* compared to *A. thaliana* under sufficient Zn supply (Krämer et al., 2007). These transporters are all candidates for non-selective uptake of toxic Cd^{2+} ions into *A. halleri* roots, but up to now, there has been no clear evidence to support the role of candidate genes for Cd uptake from soil in *A. halleri* (Meyer and Verbruggen 2012). The investigation of predominantly expressed genes in the roots of *N. caerulea* suggested *ZIP6* as a candidate gene for Cd hyperaccumulation (Halimaa et al., 2014). In addition, it was shown that the expression of *TcZNT6* (*AtZIP6* ortholog)

Discussion

enhanced Cd sensitivity in transgenic *A. thaliana* without changing metal profiles in roots and shoots (Wu et al., 2009). This study provided first evidence for the role of *AhZIP6* in Cd uptake in *A. halleri*. We suggest that *AhZIP6* is responsible for taking up Cd to the root cells in *A. halleri* and its down regulation led to lesser uptake of Cd in short-term and consequently increase in tolerance towards Cd. We speculate that after 3 weeks of Cd treatment due to compensatory effect of other metal uptake and transporter genes from the ZIP transporter family or other metal uptake groups, *AhZIP*-suppressed lines accumulate similar level of Cd in their root and shoot as wild-type plants. At this stage, we are unable to clarify if ZIP6 uptake activity is restricted to Cd or it also takes up other metals such as Zn, Fe and Mn. We assume that ZIP6 like other essential metal transporters such as the IRT1 in *A. thaliana* and ZNT1 in *Noccea caerulescens* which facilitate Cd uptake (Cailliatte et al., 2009; Vert et al., 2002; Verbruggen et al., 2009b), plays a role in Zn uptake and translocation in *A. halleri*. Further studies with micronutrient isotopes need to be performed to assess this hypothesis. Also, it will be of central importance to identify the two copies of *ZIP6* in *A. halleri* as predicted by (Becher et al., 2004 ; Talke et al., 2006). Subcellular localization and functional characterization of *ZIP6* copies in *A. halleri* has yet to be performed. The expression of *AhZIP6* copies in heterologous systems like yeast and finally the expression of *AhZIP6* in *A. thaliana* transgenic lines to find direct roles of gene in Cd uptake and tolerance other important aspects to be investigated.

4.4 *AhCAX1* is essential for suppressing Cd-induced generation of reactive oxygen species in roots of *A. halleri*

The *Auby* individual crossed with *A. lyrata* to generate the population used for mapping the Cdtol QTLs does not form calli in culture and therefore could not be transformed (Fig. 3.6). Thus, *AhCAX1*-RNAi lines were generated from the *C-line* individual from the Langelsheim population in the Harz mountains in Germany. This population is closely related to the population the *Auby* individual originated from in Northern France (Pauwels et al., 2012). It has been shown that *A. halleri* plants from both regions are Cd hypertolerant (Meyer et al., 2015). It was confirmed that, relative transcript levels of *AhCAX1* in shoots of *C-line* and *Auby* individuals were similar and therefore *AhCAX1*-RNAi lines were suitable to explore the role of *AhCAX1* in Cdtol QTLs (Fig. 3.47). Suppression of 89% and 95% of relative *CAX1* transcript abundance was accomplished in shoots of two independent transgenic *A. halleri* lines compared to the wild-type via transformation with an *AhCAX1*-RNAi construct (Fig. 3.48).

4.4.1 Suppression of *AhCAX1* has no visible phenotypical effects on *A. halleri* grown under sequential Cd tolerance assay

When plants were subjected to the Cd tolerance assay and transferred to a regime of weekly increasing Cd exposure with a range of 50, 100, 150, and 200 μM Cd according to (Courbot et al., 2007), no significant differences in relative shoot fresh weight were found between two *AhCAX1*-suppressed lines and wild-type (Fig. 3.49). It had been shown the contribution of second major QTL to Cd tolerance, Cdtol2, only explains 23.7% of the difference in Cd tolerance between the *A. lyrata* and *A. halleri* parents in the original cross. This might explain why variation in Cd response between two *AhCAX1*-suppressed lines and wild-type plants was not detectable in *A. halleri* upon sequential Cd tolerance test.

4.4.2 Suppression of *AhCAX1* leads to an increase in H₂O₂ and superoxide accumulation following Cd treatment in *A. halleri* roots

AhCAX1 has been identified as a candidate gene for the second major QTL for Cd tolerance, *Cdtol2*, and interestingly, *Cdtol2* was Ca-dependent and only was detectable in the presence of low Ca²⁺ concentrations (Baliardini et al., 2015). It was shown that in *A. thaliana* the *cax1* mutation dramatically enhances concentrations of reactive oxygen species in roots while differences in root growth between wildtype and *cax1* mutants upon Cd²⁺ exposure were minimal (Baliardini et al., 2015). Therefore, analogous experiments were performed with the *A. halleri* *CAX1-RNAi* lines and ROS production quantified in control and Cd²⁺-treated plants. At the selected Cd²⁺ concentration of 10 µM, which does not cause growth inhibition, the roots of wild-type and control RNAi plants did not show an increase in H₂O₂ accumulation relative to untreated plants while in *AhCAX1*-suppressed plants H₂O₂ accumulation was about a 4-fold higher upon Cd²⁺ exposure. This increase was completely absent when plants were cultivated in medium with the higher Ca²⁺ concentration (Fig. 3.50). Generation of superoxide radical assayed in a similar fashion and quantification by NBT staining again showed a strongly Ca²⁺ dependent and highly significant increase only in roots of *AhCAX1*-suppressed lines and wild-type and control RNAi plants did not show enhanced superoxide radical accumulation when exposed to Cd²⁺ (Fig. 3.51). These results are consistent with what have been reported by Baliardini et al., (2015) as no accumulations of ROS species in *A. halleri* wild-type and control lines after exposure to Cd in low and high Ca conditions were detected. In addition, Baliardini et al., (2015) have shown that loss of *CAX1* function in *A. thaliana* led to an enhancement in accumulation of ROS following Cd treatment, it was confirmed that suppression of *CAX1* in *A. halleri* led to enhanced accumulation of ROS species after exposure to Cd specifically in low Ca conditions. Plant cation/H⁺ exchangers (*CAXs*) are members of a multigene family which are energized by the proton gradient and membrane potential and are able to transport a broad range of cations (Manohar et al., 2011). *A. thaliana* *CAX2* and *CAX4* can mediate Cd²⁺ sequestration into the vacuole and therefore confer Cd tolerance (Edmond et al., 2009; Hirschi et al., 2000; Korenkov et al., 2007; Mei et al., 2009). The *CAX1* has a higher affinity for Ca²⁺ compared to *CAX2* and was shown to be the major tonoplast Ca²⁺ transporter (Cheng et al., 2003; Hirschi et al., 2000; Shigaki and Hirschi, 2006). *A. thaliana* *cax1* mutant showed a 50% reduction in vacuolar Ca²⁺/H⁺ exchange activity and was sensitive to high concentrations of Ca²⁺ (Cheng et al., 2003). While no Cd²⁺/H⁺ exchange activity has been reported for *CAX1*, the *CAXcd* version which has only one amino acid change in the selectivity domain in N-terminus of *CAX1*, showed high Cd transport activity (Shigaki et al., 2005) and *Petunia* plants expressing this *CAXcd* accumulated more Cd and were more tolerant towards Cd than control plants (Wu et al., 2011). Baliardini et al., (2015) showed constitutively higher expression of *CAX1* in the roots of *A. halleri* compared to *A. thaliana*, while the expression level in shoots was similar. The amino acid sequences analysis showed the annotated functional domains including the selectivity domain were entirely conserved in *A. thaliana* and *A. halleri* *Cax1*. Thus, the same substrate specificity was assumed for *A. thaliana* *Cax1* and *A. halleri* *Cax1* proteins (Baliardini et al., 2015). They suggested that the absence of H₂O₂ accumulation in the *A. halleri* roots could be due to the efficient root to shoot translocation of Cd or the stable maintenance of Ca homeostasis in the cytosol of *A. halleri* root cells, because of the constitutive high level of *CAX1* expression or synergistic action of both mechanisms. It was shown that the *CdTol2* QTL was only detectable at low Ca concentration (Courbot et al., 2007). This study and Baliardini et al., (2015) confirmed that regardless of different *CAX1* expression level in roots of *A. halleri* and *A. thaliana*, suppression of *CAX1* resulted in 4 to 5-fold higher accumulation of ROS in roots of both *A. halleri*

Discussion

and *A. thaliana* species in low Ca conditions. Therefore, we suggest that the proper expression of *CAX1* is necessary for the stable maintenance of Ca homeostasis in the cytosolic compartments of *A. halleri* and *A. thaliana* root cells and disruption in expression of *CAX1* led to increase in ROS accumulation in both species. We speculate that absence of CdTol2 QTL detection, the lower accumulation of H₂O₂ in roots of *A. halleri* suppressed lines in the presence of higher Ca could be due to the higher competition between Ca and Cd at Ca-binding motifs of structural proteins and enzymes in the presence of extra Ca in medium. These data strongly support the hypothesis that *AhCAX1* is indeed explaining the QTL Cdtol2 and represents the second Cd hypertolerance factor identified in plants besides HMA4. At this stage, our information about the expression level of other members of CAX family in *A. halleri* and their role in Cd homeostasis is limited. The exact mechanisms that explain the role of *AhCAX1* in Ca homeostasis and in preventing ROS production in response to Cd stress remain to be elucidated. In further studies the possible effects of *AhCAX1* suppression on Ca and Cd accumulation in *A. halleri* plants under control and Cd stress conditions in low and high Ca supply in medium need to be addressed.

4.5 *AhNRAMP3* has no major contribution to metal hyperaccumulation and hypertolerance in *A. halleri*

4.5.1 Suppression of *AhNRAMP3* did not reveal any physiological role in *A. halleri*

In *A. thaliana* disruption of the *AtNRAMP3* gene slightly enhanced tolerance towards Cd and increased root growth while over expression of *AtNRAMP3* resulted in Cd hypersensitivity in *A. thaliana* (Thomine et al., 2000). Oomen et al., (2009) showed that the *TcNRAMP3* in *N. caerulescens* expressed at higher levels than its *A. thaliana* homologue and is able to transport Fe, Mn and Cd. The *TcNRAMP3* expression fully restored the Zn and Cd sensitivity in *nramp3 nramp4* double mutant to wild-type levels (Oomen et al., 2009). The disruption of *NRAMP3* in *A. thaliana* resulted in Mn and Zn accumulation in roots and overexpression of it decreased Mn accumulation (Thomine et al., 2003). The initial hypothesis based on the comparative transcriptome analysis between *A. halleri* and *A. thaliana* was that since *AhNRAMP3* is constitutively highly expressed in *A. halleri*, it might play a role in metal hyperaccumulation or hypertolerance in *A. halleri*. In this study, knockdown RNAi lines of *A. halleri* in which transcript level of *AhNRAMP3* was significantly reduced, were used to dissect the possible role of *AhNRAMP3* gene in metal hyperaccumulation and hypertolerance. We showed that in both Cd and Ni stress conditions altered *AhNRAMP3* did not change Cd and Ni tolerance in *A. halleri*. All plants showed reduction in root elongation in response to Cd stress conditions with no detectable differences between two *AhNRAMP3*-suppressed and control lines (Fig. 3.53). Likewise, in Ni stress conditions all plants showed leaf chlorosis with no differences in root growth and plant biomass detected between two *AhNRAMP3*-suppressed and control plants upon Ni stress conditions (Fig. 3.55). In addition it has been shown in *A. thaliana* that *AtNRAMP3* gene is upregulated by Fe starvation and the elevated expression of it by mobilizing vacuolar metal pool to cytosol downregulated the primary Fe uptake genes like *IRT1* and *FRO2* (Thomine et al., 2000, 2003). Therefore, it was suggested that the high expression of *NRAMP3* in *A. halleri* (Weber et al., 2004) might play a role in maintaining Fe homeostasis. There were no differences in root length, root and shoot biomass between control and *AhNRAMP3*-suppressed lines upon Fe deficiency (Fig. 3.56). Elemental profiling of plants hydroponically grown in control conditions or under Fe limiting treatment showed no significant differences in root and shoot Fe, Zn and Mn contents between

Discussion

AhNRAMP3-suppressed and control lines (Fig. 3.57). These results showed that suppression of the *AhNRAMP3* gene has no effect on tolerance towards Fe deficiency in *A. halleri*. Since it has been shown in *A. thaliana* that NRAMP3 and NRAMP4 are tonoplast metal influx transporters (Thomine et al., 2003; Lanquar et al., 2005), further studies could focus on subcellular localization of NRAMP3 protein in *A. halleri*, functional characterization of *AhNRAMP3* gene and assess the possible role of *AhNRAMP3* on fate of Cd induced cytosolic ROS accumulation in plant. It also would be interesting to explore the possible effects of *AhNRAMP3* suppression on *AhNRAMP4* transcription.

References

Pinto AP, Simões I, Mota AM. (2008) Cadmium Impact on Root Exudates of Sorghum and Maize Plants: A Speciation Study, *Journal of Plant Nutrition* **31**, 1746–1755.

Alloway BJ. (2008). Zinc in soils and crop nutrition. Paris, France: IFA; and Brussels, Belgium: IZA.

Amoah BK, Wu H, Sparks CA, Jones HD. (2001) Factors influencing *Agrobacterium*-mediated transient expression of *uidA* in wheat inflorescence tissue. *Journal of Experimental Botany* **52**, 1135–1142.

Anderson JA. (2002). Catalase activity, hydrogen peroxide content and thermotolerance of pepper leaves. *Scientia Horticulturae* **95**, 277–284.

Andreini C, Bertini I, Rosato A. (2009). Metalloproteomes: A bioinformatic approach. *Accounts of Chemical Research* **42**, 1471–1479.

Arrivault S, Senger T, Krämer U. (2006). The Arabidopsis metal tolerance protein AtMTP3 maintains metal homeostasis by mediating Zn exclusion from the shoot under Fe deficiency and Zn oversupply. *The Plant Journal* **46**, 861–79.

Audet P, Charest C. (2008). Allocation plasticity and plant-metal partitioning : Meta-analytical perspectives in phytoremediation. *Environmental Pollution* **156**, 290–296.

Baker AJM. (1981). Accumulators and excluders -strategies in the response of plants to heavy metals. *Journal of Plant Nutrition* **3**, 643-654.

Baker AJM, Brooks RR. (1989). Terrestrial higher plants which hyperaccumulate metallic elements - A review of their distribution, Ecology and Phytochemistry. *Biorecovery* **1**, 81-126.

Baliardini C, Meyer C-L, Salis P, Saumitou-Laprade P, Verbruggen N. (2015) CATION EXCHANGER1 cosegregates with cadmium tolerance in the metal hyperaccumulator *Arabidopsis halleri* and plays a role in limiting oxidative stress in *Arabidopsis* Spp. *Plant Physiology* **169**, 549-559.

Banerjee S, Flores-Rozas H. (2005). Cadmium inhibits mismatch repair by blocking the ATPase activity of the MSH2-MSH6 complex. *Nucleic Acids Res* **33**, 1410-1419.

Bashir K, Ishimaru Y, Shimo H, Nagasaka S, Fujimoto M, Takanashi H, Tsutsumi N, An G, Nakanishi H, Nishizawa N.K. (2011). The rice mitochondrial iron transporter is essential for plant growth. *Nature Communications*. **2**, 322-327.

Becher M, Talke IN, Kramer U. (2004). Cross-species microarray transcript profiling reveals high constitutive expression of metal homeostasis genes in shoots of the zinc hyperaccumulator *Arabidopsis halleri*. *Plant J* **37**, 251–268.

References

- Benes I, Schreiber, K, Ripperger H, Kirsceiss A.** (1983). Metal complex formation of nicotianamine, a possible phytosiderophore. *Experientia* **39**, 261–262.
- Bernal M, Casero D, Singh V, Wilson G.T, Grande A, Yang H, Dodani S.C, Pellegrini M, Huijser P, Connolly E.L, Merchant S.S, Krämer U,** (2012). Transcriptome Sequencing Identifies SPL7-Regulated Copper Acquisition Genes FRO4/FRO5 and the Copper Dependence of Iron Homeostasis in *Arabidopsis*. *Plant Cell* **24**, 738-761.
- Bert V, Bonnin I, Saumitou-Laprade P, de Laguerie P, Petit D.** (2002). Do *Arabidopsis halleri* from nonmetallicolous populations accumulate zinc and cadmium more effectively than those from metallicolous populations? *New Phytologist* **155**, 47-57.
- Besson-Bard A, Gravot A, Richaud P, Auroy P, Duc C, Gaymard F et al.** (2009). Nitric oxide contributes to cadmium toxicity in *Arabidopsis* by promoting cadmium accumulation in roots and by up-regulating genes related to iron uptake. *Plant Physiol* **149**, 1302–1315.
- Bhattacharjee B, Mohan M, Nair S.** (2010). Transformation of chickpea: Effect of genotype, explant, *Agrobacterium*-strain and composition of culture medium. *Biologia Plantarum* **54**, 21–32.
- Boardman R, McGuire DO.** (1990). The role of zinc in forestry. I. Zinc in forest environments, ecosystems and tree nutrition. *Forest Ecology and Management* **37**, 167-205.
- Bouma D.** (1983). Diagnosis of Mineral Deficiencies Using Plant Tests. *Inorganic Plant Nutrition*, Vol. **15**: Springer Berlin Heidelberg, 120-146.
- Bradford MM.** (1976). A rapid and sensitive method for the quantitation of microgram quantities of protein utilizing the principle of protein–dye binding. *Analytical Biochemistry* **72**, 248–254.
- Broadley MR, White PJ, HammondJP, Zelko I, Lux A.** (2007). Zinc in plants: Tansley review. *New Phytologist* **173**, 677–702.
- Brown PH.** (2008). Micronutrient use in agriculture in the United States of America. *Micronutrient deficiencies in global crop production*, 1–353.
- Cailliatte R, Lapeyre B, Briat JF, Mari S, Curie C.** (2009). The NRAMP6 metal transporter contributes to cadmium toxicity. *Biochem. J.* **422**, 217–228.
- Cakmak I.** (2008). Enrichment of cereal grains with zinc: Agronomic or genetic biofortification? *Plant and Soil* **302**, 1–17.
- Cakmak I, Kalayci M, Ekiz H, Braun H J, Kiliç Y, Yilmaz A.** (1999). Zinc deficiency as a practical problem in plant and human nutrition in Turkey: A NATO-science for stability project. *Field Crops Research* **60**, 175–188.
- Chao DY, Silva A, Baxter I, Huang YS, Nordborg M, Danku J, Lahner B, Yakubova E, Salt DE.**

References

(2012). Genome-wide association studies identify heavy metal ATPase3 as the primary determinant of natural variation in leaf cadmium in *Arabidopsis thaliana*. *PLoS Genet* **8**, e1002923.

Chen J, Yang L, Gu J, Bai X, Ren Y, Fan T, Han Y, et al. (2015). MAN3 gene regulates cadmium tolerance through the glutathione-dependent pathway in *Arabidopsis thaliana*, *New Phytologist* **205**, 570–582.

Cheng NH, Pittman JK, Barkla BJ, Shigaki T, Hirschi KD. (2003). The *Arabidopsis* *cax1* mutant exhibits impaired ion homeostasis, development, and hormonal responses and reveals interplay among vacuolar transporters. *Plant Cell* **15**, 347-364.

Cheng NH, Pittman JK, Shigaki T, Lachmansingh J, LeClere S, Lahner B, Salt DE, Hirschi KD. (2005). Functional association of *Arabidopsis* CAX1 and CAX3 is required for normal growth and ion homeostasis. *Plant Physiol* **138**, 2048-2060.

Chiang HC, Lo JC, Yeh KC. (2006) Genes associated with heavy metal tolerance and accumulation in Zn/Cd hyperaccumulator *Arabidopsis halleri*: a genomic survey with cDNA microarray. *Environ Sci Technol* **40**, 6792–6798.

Cho UH, Seo NH. (2005). Oxidative stress in *Arabidopsis thaliana* exposed to cadmium is due to hydrogen peroxide accumulation. *Plant Sci.* **168**, 113–120.

Clemens S. (2001). Molecular mechanisms of plant metal tolerance and homeostasis. *Planta* **212**, 475-486.

Clemens S, Palmgren MG, Krämer U. (2002). A long way ahead: understanding and engineering plant metal accumulation. *Trends Plant Sci* **7**, 309-315.

Clemens S. (2006a). Evolution and function of phytochelatin synthases. *J Plant Physiol* **163**, 319-332.

Clemens S. (2006b). Toxic metal accumulation, responses to exposure and mechanisms of tolerance in plants. *Biochimie* **88**, 1707-1719.

Clemens S. (2010). Zn – A Versatile Player in Plant Cell Biology. In: Hell, R. and Mendel, R. R. eds. *Cell Biology of Metals and Nutrients*. Springer-Verlag, Heidelberg, 281-298.

Clemens S, Aarts MG, Thomine S, Verbruggen N. (2013a). Plant science: the key to preventing slow cadmium poisoning. *Trends Plant Sci* **18**(2): 92-99.

Clemens S, Deinlein U, Ahmadi H, Höreth S, Uraguchi S. (2013b). Nicotianamine is a major player in plant Zn homeostasis. *Biometals* **26**, 623-632.

Clemens S., Ma JF. (2016). Toxic Heavy Metal and Metalloid Accumulation in Crop Plants and Foods, *Annu. Rev. Plant Biol* **67**, 1–24.

References

Colangelo EP, Guerinot ML. (2006). Put the metal to the petal: Metal uptake and transport throughout plants. *Curr. Opin. Plant Biol.* **9**, 322–330.

Cornu J-Y, Deinlein U, Höreth S, Braun M, Schmidt H, Weber M, Persson DP, Husted S, Schjoerring JK, Clemens S. (2015). Contrasting effects of nicotianamine synthase knockdown on zinc and nickel tolerance and accumulation in the zinc/cadmium hyperaccumulator *Arabidopsis halleri*. *New Phytol* **206**, 738-750.

Courbot M, Willems G, Motte P, Arvidsson S, Roosens N, Saumitou-Laprade P, Verbruggen N. (2007). A major quantitative trait locus for cadmium tolerance in *Arabidopsis halleri* colocalizes with HMA4, a gene encoding a heavy metal ATPase. *Plant Physiol* **144**, 1052-1065.

Curie C, Cassin G, Couch D, Divol F, Higuchi K, Le Jean M, Misson J, Schikora A, Czernic P, Mari S. (2009). Metal movement within the plant: contribution of nicotianamine and yellow stripe 1-like transporters. *Ann Bot* **103**, 1-11.

Curie C, Panaviene Z, Loulergue C, Dellaporta SL, Briat JF, Walker EL. (2001). Maize YELLOWSTRIPE1 encodes a membrane protein directly involved in Fe(III) uptake. *Nature* **409**, 346–349.

Cuyper A, Plusquin M, Remans T, Jozefczak M, Keunen E, Gielen H, Opdenakker K, Nair AR, Munters E, Artois TJ, Nawrot T, Vangronsveld J, Smeets K. (2010). Cadmium stress: an oxidative challenge. *Biomaterials* **23**, 927-940.

DalCorso G, Farinati S, Furini A. (2010). Regulatory networks of cadmium stress in plants. *Plant Signal Behav* **5**, 663-667.

DalCorso G, Farinati S, Maistri S, Furini A. (2008). How plants cope with cadmium: staking all on metabolism and gene expression. *J Integr Plant Biol* **50**, 1268-1280.

Daudi A, Cheng Z, O'Brien JA, Mammarella N, Khan S, Ausubel FM, Bolwell GP. (2012). The apoplastic oxidative burst peroxidase in *Arabidopsis* is a major component of pattern-triggered immunity. *Plant Cell* **24**, 275-287.

Deinlein U, Weber M, Schmidt H, Rensch S, Trampczynska A, Hansen TH, Husted S, Schjoerring JK, Talke IN, Krämer U, Clemens S. (2012). Elevated nicotianamine levels in *Arabidopsis halleri* roots play a key role in zinc hyperaccumulation. *Plant Cell* **24**, 708-723.

di Toppi LS, Gabbriellini R (1999) Response to cadmium in higher plants. *Environ Exp Bot* **41**, 105–130.

DiDonato RJ Jr, Roberts LA, Sanderson T, Easley RB, Walker EL. (2004). *Arabidopsis* Yellow Stripe-Like2 (YSL2): a metal-regulated gene encoding a plasma membrane transporter of nicotianamine-metal complexes. *The Plant Journal* **39**, 403–414.

Divol F, Couch D, Conejero G., Roschzttardtz H, Mari S, Curie C. (2013). The *Arabidopsis* Yellow Stripe LIKE4 and 6 transporters control iron release from the chloroplast. *Plant Cell* **25**, 1040–

References

1055.

Douchkov D, Gryczka C, Stephan UW, Hell R, Baumlein H. (2005). Ectopic expression of nicotianamine synthase genes results in improved iron accumulation and increased nickel tolerance in transgenic tobacco. *Plant, Cell & Environment* **28**, 365–374.

Dräger DB, Desbrosses-Fonrouge AG, Krach C, Chardonnens AN, Meyer RC, Saumitou-Laprade P, Krämer U. (2004). Two genes encoding *Arabidopsis halleri* MTP1 metal transport proteins co-segregate with zinc tolerance and account for high MTP1 transcript levels. *Plant J* **39**, 425-439.

Durrett TP, Gassmann W, Rogers EE. (2007). The FRD3-mediated efflux of citrate into the root vasculature is necessary for efficient iron translocation. *Plant Physiol* **144**, 197-205.

Edmond C, Shigaki T, Ewert S, Nelson M, Connorton JM, Chalova V, Pittman JK. (2009). Comparative analysis of CAX2-like cation transporters indicates functional and regulatory diversity. *Biochemical Journal* **418**, 145–154.

Eide D, Broderius M, Fett J, Guerinot ML. (1996). A novel iron-regulated metal transporter from plants identified by functional expression in yeast. *Proc Natl Acad Sci U S A* **93**, 5624-5628.

Eide D. (2006). Zinc transporters and the cellular trafficking of zinc. *Biochim. Biophys. Acta* **1763**, 711–722.

Ercal N, Gurer-Orhan H, Aykin-Burns N. (2001). Toxic metals and oxidative stress part I: mechanisms involved in metal-induced oxidative damage. *Curr Top Med Chem* **1**, 529-539.

Faller P, Kienzler K, Krieger-Liszkay A. (2005). Mechanism of Cd²⁺ toxicity: Cd²⁺ inhibits photoactivation of photosystem II by competitive binding to the essential Ca²⁺ site. *Biochim. Biophys. Acta* **1706**, 158–164.

Filatov V, Dowdle J, Smirnoff N, Ford-Lloyd B, Newbury HJ, Macnair MR. (2006). Comparison of gene expression in segregating families identifies genes and genomic regions involved in a novel adaptation, zinc hyperaccumulation. *Mol Ecol* **15**, 3045-3059.

Fischer S, Kühnlenz T, Thieme M, Schmidt H, Clemens S. (2014). Analysis of plant Pb tolerance at realistic submicromolar concentrations demonstrates the role of phytochelatin synthesis for Pb detoxification. *Environmental Science and Technology*, **48**, 7552–7559.

Fourcroy P, Siso-Terraza P, Sudre D, Saviron M, Reyt G, Gaymard F et al. (2013). Involvement of the ABCG37 transporter in secretion of scopoletin and derivatives by *Arabidopsis* roots in response to iron deficiency. *New Phytol.* **201**, 155–167.

Gamalero E, Lingua G, Berta G, Glick BR. (2009). Beneficial role of plant growth promoting bacteria and arbuscular mycorrhizal fungi on plant responses to heavy metal stress. *Can J Microbiol* **55**, 501–514.

Gelvin SB. (2003). *Agrobacterium*-mediated plant transformation: the biology behind the “gene-

References

jockeying” tool. *Microbiology and Molecular Biology Reviews* : *MMBR*, **67**, 16–37.

Gendre D, Czernic P, Conejero G, Pianelli K, Briat JF, Lebrun M, Mari S. (2007). TcYSL3, a member of the YSL gene family from the hyper-accumulator *Thlaspi caerulescens*, encodes a nicotianamine-Ni/Fe transporter. *Plant J* **49**, 1-15.

Ghasemi R, Ghaderian M, Krämer U. (2009). Interference of nickel with copper and iron homeostasis contributes to metal toxicity symptoms in the nickel hyperaccumulator plant *Alyssum inflatum*. *New Phytol.* **184**, 566–580.

Gnasekaran P, James-Antony JJ, Uddain J, Subramaniam S. (2014). *Agrobacterium*-mediated transformation of the recalcitrant *Vanda* Kasem’s delight orchid with higher efficiency. *The Scientific World Journal*, 14–16.

González-Guerrero M, Escudero V, Saéz Á, Tejada-Jiménez M. (2016). Transition Metal Transport in Plants and Associated Endosymbionts: Arbuscular Mycorrhizal Fungi and Rhizobia. *Front Plant Sci.* **7**, 1–21.

Green LS, Rogers EE. (2004). FRD3 controls iron localization in Arabidopsis. *Plant Physiol* **136**, 2523-2531.

Grillet L, Mari S, Schmidt W. (2014). Iron in seeds – loading pathways and subcellular localization. *Front Plant Sci.* **4**, 1–8.

Guerinot ML. (2000). The ZIP family of metal transporters. *Biochim. Biophys. Acta* **1465**, 190–198.

Halimaa P, Lin YF, Ahonen VH, Blande D, Clemens S, Gyenesei A, Haikio E, Karenlampi SO, Laiho A, Aarts MG, Pursiheimo JP, Schat H, Schmidt H, Tuomainen MH, Tervahauta AI. (2014). Gene expression differences between *Noccaea caerulescens* ecotypes help to identify candidate genes for metal phytoremediation. *Environ Sci Technol* **48**, 3344-3353.

Hall JL, Williams LE. (2003). Transition metal transporters in plants. *J Exp Bot* **54**, 2601–2613.

Hanikenne M, Nouet C. (2011). Metal hyperaccumulation and hypertolerance: a model for plant evolutionary genomics. *Curr Opin Plant Biol* **14**, 252-259.

Hanikenne M, Talke IN, Haydon MJ, Lanz C, Nolte A, Motte P, Kroymann J, Weigel D, Krämer U. (2008). Evolution of metal hyperaccumulation required cis-regulatory changes and triplication of HMA4. *Nature* **453**, 391-395.

Hänsch R, Mendel RR. (2009) Physiological functions of mineral micronutrients (Cu, Zn, Mn, Fe, Ni, Mo, B Cl). *Curr. Opin. Plant Biol.* **12**, 259–266

Haydon MJ, Cobbett CS. (2007a). A novel major facilitator superfamily protein at the tonoplast influences zinc tolerance and accumulation in Arabidopsis. *Plant Physiol.* **143**, 1705–19.

References

- Haydon MJ, Cobbett CS.** (2007b). Transporters of ligands for essential metal ions in plants. *New Phytol.* **174**, 499–506.
- Haydon MJ, Kawachi M, Wirtz M, Hillmer S, Hell R, Krämer U.** (2012). Vacuolar Nicotianamine Has Critical and Distinct Roles under Iron Deficiency and for Zinc Sequestration in Arabidopsis. *Plant Cell.* **24**, 724–737
- He Y, HD Jones, S Chen, XM Chen, DW Wang, KX Li, DS Wang, LQ Xia.** (2010). *Agrobacterium*-mediated transformation of durum wheat (*Triticum turgidum* L. var. durum cv. Stewart) with improved efficiency. *J. Expt. Bot.* **61**:1567–1581.
- Hell R, Stephan UW.** (2003). Iron uptake, trafficking and homeostasis in plants. *Planta* **216**, 541–51.
- Helliwell CA, Wesley SV, Wielopolska AJ, Waterhouse PM.** (2002). High-throughput vectors for efficient gene silencing in plants. *F. Plant Biol.* **29**, 1217-1225.
- Henriques R, Jasik J, Klein M, Martinoia E, Feller U, Schell J, Pais MS, Koncz C.** (2002) Knock-out of Arabidopsis metal transporter gene IRT1 results in iron deficiency accompanied by cell differentiation defects. *Plant Mol. Biol.* **50**, 587–597.
- Hernandez LE, Carpena-Ruiz R, Gárate A.** (1996). Alterations in the mineral nutrition of pea seedlings exposed to cadmium. *J. Plant Nutr.* **19**, 1581–1598.
- Hirschi KD, Korenkov VD, Wilganowski NL, Wagner GJ.** (2000). Expression of Arabidopsis CAX2 into tobacco. Altered metal accumulation and increased manganese tolerance. *Plant Physiol.* **124**, 125-133.
- Hossain MA, Piyatida P, da Silva Ja, Fujita M.** (2012). Molecular Mechanism of Heavy Metal Toxicity and Tolerance in Plants: Central Role of Glutathione in Detoxification of Reactive Oxygen Species and Methylglyoxal and in Heavy Metal Chelation. *Journal of Botany.* 1–37.
- Hussain D, Haydon MJ, Wang Y, Wong E, Sherson SM, Young J, Camakaris J, Harper JF, Cobbett CS.** (2004). P-type ATPase heavy metal transporters with roles in essential zinc homeostasis in Arabidopsis. *Plant Cell.* **16**, 1327–1339.
- Inaba T, Kobayashi E, Suwazono Y, Uetani M, Oishi M, Nakagawa H, Nogawa K.** (2005). Estimation of cumulative cadmium intake causing Itai-itai disease. *Toxicol Lett.* **159**, 192-201.
- Jain A, Connolly EL.** (2013). Mitochondrial iron transport and homeostasis in plants. *Front Plant Sci.* **4**, 1–6.
- James DJ, Uratsu S, Cheng J, Negri P, Viss P, Dandekar AM** (1993) Acetosyringone and osmoprotectants like betaine or proline synergistically enhance *Agrobacterium*-mediated transformation of apple. *Plant Cell Reports.* **12**, 559-563.
- Järup L.** (2003). Hazards of heavy metal contamination. *British Medical Bulletin.* **68**, 167–182.

References

- Jeong J, Cohu C , Kerkeb L, Pilon M, Connolly EL, Guerinot ML.** (2008). Chloroplast Fe(III) chelate reductase activity is essential for seedling viability under iron limiting conditions. *Proc. Natl.Acad.Sci.USA.* **105**, 10619–10624.
- Johri N, Jacquillet G, Unwin R.** (2010). Heavy metal poisoning: the effects of cadmium on the kidney.*Biometals.* **23**, 783–792.
- Jozefczak M, Keunen E, Schat H, Bliet M, Hernandez LE, Carleer R, Remans T, Bohler S, Vangronsveld J, Cuypers A.** (2014). Differential response of Arabidopsis leaves and roots to cadmium: glutathione-related chelating capacity vs antioxidant capacity. *Plant Physiol Biochem* **83**, 1-9.
- Jozefczak M, Remans T, Vangronsveld J, Cuypers A.** (2012). Glutathione is a key player in metalinduced oxidative stress defenses. *Int J Mol Sci* **13**(3), 3145-3175.
- Khan,MA,Castro-guerrero N, Mendoza-cozatl DG.** (2014). Moving toward a precise nutrition : preferential loading of seeds with essential nutrients over non-essential toxic elements. *Front Plant Sci.* **5**, 1-7.
- Kim SA, Punshon T, Lanzirotti A, Li L, Alonso JM., Ecker JR.,Kaplan J, Guerinot M.L.** (2006). Localization of iron in Arabidopsis seed requires the vacuolar membrane transporter VIT1. *Science.* **314**, 1295–1298.
- Kim S, Takahashi M, Higuchi K, Tsunoda K, Nakanishi H, Yoshimura E, Mori S, Nishizawa NK** (2005) Increased nicotianamine biosynthesis confers enhanced tolerance of high levels of metals, in particular nickel, to plants. *Plant Cell Physiol.* **46**, 1809–1818.
- Klatte M, Schuler M, Wirtz M, Fink-Straube C, Hell R, Bauer P.** (2009). The analysis of Arabidopsis nicotianamine synthase mutants reveals functions for nicotianamine in seed iron loading and iron deficiency responses. *Plant Physy.* **150**, 257–271.
- Kobayashi T, Nishizawa NK.** (2012) Iron uptake, translocation, and regulation in higher plants. *Annu Rev Plant Biol.* **63**, 131–152.
- Kobayashi T, Nishizawa NK.** (2014) Iron sensors and signals in response to iron deficiency. *Plant Science,* **224**, 36–43.
- Koch MA, Matschinger M.** (2007) Evolution and genetic differentiation among relatives of Arabidopsis thaliana. *Proc Natl Acad Sci USA* **104**: 6272–6277.
- Korenkov V, Park S, Cheng NH, Sreevidya C, Lachmansingh J, Morris J, Hirschi K, Wagner GJ.** (2007). Enhanced Cd²⁺ -selective root-tonoplast-transport in tobaccos expressing Arabidopsis cation exchangers. *Planta* **225**, 403-411.
- Krämer U.** (2010). Metal hyperaccumulation in plants. *Annu Rev Plant Biol* **61**, 517-534.
- Krämer U, Talke IN, Hanikenne M.** (2007). Transition metal transport. *FEBS Lett* **581**, 2263-2272.

References

- Krüger C, Berkowitz O, Stephan UW, Hell R.** (2002). A Metal-binding Member of the Late Embryogenesis Abundant Protein Family Transports Iron in the Phloem of *Ricinus communis* L. *J. Biol. Chem.* **227**, 25062-25069
- Kum C, Won, E, Cobbett CS.** (2009). HMA P-type ATPases are the major mechanism for root-to-shoot Cd translocation in *Arabidopsis thaliana*, *New Phytologist* **181**, 71–78.
- Kumlehn J, Serazetdinova L, Hensel G, Becker D, Loerz H.** (2006). Genetic transformation of barley (*Hordeum vulgare* L.) via infection of androgenetic pollen cultures with *Agrobacterium tumefaciens*. *Plant Biotechnol. J.* **4**, 251- 261.
- Laity JH, Lee BM, Wright PE.** (2001). Zinc finger proteins: new insights into structural and functional diversity. *Current Opinion in Structural Biology* **11**, 39-46.
- Lanquar V, Lelièvre F, Barbier-brygoo H, Thomine S.** (2004). Regulation and function of AtNRAMP4 metal transporter protein. *Soil Sci. Plant Nutr.* **50**, 1141–1150.
- Lanquar V, Lelièvre F, Bolte S, Hamès C, Alcon C, Neumann D, Vansuyt G, Curie C, Schröder A, Krämer U, Barbier-Brygoo H, Thomine S.** (2005). Mobilization of vacuolar iron by AtNRAMP3 and AtNRAMP4 is essential for seed germination on low iron. *EMBO J.* **24**, 4041–4051.
- Le Jean M, Schikora A, Mari S, Briat JF, Curie C.** (2005). A loss-of-function mutation in AtYSL1 reveals its role in iron and nicotianamine seed loading. *The Plant Journal.* **44**, 769–782.
- Li S, Zhou X, Huang Y, Zhu L, Zhang S, Zhao Y, Gou J, Chen J, Chen R.** (2013). Identification and characterization of the zinc-regulated transporters, iron-regulated transporter-like protein (ZIP) gene family in maize. *BMC Plant Biology*, **13**, 1-14.
- Lin YF, Aarts MG.** (2012). The molecular mechanism of zinc and cadmium stress response in plants. *Cell Mol Life Sci* **69**, 3187-3206.
- Long TA, Tsukagoshi H, Busch W, Lahner B, Salt D, Benfey PN.** (2010). The bHLH transcription factor POPEYE regulates response to iron deficiency in *Arabidopsis* roots. *Plant Cell* **22**, 2219–36.
- López-Millán AF, Grusak MA, Abadía A, Abadía J.** (2013). Iron deficiency in plants: an insight from proteomic approaches. *Front Plant Sci* **4**, 1-16.
- Maestri E, Marmiroli M, Visioli G, Marmiroli N.** (2010). Metal tolerance and hyperaccumulation: Costs and trade-offs between traits and environment. *Environ Exp Bot* **68**, 1–13
- Manjul D, Vladimir O, Jude G.** (2009). Cultivar-dependent Gene Transfer into Citrus using *Agrobacterium*, *Proc. Fla. State Hort. Soc.* **122**, 85–89.
- Manohar M, Shigaki T, Hirschi KD.** (2011). Plant cation/H⁺ exchangers (CAXs): biological functions and genetic manipulations. *Plant Biol* **13**, 561-569.

References

- McLean E, Cogswell M, Egli I, Wojdyla D, de Benoist B.** (2009). Worldwide prevalence of anaemia, WHO Vitamin and Mineral Nutrition Information System, 1993–2005. *Public Health Nutrition*, **12**, 444–454.
- Mei H, Cheng NH, Zhao J, Park S, Escareno RA, Pittman JK, Hirschi KD.** (2009). Root development under metal stress in *Arabidopsis thaliana* requires the H⁺/cation antiporter CAX4. *New Phytol* **183**, 95-105.
- Mendoza-Cozatl DG, Butko E, Springer F, Torpey JW, Komives EA, Kehr J, Schroeder JI.** (2008). Identification of high levels of phytochelatin, glutathione and cadmium in the phloem sap of *Brassica napus*. A role for thiol-peptides in the long-distance transport of cadmium and the effect of cadmium on iron translocation. *Plant J* **54**, 249-259.
- Meyer C-L, Verbruggen N (2012).** The use of the model species *Arabidopsis halleri* towards phytoextraction of cadmium polluted soils. *New Biotechnology* **30**, 9–14.
- Meyer CL, Juraniec M, Huguet S, Chaves-Rodriguez E, Salis P, Isaure MP, Goormaghtigh E, Verbruggen N.** (2015). Intraspecific variability of cadmium tolerance and accumulation, and cadmium-induced cell wall modifications in the metal hyperaccumulator *Arabidopsis halleri*. *J Exp Bot* **66**, 3215-3227.
- Milner MJ, Kochian LV.** (2008). Investigating heavy-metal hyperaccumulation using *Thlaspi caerulescens* as a model system. *Ann Bot* **102**, 3-13.
- Milner M, Seamon J, Craft E, Kochian L.** (2013). Transport properties of members of the ZIP family in plants and their role in Zn and Mn homeostasis. *J. Exp. Bot.* **64**, 369–381.
- Mizuno D, Higuchi K, Sakamoto T, Nakanishi H, Mori S, Nishizawa NK.** (2003). Three nicotianamine synthase genes isolated from maize are differentially regulated by iron nutritional status. *Plant Physiology* **132**, 1989–1997.
- Mondal TK, Bhattacharya A, Ahuja PS, Chand PK** (2001) Transgenic tea (*Camellia sinensis* (L) O. Kuntze cv. Kangra Jat) plants obtained by *Agrobacterium*-mediated transformation of somatic embryos. *Plant Cell Reports* **20**, 712-720
- Morel M, Crouzet J, Gravot A, Auroy P, Leonhardt N, Va2016seur A, Richaud P.** (2009). AtHMA3, a P_{1B}-ATPase allowing Cd/Zn/Co/Pb vacuolar storage in *Arabidopsis*. *Plant Physiol* **149**, 894-904.
- Morrissey J, Guerinot ML.** (2009) Iron uptake and transport in plants: the good, the bad, and the lonome. *Chem Rev* **109**, 4553–4567.
- Morrissey J, Baxter I., Lee J, Li LT, Lahner B, Grotz N, Kaplan J, Salt DE, Guerinot ML.** (2009). The ferroportin metal efflux proteins function in iron and cobalt homeostasis in *Arabidopsis*. *Plant Cell* **21**, 3326–3338.
- Van Roekel J, Damm B, Melchers I, Hoekema A.** (1993). Factors influencing transformation

References

frequency of tomato (*Lycopersicon esculentum*) *PlantCell Reports* **12**, 644-647.

Mustroph A, Zanetti ME, Jang CJ, Holtan HE, Repetti PP, Galbraith DW, Girke T, Bailey-Serres J. (2009). Profiling translomes of discrete cell populations resolves altered cellular priorities during hypoxia in Arabidopsis. *Proc. Natl. Acad. Sci. USA* **106**, 18843–18848.

Nakanishi H, Ogawa I, Ishimaru Y, Mori S, Nishizawa NK. (2006). Iron deficiency enhances cadmium uptake and trans- location mediated by the Fe²⁺ transporters OsIRT1 and OsIRT2 in rice. *Soil Sci. Plant Nutr.* **52**, 464–469.

Nam J, Matthyse AG, Gelvin SB. (1997). Differences in susceptibility of Arabidopsis ecotypes to crown gall disease may result from a deficiency in T-DNA integration. *Plant Cell* **9**,317-333.

Nevo Y, Nelson N. (2006). The NRAMP family of metal-ion transporters. *Biochim.Biophys.Acta* **1763**, 609–620.

Nishiyama R, Kato M, Nagata S, Yanagisawa S, Yoneyama T. (2012). Identification of Zn-nicotianamine and Fe-2'-deoxymugineic acid in the phloem sap from rice plants (*Oryza sativa* L.). *Plant Cell Physiol.* **53**, 381–390.

Nouet C, Motte P, Hanikenne M. (2011). Chloroplastic and mitochondrial metal homeostasis. *Trends Plant Sci*, **16**, 395–404.

Nozoye T, Nagasaka S, Kobayashi T, Takahashi M, Sato Y, Uozumi N, Nakanishi H, Nishizawa N. (2011). Phytosiderophore efflux transporters are crucial for iron acquisition in graminaceous plants. *J. Biol. Chem* **286**, 5446–5454.

Das S, Green A. (2013). Importance of zinc in crops and human health. *J SAT Agri.Research* **11**, 1-7.

Ohki K. (1984). Zinc Nutrition Related to Critical Deficiency and Toxicity Levels for Sorghum. *Agronomy Journal* **76**, 253-256.

Olsen LI, Palmgren MG. (2014). Many rivers to cross: the journey of zinc from soil to seed. *Front. Plant Sci.* **5**,30.

Oomen RJ, Wu J, Lelievre F, Blanchet S, Richaud P, Barbier-Brygoo H, Aarts MG, Thomine S. (2009). Functional characterization of NRAMP3 and NRAMP4 from the metal hyperaccumulator *Thlaspi caerulescens*. *New Phytol* **181**, 637–650.

Păcurar DI, Thordal-Christense H, Păcurar ML, Pamfil D, Botez ML, Bellini C. (2011). *Agrobacterium tumefaciens*: From crown gall tumors to genetic transformation. *Physiological and Molecular Plant Pathology* **76**, 76–81.

Palmer CM, Guerinot ML. (2009). Facing the challenges of Cu, Fe and Zn homeostasis in plants. *Nat Chem Biol* **5**, 333-340.

References

- Palmer CM, Hindt MN, Schmidt H, Clemens S, Guerinot ML.** (2013). MYB10 and MYB72 Are Required for Growth under Iron-Limiting Conditions, *PLoS Genet* **9**, 11.
- Palmgren M.G, Clemens S, Williams LE, Kramer U, Borg S, Schjorring JK, Sanders D.** (2008). Zinc biofortification of cereals: problems and solutions. *Trends Plant Sci*, **13**, 464–473.
- Park J, Song WY, Ko D, Eom Y, Hansen TH, Schiller M, Lee TG, Martinoia E, Lee Y.** (2012). The phytochelatin transporters AtABCC1 and AtABCC2 mediate tolerance to cadmium and mercury. *Plant J* **69**, 278–288.
- Pauwels M, Vekemans X, Gode C, Frerot H, Castric V, Saumitou-Laprade P.** (2012). Nuclear and chloroplast DNA phylogeography reveals vicariance among European populations of the model species for the study of metal tolerance, *Arabidopsis halleri* (Brassicaceae). *New Phytol* **193**, 916– 928.
- Pence NS, Larsen PB, Ebbs SD, Letham DLD, Lasat MM, Garvin DF, Eide D, Kochian LV.** (2000). The molecular physiology of heavy metal transport in the Zn/Cd hyperaccumulator *Thlaspi caerulescens*. *Proc Natl Acad Sci USA* **97**, 4956–4960.
- Person RJ, Tokar EJ, Xu Y, Orihuela R, Ngalame NN, Waalkes MP.** (2013). Chronic cadmium exposure in vitro induces cancer cell characteristics in human lung cells. *Toxicol Appl Pharmacol* **273**, 281–288.
- Persson DP, Chen A, Aarts MG, Salt DE, Schjoerring JK, Husted S.** (2016). Multi-Element Bioimaging of *Arabidopsis thaliana*. *Plant Physiology* **172**, 835–847.
- Petrov V, Hille J, Mueller-Roeber B, Gechev TS.** (2015). ROS-mediated abiotic stress-induced programmed cell death in plants. *Front Plant Sci* **6**, 69.
- Pich A, Manteuffel R, Hillmer S, Scholz G, Schmidt W.** (2001). Fe homeostasis in plant cells: does nicotianamine play multiple roles in the regulation of cytoplasmic Fe concentration? *Planta* **213**, 967–976.
- Pilon-Smits EA, Quinn CF, Tapken W, Malagoli M, Schiavon M.** (2009). Physiological functions of beneficial elements. *Curr Opin Plant Biol* **12**, 267–274.
- Pittman JK, Hirschi KD.** (2016). CAX-ing a wide net: Cation/H⁺ transporters in metal remediation and abiotic stress signalling. *Plant Biology*, **18**, 741–749.
- Pitzschke A.** (2013). *Agrobacterium* infection and plant defense-transformation success hangs by a thread. *Front Plant Sci*, **4**, 519.
- Pitzschke A, Hirt H.** (2010). New insights into an old story: *Agrobacterium*-induced tumour formation in plants by plant transformation. *EMBO Journal*, **29**, 1021–32.
- Pollard AJ, Dandridge PK, Harper FA, Smith JA.** (2002). The genetic basis of metal hyperaccumulation in plants. *Crit. Rev. Plant Sci.* **21**, 539–566.

References

- Porra R, Thompson W, Kriedemann P.** (1989). Determination of accurate extinction coefficients and simultaneous equations for assaying chlorophylls a and b extracted with four different solvents: verification of the concentration of chlorophyll standards by atomic absorption spectroscopy. *Biochim Biophys Acta (BBA)-Bioenergetics* **975**, 384-394.
- Qu LJ, Zhu YX** (2006) Transcription factor families in Arabidopsis: major progress and outstanding issues for future research. *Curr Opin Plant Bio* **9**, 544–549
- Ramel F, Sulmon C, Bogard M, Couee I, Gouesbet G.** (2009). Differential patterns of reactive oxygen species and antioxidative mechanisms during atrazine injury and sucrose-induced tolerance in *Arabidopsis thaliana* plantlets. *BMC Plant Biol* **9**, 28.
- Rascio N, Navari-Izzo F.** (2011). Heavy metal hyperaccumulating plants: how and why do they do it? And what makes them so interesting? *Plant Sci* **180**, 169-181.
- Raven JA, Evans MCW, Korb RE.** (1999). The role of trace metals in photosynthetic electron transport in O₂-evolving organisms. *Photosynthesis Research* **60**, 111-150.
- Reichman SM.** (2002). The Responses of Plants to Metal Toxicity: A Review Focusing on Copper, Manganese and Zinc. Melbourne: Australian Minerals and Energy Environment Foundation.
- Reichman SM, Parker DR.** (2002) Revisiting the metal-binding chemistry of nicotianamine and 2'-deoxymugineic acid. Implications for iron nutrition in strategy II plants. *Plant Physiol.* **129**, 1435–1438.
- Rellán-Alvarez R, Abadia J, Alvarez-Fernandez A.** (2008). Formation of metal-nicotianamine complexes as affected by pH, ligand exchange with citrate and metal exchange: a study by electrospray ionization time-of-flight mass spectrometry. *Rapid Communications in Mass Spectrometry* **22**, 1553–1562.
- Rellán-Alvarez R, Giner-Martinez-Sierra J, Orduna J, Orera I, Rodriguez-Castrillon JA, Garcia-Alonso JI, Abadia J, Alvarez-Fernandez A.** (2010). Identification of a tri-iron(III), tri-citrate complex in the xylem sap of iron-deficient tomato resupplied with iron: new insights into plant iron long-distance transport. *Plant Cell Physiol* **51**, 91-102.
- Rivetta A, Negrini N, Cocucci M.** (1997). Involvement of Ca²⁺-calmodulin in Cd²⁺ toxicity during the early phases of radish (*Raphanus sativus* L.) seed germination. *Plant, Cell Environ* **20**, 600–608.
- Roschttardt H, Conéjéro G, Curie C, Mari S.** (2009). Identification of the endodermal vacuole as the iron storage compartment in the Arabidopsis embryo. *Plant Physiol.* **151**, 1–10.
- Roschttardt H, Conèjèro G, Divol F, Alcon C, Verdeil J-L, Curie C, Mari S.** (2013). New insights into Fe localization in plant tissues. *Front. Plant Sci.* **4**, 350.
- Salt DE, Prince RC, Pickering IJ, Raskin I.** (1995). Mechanisms of Cadmium Mobility and Accumulation in Indian Mustard. *Plant Physiol* **109**, 1427-1433.

References

- Sasaki A, Yamaji N, Yokosho K, Ma JF.** (2012). Nramp5 is a major transporter responsible for manganese and cadmium uptake in rice. *Plant Cell* **24**, 2155–2167.
- Schaaf G, Schikora A, Häberle J, Vert G, Ludewig U, Briat JF, Curie C, von Wirén N.** (2005). A putative function for the Arabidopsis Fe-Phytosiderophore transporter homolog AtYSL2 in Fe and Zn homeostasis. *Plant Cell Physiol* **46**, 762–774.
- Schmid NB, Giehl RFH, Doll S, Mock H-P, Strehmel N, Scheel D, Kong X, Hider CR, von Wirén N.** (2014). Feruloyl-CoA 6'-hydroxylase1-dependent coumarins mediate iron acquisition from alkaline substrates in Arabidopsis. *Plant Physiol* **164**, 160–172.
- Schmidke I, Krüger C, Frommichen R, Scholz G, Stephan U.** (1999). Phloem loading and transport characteristics of iron in interaction with plant-endogenous ligands in castor bean seedlings. *Physiologia Plantarum* **106**, 82–89.
- Schmidt H, Günther C, Weber M, Spörlein C, Loscher S, Böttcher C, Schobert R, Clemens S.** (2014). Metabolome analysis of *Arabidopsis thaliana* roots identifies a key metabolic pathway for iron acquisition. *PLoS One*, **9**.
- Schutzendubel A, Polle A.** (2002) Plant responses to abiotic stresses: heavy metal-induced oxidative stress and protection by mycorrhization. *J Exp Bot* **53**, 1351–1365.
- Schuler M, Rellán-Álvarez R, Fink-Straube C, Abadia J, Bauer P.** (2012). Nicotianamine functions in the Phloem-based transport of iron to sink organs, in pollen development and pollen tube growth in Arabidopsis. *Plant Cell* **24**, 2380-2400.
- Schuler M, Bauer P.** (2011) Heavy metals need assistance: the contribution of nicotianamine to metal circulation throughout the plant and the Arabidopsis NAS gene family. *Front Plant Sci* **2**, 69
- Shahzad Z, Gosti F, Frerot H, Lacombe E, Roosens N, Saumitou-Laprade P, Berthomieu P.** (2010). The five AHMT1 zinc transporters undergo different evolutionary fates towards adaptive evolution to zinc tolerance in Arabidopsis halleri. *PLoS Genetics* **6**, e1000911.
- Shanmugam V, Lo JC, Wu CL, Wang SL, Lai CC, Connolly EL, Huang JL, Yeh KC.** (2011). Differential expression and regulation of iron-regulated metal transporters in Arabidopsis halleri and Arabidopsis thaliana--the role in zinc tolerance. *New Phytol* **190**, 125-137.
- Sharma P, Jha AB, Dubey RS, Pessarakli M.** (2012). Reactive Oxygen Species, Oxidative Damage, and Antioxidative Defense Mechanism in Plants under Stressful Conditions. *Journal of Botany* **2012** 26
- Shigaki T, Barkla BJ, Miranda-Vergara MC, Zhao J, Pantoja O, Hirschi KD.** (2005). Identification of a crucial histidine involved in metal transport activity in the Arabidopsis cation/H⁺ exchanger CAX1. *J Biol Chem* **280**, 30136-30142.
- Shigaki T, Hirschi KD.** (2006). Diverse functions and molecular properties emerging for CAX cation/H⁺ exchangers in plants. *Plant Biol (Stuttg)* **8**, 419-429.

References

Sidorov V, Gilbertson L, Addae P, Duncan D. (2006). *Agrobacterium*-mediated transformation of seedling-derived maize callus. *Plant Cell Reports*, **25**, 320–328.

Sinclair SA, Krämer U. (2012). The zinc homeostasis network of land plants. *Biochim Biophys Acta*, **1823**, 1553–1567.

Skórzyńska-Polit E, Pawlikowska-Pawłęga B, Szczuka E, Drązkiewicz M, Krupa Z. (2006). The activity and localization of lipoxygenases in *Arabidopsis thaliana* under cadmium and copper stresses. *Plant Growth Regulation*, **48**, 29–39.

Stein RJ, Höreth S, de Melo JR, Syllwasschy L, Lee G, Garbin ML, Clemens S, Krämer U. (2016). Relationships between soil and leaf mineral composition are element-specific, environment-dependent and geographically structured in the emerging model *Arabidopsis halleri*. *New Phytol.* **213**, 11274-1286.

Stephan UW, Schmidke I, StephanVW, Scholz G. (1996). The nicotianamine molecule is made-to-measure for complexation of metal micronutrients in plants. *Biometals* **9**, 84–90.

Suryawanshi V, Talke IN, Weber M, Eils R, Brors B, Clemens S, Krämer U. (2016). Between-species differences in gene copy number are enriched among functions critical for adaptive evolution in *Arabidopsis halleri*, *BMC Genomics* **17**(Suppl 13), 1034.

Jaffre T, Brooks RR, Lee J, Reeves RD. (1976). *Sebertia acuminata*: A Hyperaccumulator of Nickel from New Caledonia. *Science* **193**, 579-580.

Takahashi M, Terada Y, Nakai I, Nakanishi H, Yoshimura E, Mori S, Nishizawa NK. (2003). Role of nicotianamine in the intracellular delivery of metals and plant reproductive development. *Plant Cell* **15**, 1263–1280.

Takahashi R, Ishimaru Y, Senoura T, Shimo H, Ishikawa S, Arai T, Nakanishi H, Nishizawa NK. (2011). The OsNRAMP1 iron transporter is involved in Cd accumulation in rice. *J. Exp. Bot.* **62**, 4843–4850.

Talke IN, Hanikenne M, Krämer U. (2006). Zinc-dependent global transcriptional control, transcriptional deregulation, and higher gene copy number for genes in metal homeostasis of the hyperaccumulator *Arabidopsis halleri*. *Plant Physiol* **142**, 148-167.

Thomine S, Wang R, Ward JM, Crawford NM, Schroeder JI. (2000). Cadmium and iron transport by members of a plant metal transporter family in *Arabidopsis* with homology to Nramp genes. *Proc. Natl. Acad. Sci. USA* **97**, 4991–4996.

Thomine S, Lelièvre F, Debarbieux E, Schroeder JI, Barbier-Brygoo H. (2003). AtNRAMP3, a multispecific vacuolar metal transporter involved in plant responses to iron deficiency. *Plant Journal* **34**, 685–695.

Thomine S, Vert G. (2013). Iron transport in plants: better be safe than sorry. *Curr Opin Plant Bio* **16**, 322–7.

References

Tottey S, Block M, Allen M, Westergren T, Albrieux C, Scheller H, Merchant S, Jensen P. (2003) Arabidopsis CHL27, located in both envelope and thylakoid membranes, is required for the synthesis of protochlorophyllide. *Proc Natl Acad Sci USA* **100**, 16119–16124

Trampczynska A, Küpper H, Meyer-Klaucke W, Schmidt H, Clemens S. (2010). Nicotianamine forms complexes with Zn(II) in vivo. *Metallomics*, **2**, 57–66.

Ueno D, Milner MJ, Yamaji N, Yokosho K, Koyama E, Clemencia Zambrano M, Kaskie M, Ebbs S, Kochian LV, Ma JF. 2011. Elevated expression of TcHMA3 plays a key role in the extreme Cd tolerance in a Cd-hyperaccumulating ecotype of *Thlaspi caerulescens*. *Plant J* **66**, 852-862.

Ueno D, Milner MJ, Yamaji N, Yokosho K, Koyama E, Clemencia Zambrano M, Kaskie M, Ebbs S, Kochian LV, Ma JF. (2011). Elevated expression of TcHMA3 plays a key role in the extreme Cd tolerance in a Cd-hyperaccumulating ecotype of *Thlaspi caerulescens*. *Plant J* **66**, 852-862.

Ueno D, Yamaji N, Kono I, Huang CF, Ando T, Yano M, Ma JF. (2010). Gene limiting cadmium accumulation in rice. *Proc. Natl. Acad. Sci. USA* **107**, 16500–16505.

UNEP (United Nations Environment Programme). 2008. Draft Final Review of Scientific Information [hazardoussubstances/Portals/9/Lead_Cadmium/docs/Interim_reviews/Final_UNEP_Cadmium_review_Nov_2008.pdf](http://www.unep.org/hazardoussubstances/Portals/9/Lead_Cadmium/docs/Interim_reviews/Final_UNEP_Cadmium_review_Nov_2008.pdf).

Uraguchi S, Kamiya T, Sakamoto T, Kasai K, Sato Y, Nagamura Y, Yoshida A, Kyojuka J, Ishikawa S, Fujiwara T. (2011). Low-affinity cation transporter (OsLCT1) regulates cadmium transport into rice grains. *Proc Natl Acad Sci USA* **108**(52): 20959-20964.

van de Mortel JE, Almar Villanueva L, Schat H, Kwekkeboom J, Coughlan S, Moerland PD, Ver Loren van Themaat E, Koornneef M, Aarts MG. (2006). Large expression differences in genes for iron and zinc homeostasis, stress response, and lignin biosynthesis distinguish roots of *Arabidopsis thaliana* and the related metal hyperaccumulator *Thlaspi caerulescens*. *Plant Physiol* **142**, 1127-1147.

Vera-Estrella R, Miranda-Vergara MC, Barkla BJ. (2009). Zinc tolerance and accumulation in stable cell suspension cultures and in vitro regenerated plants of the emerging model plant *Arabidopsis halleri* (Brassicaceae). *Planta*, **229**, 977–86.

Verbruggen N, Hermans C. (2013). Root responses to trace metallic elements in Plant Roots. In: *The Hidden Half*, 4th edition. Editors: Eshel A. and Beeckman T., **CRC Press**. ISBN 978-1-4398-4648-3.

Verbruggen N, Hermans C, Schat H. (2009a). Mechanisms to cope with arsenic or cadmium excess in plants. *Curr Opin Plant Biol* **12**, 364-372.

Verbruggen N, Hermans C, Schat H. (2009b). Molecular mechanisms of metal hyperaccumulation in plants. *New Phytol* **181**, 759-776.

References

Verbruggen N, Juraniec M, Baliardini C, Meyer CL. (2013). Tolerance to cadmium in plants: the special case of hyperaccumulators. *Biometals* **26**, 633-638.

Vert G, Grotz N, Dedaldechamp F, Gaymard F, Guerinot ML, Briat JF, Curie C. (2002). IRT1, an Arabidopsis transporter essential for iron uptake from the soil and for plant growth. *Plant Cell* **14**, 1223-1233.

Vigani G, Bashir K, Ishimaru Y, Lehmann M, Casiraghi FM, Nakanishi H, Seki M, Geigenberger P, Zocchi G, Nishizawa NK. (2015). Knocking down mitochondrial iron transporter (MIT) reprograms primary and secondary metabolism in rice plants. *J. Exp. Bot* **67**,1357-1368.

Villiers F, Ducruix C, Hugouvieux V, Jarno N, Ezann E, Garin J, Junot C, Bourguignon J. (2011). Investigating the plant response to cadmium exposure by proteomic and metabolomic approaches. *Proteomics* **11**, 1650–1663.

Vogel-Mikus ., Simcic J, Pelicon P, Budnar M, Kump P, Necemer M, Mesjasz-Przybyłowicz J, Przybyłowicz W, Regvar M. (2008). Comparison of essential and non-essential element distribution in leaves of the Cd/Zn hyperaccumulator *Thlaspi praecox* as revealed by micro-PIXE. *Plant Cell Environ*, **31**, 1484–1496.

Wasowicz P, Pauwels M, Pasierbinski A, Przedpelska-Wasowicz EM, Babst-Kostecka AA, Saumitou-Laprade P, Rostanski A. (2016) Phylogeography of *Arabidopsis halleri* (Brassicaceae) in mountain regions of Central Europe inferred from cpDNA variation and ecological niche modelling. *PeerJ* 4:e1645 <https://doi.org/10.7717/peerj.1645>.

Weber M, Harada E, Vess C, Roepenack-Lahaye E, Clemens S. (2004). Comparative microarray analysis of *Arabidopsis thaliana* and *Arabidopsis halleri* roots identifies nicotianamine synthase, a ZIP transporter and other genes as potential metal hyperaccumulation factors. *Plant J* **37**, 269-281.

Weber M, Trampczynska A, Clemens S (2006) Comparative transcriptome analysis of toxic metal responses in *Arabidopsis thaliana* and the Cd²⁺-hypertolerant facultative metallophyte *Arabidopsis halleri*. *Plant, Cell Environ* **29**, 950–963.

Wessells KR, Brown KH. (2012). Estimating the Global Prevalence of Zinc Deficiency : Results Based on Zinc Availability in National Food Supplies and the Prevalence of Stunting. *Plos One* **7**(11).

White PJ, Brown PH. (2010). Plant nutrition for sustainable development and global health. *Ann Bot* **105**, 1073-1080.

Willems G, Drager DB, Courbot M, Gode C, Verbruggen N, Saumitou-Laprade P. (2007). The genetic basis of zinc tolerance in the metallophyte *Arabidopsis halleri* ssp. *halleri* (Brassicaceae): an analysis of quantitative trait loci. *Genetics* **176**, 659-674.

Willems G, Frérot H, Gennen J, Salis P, Saumitou-laprade P, Verbruggen N (2010) Quantitative

References

trait loci analysis of mineral element concentrations in an *Arabidopsis halleri* x *Arabidopsis lyrata* petraea F 2 progeny grown on cadmium- contaminated soil. *New Phytol* **187**, 368–379.

Wirén N, Klair S, Bansal S, Briat JF, Khodr H, Shioiri T, Leigh RA, Hider RC. (1999). Nicotianamine Chelates Both FeIII and FeII. Implications for Metal Transport in Plants. *Plant Physiol* **119**, 1107-1114.

Wu AC, Lesperance L, Bernstein H. (2002). Screening for Iron Deficiency. *Pediatrics in Review* <http://doi.org/10.1542/pir.23-5-171>

Wu J; Zhao FJ, Ghandilyan A, LogotetaB, Guzman MO, Schat H, Wang X, Aarts MG. (2009) Identification and functional analysis of two ZIP metal transporters of the hyperaccumulator *Thlaspi caerulescens*. *Plant Soil* **325**, 79–95.

Wu Q, Shigaki T, Williams KA, Han J-S, Kim CK, Hirschi KD, Park S (2011) Expression of an *Arabidopsis* Ca²⁺/H⁺ antiporter CAX1 variant in petunia enhances cadmium tolerance and accumulation. *J Plant Physiol* **168**, 167–73.

Zhao FJ, McGrath SP. (2009) Biofortification and phytoremediation. *Curr. Opin. Plant Biol.* **12**, 373–380.

Zhao Z, Cai T, Tagliani L, Miller M, Wang N, Pang H, Rudert M, Schroeder S, Hondred D, Seltzer J, Pierce D (2000) *Agrobacterium*-mediated sorghum transformation. *Plant Mol Biol* **44**, 789-798.

Zhao Z, Gu W, Cai T, Tagliani L, Hondred D, Bond D, Schroeder S, Rudert M, Pierce D (2001) High throughput genetic transformation mediated by *Agrobacterium tumefaciens* in maize. *Molecular Breeding* **8**, 323-333.

Zhu XF, Zheng C, Hu YT, Jiang T, Liu Y, Dong NY, Yang JL, Zheng SJ (2011). Cadmium-induced oxalate secretion from root apex is associated with cadmium exclusion and resistance in *Lycopersicon esulentum*. *Plant Cell Environ* **34**, 1055-1064.

References

(Eidesstattliche) Versicherungen und Erklärungen

(§ 5 Nr. 4 PromO)

Hiermit erkläre ich, dass keine Tatsachen vorliegen, die mich nach den gesetzlichen Bestimmungen über die Führung akademischer Grade zur Führung eines Doktorgrades unwürdig erscheinen lassen.

(§ 8 S. 2 Nr. 5 PromO)

Hiermit erkläre ich mich damit einverstanden, dass die elektronische Fassung meiner Dissertation unter Wahrung meiner Urheberrechte und des Datenschutzes einer gesonderten Überprüfung hinsichtlich der eigenständigen Anfertigung der Dissertation unterzogen werden kann.

(§ 8 S. 2 Nr. 7 PromO)

Hiermit erkläre ich eidesstattlich, dass ich die Dissertation selbständig verfasst und keine anderen als die von mir angegebenen Quellen und Hilfsmittel benutzt habe.

(§ 8 S. 2 Nr. 8 PromO)

Ich habe die Dissertation nicht bereits zur Erlangung eines akademischen Grades anderweitig eingereicht und habe auch nicht bereits diese oder eine gleichartige Doktorprüfung endgültig nicht bestanden.

(§ 8 S. 2 Nr. 9 PromO)

Hiermit erkläre ich, dass ich keine Hilfe von gewerblichen Promotionsberatern bzw. -vermittlern in Anspruch genommen habe und auch künftig nicht nehmen werde.

21/12/2017

Ort, Datum, Unterschrift